

**Program to Reduce the Earthquake Hazards of
Steel Moment-Frame Structures**

**State of the Art Report on
Welding and Inspection**

DISCLAIMER

This document provides practicing engineers and building officials with a resource document for understanding the behavior of steel moment-frame buildings in earthquakes. It is one of the set of six State of the Art Reports containing detailed derivations and explanations of the basis for the design and evaluation recommendations prepared by the SAC Joint Venture. The recommendations and state of the art reports, developed by practicing engineers and researchers, are based on professional judgment and experience and supported by a large program of laboratory, field, and analytical research. **No warranty is offered with regard to the recommendations contained herein, by the Federal Emergency Management Agency, the SAC Joint Venture, the individual joint venture partners, or the partner's directors, members or employees. These organizations and their employees do not assume any legal liability or responsibility for the accuracy, completeness, or usefulness of any of the information, products or processes included in this publication. The reader is cautioned to review carefully the material presented herein and exercise independent judgment as to its suitability for application to specific engineering projects.** This publication has been prepared by the SAC Joint Venture with funding provided by the Federal Emergency Management Agency, under contract number EMW-95-C-4770.

Cover Art. The beam-column connection assembly shown on the cover depicts the standard detailing used in welded steel moment-frame construction prior to the 1994 Northridge earthquake. This connection detail was routinely specified by designers in the period 1970-1994 and was prescribed by the *Uniform Building Code* for seismic applications during the period 1985-1994. It is no longer considered to be an acceptable design for seismic applications. Following the Northridge earthquake, it was discovered that many of these beam-column connections had experienced brittle fractures at the joints between the beam flanges and column flanges.

State of the Art Report on Welding and Inspection

SAC Joint Venture

A partnership of
Structural Engineers Association of California (SEAOC)
Applied Technology Council (ATC)
California Universities for Research in Earthquake Engineering (CUREe)

Prepared for the SAC Joint Venture Partnership by

Matt Johnson

Edison Welding Institute

Project Oversight Committee

William J. Hall, Chair

Shirin Ader
John M. Barsom
Roger Ferch
Theodore V. Galambos
John Gross

James R. Harris
Richard Holguin
Nestor Iwankiw
Roy G. Johnston
Len Joseph

Duane K. Miller
John Theiss
John H. Wiggins

SAC Project Management Committee

SEAOC: William T. Holmes
ATC: Christopher Rojahn
CUREe: Robin Shepherd

Program Manager: Stephen A. Mahin
Project Director for Topical Investigations:
James O. Malley
Project Director for Product Development:
Ronald O. Hamburger

Topical Investigation Team

Pingsha Dong

George Gruber/Glenn M. Light

William Mohr

Technical Advisory Panel

John M. Barsom
John W. Fisher
J. Ernesto Indacochea

Duane K. Miller
Robert Pyle

Douglas Rees-Evans
Richard I. Seals

SAC Joint Venture

SEAOC: www.seaoc.org

ATC: www.atcouncil.org

CUREe: www.curee.org

September 2000

THE SAC JOINT VENTURE

SAC is a joint venture of the Structural Engineers Association of California (SEAOC), the Applied Technology Council (ATC), and California Universities for Research in Earthquake Engineering (CUREe), formed specifically to address both immediate and long-term needs related to solving performance problems with welded, steel moment-frame connections discovered following the 1994 Northridge earthquake. SEAOC is a professional organization composed of more than 3,000 practicing structural engineers in California. The volunteer efforts of SEAOC's members on various technical committees have been instrumental in the development of the earthquake design provisions contained in the *Uniform Building Code* and the 1997 *National Earthquake Hazards Reduction Program (NEHRP) Recommended Provisions for Seismic Regulations for New Buildings and other Structures*. ATC is a nonprofit corporation founded to develop structural engineering resources and applications to mitigate the effects of natural and other hazards on the built environment. Since its inception in the early 1970s, ATC has developed the technical basis for the current model national seismic design codes for buildings; the *de facto* national standard for postearthquake safety evaluation of buildings; nationally applicable guidelines and procedures for the identification, evaluation, and rehabilitation of seismically hazardous buildings; and other widely used procedures and data to improve structural engineering practice. CUREe is a nonprofit organization formed to promote and conduct research and educational activities related to earthquake hazard mitigation. CUREe's eight institutional members are the California Institute of Technology, Stanford University, the University of California at Berkeley, the University of California at Davis, the University of California at Irvine, the University of California at Los Angeles, the University of California at San Diego, and the University of Southern California. These laboratory, library, computer and faculty resources are among the most extensive in the United States. The SAC Joint Venture allows these three organizations to combine their extensive and unique resources, augmented by subcontractor universities and organizations from across the nation, into an integrated team of practitioners and researchers, uniquely qualified to solve problems related to the seismic performance of steel moment-frame buildings.

ACKNOWLEDGEMENTS

Funding for Phases I and II of the SAC Steel Program to Reduce the Earthquake Hazards of Steel Moment-Frame Structures was principally provided by the Federal Emergency Management Agency, with ten percent of the Phase I program funded by the State of California, Office of Emergency Services. Substantial additional support, in the form of donated materials, services, and data has been provided by a number of individual consulting engineers, inspectors, researchers, fabricators, materials suppliers and industry groups. Special efforts have been made to maintain a liaison with the engineering profession, researchers, the steel industry, fabricators, code-writing organizations and model code groups, building officials, insurance and risk-management groups, and federal and state agencies active in earthquake hazard mitigation efforts. SAC wishes to acknowledge the support and participation of each of the above groups, organizations and individuals. In particular, we wish to acknowledge the contributions provided by the American Institute of Steel Construction, the Lincoln Electric Company, the National Institute of Standards and Technology, the National Science Foundation, and the Structural Shape Producers Council. SAC also takes this opportunity to acknowledge the efforts of the project participants – the managers, investigators, writers, and editorial and production staff – whose work has contributed to the development of these documents. Finally, SAC extends special acknowledgement to Mr. Michael Mahoney, FEMA Project Officer, and Dr. Robert Hanson, FEMA Technical Advisor, for their continued support and contribution to the success of this effort.

In Memory of Egor Popov, Professor Emeritus, University of California at Berkeley

TABLE OF CONTENTS

LIST OF FIGURES	vii
LIST OF TABLES	xi
1. INTRODUCTION	1-1
1.1 Purpose	1-1
1.2 Background.....	1-2
1.3 Scope.....	1-10
2. TOUGHNESS REQUIREMENTS, PERFORMANCE, AND PREQUALIFICATION OF CONSUMABLES USED FOR MOMENT FRAME CONSTRUCTION DESIGNED FOR SEISMIC RESISTANCE.....	2-1
2.1 Introduction.....	2-1
2.1.1 Class A: No Toughness Requirements	2-2
2.1.2 Class B: Moderate Toughness Requirements.....	2-2
2.1.3 Class C: High Toughness at Low Temperatures	2-2
2.2 AWS Classification Requirements	2-4
2.3 Full-Scale Testing	2-4
2.3.1 Description of Full-Scale Tests	2-4
2.3.2 CVN Impact Toughness of Full-Scale Welds	2-6
2.3.3 CTOD Toughness and Low-Cycle Behavior of Full-Scale Tests	2-12
2.3.3.1 Comparison of Full-Scale Test Welds with Laboratory Test Welds ..	2-12
2.3.3.2 Development of Fracture Toughness Requirements.....	2-13
2.3.3.3 Derivation of Equivalent Charpy V-Notch (CVN) Impact Toughness	2-17
2.3.3.4 Validation of Methodology.....	2-20
2.3.3.5 Proposed Charpy V-Notch Requirements.....	2-21
2.3.4 Tensile Properties in the Full-Scale Tests	2-22
2.4 Variables Affecting Weld Metal Toughness	2-24
2.4.1 Effect of Cooling Rate on Weld Metal Strength	2-38
2.5 Prequalification of Electrodes.....	2-40
2.5.1 Prequalification Requirements and Method	2-40
2.5.2 Discussion	2-42
2.6 Chapter Summary	2-45
3. EFFECT OF INTERMIXING OF CONSUMABLES.....	3-1
3.1 Background.....	3-1
3.2 Measurement of Intermixing Effects	3-3
3.3 Mechanical Properties of Intermixed Welds	3-3
3.4 Summary and Conclusions	3-6
4. HEAT-AFFECTED-ZONE CONSIDERATIONS.....	4-1
4.1 Introduction.....	4-1

4.2	The Heat Affected Zone Regions	4-1
4.2.1	Single Pass Welds.....	4-1
4.2.2	Multiple-Pass HAZs	4-2
4.3	Measurement of HAZ Toughness.....	4-3
4.3.1	Charpy V-Notch (CVN)	4-4
4.3.2	Crack Tip Opening Displacement (CTOD).....	4-5
4.3.3	Weld Thermal Simulation	4-8
4.4	The Effects of Post Weld Heat Treatment (PWHT)	4-10
4.4.1	Toughness in Structural Steel Shapes	4-10
4.4.1.1	ASTM A572 Gr. 50	4-10
4.4.1.2	HAZ Toughness of QST Jumbo Columns	4-16
4.4.1.3	Effect of Scrap Quality on the Toughness of A913 Steel.....	4-18
4.5	Summary and Conclusions	4-19
5.	EFFECT OF HYDROGEN ON WELD METAL PROPERTIES AND INTEGRITY	5-1
5.1	Summary	5-1
5.2	Effects of Hydrogen in Steel.....	5-1
5.2.1	Introduction of Hydrogen into the Weld Pool.....	5-2
5.2.2	Sources of Hydrogen	5-2
5.2.3	Effects of Hydrogen on the Mechanical Properties of Steel	5-6
5.2.3.1	Effect of Hydrogen on Ductility	5-7
5.2.3.2	Fisheyes in Weld Metal Fracture Surfaces	5-8
5.2.3.3	Hydrogen Assisted Cracking	5-9
5.3	Hydrogen Management in Weld Metals Deposited Using Flux-Cored Arc Welding Consumables	5-10
5.3.1	Background.....	5-10
5.3.2	Diffusible Hydrogen in FCAW Weldments	5-11
5.3.3	Hydrogen Assisted Cracking in FCAW Weldments	5-16
5.3.4	Low Temperature PWHT	5-21
5.4	Summary and Conclusions	5-25
5.5	Recommendations.....	5-25
5.5.1	Recommendations: Present Problems	5-25
5.5.2	Recommendations: Proposed Specifications.....	5-27
5.5.3	Recommendations: Future Research	5-29
6.	EFFECT OF WIND SPEED	6-1
6.1	Introduction and Background	6-1
6.2	Experimental Approach	6-4
6.2.1	Weld Metal Soundness Study.....	6-4
6.2.2	Weld Metal Mechanical Property Study	6-5
6.3	Results and Discussion	6-8
6.4	Conclusions.....	6-15
6.5	Recommendations.....	6-15
7.	INSPECTION AND ACCEPTANCE CRITERIA	7-1

7.1	Introduction.....	7-1
7.2	Overview of Inspection Methods.....	7-1
7.2.1	Visual Inspection.....	7-1
7.2.2	Penetrant Testing (PT).....	7-2
7.2.3	Magnetic Particle Testing (MT).....	7-5
7.2.4	Ultrasonic Testing (UT).....	7-6
7.2.5	Radiographic Testing (RT).....	7-8
7.2.6	Acoustic Emission Testing.....	7-10
7.2.7	New NDE Techniques.....	7-10
7.2.7.1	Semi-Automated and Fully Automated UT.....	7-10
7.2.7.2	Phased Array UT.....	7-10
7.2.8	Types of Inspectors.....	7-11
7.2.9	Inspector Qualification Requirements.....	7-11
7.3	Discussion of Ultrasonic Inspection Approaches.....	7-11
7.3.1	Summary of SAC UT Round-Robin Testing.....	7-12
7.3.2	Demonstrated Limitations of the Current D1.1 Acceptance Criteria.....	7-14
7.3.3	Contract of AWS D1.1 Annex K and API Recommended Practice 2X.....	7-16
7.3.4	Southwest Research Institute Alternative Manual UT Procedures.....	7-18
7.3.5	Ultrasonic Inspection Summary.....	7-19
7.4	Acceptance Criteria.....	7-19
7.4.1	Alternative Acceptance Criteria.....	7-20
7.4.2	More Stringent Ultrasonic Amplitude-Based Criteria.....	7-20
7.4.3	Ultrasonic Size-Based Criteria.....	7-21
7.4.3.1	Alternative Acceptance-Rejection Criteria.....	7-21
7.4.3.2	Commentary on Alternative Criteria.....	7-22
7.4.4	Acceptance Criteria Using Other Inspection Techniques.....	7-24
	REFERENCES, FEMA REPORTS, SAC REPORTS, AND ACRONYMS.....	R-1
	SAC PHASE II PROJECT PARTICIPANTS.....	S-1

LIST OF FIGURES

Figure 1-1	Typical Welded Moment-Resisting Connection Prior to 1994	1-4
Figure 1-2	Common Zone of Fracture Initiation in Beam-Column Connection	1-5
Figure 1-3	Fractures of Beam-to-Column Joints	1-5
Figure 1-4	Column Fractures	1-6
Figure 1-5	Vertical Fracture through Beam Shear Plate Connection	1-6
Figure 2-1	CVN Impact Toughness Measured in E70TG-K2 Weld Metal Deposited in the UM Full-Scale Beam-to-Column Welds and in Follow-On Testing at EWI.....	2-9
Figure 2-2	CVN Impact Toughness Measured in E70TG-K2 Weld Metal Deposited in the Lehigh University Full-Scale Beam-to-Column Welds and in Welds Deposited at EWI for Follow-on Testing	2-9
Figure 2-3	CVN Impact Toughness Measured in Full-Scale E70T-6 Welds Deposited in Full-Scale Connections Evaluated at UTA/UTAM and in Welds Deposited at EWI	2-10
Figure 2-4	Comparison of CVN Impact Energy and CTOD Values for E70TG-K2 Weld Metal Deposited in the EWI Follow-On Testing (SAC Sub-Task 5.2.8). Data from the UM and Lehigh Tests is also Included	2-13
Figure 2-5	CVN Impact Energy and CTOD Data Measured in E70T-6 Weld Metal Deposited as Part of SAC Sub-Task 5.2.8. Data from the UTA Full-Scale Tests is also Included	2-14
Figure 2-6	Initiation and Propagation of Fatigue Cracks in the University of Michigan Beam-to-Column Test Welds	2-14
Figure 2-7	Stable Crack Growth Preceded Unstable Crack Growth	2-15
Figure 2-8	Kc-CTOD-J Relationships for an A131 Steel.....	2-19
Figure 2-9	Kc Values Calculated from CTOD and CVN Upper Shelf Energy Measured in E70TG-K2 Weld Metal	2-19
Figure 2-10	Kc Values Calculated from CTOD and CVN Upper Shelf Energy Measured In E70T-6 Weld Metal	2-20
Figure 2-11	Location and Orientation of Tensile Specimens Extracted from Full-Scale Test Specimens	2-23
Figure 2-12	Yield and Tensile Strength Measured in the Full-Scale Test Welds Deposited at the University of Michigan (UM), Lehigh (LU), and the University of Texas at Austin (UTA). The Locations and Orientation of the Test Samples are Shown in Figure 2-11.	2-24
Figure 2-13	CVN Impact Toughness Measured in E70T-6 Welds Deposited with Fast Cooling Rates (33 kJ/in., <100°F Interpass), Medium Cooling Rates (53 kJ/in., <300°F), and Slow Cooling Rates (76 kJ/in., 550°F).	2-28
Figure 2-14	CVN Impact Toughness Measured in E70T-6 Weld Metal Deposited with Low, Medium and High Heat Inputs. Interpass Temperature was Maintained at 300°F. [M.A. Quintana, LEC-with permission]	2-28

Figure 2-15	CVN Impact Energy Measured in E70TG-K2 Weld Metal Deposited Under the Following Conditions: Weld A 17 kJ/in., <100 °F Interpass, Normal Electrode Extension (EE); Weld B, 43 kJ/in., 300°F, Long EE; Weld C, 43 kJ/in., 300°F, Normal EE, Weld D; 43 kJ/in., 300°F, Short EE; Weld E, 70 kJ/in., 550°F, Normal EE.....	2-29
Figure 2-16	CVN Impact Toughness Measured in E70TG-K2 Weld Metal Deposited with Medium and High Heat Inputs. Interpass Temperature was Maintained at 300°F. [M.A. Quintana, LEC-with permission]	2-29
Figure 2-17	CVN Impact Energy Measured in E71T-8 Weld Metal Deposited Under the Following Conditions: Weld A 13 kJ/in., <100°F Interpass, Normal Electrode Extension (EE); Weld B, 29 kJ/in., 300°F, Long EE; Weld C, 29 kJ/in., 300°F, Normal EE, Weld D; 29 kJ/in., 300°F, Short EE; Weld E, 43 kJ/in., 550°F, Normal EE.....	2-30
Figure 2-18	CVN Impact Toughness Measured in E71T-8 Weld Metal Deposited with Medium and High Heat Inputs. Interpass Temperature was Maintained at 300°F. [M.A. Quintana, LEC-with permission]	2-31
Figure 2-19	CVN Impact Energy of E7018 Weld Metal Deposited using the Following Welding Conditions: Weld A 17 kJ/in., <100°F Interpass, Weld B 40 kJ/in. 300°F Interpass, Weld C 70 kJ/in., 550°F Interpass.....	2-31
Figure 2-20	Summary of Low Temperature CVN Impact Energy Measured in Welds Deposited Using 3/32-in. dia. E70T-6 consumables Evaluated in the SAC Program.....	2-35
Figure 2-21	Summary of Low Temperature CVN Impact Energy Measured in E70TG-K2 Weld Metal Evaluated in the SAC Program.....	2-35
Figure 2-22	Summary of Low Temperature CVN Impact Energy Measured in E71T-8 Weld Metal Evaluated in the SAC Program.....	2-36
Figure 2-23	Comparison of the CVN Impact Energy Measured at Room Temperature in Welds Deposited Under Different Conditions Using E70T-6, E7018, E71T-8, and E70TG-K2 Electrodes.....	2-37
Figure 2-24	Effect of Electrode Type on the 50% FATT (temperature at which 50 percent of the CVN fracture surface is brittle)	2-38
Figure 2-25	Effect of Cooling Rate on the Tensile Strength of Weld Metal Deposited Using FCAW-S and SMAW Electrodes During the SAC Program. The Maximum, Minimum, and Mean Tensile Strengths Measured in A572 Gr. 50 and A913 Gr. 65 Shape Materials are also Shown for Comparison.....	2-39
Figure 2-26	Effect of Cooling Rate on the Tensile Strength of Weld Metal Deposited Using FCAW-S and SMAW Electrodes During the SAC Program. The Maximum, Minimum, and Mean Tensile Strengths Measured in A572 Gr. 50 and A913 Gr. 65 Shape Materials are also Shown for Comparison.....	2-40
Figure 3-1	Test Specimen Locations	3-3
Figure 4-1	A Schematic Illustration of the Various Single-Pass HAZ Regions with Reference to the Iron-Carbon Equilibrium Diagram. A Fe-0.15 wt. pct. Carbon Steel is Shown.....	4-2

Figure 4-2	Schematic Illustration of the Various HAZ Regions Produced During Deposition of a Multiple Pass Weld	4-4
Figure 4-3	Through Thickness Notch Sampling CGHAZ Regions.....	4-6
Figure 4-4	Schematic Illustration Showing L-type Specimens and T-type Notch Locations.....	4-7
Figure 4-5	Schematic Illustration Showing Approach Used to Quantify the Percent of Unaltered CGHAZ Region Sampled in a Through-Thickness L-type CTOD Specimen.....	4-8
Figure 4-6	Schematic Illustration of Potential Crack Paths in a Bottom Flange Weldment.....	4-12
Figure 4-7	Specimen Location and Orientation for CGHAZ Simulation as Part of the SAC Study. Samples Extracted from Column Material were Oriented and Notched so that Crack Propagation Occurred in the S-L Direction. Samples extracted from Beam Material were Oriented so that Crack Propagation Occurred in the L-S Direction.	4-13
Figure 4-8	Simulated CGHAZ in W14x398 ASTM A572 Gr. 50 Column Material	4-14
Figure 4-9	The Effect of Thermal Cycles on the CVN Toughness of As-Received W14x455 Column Material Subjected to CGHAZ Thermal Cycles Corresponding to Heat Inputs of 20 kJ/in, 70 kJ/in, and 120 kJ/in. The Column Material was Extracted from a Damaged Building in the Los Angeles Area.....	4-16
Figure 4-10	The Effect of Simulated CGHAZ Thermal Cycles on the Toughness of W36x150 ASTM A572 Gr. 50 Beam Flange Material.....	4-17
Figure 5-1	Hydrogen Remaining in a Weld Deposit as a Function of Time (Coe, 1973).....	5-3
Figure 5-2	Effect of Test Temperature and Strain Rate on the Notched Tensile Strength of Hydrogen Charged Low Alloy Steel (Graville, 1967)	5-7
Figure 5-3	Atmospheric Exposure Test Results for Mild-Steel FCAW-G Electrodes Provided by Several Manufacturers (Harwig, 1999)	5-13
Figure 5-4	Effect of Atmospheric Exposure on FCAW-S Weld Metal Diffusible Hydrogen Concentrations. Electrodes Were Tested in the As-Received Condition, After 1 Week of Exposure in a Forced-Air Humidity Cabinet at 80%RH-80°F, and After 1 Month of Exposure Under Ambient Laboratory Conditions (Johnson, 2000).	5-14
Figure 5-5	Effect of Electrode Extension and Welding Current on Diffusible Hydrogen in E71T-1 Rutile FCAW-G Weld Metal (Harwig, 1999)	5-15
Figure 5-6	Effect of Preheat on E71T-1M Weld Metal Cracking Using Low and High Welding Currents (The Nominal Heat Inputs were 0.95 and 1.85 kJ/mm Respectively)	5-17
Figure 5-7	Effect of Preheat and Hydrogen on E70T-5M Weld Metal Cracking. Welds were Produced with Heat Inputs of 0.95 and 1.85 kJ/mm. The Filled Symbols Represent Welds Produced using Dry 80/20 Ar/CO ₂ and the Open Symbols Represent Welds Produced with Moistened Gas.....	5-18

Figure 5-8	Effect of Preheat and Arc-Energy on Hydrogen-Assisted Cracking in Y-Groove Test Specimens. FCAW-S Electrodes were Used to Deposit Welds in 1-in. Thick A572Gr. 60 plate. The Nominal Diffusible Hydrogen Concentration in the FCAW-S Weld Metals Ranged from 8-12 ml H ₂ /100 g Deposited Weld Metal.	5-19
Figure 5-9	Longitudinal and Transverse Cracks Occurring in a Multipass Weldment.....	5-20
Figure 5-10	Proportion of Diffusible Hydrogen Remaining in Different Geometry Shapes after Exposure in Air for Time at Constant Temperature (Bailey, 1993)	5-23
Figure 5-11	Simplified Geometry and Assumption of Infinite Cylinder to Estimate Hydrogen Remaining after a Given Period of Time.....	5-23
Figure 6-1	Effect of Wind Speed on Nitrogen Concentration in Three FCAW-S Weld Deposits	6-2
Figure 6-2	Effect of Wind Speed on Tensile Ductility of All Weld Metal Tensile Specimens Produced Using the FCAW-G and FCAW-S Processes	6-3
Figure 6-3	Effect of Wind Speed on CVN Impact Energy Measured in Welds Deposited Using the FCAW-G and FCAW-S Processes	6-4
Figure 6-4	Schematic of Equipment Used to Vary Wind Speed. Wind Velocity was Varied by Adjusting Fan Speed and by Varying Distance to the Weld. Wind Velocity was Measured at the Weld Centerline Using a Hand-Held Anemometer.....	6-6
Figure 6-5	Groove Weld Joint Geometry, Test Plate Dimensions, and Sample Locations for the Mechanical Properties of Welds Deposited with a Wind Speed of 10 mph	6-7
Figure 6-6	Macrograph and Radiographs of the E71T-1 Bead-on-Plate Welds Deposited Under a Range of Wind Conditions.....	6-9
Figure 6-7	Radiographs of Bead-on-Plate Welds Deposited Under Different Wind Conditions Using an E70T-6 FCAW-S Consumable	6-10
Figure 6-8	CVN Impact Energy Measured in E70T-6 Multipass Welds Deposited in Still Air and Under Wind Speeds of 10 mph (4.5 m/s).....	6-11
Figure 6-9	CVN Impact Energy Measured in E70TG-K2 Multipass Welds Deposited in Still Air and Under Wind Speeds of 10 mph (4.5 m/s).....	6-12
Figure 6-10	CVN Impact Energy Measured in E71T-8 Multipass Welds Deposited in Still Air and Under Wind Speeds of 10 mph (4.5 m/s).....	6-12
Figure 6-11	CVN Impact Energy Measured in E7018 Multipass Welds Deposited in Still Air and Under Wind Speeds of 10 mph (4.5 m/s).....	6-13

LIST OF TABLES

Table 2-1	Minimum Mechanical Property Requirements for Selected Consumables	2-5
Table 2-2	Summary of CVN Properties Measured in Welds Produced as Part of the SAC Program	2-8
Table 2-3	CTOD and Calculated K _c Values from Full-Scale Specimens Fabricated at the University of Michigan, Lehigh University, and the University of Texas at Austin	2-16
Table 2-4	CTOD and Calculated K _c Values from E70TG-K2 Weld Metal Tested in SAC Sub-Task 5.2.8	2-17
Table 2-5	CTOD and Calculated K _c from E70T-6 Weld Metal Tested in SAC Sub-Task 5.2.8	2-18
Table 2-6	Summary of Experimental Welding Conditions and Electrodes Used in SAC Sub-Task 5.2.3	2-26
Table 2-7	Summary of Classification Testing Program using a 3/32-in. dia. E70TG-K2 Electrode	2-33
Table 2-8	Summary of the Classification Testing Program Using the E70T-6 Electrode ..	2-34
Table 2-9	Proposed Welding and Preheat Conditions for Determination of Prequalified Status	2-42
Table 3-1	Typical Weld Metal Chemical Compositions	3-2
Table 3-2	Impact Toughness Measured/Expected in the Region of Maximum Dilution Relative to Baseline Welds Produced with a Single Fill Electrode	3-4
Table 3-3	Typical Dilution Ranges Measured for Various Welding Processes	3-5
Table 4-1	Chemical Compositions of the Beam and Column Material Subject to CGHAZ Thermal Simulations in the SAC Study	4-15
Table 5-1	Variation of Overall Diffusivity Coefficient D, with Temperature and Material Type	5-4
Table 5-2	Effect of Atmospheric Exposure on Diffusible Hydrogen of FCAW-S Weld Metal (Johnson, 2000)	5-5
Table 5-3	Expected Time for Diffusion of 90% of Hydrogen from FCAW-S Weld Metal from Flanges of Different Thickness	5-24
Table 6-1	Welding Parameters Used to Produce the Bead-on-Plate Welds Deposited Used to Evaluate the Effect of Wind Speed on Weld Soundness	6-5
Table 6-2	Welding Parameters Used to Deposit Multipass Weld Metal Used for Mechanical Property Measurement	6-8
Table 6-3	Summary of All Weld Metal Tensile Tests from Weld Metal Deposited with a Side Wind of 10 mph (4.5 m/s) and Under Laboratory Conditions (0 mph) ..	6-14
Table 7-1	Applicability of NDE Techniques for Finding Discontinuities	7-3
Table 7-2	Applicability of NDE Techniques for Weld Joint Geometry	7-4

1. INTRODUCTION

1.1 Purpose

This report, *FEMA-355B – State of the Art Report on Welding and Inspection*, presents an overview of the technical issues that were investigated and found to be relevant to the performance of welded joints in moment-resisting steel frame structures subject to seismic loading. This state of the art report was prepared in support of the development of a series of Recommended Design Criteria documents, prepared by the SAC Joint Venture on behalf of the Federal Emergency Management Agency (FEMA) and addressing the issue of the seismic performance of moment-resisting steel frame structures. These publications include:

- *FEMA-350 – Recommended Seismic Design Criteria for New Steel Moment-Frame Buildings*. This publication provides recommended criteria, supplemental to *FEMA-302 – 1997 NEHRP Recommended Provisions for Seismic Regulations for New Buildings and Other Structures*, for the design and construction of steel moment-frame buildings and provides alternative performance-based design criteria.
- *FEMA-351 – Recommended Seismic Evaluation and Upgrade Criteria for Existing Welded Steel Moment-Frame Buildings*. This publication provides recommended methods to evaluate the probable performance of existing steel moment-frame buildings in future earthquakes and to retrofit these buildings for improved performance.
- *FEMA-352 – Recommended Postearthquake Evaluation and Repair Criteria for Welded Steel Moment-Frame Buildings*. This publication provides recommendations for performing postearthquake inspections to detect damage in steel moment-frame buildings following an earthquake, evaluating the damaged buildings to determine their safety in the postearthquake environment, and repairing damaged buildings.
- *FEMA-353 – Recommended Specifications and Quality Assurance Guidelines for Steel Moment-Frame Construction for Seismic Applications*. This publication provides recommended specifications for the fabrication and erection of steel moment frames for seismic applications. The recommended design criteria contained in the other companion documents are based on the material and workmanship standards contained in this document, which also includes discussion of the basis for the quality control and quality assurance criteria contained in the recommended specifications.

Detailed derivations and explanations of the basis for these design and evaluation recommendations may be found in a series of State of the Art Report documents prepared by the SAC Joint Venture in parallel with these design criteria. These reports include:

- *FEMA-355A – State of the Art Report on Base Metals and Fracture*. This report summarizes current knowledge of the properties of structural steels commonly employed in building construction, and the production and service factors that affect these properties.

- *FEMA-355B – State of the Art Report on Welding and Inspection.* This report summarizes current knowledge of the properties of structural welding commonly employed in building construction, the effect of various welding parameters on these properties, and the effectiveness of various inspection methodologies in characterizing the quality of welded construction.
- *FEMA-355C – State of the Art Report on Systems Performance of Steel Moment Frames Subject to Earthquake Ground Shaking.* This report summarizes an extensive series of analytical investigations into the demands induced in steel moment-frame buildings designed to various criteria, when subjected to a range of different ground motions. The behavior of frames constructed with fully restrained, partially restrained and fracture-vulnerable connections is explored for a series of ground motions, including motion anticipated at near-fault and soft-soil sites.
- *FEMA-355D – State of the Art Report on Connection Performance.* This report summarizes the current state of knowledge of the performance of different types of moment-resisting connections under large inelastic deformation demands. It includes information on fully restrained, partially restrained, and partial strength connections, both welded and bolted, based on laboratory and analytical investigations.
- *FEMA-355E – State of the Art Report on Past Performance of Steel Moment-Frame Buildings in Earthquakes.* This report summarizes investigations of the performance of steel moment-frame buildings in past earthquakes, including the 1995 Kobe, 1994 Northridge, 1992 Landers, 1992 Big Bear, 1989 Loma Prieta and 1971 San Fernando events.
- *FEMA-355F – State of the Art Report on Performance Prediction and Evaluation of Steel Moment-Frame Buildings.* This report describes the results of investigations into the ability of various analytical techniques, commonly used in design, to predict the performance of steel moment-frame buildings subjected to earthquake ground motion. Also presented is the basis for performance-based evaluation procedures contained in the design criteria documents, *FEMA-350*, *FEMA-351*, and *FEMA-352*.

In addition to the recommended design criteria and the State of the Art Reports, a companion document has been prepared for building owners, local community officials and other non-technical audiences who need to understand this issue. *A Policy Guide to Steel Moment-Frame Construction (FEMA-354)* addresses the social, economic, and political issues related to the earthquake performance of steel moment-frame buildings. *FEMA-354* also includes discussion of the relative costs and benefits of implementing the recommended criteria.

1.2 Background

For many years, the basic intent of the building code seismic provisions has been to provide buildings with an ability to withstand intense ground shaking without collapse, but potentially with some significant structural damage. In order to accomplish this, one of the basic principles inherent in modern code provisions is to encourage the use of building configurations, structural systems, materials and details that are capable of ductile behavior. A structure is said to behave in a ductile manner if it is capable of withstanding large inelastic deformations without

significant degradation in strength, and without the development of instability and collapse. The design forces specified by building codes for particular structural systems are related to the amount of ductility the system is deemed to possess. Generally, structural systems with more ductility are designed for lower forces than less ductile systems, as ductile systems are deemed capable of resisting demands that are significantly greater than their elastic strength limit. Starting in the 1960s, engineers began to regard welded steel moment-frame buildings as being among the most ductile systems contained in the building code. Many engineers believed that steel moment-frame buildings were essentially invulnerable to earthquake-induced structural damage and thought that should such damage occur, it would be limited to ductile yielding of members and connections. Earthquake-induced collapse was not believed possible. Partly as a result of this belief, many large industrial, commercial and institutional structures employing steel moment-frame systems were constructed, particularly in the western United States.

The Northridge earthquake of January 17, 1994 challenged this paradigm. Following that earthquake, a number of steel moment-frame buildings were found to have experienced brittle fractures of beam-to-column connections. The damaged buildings had heights ranging from one story to 26 stories, and a range of ages spanning from buildings as old as 30 years to structures being erected at the time of the earthquake. The damaged buildings were spread over a large geographical area, including sites that experienced only moderate levels of ground shaking. Although relatively few buildings were located on sites that experienced the strongest ground shaking, damage to buildings on these sites was extensive. Discovery of these unanticipated brittle fractures of framing connections, often with little associated architectural damage, was alarming to engineers and the building industry. The discovery also caused some concern that similar, but undiscovered, damage may have occurred in other buildings affected by past earthquakes. Later investigations confirmed such damage in a limited number of buildings affected by the 1992 Landers, 1992 Big Bear and 1989 Loma Prieta earthquakes.

In general, steel moment-frame buildings damaged by the Northridge earthquake met the basic intent of the building codes. That is, they experienced limited structural damage, but did not collapse. However, the structures did not behave as anticipated and significant economic losses occurred as a result of the connection damage, in some cases, in buildings that had experienced ground shaking less severe than the design level. These losses included direct costs associated with the investigation and repair of this damage as well as indirect losses relating to the temporary, and in a few cases, long-term, loss of use of space within damaged buildings.

Steel moment-frame buildings are designed to resist earthquake ground shaking based on the assumption that they are capable of extensive yielding and plastic deformation, without loss of strength. The intended plastic deformation consists of plastic rotations developing within the beams, at their connections to the columns, and is theoretically capable of resulting in benign dissipation of the earthquake energy delivered to the building. Damage is expected to consist of moderate yielding and localized buckling of the steel elements, not brittle fractures. Based on this presumed behavior, building codes permit steel moment-frame buildings to be designed with a fraction of the strength that would be required to respond to design level earthquake ground shaking in an elastic manner.

Steel moment-frame buildings are anticipated to develop their ductility through the development of yielding in beam-column assemblies at the beam-column connections. This yielding may take the form of plastic hinging in the beams (or, less desirably, in the columns), plastic shear deformation in the column panel zones, or through a combination of these mechanisms. It was believed that the typical connection employed in steel moment-frame construction, shown in Figure 1-1, was capable of developing large plastic rotations, on the order of 0.02 radians or larger, without significant strength degradation.

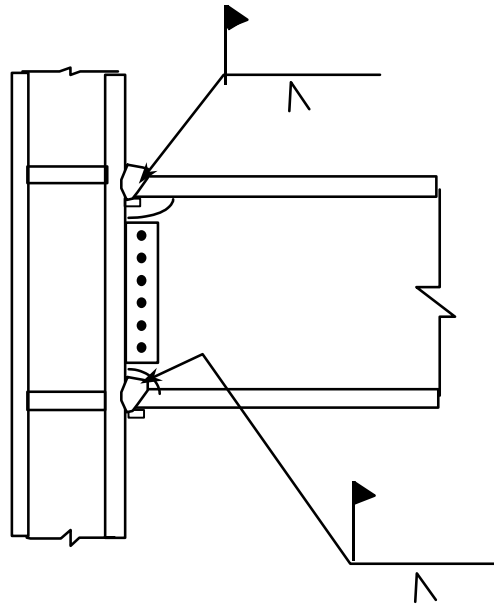


Figure 1-1 Typical Welded Moment-Resisting Connection Prior to 1994

Observation of damage sustained by buildings in the 1994 Northridge earthquake indicated that, contrary to the intended behavior, in many cases, brittle fractures initiated within the connections at very low levels of plastic demand, and in some cases, while the structures remained essentially elastic. Typically, but not always, fractures initiated at the complete joint penetration (CJP) weld between the beam bottom flange and column flange (Figure 1-2). Once initiated, these fractures progressed along a number of different paths, depending on the individual joint conditions.

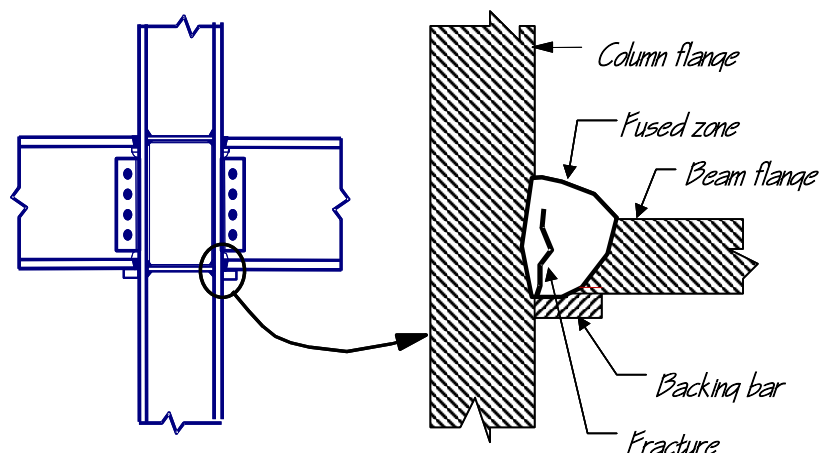


Figure 1-2 Common Zone of Fracture Initiation in Beam-Column Connection

In some cases, the fractures progressed completely through the thickness of the weld, and when fire protective finishes were removed, the fractures were evident as a crack through exposed faces of the weld, or the metal just behind the weld (Figure 1-3a). Other fracture patterns also developed. In some cases, the fracture developed into a crack of the column flange material behind the CJP weld (Figure 1-3b). In these cases, a portion of the column flange remained bonded to the beam flange, but pulled free from the remainder of the column. This fracture pattern has sometimes been termed a “divot” or “nugget” failure.

A number of fractures progressed completely through the column flange, along a near-horizontal plane that aligns approximately with the beam lower flange (Figure 1-4a). In some cases, these fractures extended into the column web and progressed across the panel zone (Figure 1-4b). Investigators have reported some instances where columns fractured entirely across the section.



a. Fracture at Fused Zone



b. Column Flange "Divot" Fracture

Figure 1-3 Fractures of Beam-to-Column Joints



a. Fractures through Column Flange



b. Fracture Progresses into Column Web

Figure 1-4 Column Fractures

Once such fractures have occurred, the beam-column connection has experienced a significant loss of flexural rigidity and strength to resist those loads that tend to open the crack. Residual flexural strength and rigidity must be developed through a couple consisting of forces transmitted through the remaining top flange connection and the web bolts. However, in providing this residual strength and stiffness, the bolted web connections can themselves be subject to failures. These include fracturing of the welds of the shear plate to the column, fracturing of supplemental welds to the beam web or fracturing through the weak section of shear plate aligning with the bolt holes (Figure 1-5).

Despite the obvious local strength impairment resulting from these fractures, many damaged buildings did not display overt signs of structural damage, such as permanent drifts or damage to architectural elements, making reliable postearthquake damage evaluations difficult. In order to determine if a building has sustained connection damage it is necessary to remove architectural finishes and fireproofing, and perform detailed inspections of the connections. Even if no damage is found, this is a costly process. Repair of damaged connections is even more costly. At least one steel moment-frame building sustained so much damage that it was deemed more practical to demolish the building than to repair it.

**Figure 1-5 Vertical Fracture through Beam Shear Plate Connection**

Initially, the steel construction industry took the lead in investigating the causes of this unanticipated damage and in developing design recommendations. The American Institute of Steel Construction (AISC) convened a special task committee in March, 1994 to collect and disseminate available information on the extent of the problem (AISC, 1994a). In addition, together with a private party engaged in the construction of a major steel building at the time of the earthquake, AISC participated in sponsoring a limited series of tests of alternative connection details at the University of Texas at Austin (AISC, 1994b). The American Welding Society (AWS) also convened a special task group to investigate the extent to which the damage was related to welding practice, and to determine if changes to the welding code were appropriate (AWS, 1995).

In September 1994, the SAC Joint Venture, AISC, the American Iron and Steel Institute and National Institute of Standards and Technology jointly convened an international workshop (SAC, 1994) in Los Angeles to coordinate the efforts of the various participants and to lay the foundation for systematic investigation and resolution of the problem. Following this workshop, FEMA entered into a cooperative agreement with the SAC Joint Venture to perform problem-focused studies of the seismic performance of steel moment-frame buildings and to develop recommendations for professional practice (Phase I of SAC Steel Project). Specifically, these recommendations were intended to address the following: the inspection of earthquake-affected buildings to determine if they had sustained significant damage; the repair of damaged buildings; the upgrade of existing buildings to improve their probable future performance; and the design of new structures to provide reliable seismic performance.

During the first half of 1995, an intensive program of research was conducted to explore more definitively the pertinent issues. This research included literature surveys, data collection on affected structures, statistical evaluation of the collected data, analytical studies of damaged and undamaged buildings, and laboratory testing of a series of full-scale beam-column assemblies representing typical pre-Northridge design and construction practice as well as various repair, upgrade and alternative design details. The findings of these tasks formed the basis for the development of *FEMA-267 – Interim Guidelines: Evaluation, Repair, Modification, and Design of Welded Steel Moment Frame Structures*, which was published in August, 1995. *FEMA-267* provided the first definitive, albeit interim, recommendations for practice, following the discovery of connection damage in the 1994 Northridge earthquake.

In September 1995, the SAC Joint Venture entered into a contractual agreement with FEMA to conduct Phase II of the SAC Steel Project. Under Phase II, SAC continued its extensive problem-focused study of the performance of moment resisting steel frames and connections of various configurations, with the ultimate goal of developing reliable seismic design criteria for steel construction. This work has included: extensive analyses of buildings; detailed finite element and fracture mechanics investigations of various connections to identify the effects of connection configuration, material strength, and toughness and weld joint quality on connection behavior; as well as more than 120 full-scale tests of connection assemblies. As a result of these studies, and independent research conducted by others, it is now known that the typical moment-resisting connection detail employed in steel moment-frame construction prior to the 1994 Northridge earthquake, and depicted in Figure 1-1, had a number of features that rendered it inherently susceptible to brittle fracture. These included the following:

- The most severe stresses in the connection assembly occur where the beam joins to the column. Unfortunately, this is also the weakest location in the assembly. At this location, bending moments and shear forces in the beam must be transferred to the column through the combined action of the welded joints between the beam flanges and column flanges and the shear tab. The combined section properties of these elements, for example the cross sectional area and section modulus, are typically less than those of the connected beam. As a result, stresses are locally intensified at this location.
- The joint between the bottom beam flange and the column flange is typically made as a downhand field weld, often by a welder sitting on top of the beam top flange, in a so-called “wildcat” position. To make the weld from this position each pass must be interrupted at the beam web, with either a start or stop of the weld at this location. This welding technique often results in poor quality welding at this critical location, with slag inclusions, lack of fusion and other defects. These defects can serve as crack initiators, when the connection is subjected to severe stress and strain demands.
- The basic configuration of the connection makes it difficult to detect hidden defects at the root of the welded beam-flange-to-column-flange joints. The backing bar, which was typically left in place following weld completion, restricts visual observation of the weld root. Therefore, the primary method of detecting defects in these joints is through the use of ultrasonic testing (UT). However, the geometry of the connection also makes it very difficult for UT to detect flaws reliably at the bottom beam flange weld root, particularly at the center of the joint, at the beam web. As a result, many of these welded joints have undetected significant defects that can serve as crack initiators.
- Although typical design models for this connection assume that nearly all beam flexural stresses are transmitted by the flanges and all beam shear forces by the web, in reality, due to boundary conditions imposed by column deformations, the beam flanges at the connection carry a significant amount of the beam shear. This results in significant flexural stresses on the beam flange at the face of the column, and also induces large secondary stresses in the welded joint. Some of the earliest investigations of these stress concentration effects in the welded joint were conducted by Richard, et al. (1995). The stress concentrations resulting from this effect resulted in severe strength demands at the root of the complete joint penetration welds between the beam flanges and column flanges, a region that often includes significant discontinuities and slag inclusions, which are ready crack initiators.
- In order that the welding of the beam flanges to the column flanges be continuous across the thickness of the beam web, this detail incorporates weld access holes in the beam web, at the beam flanges. Depending on their geometry, severe strain concentrations can occur in the beam flange at the toe of these weld access holes. These strain concentrations can result in low-cycle fatigue and the initiation of ductile tearing of the beam flanges after only a few cycles of moderate plastic deformation. Under large plastic flexural demands, these ductile tears can quickly become unstable and propagate across the beam flange.
- Steel material at the center of the beam-flange-to-column-flange joint is restrained from movement, particularly in connections of heavy sections with thick column flanges. This condition of restraint inhibits the development of yielding at this location, resulting in locally

high stresses on the welded joint, which exacerbates the tendency to initiate fractures at defects in the welded joints.

- Design practice in the period 1985-1994 encouraged design of these connections with relatively weak panel zones. In connections with excessively weak panel zones, inelastic behavior of the assembly is dominated by shear deformation of the panel zone. This panel zone shear deformation results in a local kinking of the column flanges adjacent to the beam-flange-to-column-flange joint, and further increases the stress and strain demands in this sensitive region.

In addition to the above, additional conditions contributed significantly to the vulnerability of connections constructed prior to 1994.

- In the mid-1960s, the construction industry moved to the use of the semi-automatic, self-shielded, flux-cored arc welding process (FCAW-S) for making the joints of these connections. The welding consumables that building erectors most commonly used inherently produced welds with very low toughness. The toughness of this material could be further compromised by excessive deposition rates, which unfortunately were commonly employed by welders. As a result, brittle fractures could initiate in welds with large defects, at stresses approximating the yield strength of the beam steel, precluding the development of ductile behavior.
- Early steel moment frames tended to be highly redundant and nearly every beam-column joint was constructed to behave as part of the lateral-force-resisting system. As a result, member sizes in these early frames were small and much of the early acceptance testing of this typical detail was conducted with specimens constructed of small framing members. As the cost of construction labor increased, the industry found that it was more economical to construct steel moment-frame buildings by moment-connecting a relatively small percentage of the beams and columns and by using larger members for these few moment-connected elements. The amount of strain demand placed on the connection elements of a steel moment frame is related to the span-to-depth ratio of the member. Therefore, as member sizes increased, strain demands on the welded connections also increased, making the connections more susceptible to brittle behavior.
- In the 1960s and 1970s, when much of the initial research on steel moment-frame construction was performed, beams were commonly fabricated using A36 material. In the 1980s, many steel mills adopted more modern production processes, including the use of scrap-based production. Steels produced by these more modern processes tended to include micro-alloying elements that increased the strength of the materials so that despite the common specification of A36 material for beams, many beams actually had yield strengths that approximated or exceeded that required for grade 50 material. As a result of this increase in base metal yield strength, the weld metal in the beam-flange-to-column-flange joints became under-matched, potentially contributing to its vulnerability.

At this time, it is clear that in order to obtain reliable ductile behavior of steel moment-frame construction a number of changes to past practices in design, materials, fabrication, erection and quality assurance are necessary. The recommendations contained in this document, and the companion publications, are based on an extensive program of research into materials, welding

technology, inspection methods, frame system behavior, and laboratory and analytical investigations of different connection details.

1.3 Scope

Following the 1994 Northridge earthquake several concerns and questions pertaining to welding and inspection as implemented in common practice were raised with regard to their adequacy to provide reliable seismic performance in steel frame structures. There are a considerable number of factors which can impact the performance of welded connections under seismic loading. Under the SAC project, a series of investigative tasks was pursued to address the following technical issues with respect to reduction of failure at the weld or heat affected zone regions:

- How strong should the weld be? (i.e. is an overmatching condition necessary or even desirable?)
- Is it possible to use small scale mechanical tests (T-Stubs, wide plates, CVN, CTOD) to determine suitability of a consumable and welding procedure for seismic applications?
- How tough does the weld have to be? What temperature ranges should be considered?
- What effect will variations in welding procedure have on the mechanical properties of welds deposited with consumables designed to deposit weld metal with a specified minimum level of CVN toughness?
- Are current inspection methods accurate enough to detect flaws in a number of locations and are there other inspection techniques available that are inherently superior?
- Given an improvement in weld metal toughness, can alternate acceptance criteria be developed for review and acceptance of weld defects?
- Is the heat affected zone of concern when using hot-rolled structural shapes?
- Is hydrogen assisted cracking an issue when using the newer, more highly alloyed welding consumables?

This report addresses these issues in the following chapters:

Chapter 2: Toughness requirements, consumable performance, and prequalification of consumables used for moment frame construction for seismic applications

Chapter 3: Effect of intermixing of consumables

Chapter 4: Base metal and heat-affected zone considerations

Chapter 5: Effect of hydrogen on weld metal integrity and properties

Chapter 6: Inspection and acceptance criteria

Chapter 7: Effect of wind speed

Considering the long development history of steel welding, metallurgy, welding consumables, inspection, and fracture mechanics, it would be possible to write entire State of the Art reports on each of these topics alone. Where appropriate, the reader is referred to technical documents in the literature that review prior art. Effort in this report is made to provide detail of new technical information that is directly applicable to steel moment frame construction as developed in the FEMA/SAC program to reduce seismic hazards in steel moment-resisting frames.

2. TOUGHNESS REQUIREMENTS, PERFORMANCE, AND PREQUALIFICATION OF CONSUMABLES USED FOR MOMENT FRAME CONSTRUCTION DESIGNED FOR SEISMIC RESISTANCE

2.1 Introduction

A number of structural welding processes are applicable to the fabrication and erection of steel building structures. These include shielded metal arc welding (SMAW), gas-shielded flux cored arc welding (FCAW-G), self shielded flux cored arc welding (FCAW-S), Gas Metal Arc Welding (GMAW), and Submerged Arc Welding (SAW). Of these, the most commonly employed processes in building construction in the United States today are those employing flux cored arc welding, with FCAW-S used almost exclusively in field erection, and either FCAW-S or FCAW-G being employed in shop fabrication.

The factors affecting the mechanical properties of SMAW welding deposits have been the subject of numerous literature reviews published since the early 1940's. Reviews by Campbell (Sagan and Campbell, 1960), Masubuchi (Masubuchi et al., 1966), Abson (Abson and Pargeter, 1986), Grong (Grong and Matlock, 1986), Evans (Evans and Bailey, 1997), Svensson (Svensson, 1994), Widgery (Widgery, 1994), and Boniszewski (Boniszewski, 1992) provide extensive discussion of the factors controlling mild steel weld metal microstructures and properties. While the content of many of these reviews apply directly to both SMAW and FCAW-G (E70T-1 and E70T-5) weld metals, the chemical composition and nature of FCAW-S electrodes are substantially different and should be considered separately. Compared to the number of studies related to the mechanical properties in SMAW weld metals, relatively few studies have been conducted on the topic of FCAW-S electrodes.

The basic operation and properties of FCAW-S electrodes is reviewed by Boniszewski, Kotecki (Kotecki and Moll, 1972), Kaplan (Kaplan and Hill, 1976), and Killing (Killing, 1980). While SMAW electrodes rely on coating decomposition to provide protection of the molten weld metal during welding, and shielding gas is used during FCAW-G welding, most FCAW-S consumables utilize either aluminum or titanium to deoxidize the weld metal and tie up nitrogen in the molten weld pool. While titanium is used as the primary deoxidant in some single pass electrodes, aluminum is generally used in most multipass FCAW-S consumables. Aluminum concentrations of up to 1.8 wt. pct. are measured in some FCAW-S deposits. Titanium and aluminum are both strong ferrite stabilizers. In order to prevent stabilization of the high temperature δ -ferrite at low temperatures, aluminum is often balanced with an austenite stabilizing element such as carbon, manganese, or nickel.

Following a similar line of discussion presented by Boniszewski (Boniszewski, 1992), SMAW and FCAW-S electrodes can be divided into three toughness classes:

2.1.1 Class A: No Toughness Requirements

Similar to SMAW electrodes, a range of weld metal properties can be achieved in FCAW-S electrodes depending on the type of consumable specified. Depending on design requirements, weld metal with minimum notch toughness may or may not be required. In cases where notch tough weld metal is not specified, E6013, E7014, or E7024 SMAW electrodes are commonly used. Similarly, E70T-4, E70T-7, E70T-3, and E70T-10 FCAW-S electrodes are typically employed when notch toughness is not specified. These electrodes are typically capable of high deposition rates and have considerable operator appeal. The aluminum concentration in FCAW-S electrodes where notch tough weld metal is not expected will typically range between 1.5 and 1.8 wt. pct. In these electrodes, aluminum is typically balanced by the addition of up to 0.3 wt. pct. carbon. The resulting microstructures typically consist of coarse δ -ferrite (stable at room temperature) and pearlite.

2.1.2 Class B: Moderate Toughness Requirements

When notch toughness is required at temperatures above the -20°F to 0°F range, E7024-1, E7028, E7016, and E7018 SMAW electrodes are often specified. Corresponding FCAW-S electrodes include E70T-6 and E71T-8 type consumables classified to deposit weld metal with a minimum toughness of 20 ft-lbf. at -20°F . Relative to the Class A electrodes, higher toughness is achieved in E70T-6 and E71T-8 weld metal by reducing the aluminum (typically ~ 1 wt. pct. Al) and carbon concentrations while increasing the manganese and/or nickel concentrations. Most E70T-1 and E70T-5 electrodes would fall into this category also.

2.1.3 Class C: High Toughness at Low Temperatures

When high toughness is required at temperatures below -20°F , E7018-1 type SMAW electrodes and E61T8-K6/E71T8-K6 electrodes have been shown to provide acceptable performance. FCAW-S electrodes designed to deposit weld metal with high toughness at low temperatures typically have aluminum concentrations of less than 1 wt. pct., carbon concentrations of less than 0.1 wt. pct., manganese concentrations ranging from 1-1.8 wt. pct., and nickel concentrations up to and exceeding 1 wt. pct. Along with a modified chemical composition, welding procedures have been developed to ensure high toughness in the Class C FCAW-S consumables.

Specific welding procedures must also be utilized to maintain high toughness when using the Class C E61T8-K6/E71T8-K6 electrodes. Several key studies in the late 1970's and early 1980's discuss procedural variables required for high toughness in welds deposited by smaller diameter FCAW-S weld metals (Dorling, et al., 1976), (Dorling and Rogerson, 1977), (Keeler, 1981), (Pisarkski, et al., 1987), (Rogers and Lockhead, 1987), and (Grong, et al., 1988). While the individual documents should be consulted for specific details, the following procedures have been shown to provide high toughness:

- Welding procedures that maximize weld metal refinement such as deposition of narrow stringer beads. When welding in the 3G position, vertical down welds are required. AWS

D1.1 does not permit prequalified welding procedures to be used when welding vertical down. Such Welding Procedure Specifications (WPS) are required to be qualified by test.

- Deposition of shallow weld beads using “thin layer” techniques where wire, welding position, Wire Feed Speed (WFS), current, and voltage are fixed, and layer thickness is controlled by travel speed. Alternately, a wide shallow weave has been successfully employed. Depending on welding position, layer thickness of 2.5 - 3.8 mm have been specified to ensure high toughness.
- In order to ensure consistent quality when using FCAW-S electrodes for offshore applications, fabricators will set the WFS/voltage prior to welding and prohibit changes during fabrication. Additionally, the use of data acquisition and detailed visual inspection (based on weld bead width for various welding procedures) will often be specified to ensure proper travel speed is maintained.

Despite the higher deposition rates (relative to SMAW) and higher toughness afforded by the use of E61T8-K2/E71T8-K2 consumables, the use of Class C electrodes in moment frame construction has been limited for the following reasons:

- The need for the very high weld metal toughness produced by these consumables has not been justified.
- The lower deposition rates of these electrodes increases welding costs.
- Welders with appropriate skill and training are not available.
- The cost of QA/QC when using specialized welding procedures would add to the fabrication costs.
- There would be higher consumable costs (relative to other FCAW-S consumables).
- The benefits of using higher toughness welding consumables is limited when joining hot-rolled structural shapes.

The need for relatively economical alternatives that could produce welded joints of sufficient toughness for high-demand seismic applications in buildings has led many contractors to select and use Class B type consumables such as the E70T-6 and E71T-8 consumables. Following the Northridge earthquake, the NR311Ni (E70TG-K2) consumable has also been widely used. Published literature related to factors that affect the properties of higher deposition rate FCAW-S consumables with a moderate degree of toughness is currently in short supply. Due to the larger bead sizes deposited when using these consumables and differences in chemical composition (mainly higher aluminum and lower Mn/Ni concentrations), lessons learned when developing high toughness welding procedures for use with the Class C consumables are not generally applicable. As part of the FEMA/SAC program to reduce seismic hazards in steel frames, the

suitability of the Class B type consumables for seismic applications of moment frame construction have been evaluated in full-scale tests and T-stub tests.

The purpose of this chapter is to consider the performance of consumables used in the fabrication of moment connections using various connection designs. Specifically, establishment of minimum toughness requirements, minimum strength requirements, and evaluation of weld metal robustness are considered in this section. Based on the strength and toughness conditions, recommendations are provided regarding suitability of AWS classification requirements and whether or not tight control of welding procedures is required to maintain notch toughness and minimum strength levels.

2.2 AWS Classification Requirements

Specification of electrodes capable of depositing notch-tough weld metal is now required for building construction in seismic regions. FEMA 267 (SAC, 1995) specifies the use of electrodes capable of depositing weld metal meeting a minimum CVN impact toughness of 20 ft-lbf. at 0°F when welds are deposited according to AWS classification procedures. Current AISC specifications require the use of consumables meeting a minimum CVN impact toughness of 20 ft-lbf. at -20°F when welds are deposited according to AWS classification procedures. The E70TG-K2 electrodes and the E70T-6 electrodes used to deposit the beam to column welds in the SAC investigations are classified to the AWS A5.20 and A5.29 electrode specifications. Once a year, consumable manufacturers produce classification test welds following welding and testing procedures outlined in the respective specifications and AWS B 4.0 (AWS, 1998a). Consumables classified to the AWS E70T-6 (AWS, 1995) and E70TG-K2 (AWS, 1998b) classifications are required to deposit weld metal under classification test conditions, with a minimum CVN impact energy of 20 ft-lbf. at -20°F. Other electrodes such as E71T-8, E7018 (AWS, 1991), and E70T-1 electrodes are also used. Of these, E70T-1 electrodes are now commonly used in shop fabrication while the other electrodes are used for field fabrication. The toughness requirements of several types of electrodes applicable to fabrication of moment connections are summarized in Table 2-1.

2.3 Full-Scale Testing

2.3.1 Description of Full-Scale Tests

Development of minimum mechanical property requirements and collection of data for modeling of connection behavior requires an understanding of the mechanical properties of the material used in full-scale testing. As part of the SAC connection testing program, supplemental mechanical property tests were carried out to measure the weld metal mechanical properties in the beam-to-column connections subject to testing at the University of Michigan (Kwasiewski, Goel, and Stodjdonovic, 1999), Lehigh University (Ricles, 2000), the University of Texas at Austin (Venti and Engelhardt, 2000), and Texas A&M (Engelhardt, Fry, and Jones, 2000).

Table 2-1 Minimum Mechanical Property Requirements for Selected Consumables

Electrode	Toughness (ft-lbf)	Test Temperature (F)	Yield Strength (ksi)	Tensile Strength (ksi)	Elong. (%)
SMAW ^{a)}					
E7018, E7015, E7027, E7048, E7016	20	-20	58	70	22
E7028	20	0	58	70	22
E7014, E7024	N/A	N/A	58	70	17
E7018-1	20	-50	58	70	22
E7018-C1L	20	-100	58	70	22
E7018-C2L	20	-150	58	70	22
FCAW-G ^{b)}					
E7XT-1	20	0	58	70	22
E7XT-5	20	-20	58	70	22
E7XT-12	20	-20	58	70	22
FCAW-S					
E7XT-4	N/A	N/A	58	70	22
E7XT-6 ^{b)}	20	-20	58	70	22
E7XT-7	N/A	N/A	58	70	22
E7XT-8 ^{b)}	20	-20	58	70	22
E70TG-K2 ^{c)}	20	-20	58	70	22

Notes:

- a) As-welded condition for SMAW
- b) Can also be specified with optional "J" designator providing 20 ft-lbf. at -40°F
- c) Properties as agreed upon by supplier and purchaser

During fabrication of test specimens for full-scale testing, additional moment connections were fabricated under identical conditions using the same welding procedures. Following fabrication of the full-scale mock-ups, mechanical test specimens were extracted from the weld and column material. The primary focus of this testing was the evaluation of weld metal tensile properties, weldment tensile properties, weld metal CVN impact properties, and limited evaluation of weld metal crack tip opening dimension (CTOD) properties (Johnson, et al., 2000c). Mechanical test specimens were extracted from welds deposited in the following full-scale connections:

University of Texas at Austin/Texas A&M

- Post-Northridge RBS with W14x298 column and W36 x 150 beam welded with E70T-6 (NR305)

University of Michigan

- Pre-Northridge design with W24x68 beam and W14/120 (A572 Gr. 50). Column welded with E70T-4. (Specimen 1.1)
- Post-Northridge design with W24x99 beam and W14x176 column (A572 Gr. 50) welded with E70TG-K2 (NR 311Ni). (Specimen 5.1)
- Post-Northridge design with W36x150 beam and W14x257 column welded with E70TG-K2 (NR311Ni). (Specimen 7.1)

Lehigh University

- Post-Northridge W14x311 column and W36 x150 column welded with E70TG-K2 (NR311Ni)

2.3.2 CVN Impact Toughness of Full-Scale Welds

For this section, see Johnson, M., Mohr, W., and Barsom, J., (2000c). All the column and beam materials described above were manufactured to ASTM A572 Gr. 50 specification. All welding was conducted using welding parameters specified by the consumable manufacturer with a minimum preheat of 150°F and a maximum interpass temperature of 550°F. CVN specimens from the Lehigh University and UTA/UTAM full-scale test specimens were extracted from the near-surface location, mid-thickness location, and root locations. The CVN notch was positioned in the weld metal at a location 2.5 mm from the fusion line. CVN specimens were extracted from the three UM weldments at the mid-thickness location. Three full thickness Bx2B CTOD specimens were extracted from weldments produced in each investigation. CTOD specimens were evaluated at room temperature.

Although it was generally assumed that the consumables used to deposit the weld metal in the full-scale connections were capable of meeting minimum respective AWS A5.X classification toughness requirements, AWS A5 test welds were not produced at the time of full-scale connection fabrication. The A5 classification test requirements specify CVN testing be conducted at a test temperature of -20°F, which is much lower than the ambient temperature when the full-scale tests were conducted. Since the full-scale test welds were conducted at room temperature, the CVN toughness measured at room temperature may be more relevant to full-scale test performance than the toughness measured at lower service temperatures. In addition to developing data that can be used for modeling purposes, the mechanical property data measured from the full-scale test conditions can also be used to infer mechanical property requirements that can be specified in classification test welds.

The CVN toughness of welds extracted from the full-scale connection mock-ups is shown in Figures 2-1 to 2-3. Table 2-2 also summarizes the toughness measured in E70T-6, E70TG-K2, E7018, and E71T-8 weld metals deposited in various sub-tasks during the SAC program. Figure 2-1 shows full transition curves for the E70TG-K2 weld metal deposited in the University of Michigan full-scale test welds. Toughness of welds deposited for SAC Sub-Task 5.2.8 is also shown in Figure 2-1. Room temperature toughness in the E70TG-K2 welds ranged from 60 to 80 ft-lbf. The temperature at which 20 ft-lbf. (V_{20}) was absorbed also varied in the two E70TG-K2 welds from -20°F in Specimen 7.1 to $+12^{\circ}\text{F}$ in Specimen 5.1. The 50% FATT (50 percent fracture appearance transition temperature) i.e., the temperature at which half of the fracture surface is ductile and half of the fracture surface is brittle, was 68 and 63°F respectively.

Figure 2-2 shows the toughness measured in welds deposited in the Lehigh University full-scale tests using the E70TG-K2 consumable. The highest toughness was measured in the root location with lower toughness measured in the near-surface and mid-thickness locations. When compared to the toughness measured in the University of Michigan welds extracted from the mid-thickness location, slightly lower toughness was measured in the Lehigh University connection welds. The room temperature CVN toughness in the Lehigh weldments ranged from 32 to 54 ft-lbf., and the temperature at which 20 ft-lbf. was absorbed ranged from -8°F to $+20^{\circ}\text{F}$. The 50% FATT for the root, mid-thickness, and near-surface locations was 62, 83, and 80°F respectively. The reason for the lower toughness in the Lehigh near surface and mid-thickness locations is unclear. The higher toughness in the root location may be attributed to grain refinement and tempering of the root region during removal of the backing bar and subsequent weld repair.

The toughness of the E70T-6 welds deposited in the full-scale test specimens evaluated at UTA/UTAM is shown in Figure 2-3. Compared to the E70TG-K2 welds, the E70T-6 weldments have slightly lower upper shelf energies and lower transition temperatures. Although refinement of the root region may occur during removal of the backing bar and subsequent deposition of repair welds, the effect of CVN specimen location in the E70T-6 welds was not consistent with that measured in the Lehigh connections. In the case of the E70T-6 welds, V_{20} temperatures (the temperature at which 20 ft-lbf. was absorbed) of -8 , -28 , and -30°F were measured in the root, mid-thickness, and near-surface locations. Although the effect of backing bar removal/repair procedures on the mechanical properties of connection welds may provide improvement in root toughness in some weld metals, this topic was beyond the scope of the SAC investigation. The CVN impact energy measured at room temperature in the root, mid-thickness, and near-surface locations was 51, 57, and 53 ft-lbf. respectively. The 50% FATT at the root, mid-thickness, and surface locations was 20, 0, and 5°F . Considering the scatter inherent in CVN testing, the CVN behavior at the root, mid-thickness, and near surface locations was similar.

Table 2-2 Summary of CVN Properties Measured in Welds Produced as Part of the SAC Program

Weld	Electrode	Weld	Heat Input (kJ/in.)	Location	20 ft-lbf Temp. (°F)	CVN _E at 68°F ft-lbf	50% FATT °F	CVN _E at 0 °F ft-lbf	CVN _E at -20°F ft-lbf
1	E70T-6	EWI A	33	Mid-Thick	25	31	44	17	10
2	E70T-6	EWI C	53	Mid-Thick	-4	36	20	21	17
3	E70T-6	EWI E	70	Mid-Thick	13	47	29	14	11
4	E70T-6	UTA (1)	45	Mid-Thick	-20	45	15	25	20
5	E70T-6	UTA(2)-R	45	Root	-8	51	20	23	16
6	E70T-6	UTA (2)-M	45	Mid-Thick	-28	57	0	33	24
7	E70T-6	UTA (2)-N	45	Near Surf.	-30	53	5	32	24
8	E70T-6	EWI5.2.8	47	Mid-Thick	-43	55	0	34	28
9	E70T-6	EWI AWS	47	Mid-Thick	N/A	44	N/A	26	24
10	E70T-6	SAC Low HI	30	Mid-Thick	N/A	43	N/A	27	23
11	E70T-6	SAC High HI	70	Mid-Thick	N/A	58	N/A	28	23
12	E70T-6	LEC Low HI	25	Mid-Thick	N/A	40	N/A	25	23
13	E70T-6	LEC Med HI	42	Mid-Thick	N/A	N/A	N/A	27	21
14	E70T-6	LEC High HI	82	Mid-Thick	N/A	N/A	N/A	30	27
15	E7018	EWI A	17	Mid-Thick	-100	186	-16	73	62
16	E7018	EWI C	47	Mid-Thick	-103	136	-11	105	89
17	E7018	EWI E	74	Mid-Thick	-106	106	-14	128	104
18	E71T-8	EWI A	13	Mid-Thick	-63	85	-29	56	41
19	E71T-8	EWI B	29	Mid-Thick	-77	75	-8	47	39
20	E71T-8	EWI C	29	Mid-Thick	-90	78	0	49	42
21	E71T-8	EWI D	29	Mid-Thick	-63	64	8	39	32
22	E71T-8	EWI E	43	Mid-Thick	-98	91	0	57	48
23	E70TG-K2	EWI B	43	Mid-Thick	-42	117	35	54	34
24	E70TG-K2	EWI C	43	Mid-Thick	-27	61	75	30	22
25	E70TG-K2	EWI D	43	Mid-Thick	-20	59	67	26	20
25	E70TG-K2	EWI E	70	Mid-Thick	-27	80	64	26	23
27	E70TG-K2	UM 5.1	40	Mid-Thick	-20	84	63	32	20
28	E70TG-K2	UM 7.1	40	Mid-Thick	12	60	68	14	8
29	E70TG-K2	LU-R	43	Root	-8	54	62	24	15
30	E70TG-K2	LU-M	43	Mid-Thick	20	32	83	16	13
31	E70TG-K2	LU-NS	43	Near Surf.	20	36	80	15	11
32	E70TG-K2	EWI5.2.8	39	Mid-Thick	23	78	70	12	9
33	E70TG-K2	EWI AWS	39	Mid-Thick	N/A	52	N/A	21	18
34	E70TG-K2	SAC Low HI	30	Mid-Thick	N/A		N/A		
35	E70TG-K2	SAC High HI	70	Mid-Thick	N/A	71	N/A	19	11
36	E70TG-K2	LEC Med HI	58	Mid-Thick	N/A	N/A	N/A	60	40
37	E70TG-K2	LEC High HI	74	Mid-Thick	N/A	N/A	N/A	37	20
39	E71T-8	LEC Low HI	25	Mid-Thick	N/A	N/A	N/A	45	60
40	E71T-8	LEC Med HI	42	Mid-Thick	N/A	N/A	N/A	73	64
41	E71T-8	LEC Med HI	40	Mid-Thick	-100	110	-18	63	58
42	E71T-8	LEC High	56	Mid-Thick	N/A	N/A	N/A	70	65
43	E71T-8	LEC V-Up	61	Mid-Thick	-80	70	8	45	38

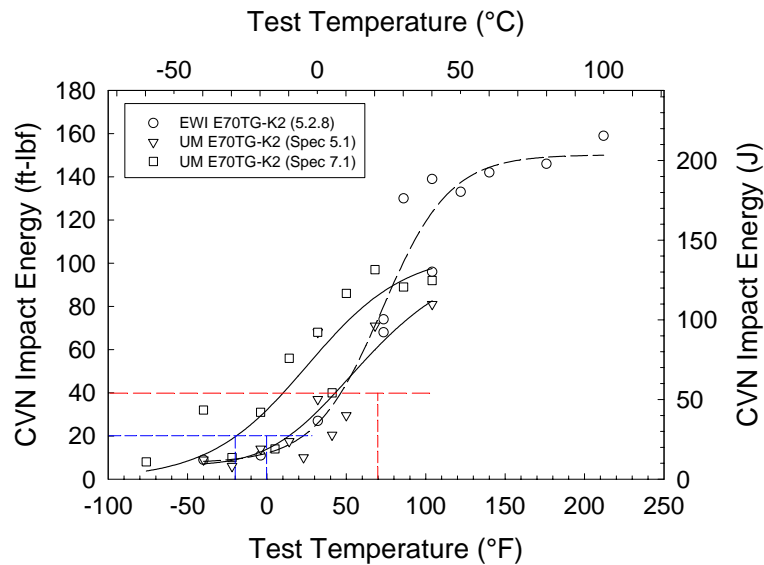


Figure 2-1 CVN Impact Toughness Measured in E70TG-K2 Weld Metal Deposited in the UM Full-Scale Beam-to-Column Welds and in Follow-On Testing at EWI

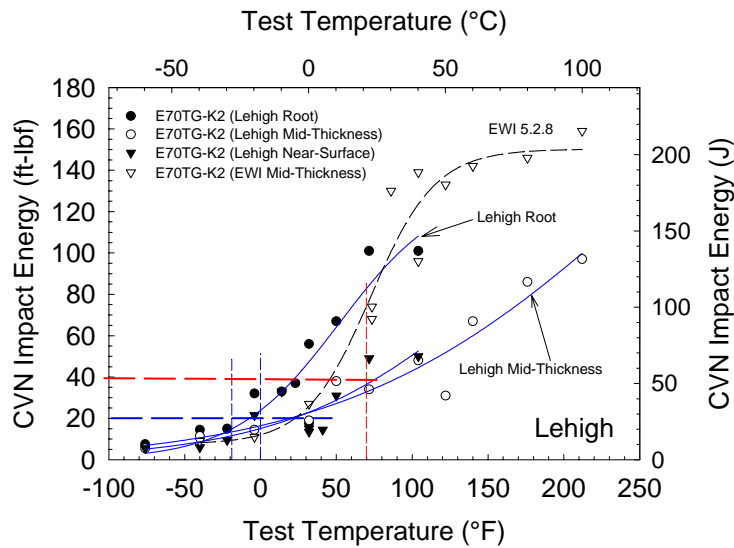


Figure 2-2 CVN Impact Toughness Measured in E70TG-K2 Weld Metal Deposited in the Lehigh University Full-Scale Beam-to-Column Welds and in Welds Deposited at EWI for Follow-On Testing

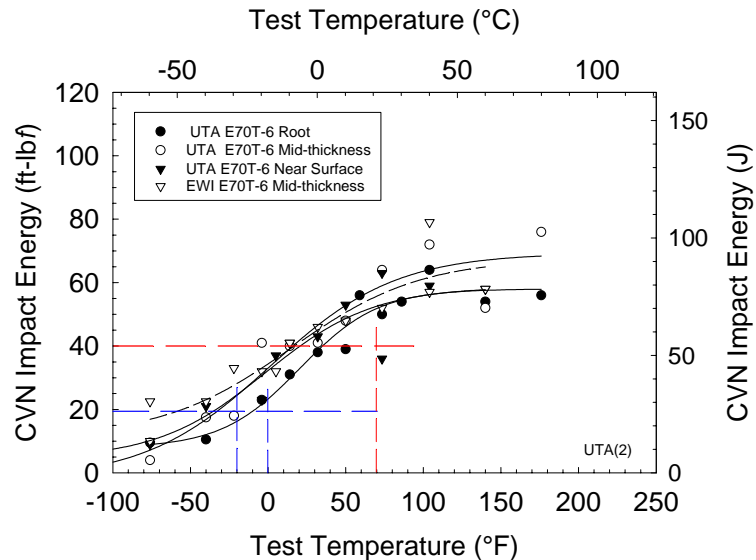


Figure 2-3 CVN Impact Toughness Measured in Full-Scale E70T-6 Welds Deposited in Full-Scale Connections Evaluated at UTA/UTAM and in Welds Deposited at EWI

The E70T-6 and E70TG-K2 consumables have been successfully used in over 100 full-scale connection tests as part of the SAC program. Although full plastic rotation may not have been developed in some of the connections evaluated in the SAC program, brittle fracture of the weld metal was not observed. From the standpoint of avoiding brittle fracture in the weld metal during full-scale connection tests, the E70T-6 and E70TG-K2 consumables have demonstrated acceptable behavior when tested at room temperature.

Based on the performance of the full-scale test connections evaluated at LU, UM, and UTA/UTAM and the success of these consumables in the SAC connection tests, it is evident that welds deposited using these two consumables should provide acceptable performance relative to the risk of brittle weld metal fracture provided the following criteria are met:

- connections are designed in accordance with the general procedures outlined in FEMA 350,
- welding procedures used in the field are similar to those used in the investigations,
- workmanship meets minimum requirements specified in AWS D1.1 and recommended herein,
- connection service temperature is near room temperature, and
- demand on connections evaluated in the SAC investigations are representative of conditions expected in an actual earthquake.

Although acceptable weld metal performance (no brittle weld fractures) has been achieved in connections when using the E70T-6 and E70TG-K2 consumables, a lower bound toughness requirement has yet to be identified using post-Northridge connection designs. Establishment of the lower bound toughness is important for determining the critical permitted flaw sizes and specifying permissible service temperatures. The CVN toughness characteristics of welds deposited using the E70T-6 and E70TG-K2 consumables are different. Perhaps one of the most important differences is the transition temperature measured in each type of weld. At this point, the transition behavior has been characterized using only CVN specimens that are rapidly loaded. Decreasing strain rate should effectively reduce the transition temperature. The transition behavior in these two welds will be discussed in more detail later.

From the point of specifying minimum toughness requirements, it is difficult to determine whether to consider the room temperature toughness, lower temperature toughness (-20°F or 0°F) or both. Depending on the application, constraint, and service conditions, a minimum CVN toughness of 20 ft-lbf. is typically specified at the service temperature or well below the service temperature. Based on the full-scale testing completed in the FEMA/SAC program, the following minimum toughness criteria can now be proposed for connections in service at room temperature:

- CVN toughness higher than 20 ft-lbf. at 0°F
- CVN toughness higher than 40 ft-lbf. at 70°F

The above criteria are based on the full-scale testing conducted in the FEMA/SAC investigations and the fact that failure of the connections did not occur in the weld metal in a brittle manner. Without additional full-scale testing, it is difficult to identify a minimum toughness that will provide acceptable service at lower temperatures.

It is clear from the testing above that it is inappropriate to rely solely upon the AWS Consumable Classification Requirements for consumable selection. Specification of only low temperature toughness may preclude use of filler metals depositing weld metal with room temperature behavior similar to that of the consumables used in this study. Specification of toughness only at room temperature may permit the use of weld metal that meets room temperature toughness requirements with a sharp ductile to brittle transition behavior. Additionally, electrodes produced to the same AWS classification by a given manufacturer or by different manufacturers may have entirely different operating characteristics, properties, and operating ranges that should be considered.

Throughout this document, reference is made to both the AWS classification and Lincoln Electric trade names for weld filler metals. Technical writing protocol typically encourages the use of generic AWS designation (i.e., E70T-6, E71T-8, etc.) and discourages the use of trade names (i.e., Innershield NR305, Innershield NR232). Specific reference to trade names in this publication is intentional since other consumables and products were not explicitly evaluated. Electrodes classified to the same AWS specification can often yield substantially different mechanical properties. It is assumed that other electrodes capable of meeting the

minimum specified mechanical properties under the proposed connection prequalification welding conditions (to be discussed later) will be suitable for use.

2.3.3 CTOD Toughness and Low-Cycle Behavior of Full-Scale Tests

A more fundamental approach was taken to justify the toughness values proposed above. Insufficient data was available from the full-scale connection tests to allow extrapolation of the room temperature test results to lower test temperatures. Additional test welds were produced as part of the FEMA/SAC Task 5.2.8 investigation (Johnson et al., 2000c) so that CTOD and CVN behavior could be investigated further.

2.3.3.1 Comparison of Full-Scale Test Welds with Laboratory Test Welds

Figures 2-4 and 2-5 show the CVN/CTOD relationships measured in supplemental testing conducted as part of FEMA/SAC Investigation 5.2.8. In this study, single-bevel welds were deposited in A572 Gr. 50 plate using E70TG-K2 and E70T-6 electrodes and welding procedures similar to those used in the full-scale connection tests. Figures 2-1 through 2-3 show that the CVN toughness measured in the welds deposited in the Task 5.2.8 study is consistent with the CVN toughness of the welds deposited in the full-scale connection tests. Direct comparison of the room temperature CTOD properties measured in the full-scale connections with those measured in the Task 5.2.8 welds also suggest that the weld metal deposited in the Task 5.2.8 study is representative of the toughness measured in the full-scale tests.

Consistent with the CVN data, a steep transition in CTOD was measured in the E70TG-K2 weld metals as shown in Figure 2-4. The CTOD data plotted in Figure 2-4 also suggests that the minimum CTOD toughness above which low-cycle fatigue is predominant (CTOD of 0.0016-in. or 0.0406 mm) may not be achieved in E70TG-K2 weld metals when the service temperature drops below 55°F.

Higher CTOD toughness was measured in the E70T-6 weld metals, Figure 2-5. The minimum toughness threshold of 0.0016-in. was exceeded even at very low temperatures. Consideration of the CTOD test data suggests that initial assumptions regarding the relative toughness of the E70TG-K2 and E70T-6 should be reconsidered. Although the upper shelf behavior of the E70TG-K2 is higher, the E70T-6 consumables may provide better performance when components are in service at temperatures below room temperature. Welds deposited using both consumables may have high enough fracture toughness such that fracture toughness of the weld metal is not a consideration in the connection performance.

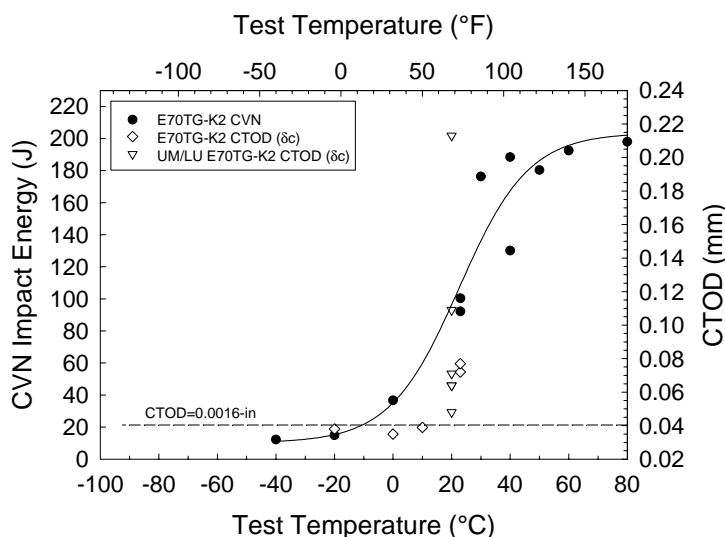


Figure 2-4 Comparison of CVN Impact Energy and CTOD Values for E70TG-K2 Weld Metal Deposited in the EWI Follow-On Testing (SAC Sub-Task 5.2.8). Data from the UM and Lehigh Tests is also Included.

2.3.3.2 Development of Fracture Toughness Requirements

The full-scale specimens evaluated at UM, UTA/UTAM, and LU were subjected to simulated seismic loads developed by the FEMA/SAC steel program. These loads induce low-cycle plastic deformation in the weldment joining the beam flanges to the column. The following discussion was also presented in greater detail at the fourth US/Japan Workshop on Steel Fracture Issues (Barsom, 2000).

Failure analysis of unreinforced welded moment frame connections subjected to simulated seismic loads during testing at the University of Michigan and Lehigh University showed that fracture was caused by the initiation and propagation of fatigue cracks, as shown in Figure 2-6 (Barsom, 1999). The fatigue cracks initiated at the web-to-flange intersection at the weld access hole, the valleys of the flame cut weld access hole surface, the weld toe, and weld imperfections. The applied cyclic loads increased the size of the fatigue crack until it reached a critical dimension where unstable crack extension severed the beam flange (see Figure 2-7 and Barsom, 1999). The fatigue cracks in all the tested specimens exhibited stable ductile tearing under the applied cyclic loads. Subsequent unstable crack extension was ductile in some specimens and brittle in others. Regardless of the mode of unstable crack extension, the critical crack size at fracture was large and the remaining fatigue life under the simulated seismic loads was negligible. Examination of fatigue cracks that initiated from weld imperfections indicated that the critical crack size was either a 0.5-in. deep part-through crack or about a 1-1/2-in. through-thickness crack (Johnson, et al., 2000c; Barsom and Rolfe, 1987). These crack sizes in combination with the applied stresses were used to estimate the critical stress intensity factor K_{Ic} (i.e., fracture toughness) of the E70TG-K2 weld metal used to fabricate the weldments.

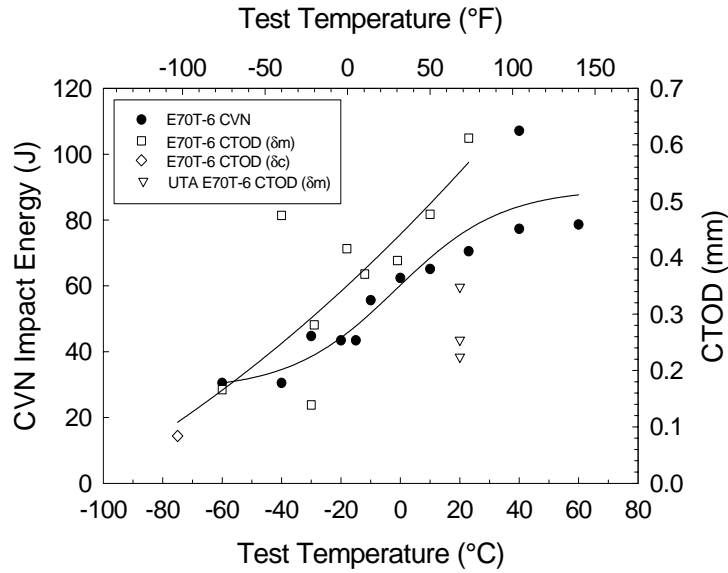


Figure 2-5 CVN Impact Energy and CTOD Data Measured in E70T-6 Weld Metal Deposited as Part of SAC Sub-Task 5.2.8. Data from the UTA Full-Scale Tests is also Included.

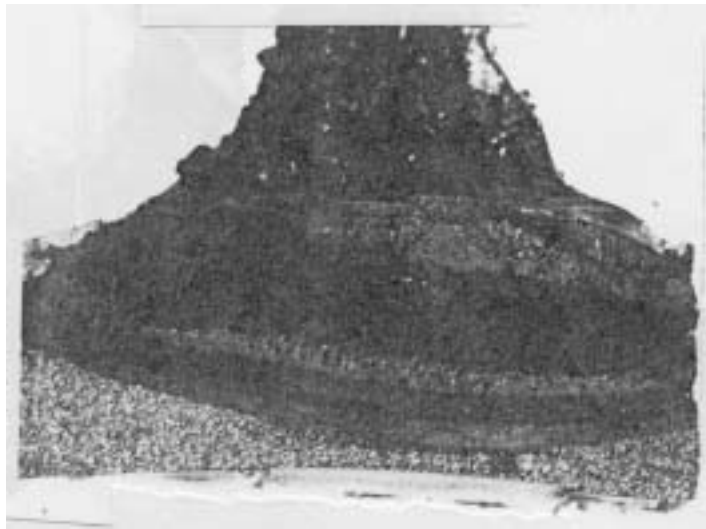


Figure 2-6 Initiation and Propagation of Fatigue Cracks in the University of Michigan Beam-to-Column Test Welds



Figure 2-7 Stable Crack Growth Preceded Unstable Crack Growth

The yield strength and tensile strength of E70TG-K2 weld metal were 76 and 90 ksi, respectively. Because the moment frame weldments experienced plastic deformation under the simulated seismic loads the flow stress, $\sigma_{flow} = \frac{\sigma_{yield} + \sigma_{Tensile}}{2}$ of 83 ksi was used to calculate the critical stress intensity factor, K_C , from the relationships (Barsom and Rolfe, 1987):

$$K_C = 1.12\sigma_{flow}\sqrt{\pi a_c} \quad (2-1)$$

for an edge crack (i.e., part-through crack of infinite length), with $a_c=0.5$ in., and

$$K_C = \sigma_{flow}\sqrt{\pi a_c} \quad (2-2)$$

for a through thickness crack with $2a_c=1.5$ in. Equations 2-1 and 2-2 above estimate the K_C values for E70TG-K2 weld metal to be 117 and 127 ksi \sqrt{in} (see Table 2-3).

The CTOD values measured for E70TG-K2 weld metal are presented in Table 2-3 and Table 2-4. Additionally, CTOD values measured in the E70T-6 weld metal are given in Table 2-3 and Table 2-5. Critical stress intensity factors, K_C , were calculated from these CTOD values by using the relationship:

$$K_C = \sqrt{1.7\sigma_{flow}E\delta} \quad (2-3)$$

Table 2-3 CTOD and Calculated K_c Values from Full-Scale Specimens Fabricated at the University of Michigan, Lehigh University, and the University of Texas at Austin

Electrode	Test Temperature (°F)	CTOD (mm)	CTOD (in.)	Mode	K_c (CTOD) Nmm ^{-3/2}	K_c (CTOD) ksi($\sqrt{\text{in}}$)
E70T-6	UTA (70)	0.224	0.0088	m	6552	190
E70T-6	UTA(70)	0.348	0.0137	m	8172	237
E70T-6	UTA(70)	0.254	0.0100	m	6966	202
E70TG-K2	LU(70)	0.064	0.0025	c	3483	101
E70TG-K2	LU(70)	0.064	0.0025	c	3483	101
E70TG-K2	LU(70)	0.071	0.0028	c	3690	107
E70TG-K2	UM(70)	0.109	0.0043	u	4586	133
E70TG-K2	UM(70)	0.213	0.0084	c	6379	185
E70TG-K2	UM(70)	0.048	0.0019	c	3034	88

where E is Young's modulus in psi, and δ is the CTOD in inches (Barsom and Rolfe, 1987). As shown in Figure 2-8, the measured CTOD values correspond to calculated K_c values between 88 and 185 ksi $\sqrt{\text{in}}$ and are consistent with the 117 and 127 ksi $\sqrt{\text{in}}$ values calculated by using the observed critical crack sizes and the flow stress.

The minimum acceptable fracture toughness, K_c , value for weld metal in unreinforced moment frame connections was derived from the fatigue crack growth behavior in metals (Barsom and Rolfe, 1987). Fatigue cracks subjected to low stress-intensity factor fluctuations, ΔK , extend by a striation forming mechanism. As ΔK increases, it approaches a fatigue critical value above which the fatigue crack propagation rate increases significantly. This acceleration in growth rate is caused by superposition of a brittle or a ductile subcritical crack extension onto the striations. To ensure a ductile subcritical crack extension, the fracture toughness of the metal should be larger than about 0.0016-in. (0.0406 mm) CTOD (Figure 2-8). Consequently, the critical fracture toughness, K_c , value for the weld metal should be larger than 81 ksi $\sqrt{\text{in}}$, Equation 2-1.

**Table 2-4 CTOD and Calculated K_c Values from E70TG-K2 Weld Metal Tested in SAC
Sub-Task 5.2.8**

Electrode	Test Temperature (F)	CTOD mm	CTOD (in.)	Mode	K _c (CTOD) Nmm ^{-3/2}	K _c (CTOD) ksi(\sqrt{in})
E70TG-K2*	100	0.081	0.0032	c	3931	114
E70TG-K2	73	0.071	0.0028	c	3690	107
E70TG-K2	73	0.076	0.0030	c	3828	111
E70TG-K2*	73	0.056	0.0022	c	3276	95
E70TG-K2	50	0.038	0.0015	c	2690	78
E70TG-K2*	50	0.086	0.0034	c	4069	118
E70TG-K2	32	0.036	0.0014	c	2621	76
E70TG-K2*	-1	0.033	0.0013	c	2517	73
E70TG-K2	-4	0.038	0.0015	c	2690	78

* indicates intentional delay in testing of specimen for a period of 30 to 60 days

2.3.3.3 Derivation of Equivalent Charpy V-Notch (CVN) Impact Toughness

The discussion in the preceding section indicates that the fracture toughness, K_c , of E70TG-K2 weld metal from full-scale test specimens and from CTOD tests of weldments ranged from 88 to 185 ksi \sqrt{in} (Figure 2-9). Likewise, the fracture toughness of the E70T-6 weld metal extracted from the full-scale specimens ranged from 190 to 237 ksi \sqrt{in} (Figure 2-10). Also, ductile tearing preceded unstable crack extension in all the tested specimens. These observations indicate that acceleration in the rate of fatigue crack growth expected at 81 ksi \sqrt{in} should be by ductile tear. Therefore, a minimum K_c value of 90 ksi \sqrt{in} was used to derive an equivalent minimum impact CVN foot bound value that can be used as a screening test for weld metal. A correlation between CTOD data and impact CVN toughness does not exist. Therefore, a procedure was developed based on the general behavior of CTOD test results as a function of temperature (Barsom and Rolfe, 1987) and by evaluating existing K_c -CVN correlations.

**Table 2-5 CTOD and Calculated K_c from E70T-6 Weld Metal Tested in
SAC Sub-Task 5.2.8**

Electrode	Test Temperature (F)	CTOD (mm)	CTOD (in.)	Mode	K _c (CTOD) Nmm ^{-3/2}	K _c (CTOD) ksi(√in)
E70T-6	73	0.612	0.0241	m	10828	314
E70T-6	50	0.478	0.0188	m	9552	277
E70T-6	30	0.394	0.0155	m	8690	252
E70T-6	10	0.371	0.0146	m	8414	244
E70T-6	0	0.417	0.0164	m	8931	259
E70T-6	-20	0.282	0.0111	u	7345	213
E70T-6	-22	0.140	0.0055	m	5172	150
E70T-6	-40	0.475	0.0187	m*	9552	277
E70T-6	-76	0.165	0.0065	m	5621	163
E70T-6	-103	0.084	0.0033	c	4000	116

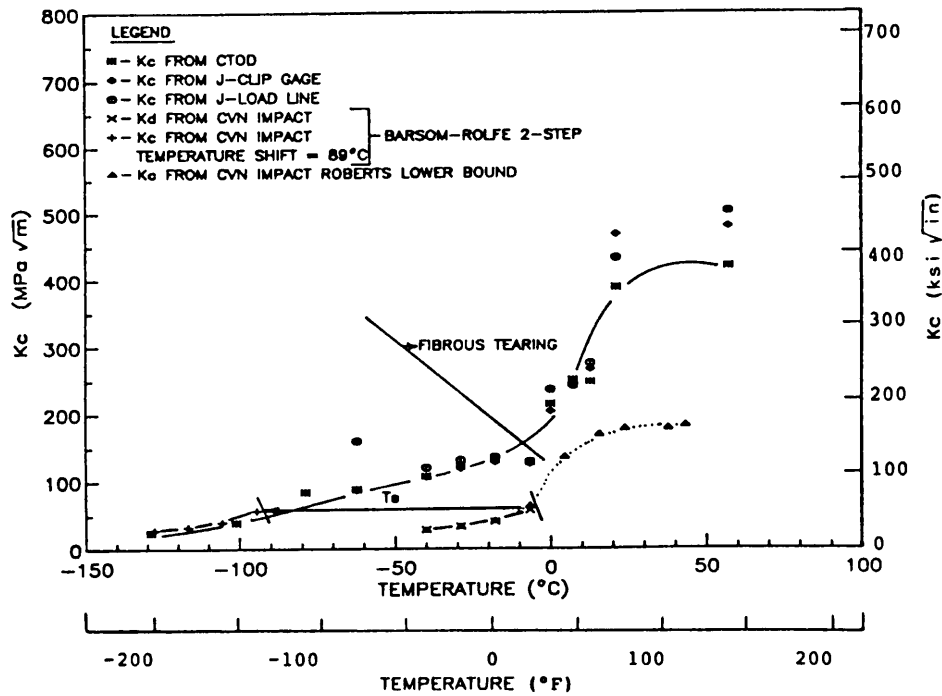


Figure 2-8 Kc-CTOD-J Relationships for an A131 Steel

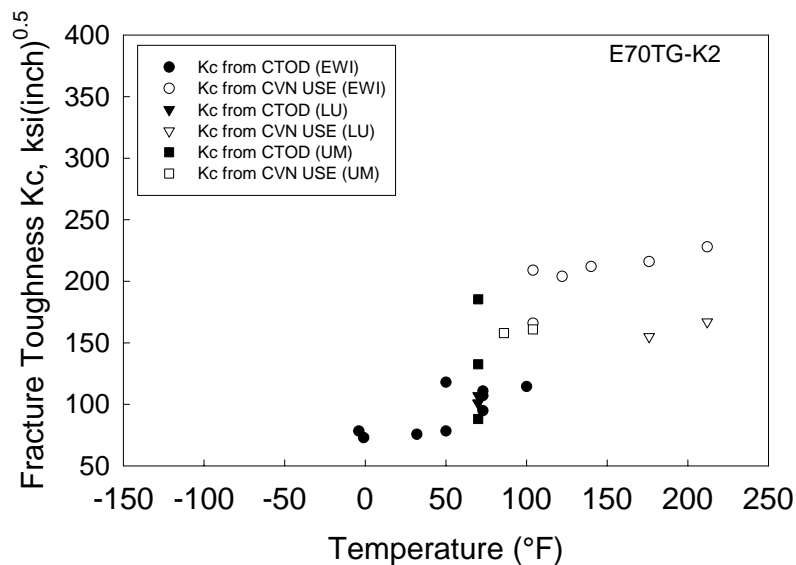


Figure 2-9 Kc Values Calculated from CTOD and CVN Upper Shelf Energy Measured in E70TG-K2 Weld Metal

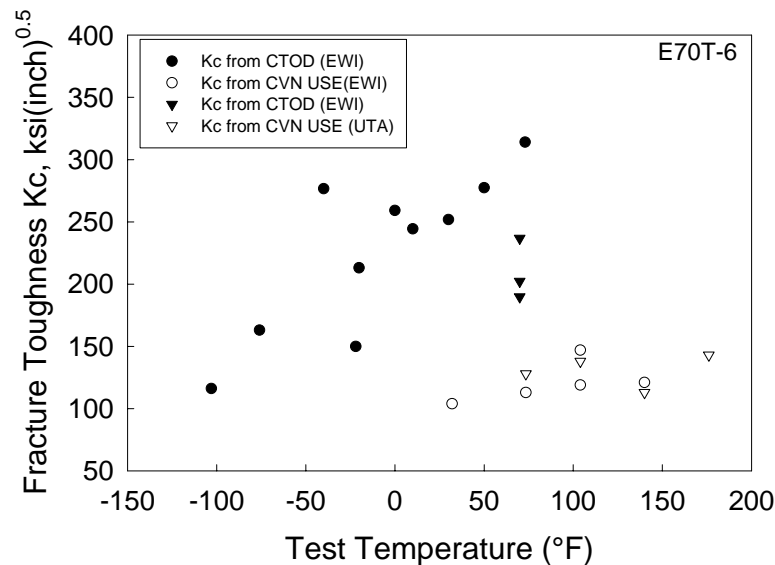


Figure 2-10 K_c Values Calculated from CTOD and CVN Upper Shelf Energy Measured in E70T-6 Weld Metal

CTOD values for structural steels increase as the test temperature increases. Initially, the increase is gradual, then increases rapidly as the test temperature zone where stable ductile tearing prior to unstable crack extension becomes visible on the fracture surface of the CTOD specimens. Because stable ductile tearing prior to fracture occurred in the specimen that had a K_c of about $90 \text{ ksi} \sqrt{\text{in}}$, this value was judged to represent the fracture toughness level above which rapid crack extension should be expected.

Having defined a K_c of $90 \text{ ksi} \sqrt{\text{in}}$ to be the desired minimum fracture toughness, an equivalent CVN impact energy absorption value had to be established. An evaluation of existing correlations suggested that the Roberts-Newton correlation may be helpful. Extreme care should be exercised in the use of this correlation. It is used here only because the K_c values calculated from the upper shelf impact CVN energy absorption appear to approximate the K_c value above which stable ductile (fibrous) tearing precedes unstable crack extension (Figure 2-4 and Barsom and Rolfe, 1999). The Roberts-Newton correlation is (Barsom and Rolfe, 1999):

$$K_c = 9.35(\text{CVN}, \text{ft} - \text{lbf})^{0.63} \quad (2-4)$$

Thus, a K_c equal to $90 \text{ ksi} \sqrt{\text{in}}$ would be equivalent to an impact CVN upper-shelf value of about 37 ft-lb. A conservative value of 40 ft-lb was selected.

2.3.3.4 Validation of Methodology

The methodology used to derive a minimum impact CVN energy absorption for beam-to-column weld metal subjected to simulated seismic loads was based on several assumptions and limited data. Consequently, weldments were fabricated with the E70T-6 and E70TG-K2 filler

metals. Additional CTOD and CVN tests were conducted to determine the validity of the assumptions. Figures 2-9 and 2-10 show the CTOD and CVN toughness test results measured in E70TG-K2 and E70T-6 weld metal in terms of equivalent K_c values calculated by using Equations 2-3 and 2-4. Although the chemical composition and strength levels of weld metal deposited using both weld metals is similar, the CTOD/CVN relationships in the respective weld metals was quite different. In general, acceptable correlation was observed in the E70T-6 weld metal while the E70TG-K2 weld metal will require further study.

Some concern was expressed that the lower K_c values measured in the E70TG-K2 weld metals might have been due to hydrogen effects. This is most likely not the case for the following reasons:

- The chemical composition and weld metal diffusible hydrogen concentrations of the two weld metals are approximately similar, and thus the diffusion of hydrogen from the weld metal should also be similar.
- In each case, one to two months elapsed between welding and testing. Based on simple calculations, hydrogen should have been substantially reduced due to natural aging prior to testing.

Comparison of the estimates of K_c suggests that the E70T-6 should generally be capable of exceeding the proposed minimum K_c toughness at temperatures below 0°F while the toughness of the E70TG-K2 weld may drop below 90 ksi \sqrt{in} in the temperature range of +50 to 70°F. Despite the difference in toughness behavior, the data support the assumption that the K_c value above which stable ductile tearing precedes unstable crack extension can be approximately calculated from the upper-shelf impact CVN energy absorption.

2.3.3.5 Proposed Charpy V-Notch Requirements

The discussion in the preceding sections suggests that the weld metal in a rigid moment connection subjected to seismic loads should exhibit a minimum CVN energy of 40 ft-lbs at 70°F. This requirement may be conservative, because seismic load rates are at least three orders of magnitude slower than the impact CVN load rate. Also, some of the plastic work that occurs in a weldment under seismic loads converts to thermal energy, which elevates the temperature of the weldment. Considering these effects and using the impact CVN test results for E70TG-K2 and E70T-6, it is possible to demonstrate that with a 40 ft-lbf. requirement in the transition region, these weld metals should exhibit ductile subcritical crack extension similar to a weld metal with 40 ft-lbf. upper-shelf requirement.

All component tests conducted in the SAC Project have been conducted at room temperature (~70 °F). Thus, the results of these tests are applicable to interior framed buildings. The minimum interior operating temperature for buildings, as expressed by several participants in the SAC Steel Project, is +50°F. Considering the difference in loading rate between seismic and CVN impact loads and the temperature increase of weldments under seismic loads, CVN

requirements at 70°F should be adequate for use at +50°F. No tests have been conducted to establish the toughness requirements for moment frames exposed to temperatures below 50°F.

Finite element analysis and strain measurements by Fry, et al. (1999) demonstrate that the strain demands on the weld metal in unreinforced connections are very high even for reduced beam section (RBS) configurations. The data shows that the strain demand on the weld metal is eight times the yield strain for a welded unreinforced connection configuration (WUF-W) and is five times the yield strain for an RBS connection. Consequently, the CVN requirements should be equally applicable to both connections.

The significance of the present 20 ft-lb at -20°F requirement for a moment frame connection exposed to 50°F and higher is not obvious. Although no data are available to investigate the significance, the 40 ft-lb at 70°F requirement may be used to justify relaxing the low temperature requirement to at least 20 ft-lb at 0°F.

In summary, based on the discussions presented in the preceding section, it is proposed that the impact requirement for filler metals used in the fabrication of highly strained joints in moment-resisting frames intended for seismic applications be:

40 ft-lb at +70°F
and
20 ft-lb at 0°F

where service temperatures are anticipated to be on the order of +50°F temperatures or higher. Further research is needed to define the CVN requirements for connections exposed to temperatures below +50°F. Additionally, some consideration should be given to evaluation of the fracture toughness of weld metal using a test such as the CTOD.

2.3.4 Tensile Properties in the Full-Scale Tests

In addition to measuring the toughness of the weld metal in the full-scale test specimens, tensile specimens were extracted at various locations as shown in Figure 2-11. The tensile specimen orientation and gage length were machined so that the tensile properties of the following regions could be directly measured (refer to Figure 2-11):

- Sample A: All weld metal tensile properties.
- Sample B: Transverse weld metal tensile specimen with gage length (g.l.) in the weld metal.
- Sample C: Transverse tensile specimen with g.l. in Weld + heat affected zone (HAZ) + base metal (BM).
- Sample D: Tensile specimen to measure column flange strength in the short-transverse direction.

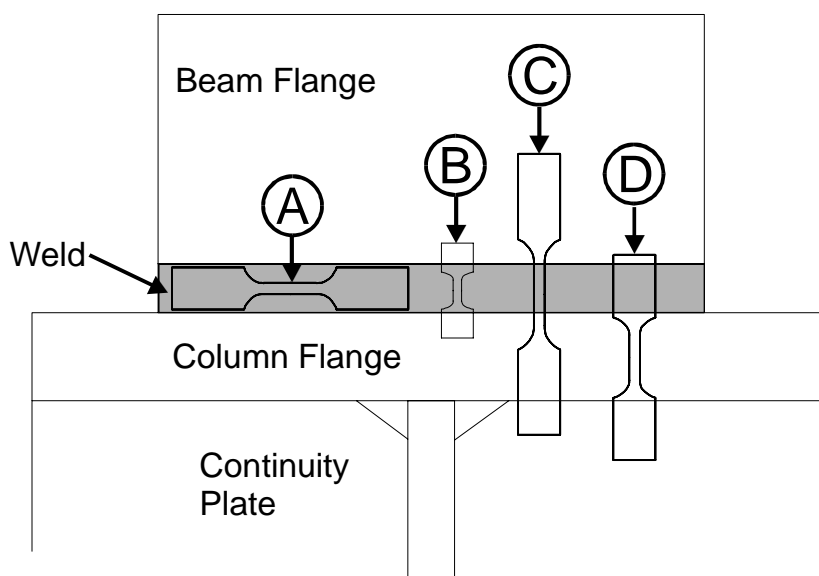


Figure 2-11 Location and Orientation of Tensile Specimens Extracted from Full-Scale Test Specimens

The tensile properties of the weld metal, weldment (weld + HAZ + BM), and column flange regions are plotted in Figure 2-12. All specimens were tested in the as-welded condition. Considering the weld metal tensile specimens, specimen orientation had very little effect on the weld metal tensile properties. The tensile properties of the E70T-6 and E70TG-K2 weld metals were consistent with the properties expected in welds deposited using these consumables using moderate heat inputs. Lower than expected (based on AWS specified minimum strength requirements for this electrode) weld metal tensile properties were measured in the E70T-4 weld metal deposited at the University of Michigan. Although the tensile strength of the E70T-4 weld metal essentially exceeded the expected base metal properties, a weld metal yield strength of approximately 50 ksi was measured. The lower strength measured in the E70T-4 deposits may be due to the deposition of higher heat input welds on thin sections. Under these conditions, the cooling rate in the weld metal can be slow and may result in lower strength weld metal. For this reason, heat input should be restricted when welding lightweight shapes.

As expected, the tensile properties of the weldment (Sample C in Figure 2-11) were representative of the tensile properties expected in the lowest strength region (the base metal in this case). Failure occurred in the parent material when the weldment (Sample C) was tested. With the exception of the E70T-4 weld deposits, the weld metal yield and tensile strengths essentially overmatched the tensile strength of the column flanges.

It is clear from the full-scale tests that a matching or slight overmatching condition is expected when A572/A992 Gr. 50 shapes are welded with E70T-6 and E70TG-K2 consumables. As will be discussed below, the weld metal tensile properties will depend on factors such as the heat input used and the thickness of the parts being welded. Based on the results obtained from the full-scale tests, tests conducted at Battelle (Dong, 1999), and other large-scale testing where some degree of constraint exists, slight weld metal undermatching (< 10%) is not expected to

result in localized deformation in the weld metal. These results also demonstrate that there is no real value in depositing weld metal that substantially overmatches the base metal properties.

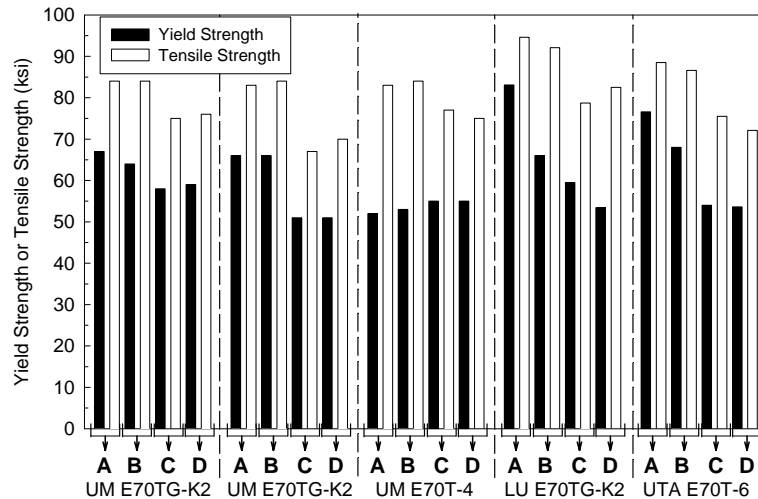


Figure 2-12 Yield and Tensile Strength Measured in the Full-Scale Test Welds Deposited at the University of Michigan (UM), Lehigh (LU), and the University of Texas at Austin (UTA). The Locations and Orientation of the Test Samples are Shown in Figure 2-11.

2.4 Variables Affecting Weld Metal Toughness

Although the factors influencing toughness in welds deposited using SMAW, FCAW-G, SAW, and small diameter FCAW-S consumables has been documented in the literature, similar studies on factors affecting the toughness of welds deposited using larger diameter FCAW-S consumables are limited. The formulation and welding characteristics of larger diameter FCAW-S consumables are unique. Compared to welds deposited using the smaller diameter FCAW-S consumables (E61T8-K6, E71T8-K6) employed for construction of offshore structures, reduced welding costs are achieved in a number of ways when using larger diameter FCAW-S consumables. First, higher deposition rates are measured in welds deposited with the larger diameter electrodes used in the FEMA/SAC Project. Second, higher aluminum concentrations are usually measured in welds deposited using larger diameter consumables and the use of magnesium or other volatile components that provide a secondary shielding gas are not employed.

While some of the most important factors governing structural integrity are related to proper design and quality control, material selection is also critical. For the connection to behave as expected, selection of consumables and welding procedures that will deposit weld metal that consistently, if not always, meets minimum specified mechanical properties is important. From a very simplistic standpoint, factors affecting mechanical properties of a weld deposit can be divided into two basic areas as follows:

1. Factors that influence chemical composition of the weld metal.
2. Factors that influence the thermal history of the weld metal.

The combination of chemical composition and thermal history (cooling rate and weld sequencing) determine the microstructure and distribution of weld metal microstructures in a weld deposit.

Considering SMAW and FCAW-S weld metal, the deposit chemistry will be closely related to consumable formulation. FCAW-G and GMAW weld deposits will also be influenced by the type of shielding gas employed. Other factors such as dilution from the base metal (or from weld metal of different composition) and arc length can also have a pronounced effect on weld metal chemical composition and hence mechanical properties.

Factors affecting the thermal history of a weld deposit can be further divided into factors that affect cooling rate and factors that influence the amount of primary weld metal in a given weld deposit. The primary factors controlling cooling rate of a weld deposit are the arc energy, preheat/interpass temperature, and plate thickness. Fast cooling rates produce welds with higher strength, while slower cooling rates produce welds with lower strengths. Faster cooling rates are promoted by welding with lower arc energies, lower preheats, and welding of thicker sections. On the other hand, cooling rate is reduced when depositing welds on thin sections with high arc energy and preheat/interpass temperatures.

During deposition of multipass welds, a variety of weld metal microstructures are produced by the thermal cycles associated with the various weld passes. Toughness and strength in ferritic materials is improved with a reduction in grain size. During deposition of a single pass weld, the as-welded (or primary microstructure) will depend on the composition of the weld metal and cooling rate. The toughness of this primary weld metal can be quite high in welds that contain a substantial proportion of fine acicular ferrite with small amounts of martensite, bainite, or primary grain boundary ferrite. Formation of substantial quantities of acicular ferrite in FCAW-S consumables is generally not observed due to the deoxidation sequence and inclusion composition.

The primary route to high toughness when using FCAW-S consumables has been to deposit a large number of small weld passes. By depositing a large number of small weld passes, the primary weld metal microstructure is effectively re-transformed to a refined microstructure consisting of fine equiaxed ferrite. When using small diameter FCAW-S consumables for high toughness applications, factors such as wire feed speed, electrode extension, and travel speed are strictly controlled. With the use of larger diameter FCAW-S consumables, such control is not practical when attempting to achieve high deposition rates and given the technology utilized in most structural fabrication environments. Depending on the weld metal microstructural characteristics, the proportion of primary weld metal sampled by a CVN notch or CTOD crack tip can have a substantial influence on the resultant toughness.

As part of the FEMA/SAC investigations, several factors influencing the toughness of welds deposited using larger diameter FCAW-S consumables were investigated. As part of Task 5.2.3 (Johnson, 2000a), the effect of FCAW-S type, cooling rate, and electrode extension on weld metal mechanical properties was investigated. Table 2-6 summarizes the experimental conditions investigated in the Task 5.2.3 study. Welds were deposited under welding conditions that produced fast, medium, and slow weld metal cooling rates. Controlling interpass temperature and varying the heat input produced a large change in cooling rate. The fast and slow cooling rate conditions evaluated in the Task 5.2.3 study were representative of extreme conditions that might be encountered while welding using manufacturer recommended parameters in the field depending on ambient temperature, section thickness, and welding technique. The heat input used to produce the fast cooling rate weld deposits was quite low. Although not economically feasible, such conditions may exist when the ambient temperature of the steel is near freezing or during the deposition of column splice welds. The effect of electrode extension when using the E71T-8 and E70TG-K2 consumables was also evaluated.

Table 2-6 Summary of Experimental Welding Conditions and Electrodes Used in SAC Sub-Task 5.2.3

Electrode	Fast Cooling Rate			Medium Cooling Rate			Slow Cooling Rate		
	Preheat/ Interpass (°F)	Heat Input (kJ/in)	$\Delta t_{8/5}$ (s)	Preheat/ Interpass (°F)	Heat Input (kJ/in)	$\Delta t_{8/5}$ (s)	Preheat/ Interpass (°F)	Heat Input (kJ/in)	$\Delta t_{8/5}$ (s)
E71T-8	<100	13	1.4	300±25	29	4.8	550±25	43	18
E70TG-K2	<100	17	1.6	300±25	43	6.8	550±25	70	23
E70T-6	<100	33	2.4	300±25	53	8.7	550±25	76	24
E7018	<100	17	1.6	300±25	47	7	550±25	74	24

In an internal study, Lincoln Electric evaluated the effect of heat input and welding position (for E71T-8 only) on the CVN impact properties of welds deposited using E70T-6, E70TG-K2, and E71T-8 consumables. For the Lincoln Electric study, the joint geometry and specimen location corresponded to the joint geometry employed in standard A5.20 classification tests. Due to the range of heat inputs employed in the Lincoln Electric Study, the AWS layer/pass requirements may not have been met. The CVN impact results from the Task 5.2.3 study and Lincoln Electric study are shown graphically in Figures 2-13 through 2-19. The data shown in Figures 2-13 to 2-19 are also summarized in Table 2-2 and in Figures 2-20 to 2-24.

The CVN transition behavior observed in weld metal deposited using 3/32-in. dia. E70T-6 electrodes and welding procedures to produce fast, medium, and slow cooling rates is shown in Figures 2-13 and 2-14. As shown in Figure 2-13, welds deposited with intermediate cooling rates (typical of most field welding conditions) had CVN impact energies that exceed 20 ft-lbf. at 0°F and have a room temperature toughness of approximately 38 ft-lbf. Increasing cooling rate

resulted in a reduction of the lower temperature toughness and reduction of the upper shelf energy. Decreasing cooling rate (increasing heat input/interpass) resulted in an increase in upper shelf energy. The increase in the upper shelf energy with decreasing cooling rates is consistent with the associated strength changes measured in the experimental welds. Upper shelf energy is strongly dependent on the strength of the material under consideration. Slightly higher toughness was measured in the E70T-6 weld metal deposited in the Lincoln Electric investigation (Figure 2-14). Although the lowest toughness was measured in weld metal deposited using a heat input of 25 kJ/in., it appears that a CVN toughness of 20 ft-lbf. at -20°F was surpassed on a consistent basis.

The CVN behavior of the weld metal deposited using 3/32-in. dia. E70TG-K2 electrodes was substantially different than the E70T-6 weld metal. Figure 2-15 shows the toughness measured in E70TG-K2 welds deposited under the conditions described in Table 2-6. When compared to the E70T-6 weld metal, higher transition temperatures and higher upper shelf energy was typically measured in the E70TG-K2 deposits. The highest toughness was measured in welds deposited using a long electrode extension and intermediate heat inputs. The higher toughness in Weld B was attributed to a lower nitrogen concentration. Due to the scatter in the CVN data at lower test temperatures, it is not clear whether or not a toughness of 20 ft-lbf. at -20°F would be consistently met. Similar CVN toughness was measured in the Lincoln Electric study as shown in Figure 2-16. Due to the high degree of scatter in the Lincoln Electric data, it was difficult to draw any conclusions regarding the low temperature CVN toughness of LEC E70TG-K2 weld deposits.

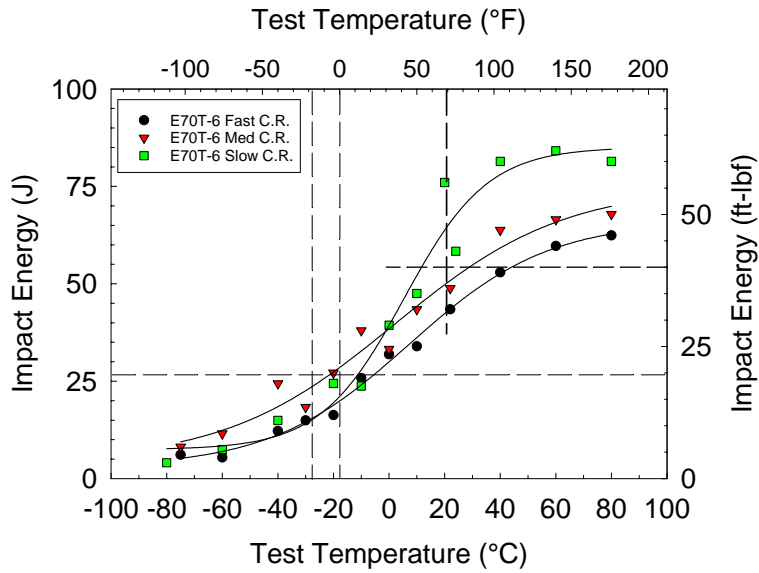


Figure 2-13 CVN Impact Toughness Measured in E70T-6 Welds Deposited with Fast Cooling Rates (33 kJ/in., <100°F Interpass), Medium Cooling Rates (53 kJ/in., 300°F), and Slow Cooling Rates (76 kJ/in., 550°F).

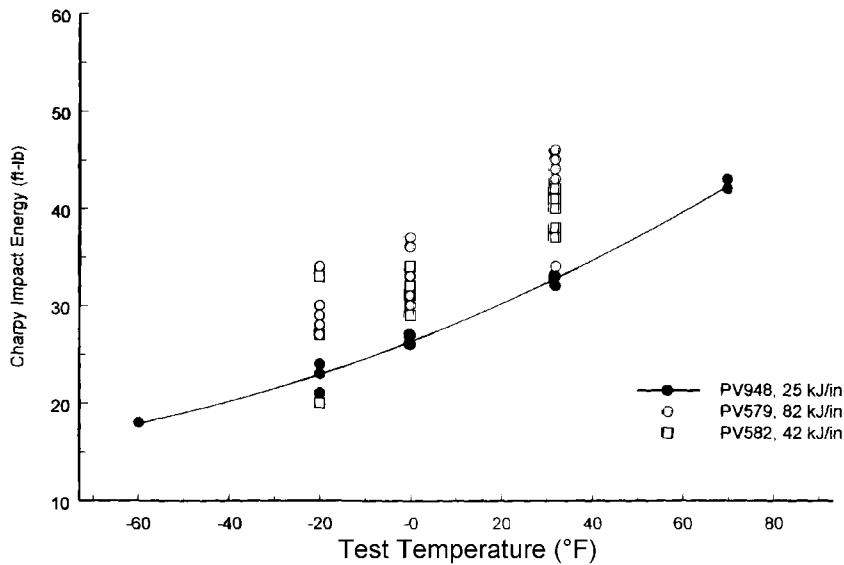


Figure 2-14 CVN Impact Toughness Measured in E70T-6 Weld Metal Deposited with Low, Medium and High Heat Inputs. Interpass Temperature was Maintained at 300°F. [M.A. Quintana, LEC-with permission]

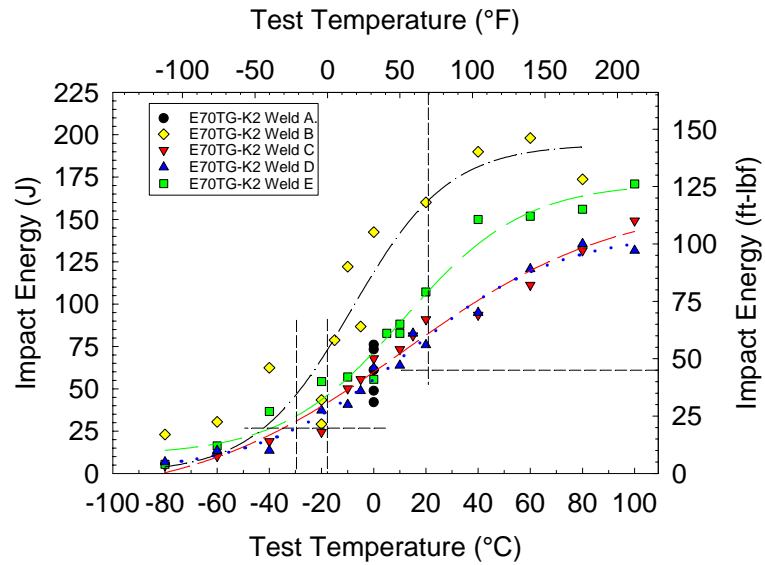


Figure 2-15 CVN Impact Energy Measured in E70TG-K2 Weld Metal Deposited Under the Following Conditions: Weld A 17 kJ/in., <100°F Interpass, Normal Electrode Extension (EE); Weld B, 43 kJ/in., 300°F, Long EE; Weld C, 43 kJ/in., 300°F, Normal EE, Weld D; 43 kJ/in., 300°F, Short EE; Weld E, 70 kJ/in., 550°F, Normal EE

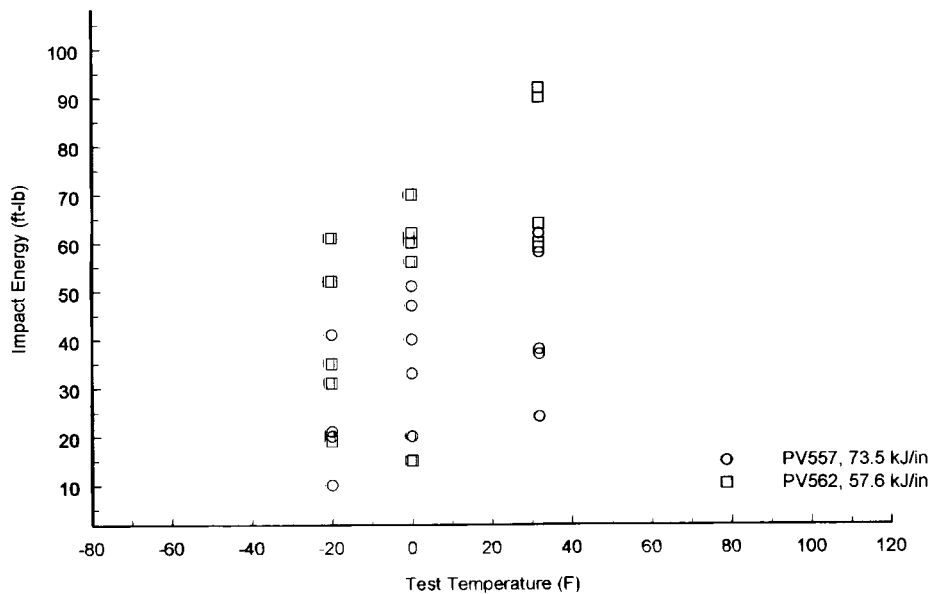


Figure 2-16 CVN Impact Toughness Measured in E70TG-K2 Weld Metal Deposited with Medium and High Heat Inputs. Interpass Temperature was Maintained at 300°F. [M.A. Quintana, LEC-with permission]

Welds deposited using the 5/64-in. dia. E71T-8 consumable were very robust. Figure 2-17 shows that significant change in cooling rate and electrode extension had very little effect on the CVN impact behavior. At lower test temperatures, minimum AWS and recommended SAC toughness requirements were exceeded on a consistent basis. Likewise, relatively high upper shelf CVN impact toughness was measured in the E71T-8 weld metals. Similar results were observed in the Lincoln Electric study although a decrease in toughness was measured in vertical up E71T-8 welds produced using relatively high heat inputs. Although higher toughness was measured in the E71T-8 weld deposits, the use of this electrode is typically limited to deposition of out-of-position welds due to lower deposition rates and lower welder appeal.

Decreasing cooling rate had a pronounced effect on the E7018 weld metal toughness as shown in Figure 2-19. Although toughness decreased in welds deposited with low heat inputs and low interpass temperatures, toughness of the E7018 weld metals should be expected to consistently exceed AWS and SAC recommended minimum toughness requirements. As with the E71T-8 consumables, the use of E7018 consumables for beam-to-column welds is limited due to the lower deposition rates.

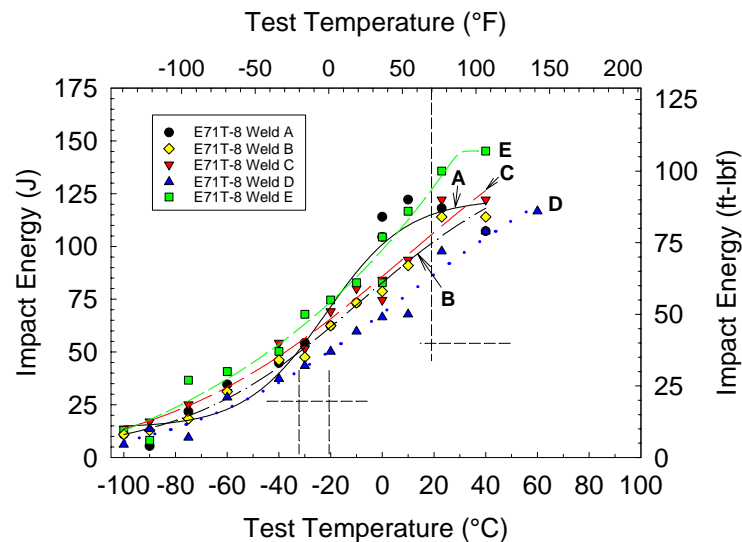


Figure 2-17 CVN Impact Energy Measured in E71T-8 Weld Metal Deposited Under the Following Conditions: Weld A 13 kJ/in., <100°F Interpass, Normal Electrode Extension (EE); Weld B, 29 kJ/in., 300°F, Long EE; Weld C, 29 kJ/in., 300°F, Normal EE, Weld D; 29 kJ/in., 300°F, Short EE; Weld E, 43 kJ/in., 550°F, Normal EE

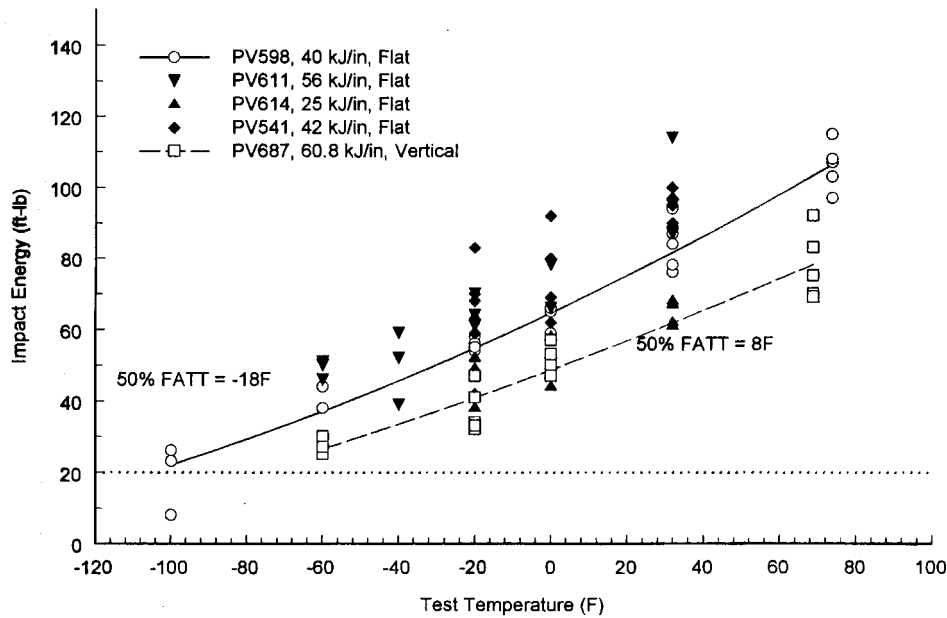


Figure 2-18 CVN Impact Toughness Measured in E71T-8 Weld Metal Deposited with Medium and High Heat Inputs. Interpass Temperature was Maintained at 300°F. [M.A. Quintana, LEC-with permission]

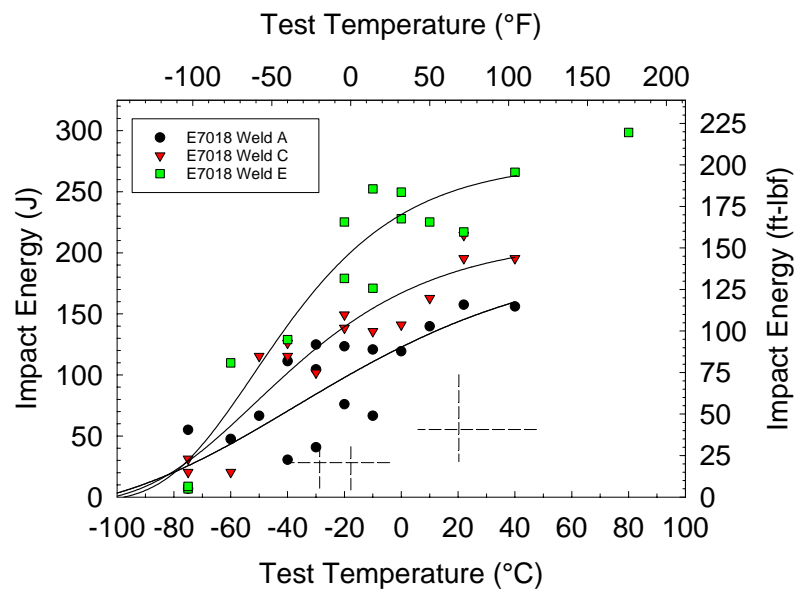


Figure 2-19 CVN Impact Energy of E7018 Weld Metal Deposited using the Following Welding Conditions: Weld A 17 kJ/in., <100°F Interpass, Weld B 40 kJ/in., 300°F Interpass, Weld C 70 kJ/in., 550°F Interpass

As discussed above, tight control of welding procedures are required to maintain high toughness when using smaller diameter FCAW-S electrodes employed in offshore fabrication. Such specific welding procedures are required to ensure deposition of small weld beads. While the toughness measured in the FCAW-S weld metal evaluated as part of the Task 5.2.3 investigation was lower than that typically measured in welds deposited using small diameter FCAW-S electrodes, the toughness of the Task 5.2.3 welds did not substantially change with small changes in welding procedure. This data suggests that a range of welding procedures can be used with the FCAW-S consumables investigated in the FEMA/SAC program (Johnson, 2000a) without significant degradation of toughness provided that:

- Manufacturers recommended operating ranges are used.
- Heat input is effectively maintained between 30 and 80 kJ/in. (or a range specified by the manufacturer).
- Interpass temperature is limited to a maximum of 550°F.

As part of investigation Task 5.2.8, additional testing was conducted to develop welding procedures that could be used to evaluate potential electrodes under a range of welding conditions. As part of this investigation, welds were deposited under AWS classification test procedures and welding procedures that produce fast and slow cooling rates. The joint geometry, welding procedures, and test results are given in Tables 2-7 and 2-8. Additional discussion of recommended “Prequalified Electrode Classification Procedures” will follow in the next section. Data from the Task 5.2.8 study is included in Table 2-2 and Figures 2-20 through 2-24.

Unlike the large number of heats of structural shapes evaluated in the FEMA/SAC program, evaluation of only a limited number of “lots” of electrodes were considered. Data available from the investigation program are summarized in Figures 2-20 through 2-24. Figure 2-20 shows a summary of the low temperature toughness measured in welds produced using 3/32-in. dia. E70T-6 consumables under a range of conditions as part of the investigation program. Welds deposited using four consumables are represented in Figure 2-20. Excluding the welds produced with fast and slow cooling rates as part of Task 5.2.3 (welds 1 and 3) that were deposited using extreme welding procedures, it is apparent that recommended minimum toughness requirements of 20 ft-lbf. at 0°F were met in most of the experimental welds. Given the wide range of welding procedures employed, the low temperature toughness of the E70T-6 weld metal is reasonably consistent.

Table 2-7 Summary of Classification Testing Program using a 3/32-in. dia. E70TG-K2 Electrode

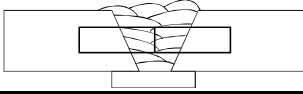


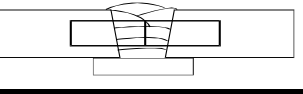


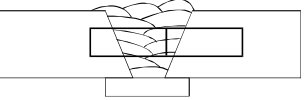
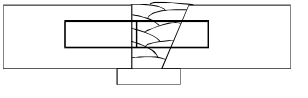
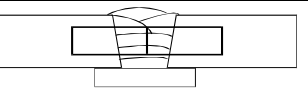

Test ID	Electrode	Heat Input (kJ/in)	Interpass Temp (F)	Joint Geometry and Sample Location	Test Temp (F)	Toughness (Ft-lbf)	YS ksi	UTS ksi	Elongation percent
AWS A5 WCL	3/32 E70TG-K2	47	300		-20	AVG. 18	76	90	25
					0	AVG. 21			
					70	AVG. 52			
AWS A5 Off-Center	3/32 E70TG-K2	47	300		-20	AVG. 8	76	90	25
					0	N/A			
					70	AVG. 33			
SAC Med	3/32 E70TG-K2	47	150 min		-20	9	82	95	23
					0	12			
					70	70			
SAC High	3/32 E70TG-K2	70	500		-20	AVG 11	51	77	32
					0	AVG 19			
					70	AVG 71			
SAC Low	3/32 E70TG-K2	30	<100		-20	AVG. 9	87	99	29
					0	AVG. 11			
					70	AVG. 45			

Table 2-8 Summary of the Classification Testing Program Using the E70T-6 Electrode

Test ID	Electrode	Heat Input (kJ/in)	Interpass Temp (F)	Joint Geometry and Sample Location	Test Temp (F)	Toughness (Ft-lbf)	YS ksi	UTS ksi	Elongation percent
AWS A5 WCL	3/32 E70T-6	47	300		-20	AVG. 24	67	92	22
					0	AVG. 26			
					70	AVG. 44			
AWS A5 Off-Center	3/32 E70T-6	47	300		-20	AVG. 24	76	90	25
					0	N/A			
					70	AVG. 41			
SAC Med	3/32 E70T-6	47	150 min		-20	28	54	76	30
					0	34			
					70	55			
SAC High	3/32 E70T-6	70	500		-20	AVG 23	78	92	26
					0	AVG 28			
					70	AVG 58			
SAC Low	3/32 E70T-6	30	<100		-20	AVG. 23	78	92	26
					0	AVG. 27			
					70	-AVG. 43			

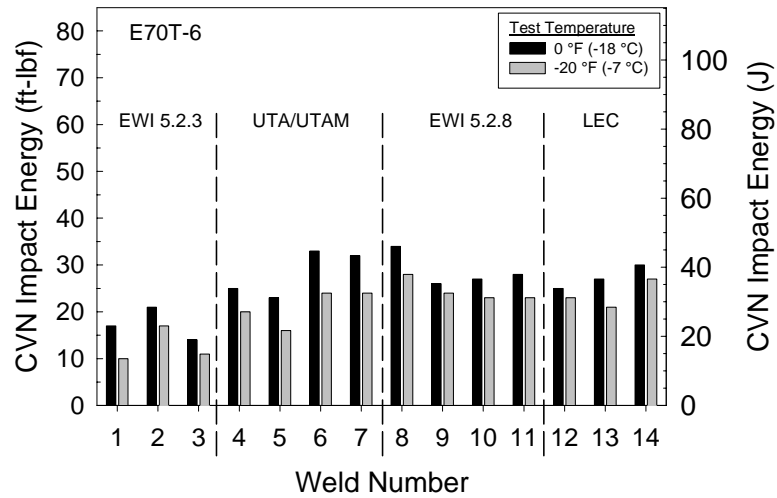


Figure 2-20 Summary of Low Temperature CVN Impact Energy Measured in Welds Deposited Using 3/32-in. dia. E70T-6 Consumables Evaluated in the SAC Program

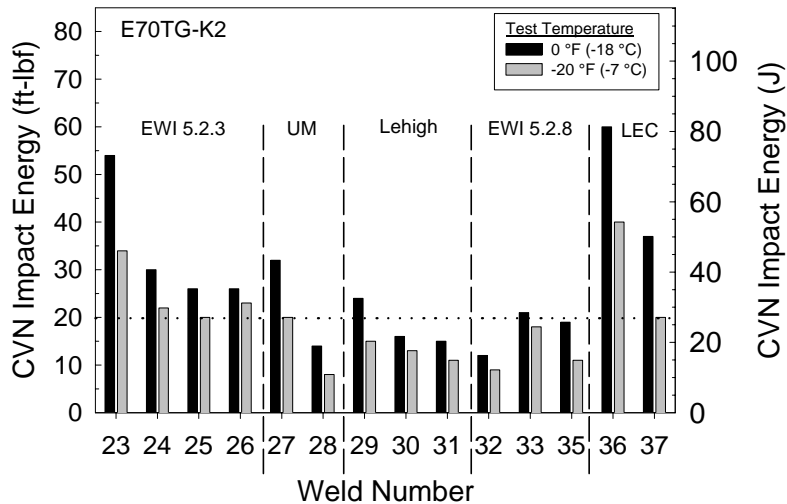


Figure 2-21 Summary of Low Temperature CVN Impact Energy Measured in E70TG-K2 Weld Metal Evaluated in the SAC Program

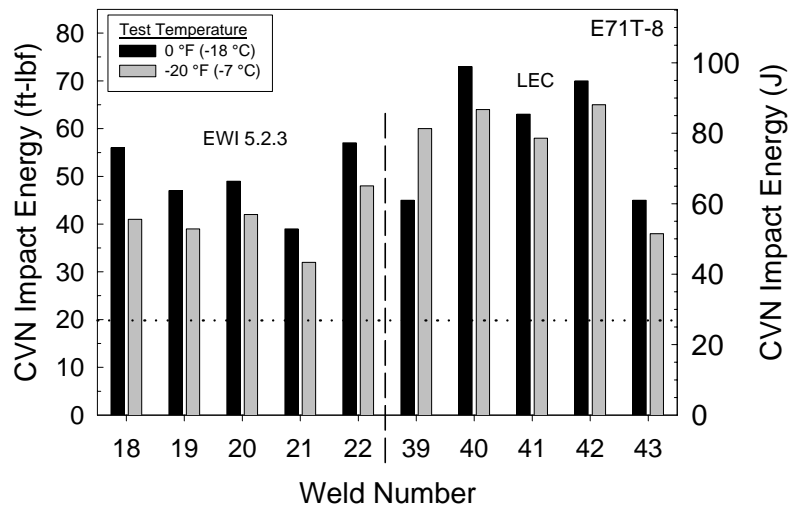


Figure 2-22 Summary of Low Temperature CVN Impact Energy Measured in E71T-8 Weld Metal Evaluated in the SAC Program

The toughness of welds deposited using the E70TG-K2 weld metal was somewhat paradoxical. At the outset of the investigation program, the E70TG-K2 electrodes were expected to deposit weld metal with higher CVN toughness than welds deposited using E70T-6 electrodes. Figure 2-16 shows that welds deposited using the E70TG-K2 consumable did not consistently exceed 20 ft-lbf. at 0°F or at -20°F. The scatter in low temperature toughness measured in E70TG-K2 weld metals may be attributed to several factors:

- The temperature range in which the transition from ductile behavior to brittle behavior occurs was relatively narrow in the E70TG-K2 welds. Some scatter is expected when evaluating toughness in the lower transition region.
- Toughness is sensitive to microstructural variation and notch location. The fraction of primary weld metal and number of large oxide/nitride inclusions sampled by the CVN has a strong effect on toughness in the E70TG-K2 weld metals. As is evident in the University of Michigan and Lehigh University test welds, notch location can be important.
- Although lot-to-lot variation as part of consumable manufacture was not specifically addressed, such variation is possible. This may be an important consideration that limits the usefulness of relying entirely on AWS classification alone.

Inspection of Figure 2-23 suggests that welds deposited using the 5/64-in. dia. E71T-8 consumables consistently exceeded 20 ft-lbf. at -20°F. Substantial changes in heat input had little effect on the lower temperature toughness in the E71T-8 welds. The toughness measured in the E71T-8 electrodes is similar to that measured in some E7018 weld metals. The higher deposition rates, acceptable out-of-position performance, and resistance to intermixing effects when welding over most FCAW-S weld metals leads many fabricators to select the E71T-8

electrode as opposed to SMAW electrodes when positional welding is required in the fabrication of moment frames.

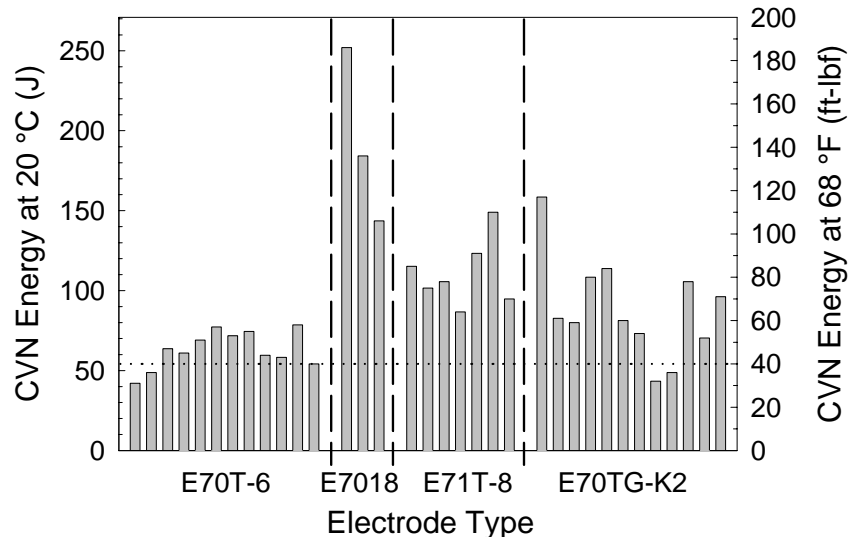


Figure 2-23 Comparison of the CVN Impact Energy Measured at Room Temperature in Welds Deposited Under Different Conditions Using E70T-6, E7018, E71T-8, and E70TG-K2 Electrodes

As previously mentioned, the CVN impact energy absorbed at room temperature may be a more important indicator determining the behavior of FCAW-S welds in moment connections than the lower temperature toughness. A minimum room temperature CVN impact energy of 40 ft-lbf. has been specified as part of SAC prequalified consumable requirements. Figure 2-23 shows that this minimum toughness was met in welds deposited using E7018 and E71T-8 consumables. The room temperature toughness measured in the E70TG-K2 weld metals were, on average, higher than the toughness measured in the E70T-6 consumables. A lower bound toughness in post-Northridge full-scale tests has not been identified. It is apparent that the consumables evaluated as part of the FEMA/SAC program should be able to meet the minimum room temperature toughness requirements proposed for pre-qualified consumable status.

The transition temperature is often an important consideration when selecting consumables or steel. It is desirable to select materials so that the service temperature does not fall in the transition region. The 50% fracture appearance transition temperature (50% FATT) in a CVN specimen is the temperature at which half of the fracture surface is cleavage and half of the fracture surface is ductile. Increasing temperature above this temperature is expected to increase the proportion of ductile fracture. Likewise, decreasing temperature below the 50% FATT will increase the likelihood of brittle fracture.

When full-CVN curves were produced during the investigation program, the CVN fracture appearance was characterized. Figure 2-24 shows the 50% FATT observed in weld metals

produced using the E70T-6, E70TG-K2, E7018, and E71T-8 weld metals. It is clear from Figure 2-19 that welds deposited using the E70T-6, E7018, and E71T-8 all had 50% FATT's well below room temperature. Higher transition temperatures were observed in the E70TG-K2 weld metals. In some cases the 50% FATT was equivalent to or above room temperature. This observation is particularly important when considering that the service temperatures of most moment connections will often drop below room temperature. All other things being equal, the E70T-6 consumable appears to be a more appropriate choice for fabrication of moment connections, particularly when lower service temperatures (<50°F) are expected.

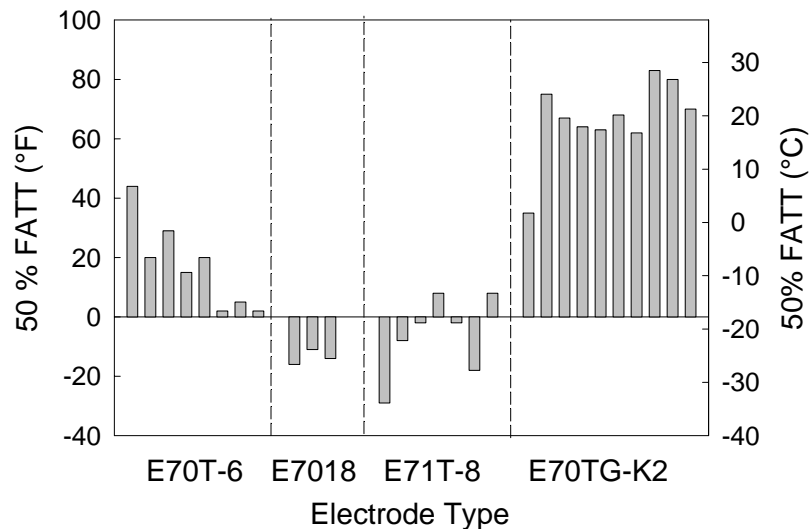


Figure 2-24 Effect of Electrode Type on the 50% FATT (temperature at which 50 percent of the CVN fracture surface is brittle)

2.4.1 Effect of Cooling Rate on Weld Metal Strength

Although it is apparent from the discussion above that the cooling rate did not have a pronounced effect on weld metal toughness, the cooling rate had a pronounced effect on weld metal tensile properties. When welding higher strength steel (yield strength > 90 ksi) it is desirable in some cases to undermatch weld metal strength relative to that measured in the base metal. Deliberate undermatching of high strength steel often reduces the risk of weld metal hydrogen assisted cracking and increases the probability that minimum weld metal toughness requirements can be met. Considering ASTM A572 Gr. 50 shape material, it is not feasible to deposit weld metal that would consistently match or undermatch the tensile properties of the shape material while maintaining adequate weld metal toughness.

When the risk of weld metal hydrogen assisted cracking can be avoided and adequate weld metal toughness can be maintained, matching or slight overmatching of the weld metal tensile properties is often specified. Matching or slight overmatching is often specified to force plastic deformation into the plate material that is unlikely to contain welding related defects.

Specification of welds which substantially overmatch the base metal can increase the risk of hydrogen assisted cracking.

The effect of cooling rate ($\Delta t_{8/5}$) on the tensile and yield strengths measured in the weld metals investigated is summarized in Figures 2-25 and 2-26. For comparison purposes, the mean, minimum, and maximum tensile properties reported by six manufacturers of structural shapes are included in the plots. As shown in Figure 2-25, specification of intermediate heat inputs and interpass temperatures should result in weld metal yield strengths that overmatch most Grade 50 shape material and essentially match most ASTM A913 Gr. 65 shapes. Likewise, Figure 2-21 shows that matching or overmatching ultimate tensile strengths are expected when welding is conducted so that intermediate cooling rates are maintained. Deposition of high heat input welds on thin sections while maintaining a high interpass temperature may result in a condition where the tensile strength and yield strength both substantially undermatch the base metal properties and result in low HAZ toughness and weld metal toughness.

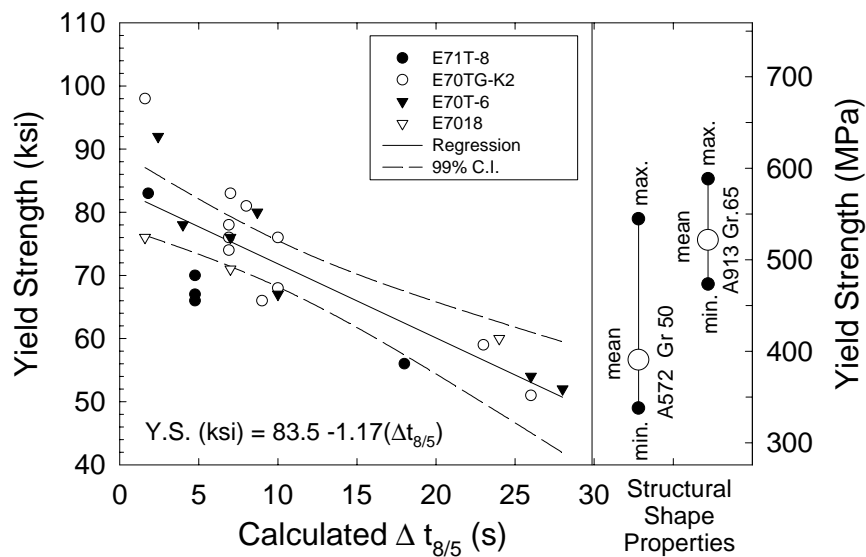


Figure 2-25 Effect of Cooling Rate on the Tensile Strength of Weld Metal Deposited Using FCAW-S and SMAW Electrodes During the SAC Program. The Maximum, Minimum, and Mean Tensile Strengths Measured in A572 Gr. 50 and A913 Gr. 65 Shape Materials are also Shown for Comparison

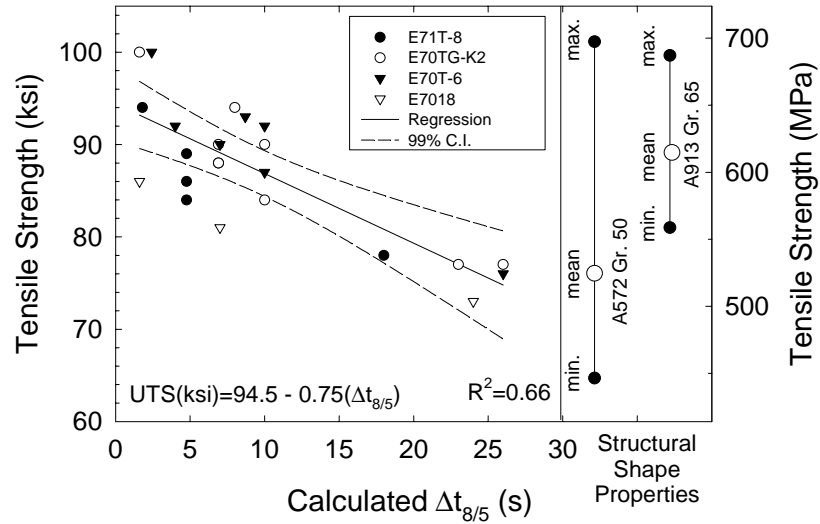


Figure 2-26 Effect of Cooling Rate on the Tensile Strength of Weld Metal Deposited Using FCAW-S and SMAW Electrodes During the SAC Program. The Maximum, Minimum, and Mean Tensile Strengths Measured in A572 Gr. 50 and A913 Gr. 65 Shape Materials are also Shown for Comparison

2.5 Prequalification of Electrodes

2.5.1 Prequalification Requirements and Method

Based on measurement of toughness from successful connection tests and a consideration of the threshold toughness above which low cycle fatigue considerations will control connection fracture, the following mechanical property requirements have been recommended for inclusion in specifications for welded joints with high strain demands due to seismic loading:

CVN Toughness:

20 ft-lbf. at 0°F

and

40 ft-lbf. at 70°F

Strength and Ductility

Yield: 50 ksi minimum

Tensile: 70 ksi minimum

Elongation: 22 percent

It is neither practical nor economically feasible to conduct full-scale test welds or T-stub specimens in order to evaluate the suitability of a particular electrode or electrode formulation for seismic service. An alternative testing protocol is required to accommodate the use of different electrodes and modifications to the electrode formulations used in the FEMA/SAC investigations.

Several approaches can be taken to provide improved confidence that weld metal deposited using a given consumable will meet minimum mechanical property requirements listed above when deposited using a wide range of welding parameters.

Potential approaches include:

1. Require the fabricator to demonstrate the suitability of each lot of electrodes and welding procedures used on a particular project following the project WPS.
2. Define a set of welding and testing conditions that are representative of the range of welding conditions likely to be used during fabrication and require the fabricator to produce a procedure qualification test for each lot/heat of electrode used in a particular job.
3. Define a set of welding and testing conditions that are representative of the range of welding conditions likely to be used during fabrication and require the manufacturer to produce a procedure qualification test for each lot/heat of electrode produced. It would be the consumable manufacturer's responsibility to demonstrate that their electrodes are generally capable of meeting minimum property requirements under the specified test conditions. Following successful completion of a demonstration program, the consumable would be "pre-qualified."

Considering the cost to the steel construction industry, it is more cost effective for the electrode manufacturers to evaluate and test their product to ensure that specified properties will be met under a wide range of welding conditions. Standardization of welding and testing procedures in order to meet recommended consumable status are discussed below.

Recommendations bracket the heat input between 30 and 80 kJ/in. and the maximum recommended interpass temperature at 550°F. Beam flange thickness can range from 3/8-in. to over 1.5-in. Conditions of a thin flange, high heat input, and high interpass temperature will result in a condition of 2-D heat flow and a slow cooling rate. Conditions of low heat input, low interpass temperature, and thick material will result in a condition of 3-D heat flow and a relatively fast cooling rate.

Considering the range of possible heat input and interpass temperatures that may be employed, it is possible to determine the critical plate thickness that defines conditions of 2-D and 3-D heat flow. Based on an analytical analysis of heat flow in thin and thick plates while considering the range of material thickness expected in many steel frame buildings, Table 2-9 presents heat input, preheat, and interpass temperature conditions that should be used to deposit classification test welds.

Two test plates should be used for each test set. The steel plates to be used may be of any AISC-listed structural grade. The joint geometry should conform to current ISO specifications. The test plate should be 3/4-in. thick with a 5/8-in. root opening and 20° included angle. Welding conditions are listed in Table 2-9. A minimum of three passes per layer should be used to fill the width. All test specimens should be taken from centerline of the weld at the mid-thickness location in order to minimize dilution effects. Alternatively, the manufacturer or contractor may elect to test a narrower range of heat inputs and interpass temperatures and clearly state these limitations on the test reports and user data sheets. Regardless of the method of selecting test heat input, the WPS as used by the Contractor must fall within the range of heat inputs and interpass temperatures tested.

Table 2-9 Proposed Welding and Preheat Conditions for Determination of Prequalified Status

Cooling Rate	Heat Input	Preheat °F	Interpass °F
Fast ($\Delta t_{8/5} \sim 5s$)	30 kJ/in.	70±25	200±50
Slow ($\Delta t_{8/5} \sim 26 s$)	80 kJ/in.	300±25	500±50

2.5.2 Discussion

At the present time, many electrode manufacturers list operating windows in which a filler metal can effectively be used to maintain a stable arc rather than a range of operating conditions that can be employed to deposit weld metal with a high probability of meeting specified mechanical properties. Uninformed users may expect that minimum AWS classification properties will be consistently, if not always, met when using a wide range of welding procedures.

The mechanical properties measured in the full-scale test welds and the Task 5.2.3 investigations demonstrate that selection of electrodes for moment frame construction based on AWS classification alone may not be sufficient for the following reasons:

- Low temperature toughness may not be the predominant factor determining the risk of brittle fracture in full-scale tests conducted at room temperature. Evaluation of CVN toughness near room temperature should also be considered.
- AWS classification test procedures evaluate weld metal deposited under one set of welding conditions at one test temperature. In reality, a single consumable may be required to deposit welds that are expected to meet minimum mechanical property requirements under a range of welding conditions. For example, when welding connections are near the bottom levels of a tall building, faster cooling rates are expected because heavier sections are being joined. Due to the larger sections, maintenance of a high interpass temperature can be difficult. As the building is completed, slower cooling rates may be encountered when welding thinner sections near the top of the building. When welding thinner sections, high interpass

temperatures are often maintained. These higher interpass temperatures will reduce the cooling rate following weld deposition. While preheat will play a minor role in weld metal strength levels in different size connections, interpass temperature during welding will effectively influence the cooling rate in a multipass weld.

- The electrodes used in this study have demonstrated satisfactory performance in full-scale test welds. However, electrodes manufactured to the same AWS classification by the same manufacturer or by a different manufacturer may not deposit weld metal that consistently meets low temperature and room temperature toughness requirements developed as part of the FEMA/SAC program.
- The electrodes evaluated in the FEMA/SAC study effectively deposited weld metal that met minimum AWS tensile requirements when a wide range of cooling rates were evaluated. Electrodes should be evaluated using welding procedures representative of fast and slow cooling rates expected in field fabrication. Evaluation of weld metal deposited using fast and slow cooling rates should increase the probability that minimum mechanical properties will be met under a wide range of conditions.

As part of the Task 5.2.8 investigations, the mechanical properties measured in standard AWS A5 classification test welds deposited using E70T-6 and E70TG-K2 welds were compared to the mechanical properties of welds deposited using the proposed SAC pre-qualification criteria. A summary of the test results is presented in Tables 2-7 and 2-8.

Before considering the relationship between the AWS A5 welding procedures and the proposed SAC welding procedures, some discussion regarding the properties measured in the A5 test welds is warranted. As previously mentioned, the AWS A5 test joint is typically filled using two passes per layer. The CVN notch is located in the central region where the two passes overlap. This region often contains very little primary weld metal and typically has higher relative toughness. The effect of notch position in the E70TG-K2 and E70T-6 AWS A5 welds was investigated. As shown in Tables 2-7 and 2-8, shifting the notch from the center position to an off-center position containing some primary weld resulted in a substantial decrease in toughness in the E70TG-K2 weld metal. The average CVN toughness of E70TG-K2 weld metal at -20°F and at room temperature dropped from 18 ft-lbf. and 52 ft-lbf. when the notch was located at the weld centerline to 8 ft-lbf. and 33 ft-lbf. when the notch was moved off-center. Similar large shifts in transition temperature (>60 °F) have been observed in AWS classification test welds using E70T-1 consumables at the Edison Welding Institute (EWI). The reduction in toughness occurs when the CVN notch samples a significant proportion of primary weld metal containing an undesirable microstructure and large oxide inclusions. A similar shift in toughness was not measured in the E70T-6 weld metals.

Comparison of the E70T-6 welds produced with the standard A5 classification test procedure with the E70T-6 welds produced with the SAC welding procedure suggests that similar toughness was measured in the A5 and SAC test welds. Furthermore, the toughness measured in the SAC tests was representative of the University of Texas at Austin full-scale test welds. As

expected, the tensile properties were strongly dependent on the weld cooling rate. Welds deposited with the high heat input procedure exhibited yield strengths above 50 ksi and tensile strength above 70 ksi. Based on these test results, it is apparent that the E70T-6 should be capable of meeting minimum recommended requirements for prequalified electrodes.

The lot of E70TG-K2 submitted to EWI for follow-up testing as part of Task 5.2.8 did not meet minimum AWS A5 low temperature CVN requirements. The minimum CVN impact energy requirements of 20 ft-lbf. at 0 °F were met when using the A5 classification test procedures. Consistent with previous tests using the E70TG-K2 electrode, higher room temperature toughness was measured in welds deposited using the A5 and FEMA/SAC welding procedures. The low temperature toughness of the E70TG-K2 weld metal deposited using the FEMA/SAC welding procedures fell below the minimum 20 ft-lbf. level at 0°F. Given the scatter expected in the E70TG-K2 welds, re-testing of the FEMA/SAC welds may produce more favorable results. An alternative approach would be to perform additional test welds at a slightly lower heat input and reduce the recommended operating range. Consideration of the CTOD properties measured in the welds produced using this particular lot of electrodes indicates that the use of this particular lot of E70TG-K2 electrode may not produce satisfactory performance at temperatures below room temperature.

The effect of cooling rate on weld metal tensile properties was consistent with the Task 5.2.3 test results. A minimum tensile strength greater than 50 ksi and a minimum tensile strength greater than 76 ksi was measured in the slow cooling rate E70TG-K2 weld metals.

It is clear that relying on the AWS A5 classification test results does not provide a useful evaluation of consumables intended for use in moment frame construction for seismic applications. Based on the data presented in Tables 2-7 and 2-8 and the discussion above, it appears that the proposed FEMA/SAC welding procedures are effective in evaluating the CVN impact energy and tensile properties for seismic applications. It is expected that additional testing by the manufacturers will be conducted to verify these results. At the present time, a proposal has been presented to the AWS A5M sub-committee to allow creation of a supplemental designator that would indicate that testing similar to that discussed here has been performed. Until the details of this supplemental designation can be resolved, the recommended testing procedure should be used to demonstrate that minimum mechanical property requirements will be met.

In comparison to SMAW electrodes, SAW fluxes, and solid wire, production of cored wire presents an additional challenge. Many manufacturers have developed appropriate production techniques and quality control routines that ensure delivery of a consistent product. Although many consumable manufacturers have documented their production and testing procedures so that they conform to ISO or ASME requirements, there is still no guarantee that a consistent product will be delivered to the end user. Although there are a variety of permitted testing schedules, most consumable manufacturers repeat classification tests on an annual basis. Reliance on current AWS A5 classification tests that evaluate toughness only once a year or perhaps less frequently may not ensure delivery of a consistent product. At the present time, the only means of ensuring that a consistent product is delivered to the end user is to require lot

testing of the electrodes by the manufacturer or by the end user. Although this is expected to increase the cost of the consumables used in the fabrication of moment frames, lot testing should be employed to ensure that the consumable is generally capable of meeting minimum mechanical properties. This is particularly relevant since the number of consumable manufacturers supplying consumables is increasing.

2.6 Chapter Summary

Two approaches have been employed to develop minimum mechanical property requirements in beam-to-column welds. As part of full-scale testing at the University of Michigan, Lehigh University, and the University of Texas at Austin, additional full-scale connections were fabricated (but not tested) for extraction of mechanical test specimens. Brittle fracture of the weld metal was not observed in the full-scale tests. Based on the mechanical properties and consideration of the flaws present in the full-scale test welds, the following minimum mechanical property requirements have been established:

<p style="text-align: center;">CVN Toughness:</p> <p style="text-align: center;">20 ft-lbf. at 0°F</p> <p style="text-align: center;">and</p> <p style="text-align: center;">40 ft-lbf. at 70°F</p> <p style="text-align: center;">Strength and Ductility</p> <p style="text-align: center;">Yield: 50 ksi minimum</p> <p style="text-align: center;">Tensile: 70 ksi minimum</p> <p style="text-align: center;">Elongation: 22 percent</p>

The robustness of E70TG-K2, E70T-6, E71T-8, and E7018 consumables was evaluated. Although the E70TG-K2 and E70T-6 electrodes have both demonstrated acceptable full-scale performance, the E70T-6 electrodes appear to have higher low temperature toughness. Variation of notch position within several full-scale weld metals had a more pronounced effect on weld metal toughness than variations in heat input, interpass temperature, or electrode extension. Variation of cooling rate had a pronounced effect on weld metal strength. All weld metals evaluated in the SAC study had tensile strengths exceeding 70 ksi and yield strengths exceeding 50 ksi. In order to ensure that the minimum mechanical property requirements are achieved, the heat input used to deposit beam-to-column welds should be maintained between 30 kJ/in. and 80 kJ/in.

As part of achieving prequalified status for electrodes for seismic applications in moment resisting frames, electrode manufacturers should specify an operating window in which their

consumables will deposit weld metal with the above minimum mechanical properties. A standard joint geometry and welding conditions have been developed for this purpose. With the exception of E7018 consumables, all consumables used in moment frame construction should be lot tested by the manufacturer. In the event that lot testing is not performed by the manufacturer, project-specific testing should be conducted to demonstrate acceptable electrode performance.

3. EFFECT OF INTERMIXING OF CONSUMABLES

3.1 Background

Welding is an integral part of most modern construction and manufacturing operations. Welding operations on any given project frequently involve a range of welding consumables and processes. Such operations may include shop welding with one consumable followed by field welding with a different consumable or tack welding with a particular consumable and deposition of weld metal of different chemical composition over the tack welds. It is often necessary to repair flaws that form as a result of service or defects created during manufacture. Repair welds are often made with welding consumables and processes that are different than those used in the original joint construction.

Pursuant to AWS standards, most welding consumables are optimized without considering dilution effects from either the underlying base metal or from a weld metal of different chemical composition. Depending on the anticipated service requirements and the operating characteristics desired, the alloy levels and slag systems of the consumable are optimized in different ways. The introduction of elements through dilution/intermixing at levels not originally intended can alter the weld metal properties and resulting weld performance.

While a great deal of study has been devoted to dilution effects from base metals, only limited study has been conducted on the effects of intermixing weld metals deposited by different processes/electrode types. Table 3-1 shows typical chemical compositions of different all-weld-metal deposits that are used for structural fabrications. It is noted that the chemical composition of FCAW-S weld metals is substantially different than weld metals deposited by other processes and consumable types. FCAW-S consumables produce very little shielding gas and rely on the addition of large amounts of deoxidizers (primarily aluminum) to react with oxygen and nitrogen from the atmosphere during metal transfer. Thus, most FCAW-S welds typically contain between 0.8 and 1.6 wt. pct. aluminum. Since aluminum is a strong ferrite former, the addition of austenite stabilizers such as carbon, manganese, or nickel are required to avoid coarse ferritic microstructures that may form if the intermediate austenite transformation is repressed. As a result, many FCAW-S weld deposits can contain substantially higher carbon (up to 0.45 wt. pct), lower manganese (as low as 0.5 wt. pct.), and lower oxygen (as low as 30 ppm). Significantly higher nitrogen (up to 700 ppm) is found in most FCAW-S weld metals when compared to weld metals produced by other arc welding processes.

While this chapter focuses primarily on the effects of dilution from FCAW-S deposits, similar effects could occur with other types of consumables or base metals. For example, Evans and Bailey (1997) has documented that even minor variation in trace elements (such as Al, Ti, V, Nb, B, etc.) in E7018 type SMAW deposits can have a profound effect on weld metal toughness. Thus, fabrication or repair procedures that result in hybrid mixtures of different weld metal types should be carefully considered (AISC, 1978) (SAC, 1995).

Table 3-1 Typical Weld Metal Chemical Compositions

Electrode Type	C	S	P	Si	Mn	Ni	Al	N (ppm)	O (ppm)
E70T-4 FCAW-S	0.23	0.003	0.011	0.28	0.50	0.02	1.5-2.0	500-700	40-70
E70T-7 FCAW-S	0.23	0.003	0.007	0.11	0.43	0.01	1.5-2.0	550-700	70-80
E70T-6 FCAW-S	0.09	0.007	0.010	0.25	1.50	0.01	0.7-1.0	300-400	450-550
E70TG-K2 FCAW-S	0.06	0.003	0.008	0.19	1.20	1.3	1.1-1.5	230-350	60-80
E71T-8 FCAW-S	0.16	0.003	0.007	0.29	0.53	0.01	0.5-0.7	200-350	250-340
ER70S-3 GMAW	0.09	0.013	0.015	0.33	0.73	0.03	<0.006	40-90	250-400
F7A2-EM12K SAW	0.06	0.010	0.013	0.36	1.25	0.07	0.020	40-90	600-800
E7018-1 SMAW	0.06	0.012	0.020	0.54	1.35	0.03	<0.010	65-110	380-450
E70T-1 FCAW-G	0.08	0.011	0.009	0.78	1.60	0.03	<0.007	45-60	550-800

Note: All chemical test results are reported in % by weight unless otherwise noted.

A review of the literature revealed that only two studies reported on the effects of intermixing of FCAW-S welds and welds produced using other processes. In the first study, Keeler and Garland (1983) report a large decrease in toughness in the root region when FCAW-S was deposited as a root pass, and high toughness SAW was used for the fill passes. The average Charpy V-notch (CVN) energy absorbed at -25°C (-13°F) was reduced from 100 J (74 ft-lbf.) when the root was deposited using a SMAW consumable to 35 J (26 ft-lbf.) when FCAW-S was used. Similarly, crack opening displacement (COD) results at -10°C (14°F) fell from an average of 0.71 mm (0.028 in.) for the SMAW root to an average of 0.14 mm (0.006 in.) for the FCAW-S root pass with failure initiating in the intermixed region. Similarly, a second study (Klimpel and Makosz, 1993) showed that the -20°C (-4°F) CVN toughness of E7018 SMAW repairs made in E70T-4 weld metal ranged from 68 J (50 ft-lbf.) when only one pass (high dilution of SMAW weld metal with E70T-4) was used to 83 J (61 ft-lbf.) when three SMAW passes (lower dilution with E70T-4) were used to make a simulated repair.

3.2 Measurement of Intermixing Effects

This chapter is intended to summarize the results of several wider investigations involving intermixed weld metals (Quintana and Johnson, 1998, 1999a, 1999b). A summary of an experimental approach used to determine weld metal toughness in intermixed weld metals is described in the following section. Further, this chapter summarizes the effects on the weld metal toughness when intermixing the non-FCAW-S and FCAW-S electrodes shown in Table 3-1.

Figure 3-1 details the weld joint geometry and location of CVN specimens. All multipass test welds were 25 mm (1 in.) thick with a joint geometry incorporating 45° included angle and 12 mm (1/2 in.) root opening. The pass/layer sequence and welding conditions were standardized to reflect standard practice in conformance test welds. Following deposition of the root layers, a two-pass-per-layer technique was employed until the finish. Charpy V-notch impact specimens were removed from three locations in the completed test welds as illustrated in Figure 3-1. The near surface and root specimens were removed from within 1.5 mm (1/16 in.) of the top and bottom plate surfaces, respectively. The specimens at maximum dilution were positioned such that the bottom surface of the CVN specimen at the weld centerline was coincident with the fusion boundary between SMAW fill passes and FCAW-S root passes. For a number of combinations, a full CVN transition curve was produced.

3.3 Mechanical Properties of Intermixed Welds

The mechanical properties of the intermixed welds were measured in weldments produced under laboratory conditions. Actual field conditions may be more or less severe than represented here. Variations in mechanical properties may be expected when welding under different conditions or using different welding parameters for the fill passes. Specifically, the mechanical properties of the intermixed welds may be influenced by several factors such as the amount of dilution with the FCAW-S layer, pass sequence (i.e., proportion of primary weld metal), and joint geometry/configuration.

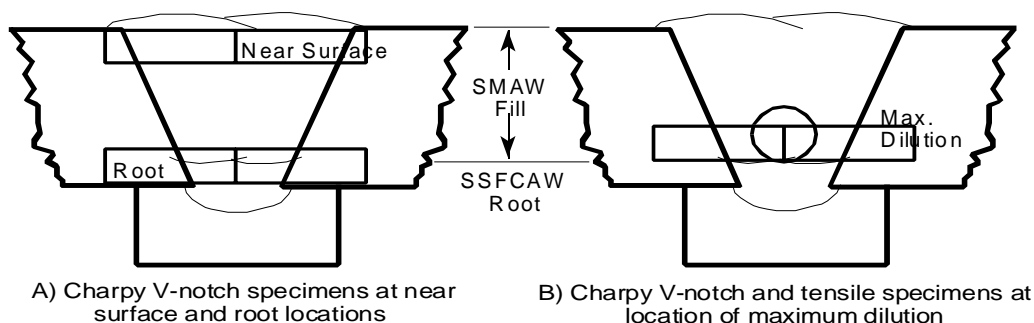


Figure 3-1 Test Specimen Locations

Table 3-2 summarizes the effects of intermixing on the toughness measured in the region of maximum dilution (as shown in Figure 3-1) in the first fill passes. The combinations presented in Table 3-2 represent the toughness that would be expected in fill passes of a given electrode when intermixing occurs. Although toughness may not be substantially reduced in some intermixed weld metal, limited toughness can be expected in the root welds produced by certain electrodes. For example, minimum levels of CVN impact toughness are not required for electrode classifications such as E70T-4 and E70T-7. The toughness measured in E70T-4/E70T-7 electrodes may not exceed 20 ft-lbf. even at elevated temperature. The toughness of the intermixed weld metal measured in the region of maximum dilution with respect to baseline welds is classified in Table 3-2 as follows:

- A. No reduction of CVN toughness was measured in the intermixed weld. Toughness of the intermixed weld is commensurate with that of the fill electrode.
- B. Some reduction in CVN toughness was measured in the intermixed weld metal relative to welds produced using a single fill electrode. The toughness of the intermixed weld metal consistently exceeded 27 J (20 ft-lbf.) at both -18°C and -29°C (0°F and -20°F).
- C. Some reduction in CVN toughness was measured in the intermixed weld metal relative to welds produced using a single fill electrode. The toughness of the intermixed weld metal consistently exceeded 27 J (20 ft-lbf.) at -18°C (0°F) but toughness did not consistently exceed 27 J (20 ft-lbf.) at -29°C (-20°F).
- D. Significant reduction in CVN toughness was measured in the intermixed weld metal relative to welds produced using a single fill electrode. The toughness of the intermixed weld metal may not consistently exceed 27 J (20 ft-lbf.) at 18°C or -29°C (0°F or -20°F).
- E. Substantial reduction in CVN toughness was measured in the intermixed weld metal. Toughness is not expected to exceed 27 J (20 ft-lbf.) at either -18°C or -29°C (0°F or -20°F).

Table 3-2 Impact Toughness Measured/Expected in the Region of Maximum Dilution Relative to Baseline Welds Produced with a Single Fill Electrode

Root Electrode	Fill Electrode						
	E7018	E7018-1	E70T-1	ER70S-6	E71T-8	E70T-6	E70TG-K2
E70T-6	B	B	E	D/E*	A	--	--
E71T-8	B	B	E	D	--	A	A
E70TG-K2	B	B	E	D/E*	A	--	--
E70T-4	C/D	C	E	E*	B	--	--
E70T-7	C/D	C	E	E*	B	--	--
E7018	--	--	--	--	A	A	D
E7018-1	--	--	--	--	A	A	D
F7A2-EM12K	--	--	--	--	A	A	D
E70T-1	--	--	--	--	A	C	D

*Toughness expected, not measured -- No tests conducted

As previously mentioned, intermixing effects in SMAW consumables have been extensively characterized as part of a larger test program (Quintana and Johnson, 1998, 1999a, 1999b). These studies concluded that there was no measurable effect of dilution from the FCAW-S layers on the ultimate tensile strength, yield point, or yield strength of the intermixed weld metals. There was a slight reduction in tensile ductility and reduction in area for the E7018 deposits only. Tensile ductility in diluted E7018-1 deposits was unchanged from the baseline levels. Reduction of toughness relative to typical E7018 and E7018-1 performance was measured in both the region of maximum dilution and root CVN locations for all weld metals tested. While a significant reduction in root CVN impact toughness was measured as a result of dilution from FCAW-S root passes, both E7018 and E7018-1 electrodes are expected to produce impact energies exceeding 20 ft-lbf. (27 J) at 0°F (-18°C). Changes in microstructure and chemical composition found in the region of maximum dilution were limited only to a small region of weld metal, typically the first pass deposited.

In order to minimize a potential reduction in impact toughness, processes and welding procedures that result in deep penetration or high levels of dilution should be avoided.

Table 3-3 shows typical dilution levels produced by various processes. A more complete review of how welding parameters and technique will effect dilution can be found in the AWS Welding Handbook. Depending on the electrode type and welding procedure, dilution can vary considerably within a specific process. While SMAW welds produced with basic electrodes typically give dilution values of 20-30%, higher levels of dilution can be encountered in GMAW, SAW, and FCAW. Therefore, if these processes are to be used to deposit weld metal over FCAW-S processes, some consideration should be given to approaches that minimize the amount of dilution. As summarized in Table 3-2, a detrimental effect of dilution from FCAW-S weld metals is clearly evident in the ER70S-3 GMAW deposits and the E70T-1 FCAW-G deposits. In both cases, a substantial decrease in impact toughness was measured, and the toughness values of these intermixed weld metals located in the region of maximum dilution are not expected to exceed 20 ft-lbf. (27 J) at temperatures above 0°F (-18°C).

Table 3-3 Typical Dilution Ranges Measured for Various Welding Processes

Process	Dilution (%)
SMAW	10-40
GMAW	15-60
FCAW	15-60
GTAW	20-80
SAW	20-70

$$\text{Dilution}(\%) = \frac{\text{Weight of Parent Material Melted}}{\text{Total Weight of Fused Metal}} \times 100$$

The results shown in Table 3-2 and discussed in this paper are intended to provide guidance in the selection of appropriate consumables for fabrication and/or repair or weldments that may involve intermixing weld metals deposited with different consumables/process types. Consequently, fabricators should be encouraged to verify that acceptable performance can be achieved with their particular welding procedure and consumables.

3.4 Summary and Conclusions

Significant changes in the toughness of intermixed weld metals can occur as a part of normal fabrication or during repair welding. The introduction of elements through dilution/intermixing at levels not originally intended can alter the weld metal properties and resulting weld performance. Such effects are not limited to dilution from FCAW-S consumables and careful consideration should be given to potential adverse effects that may be caused when intermixing different consumables with the same welding process, or similar consumables from different processes. A significant reduction in CVN impact toughness was measured as a result of dilution from FCAW-S root passes in weld metals produced with E7018 and E7018-1 electrodes; however, the results presented in this paper suggest that these electrodes are capable of depositing weld metal with impact energies exceeding 20 ft-lbf. (27 J) at 0°F (-18°C). Similarly, E71T-8 electrodes are also expected to deposit weld metal with toughness commensurate to that of baseline E71T-8 weld metals. Fabricators should be encouraged to verify that acceptable performance can be achieved with their particular welding procedure and consumables.

At the present time, a standardized methodology that can be utilized to determine the effects of intermixing on toughness and strength has not been developed. The approaches utilized to evaluate the effect of intermixing described in this chapter should receive additional consideration as a standard approach.

4. HEAT-AFFECTED-ZONE CONSIDERATIONS

4.1 Introduction

From a metallurgical point of view, a welded beam-to-column joint can be divided into several distinct regions: (1) unaffected column material, (2) a heat affected zone produced in the column material during deposition of the beam-to-column weld, (3) the weld metal, (4) a heat affected zone produced in the beam flange during deposition of the beam-to-column weld, and (5) unaffected beam material. Depending on the base materials selected and welding conditions employed during fabrication, the mechanical properties of the different HAZ regions can vary considerably. The manufacture and mechanical properties in the beam and column base metal are reviewed by Barsom and Frank (2000).

4.2 The Heat Affected Zone Regions

The heat affected zone (HAZ) is the portion of a welded joint that has experienced peak temperatures during welding that are high enough to produce solid-state microstructural changes but too low to cause melting. The transformations that occur during the weld thermal cycle do not occur under equilibrium conditions. Thus an equilibrium iron-carbon phase diagram cannot accurately predict the exact thermal boundaries and sites of the various microstructural regions in the HAZ. As will be discussed below, the size, microstructural characteristics, and mechanical properties of the HAZ are a function of the type of base metal being welded, chemical composition of the base metal, heat input, and part thickness. The following sections will define the various regions that are expected in a single and multipass HAZ. Factors that affect the properties of the HAZ in structural steels will be discussed.

4.2.1 Single Pass Welds

During deposition of single pass welds in C-Mn and low-carbon microalloyed steels, four microstructural regions in the HAZ can be identified as shown in Figure 4-1. The microstructure in each region of the HAZ is related to the peak temperature of the thermal cycle experienced during welding. The four general regions and their corresponding temperature ranges are:

<u>Region</u>	<u>Approximate Peak Temperature</u>
Coarse-grained HAZ (CGHAZ)	1100°C-melting point
Fine-grained HAZ (FGHAZ)	A_{c3} -1100°C
Intercritical HAZ (ICHAZ)	A_{c1} - A_{c3}
Subcritical HAZ (SCHAZ)	below A_{c1}

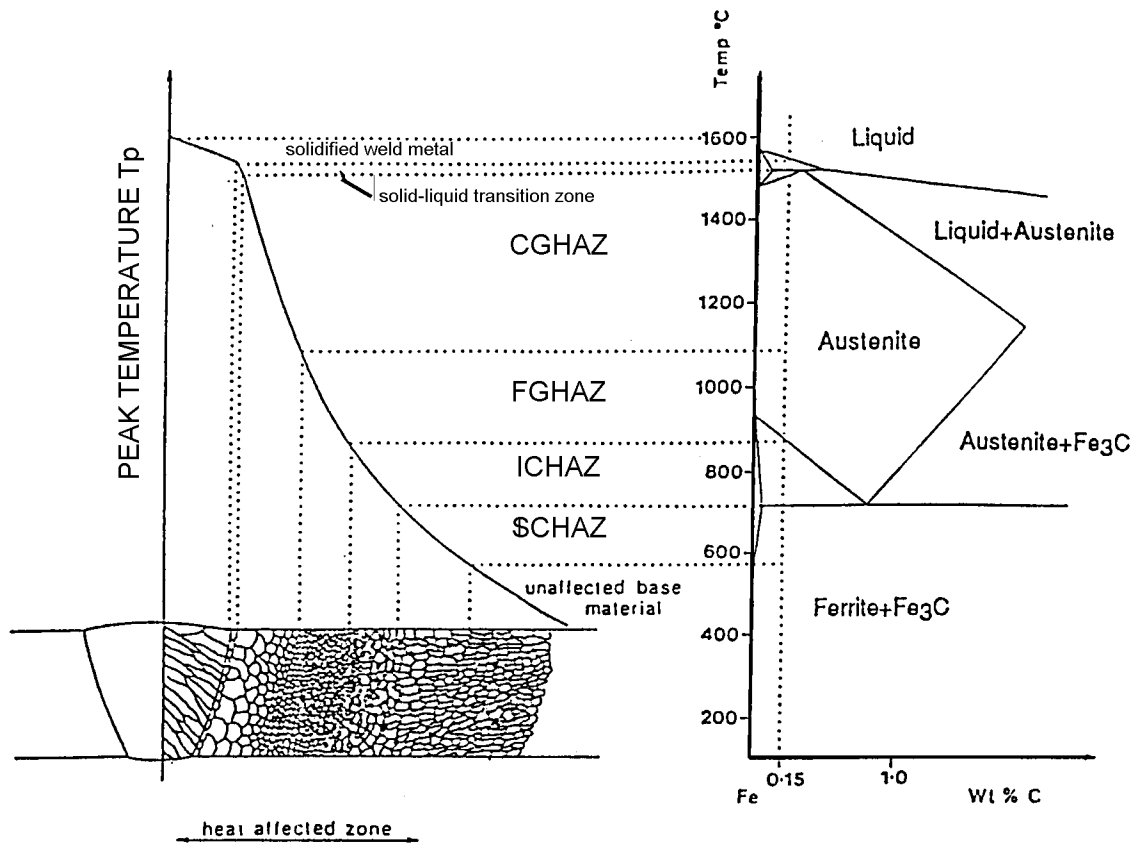


Figure 4-1 A Schematic Illustration of the Various Single-Pass HAZ Regions with Reference to the Iron-Carbon Equilibrium Diagram. A Fe-0.15 wt. pct. Carbon Steel is Shown.

Consistent with the microstructural changes induced during welding, the mechanical properties will vary across the different sub-zones. When compared to the other lower temperature HAZ sub-zones, the CGHAZ, which experiences the most severe thermal cycle, often has higher hardness and lower toughness. For this reason, much of the literature related to HAZ formation and properties has focused on the CGHAZ region. For further description of the evolution and properties in single pass weld heat affected zones, the reader is referred to the individual SAC project report on this topic (Johnson, 2000b).

4.2.2 Multiple-Pass HAZs

During the fabrication of most steel structures, multiple weld passes are required to completely fill the joint or produce a fillet weld large enough to meet minimum size requirements. During multipass welding, the HAZ microstructure of each bead in a multipass weld will be altered by the subsequent pass. Compared to a single pass weld, the HAZ microstructures are more complex.

In multipass welding, grain refinement occurs when transformation to austenite upon heating occurs without subsequent grain growth and subsequent transformation to lower temperature transformation products upon cooling. The percentage and nature of the various HAZ regions in a multipass weld will depend on the number of passes, size of the weld beads, and steel composition. As will be discussed later, the multipass process can be beneficial to HAZ toughness in many cases provided heat input is controlled. Economical requirements, however, generally lead fabricators to increase weld deposit size by using higher heat inputs and larger electrodes. The optimum weld procedure must be chosen by considering a balance between microstructure, and thus properties, and productivity.

In multipass welds deposited in C-Mn steel, each of the HAZ regions associated with each pass can experience multiple thermal cycles which can further alter the microstructure in the HAZ as illustrated in Figure 4-2 (Easterling, 1992). Figure 4-2 shows how HAZ regions in a weld can be subjected to a range of peak temperatures during the deposition of subsequent passes. For example, consider the CGHAZ of weld Y (in Figure 4-2) which has been subjected to a thermal cycle during the deposition of weld X. Portions of the CGHAZ generated during the deposition of weld Y will be subjected to thermal cycles with peak temperatures high in the austenite phase field (CGHAZ + CGHAZ), intermediate temperatures in the austenite phase field (CGHAZ + FGHAZ), peak temperatures within the intercritical region (CGHAZ + ICHAZ) or lower peak temperatures (CGHAZ + SCHAZ). For convenience these regions are often categorized into six regions as compared to the four regions (CGHAZ, FGHAZ, ICHAZ, SCHAZ) used to describe the HAZ regions of a single pass weld. For multipass welds, the two additional regions are as follows: intercritically reheated CGHAZ (ICCGHAZ), and subcritically reheated CGHAZ (SCCGHAZ). In particular, the ICCGHAZ region has been identified as a region that can often experience a substantial reduction in CTOD toughness. Extensive review of factors affecting the formation and properties in multipass weld metal heat affected zones can be found in the general literature. Readers are referred to the SAC project report (Johnson, 2000b), Francois and Burdekin (1998), and Harrison (1990) for a more detailed overview.

4.3 Measurement of HAZ Toughness

A variety of test methods can be used to measure the toughness of steel weldments. Some of these methods, Charpy V-notch (CVN), crack tip open displacement (CTOD), and weld thermal simulation, can be used to evaluate HAZ toughness (Denys and McHenry, 1988) (Fairchild, 1990). It is often difficult to measure HAZ toughness. This difficulty is due in part to the substantial microstructural gradients produced during multipass welding, the relatively small size of these regions, and difficulty in extracting mechanical test specimens that sample the HAZ region exclusively. Depending on the type of test technique, different toughness may be measured. An example of this is reported by Fairchild who documented that a substantial reduction in CTOD toughness was measured when the CTOD notch sampled ICGHAZ regions. In comparison, CVN tests with identical notch location did not experience a substantial reduction in toughness. Thus, these regions were identified as LBZ's. For critical applications, the CTOD test is superior to the Charpy impact test from the viewpoint of estimating the toughness of the non-uniform heat affected zone as a parameter of crack initiation.

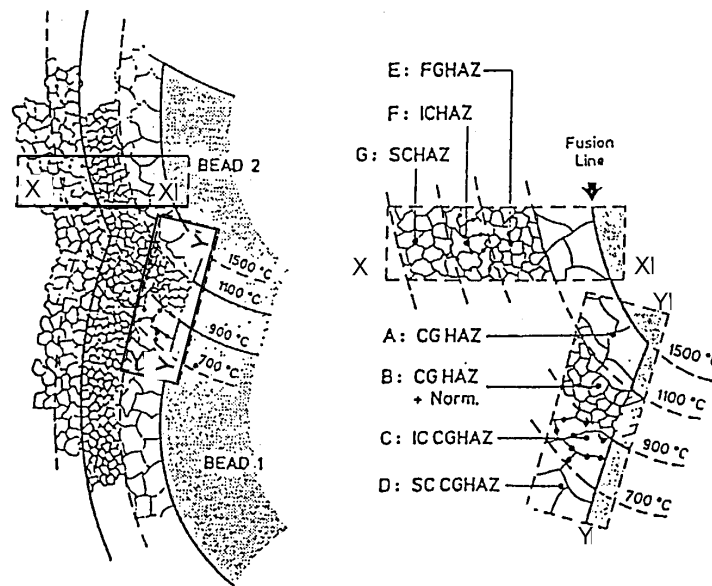


Figure 4-2 Schematic Illustration of the Various HAZ Regions Produced During Deposition of a Multiple Pass Weld

Within some weldments, some small microstructural regions can control the toughness of the entire weldment (i.e., these regions can be considered a weak link). Due to the steep thermal gradients, it is often difficult to characterize factors affecting the toughness of these critical regions. Considerable research has demonstrated that the CGHAZ and ICCGAZ regions in particular can have low toughness. Weld thermal simulation is often an inexpensive, simple, and rapid test method that can be used to produce a large volume of material with a given microstructure. Specialized equipment is used to rapidly heat and cool samples and simulate the thermal cycle experienced at a given point in a HAZ. This technique can be used to generate qualitative data comparing the effects of steel chemistry or the effect of changing weld thermal cycles (i.e., heat input). Most often, a full-size CVN specimen can be subjected to thermal cycles using a weld thermal simulator. Although weld thermal simulation is generally capable of comparing the toughness of various HAZ regions and comparing the effects of various thermal cycles on HAZ toughness, the CTOD test is usually specified to quantify the HAZ toughness produced with a given welding procedure.

4.3.1 Charpy V-Notch (CVN)

Although it is inherently difficult to locate properly the CVN notch in the desired HAZ region and ensure crack propagation through a given microstructural region, CVN tests are still used to characterize HAZ toughness. Typically in weld procedure tests, specimens are extracted at specified locations through the thickness of the plate and the notches placed at specified distances from the weld fusion boundary. For example, a typical procedure in offshore construction is to take specimens from three HAZ locations, namely, the fusion boundary (fb), fb + 2mm and, fb + 5mm (Pisarski and Pargeter, 1984). Although a certain amount of information on variation in HAZ toughness can be obtained by such tests, their primary aim is to ensure that a certain workmanship quality is maintained.

The Charpy test is not considered to be a reliable measure of a steel's sensitivity to local brittle zones (LBZs). As discussed earlier, the main problem is one of sampling. When notched in the HAZ, the Charpy crack tends to average the toughness of a variety of microstructures including the weld metal, various regions within the HAZ, and the base metal. This averaging effect is compounded by, (1) the blunt notch, which increases the volume of material exposed to the maximum normal stress, and by (2) measuring both the initiation and propagation energy of fracture. In addition to shortcomings in detecting LBZs, the Charpy test has limited value because the results provide a qualitative measure of HAZ toughness, and thus are not directly useful for fitness-for-purpose evaluations.

Some shortcomings of the Charpy tests can be overcome by measuring load and deflection during the test. From the load-deflection record, the initiation and propagation energy required to break the specimen can be evaluated separately. Furthermore, if the V-notch is replaced with the fatigue crack, CTOD procedures can be used to evaluate toughness, and post-test metallography can be used to interpret the results. Thus, the instrumented precracked Charpy test has many of the qualities of the CTOD test, but it loses the simplicity and low cost advantages of conventional Charpy testing. Instrumented precracked Charpy testing is also limited by the severe restrictions on specimen size imposed by most Charpy test machines.

In general, it is not possible with the Charpy test to assess the significance of the toughness values measured with respect to the brittle fracture resistance of a structure. The tests may provide a qualitative assessment of toughness if correlation with large scale tests or structural behavior have been established, but even so, this is an indirect measure of fracture resistance. Fracture mechanics tests, on the other hand, can provide a quantitative measure of toughness that may be used to calculate the fracture resistance of a structure.

4.3.2 Crack Tip Opening Displacement (CTOD)

The CTOD test is a common method of measuring the fracture toughness of steel weldments. The preferred specimen design is a full thickness (B), single edge notch bend specimen with a deep crack (crack length to depth ratio $a/w = 0.5$) in a BX2B cross section. The crack tip opening is measured as load is applied, and fracture occurs when the CTOD determined from this opening reaches a critical value. Using the standard procedures of BS 5762 (BSI, 1979), this value is a material property for the specific specimen size, notched location and orientation, temperature, and strain rate used in the test. By locating the crack tip in the specific region of the weldment (e.g., the HAZ), the toughness of that region can be characterized.

Standard procedures have been developed to pre-crack specimens such that the crack tip samples a specific microstructure such as the CGHAZ. Because of the large microstructural gradients that exist in a multipass weldment, it is often difficult to place the crack tip exactly. Therefore, special joint preparations and welding procedures are used to achieve a straight HAZ (often with a minimum CGHAZ percentage) to facilitate placement of the crack tip. One edge of the joint preparation is straight and perpendicular to the plate surface, i.e., a single bevel butt joint or a K-joint.

CTOD Specimens for HAZ/LBZ Testing

Figure 4-3 shows schematics illustrating how a CGHAZ might be sampled by the fatigue pre-crack in a through-thickness (TT) CTOD specimen. It is usually easier to measure HAZ toughness using the TT geometry, and the offshore industry employs this method most frequently.

With through-thickness specimens, both high and low toughness regions will be sampled by the notch front, but the fracture will tend to initiate from the lowest toughness region. On the other hand, generally only one specific region will be sampled by the crack tip in a surface notched specimen. If the fatigue crack tip samples fine grained HAZ, a higher toughness will be recorded than if the crack tip position is moved only slightly into a grain coarsened region. Thus, with surface notched specimens, small changes in crack tip depth can have a significant influence on the toughness values measured. The importance of sectioning each specimen after testing to resolve these issues is discussed in the next section.

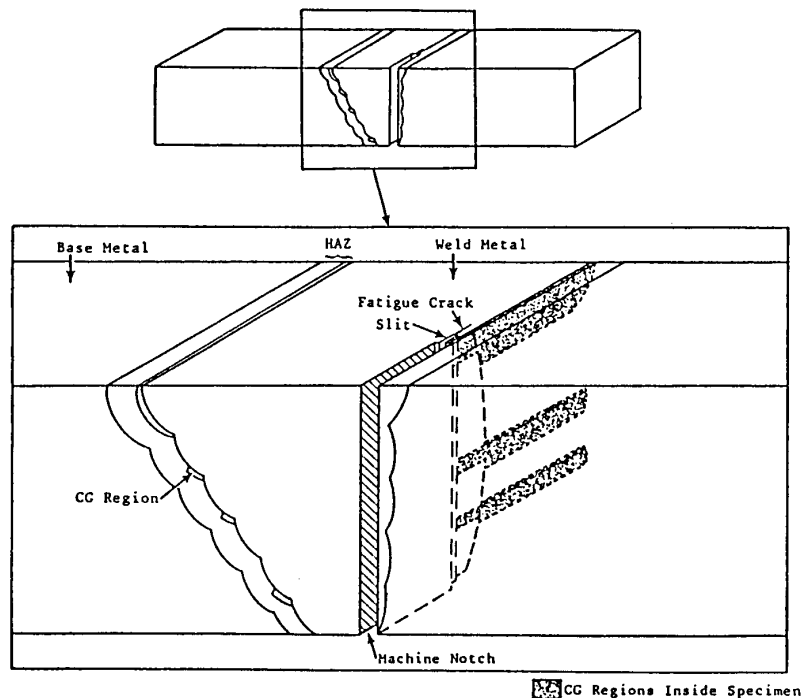


Figure 4-3 Through Thickness Notch Sampling CGHAZ Regions

L-type Specimens: The main problem concerning the CGHAZ CTOD testing is the straightness of CGHAZ regions along the weld length and scalloping of the HAZ (Squirell et al., 1986). It is obvious that waviness of the fusion line in the weld direction and weld bead irregularity in the through-thickness direction will create difficulties for the correct location of a machined notch and a fatigue crack tip in the zone of interest. Additionally, the deviation of the fatigue crack causes yet another major problem, mainly in the (Longitudinal L-type) specimens, as shown in Figure 4-4. Even if the machined notch tip is in correct position within the HAZ, the running fatigue crack may easily deviate into the base or weld metal. The microstructure gradient of the

HAZ, irregularities in the fusion line, the presence of a hardness gradient, or variation in yield strength of HAZ may play a role in fatigue crack deviation.

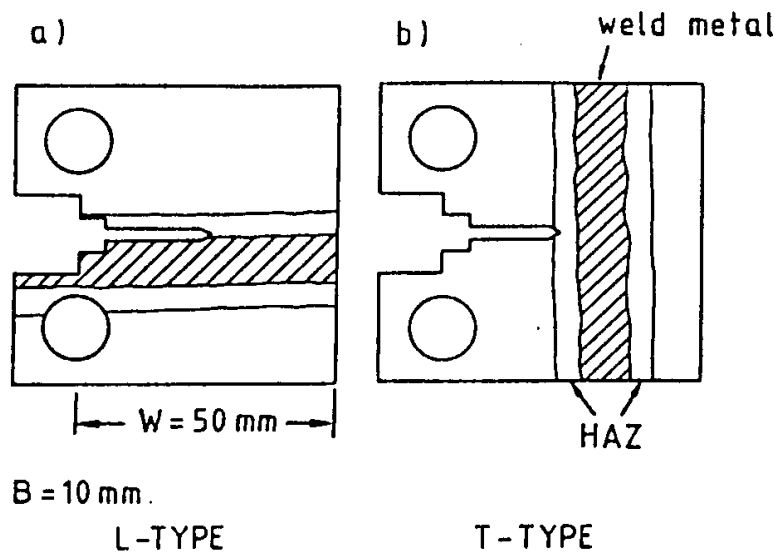


Figure 4-4 Schematic Illustration Showing L-type Specimens and T-type Notch Locations

T-type Specimens. The difficulties with regard to correctly machined notch placement, fatigue crack deviation, and the possibly great number of specimens to be tested can be reduced by using the transverse (T-type) CTOD specimens as shown in Figure 4-4. A T-type HAZ CTOD test can be carried out as a screening test for the most embrittled zone of HAZ since there is a need to identify regions of low fracture toughness for the general assessment of HAZ. The crack tip positions in various distances to the fusion line may give the complete fracture behavior of the HAZ. It seems that the L-type HAZ CTOD specimens tend to produce more difficulties than the T-type specimens to obtain valid lower-bound toughness results.

Sectioning of Specimens

Scatter of results observed when testing the HAZ can be caused by two factors. First, scatter will occur as a result of inherent material property variability within the specific HAZ region sampled, and where tests are conducted at a temperature within the transition regime, scatter can be especially high. Second, scatter will occur as a result of experimental errors brought about by the difficulty of placing the crack tip in the same HAZ region in each test. For example, very different toughness values will be measured if in one specimen the tip samples the grain coarsened HAZ, whilst in another it samples the fine grained region. By sectioning the specimens after the test to identify the microstructures sampled by the crack tip and in particular at the fracture initiation point, the sources of scatter can be isolated (Squirrell, 1986).

It is vital that all HAZ specimens are sectioned after testing and that sectioning is considered an integral part of the HAZ fracture toughness test, otherwise judgements may be made on the

basis of unrepresentative data. An example of the sectioning procedure for a through-thickness notched CTOD specimen is shown in Figures 4-3 to 4-5. However, because of the complexity of this type of sectioning procedure and the need to interpret the results obtained, the detailed requirements should be agreed upon by the parties involved.

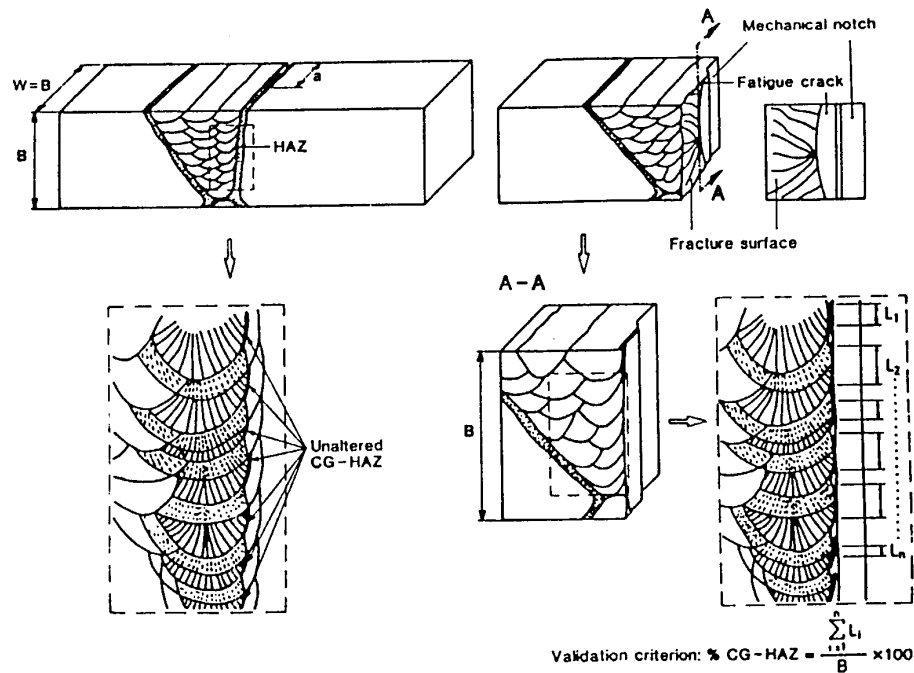


Figure 4-5 Schematic Illustration Showing Approach Used to Quantify the Percent of Unaltered CGHAZ Region Sampled in a Through-Thickness L-type CTOD Specimen

4.3.3 Weld Thermal Simulation

Weld thermal simulation is an inexpensive, simple, and rapid test method to investigate fundamental phenomena in a large number of specimens. It is used to simulate the weld thermal cycle under laboratory conditions in order to obtain information about microstructural and property changes in the HAZ. Although, in principle, these changes can be observed and measured from real welds, in practice it is more convenient to work with test pieces representative of one, not a range, of microstructures and grain sizes, particularly if mechanical property measurements are required. For this purpose weld simulators have been developed and are usually based upon resistance heating and water cooling of samples. It is possible to program the required thermal cycle to any required temperature-time profile, and to plot this thermal cycle and record phase transformations using a dilatometer. The effect of preheat or interpass temperature is easily accommodated by suitable programming of a computer.

Tests on Simulated Microstructures

The specimen size used is selected to have the typical dimensions of a Charpy V-notch sample. The usual cross-section size (10 x 10 mm) is convenient for microscopic examination,

including electron microscopy. Toughness is measured using either Charpy or CTOD specimens.

The effects of specimen size and HAZ microstructural gradients cannot be accounted for in tests on simulated microstructures. However, the results of simulation tests do yield true material properties and are indicative of microstructural and compositional factors that may influence HAZ toughness. When the weld HAZ contains large regions of microstructures that are similar to those tested in simulated specimens, CTOD tests on simulated HAZs give better correlation with weld HAZ toughness than Charpy tests (Fairchild, 1990).

Control of HAZ Grain Size

In general, the HAZ region adjacent to the weld interface has a relatively large grain size (coarse-grained HAZ). This region usually exhibits the poorest toughness. The interaction between material composition and the weld thermal cycle (primarily cooling rate) on the HAZ toughness has been shown to be very complicated and highly dependent upon grain size. Because a significant improvement in HAZ toughness results when the grain size is refined, methods to control the grain size in the HAZ are of great interest.

In most practical situations, fabricators will use high heat input welding procedures to maximize the deposition rates. At the present time, there are no limits on the maximum heat input that can be used during the welding of structural steel moment-resisting connections. The effect of using high heat input will generally reduce HAZ toughness. Recommendations are to bracket the heat input between 30 and 80 kJ/in.

For a given heat input, the distribution of HAZ microstructures is also influenced by bead size. For a constant heat input, bead size will be controlled by the ratio of wire feed speed to travel speed. A reduction in the HAZ prior austenite grain size with a consequent increase in the HAZ toughness can be achieved by using higher welding speeds. Welding speed has a marked effect on the time above the A_{c3} temperature and on the width of the transformed HAZ.

For critical applications or repairs in which higher preheat levels are not possible or PWHT is not desirable, grain refinement can also be achieved by low heat input buttering of the weld groove face, and then filling the groove using higher heat input. The half-bead technique is another method available to refine the CGHAZ by grinding the first layer to a predetermined depth. By this technique, the CGHAZ of the first layer can be refined by subsequent second layer beads without changing the welding parameters. In addition, increasing the weld interpass temperature also increases the width of the refined region.

To increase the toughness in the last-pass HAZ through tempering and grain refinement, temper-bead technique can be utilized. A temper bead is an additional weld pass critically deposited over the last pass to provide both tempering and some degree of grain refinement in the last-pass HAZ. Subsequently, the temper bead may be removed by grinding along with the weld crown to eliminate stress concentration effects. However, the temper bead technique is difficult to control in practice due to the critical requirement of bead position as well as heat input control. The beads must be positioned to achieve maximum refinement in the HAZ, but not

so close that a new coarse-grained HAZ region is created. A relatively high preheat temperature for the temper-bead passes can be helpful by increasing the tolerance for positioning of the temper bead. While this technique is not useful for primary fabrication of structural steel, it may be employed during repair operations.

Welds deposited at heat input levels below 90kJ/in. (3.6kJ/mm) produce a HAZ of greater toughness than that of the base material. However, toughness quickly falls away at higher heat input levels. The ferrite/pearlite structures showed the original grain size in the HAZ to be considerably larger than that of base metal and yet for heat inputs below 90 kJ/in the HAZ, toughness is greater than the base metal. It is therefore clear that, in these cases, refinement of the structures by preceding welds must have a large influence on the average toughness of the HAZ but, as the heat input is increased, the refinement effect diminishes.

4.4 The Effects of Post Weld Heat Treatment (PWHT)

Heat treatment is applied to welded steel constructions for two main reasons. First, it may be necessary to improve the mechanical properties across the weld region; in particular the toughness of the weld may be below that of the parent material, and an improvement is usually achieved by tempering and reducing the hardness of the microstructure. Second, heat treatment is often applied to reduce the high levels of residual stress, which are induced along and across weldments during cooling after welding. High temperature PWHT is often employed in the fabrication of pressure vessels or steel subject to sour service. The use of PWHT for structural applications following fabrication is not generally practical for most steel framed buildings. For additional discussion on this topic, the reader is referred to the SAC project report on HAZ toughness (Johnson, 2000c), or work by Shiga (1996), and Konkol (1988).

4.4.1 Toughness in Structural Steel Shapes

Relatively few studies related to the HAZ toughness of steel shapes produced from electric arc furnace (EAF) steel are available. Limited study of the CGHAZ toughness of Grade 50 EAF beam and column material was undertaken as part of the FEMA/SAC program (Johnson, 2000c). Additionally, Arbed supplied results from previous studies on QST steels intended for offshore service and construction of steel frame buildings. In the Arbed studies, consideration was given to HAZ toughness produced by several welding processes/heat inputs in Gr. 50, 60, and 65 material.

4.4.1.1 ASTM A572 Gr. 50

Figure 4-6 shows a schematic illustration of a bottom flange weldment and potential crack paths. Based on observations of full-scale connection tests at Lehigh and the University of Michigan, the crack paths shown in Figure 4-6 have been observed to initiate due to low cycle fatigue (Barsom, 1999). During full-scale testing, low-cycle fatigue cracks initiated at the intersection of the weld-access hole and the beam flange, and at the weld toes, and propagated as testing progressed. Although only limited cracking occurred in the column material, cracks may initiate and propagate in a direction parallel to the rolling direction.

As part of the FEMA/SAC investigations, weld thermal simulation was used to evaluate the CGHAZ toughness in W14x398 ASTM A572 Gr. 50 /ASTM A992 column material tested at UTA, W14x455 column material (presumably A572 Gr. 50) extracted from a building in Los Angeles, and W36x150 ASTM Gr. 50 beam material tested at Lehigh. The orientation of the test samples is shown in Figure 4-7. Samples extracted from column material were oriented and notched so that the crack propagated parallel to the rolling direction (S-L). Samples extracted from beam flange material were oriented and notched so that the crack propagated in the (L-S) direction. Thermal cycles corresponding to arc energies of 20, 70, and 120 kJ/in. were simulated.

Figure 4-8 shows that the toughness of the material in W14x398 ASTM A572 Gr. 50 /ASTM A992 column material was lower than typically expected when CVN samples are extracted from locations and orientations as specified by ASTM. The application of simulated CGHAZ thermal cycles to this material resulted in a slight improvement in toughness. The application of simulated weld thermal cycles resulted in a net microstructural refinement relative to the coarse microstructure observed in the hot rolled flange interior. The chemical composition of this material is shown in Table 4-1. This material and most of the material evaluated in the FEMA/SAC program had chemical compositions which were fairly lean and included the addition of vanadium, silicon, or both.

Figure 4-9 shows that the as-rolled toughness of the column material extracted from an older existing building in the Los Angeles area was very poor with an expected transition temperature above 200°F. This poor toughness was likely caused by the sample orientation and coarse microstructure in the central portion of the column flange. The application of simulated weld thermal cycles resulted in a net improvement of toughness relative to the hot rolled product. The impact toughness measured in the simulated material would exceed minimum base metal specifications required as part of the current ASTM A992 specification. Comparison of the toughness of the simulated CGHAZ regions suggests that increasing heat inputs in this material would be detrimental to toughness. The chemical composition of this material is shown in Table 4-1. The higher copper and phosphorous concentrations indicate that this material may have been produced using the EAF process.

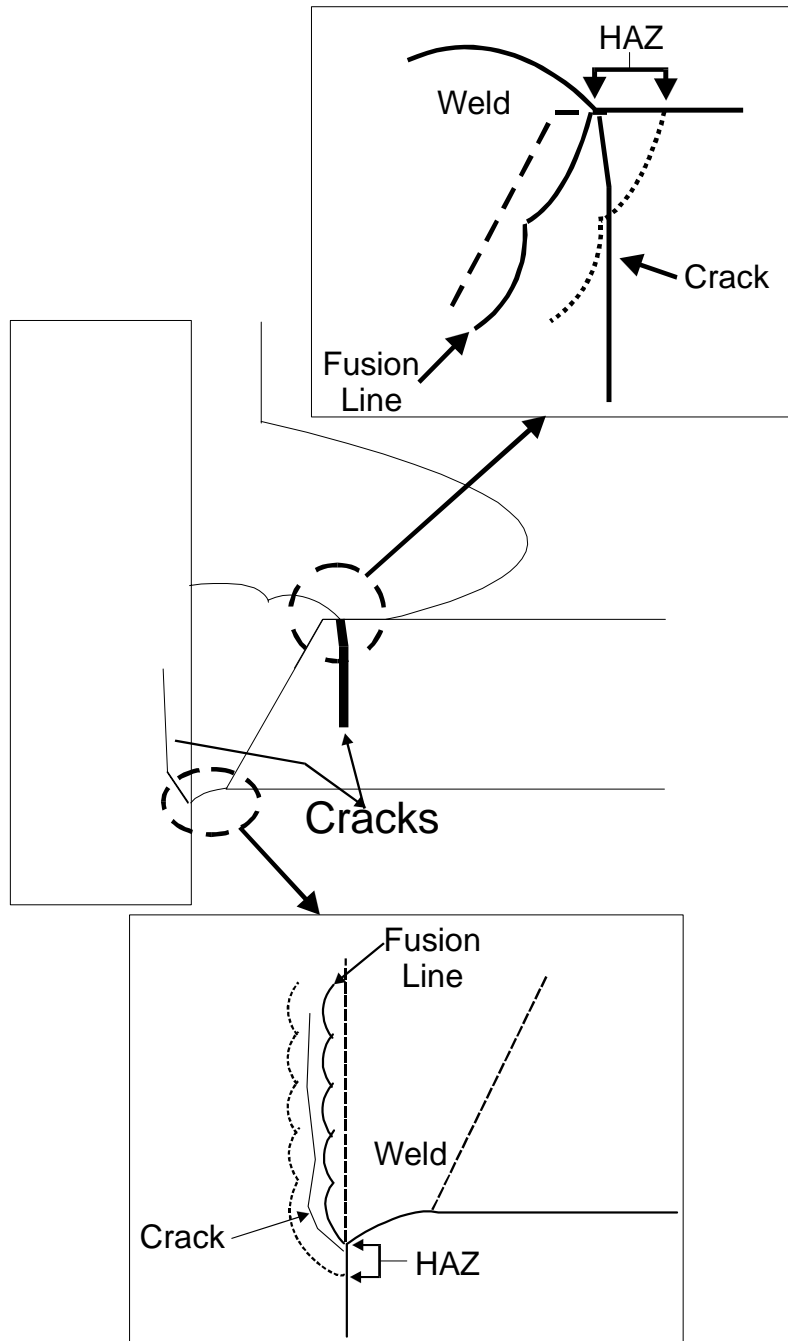
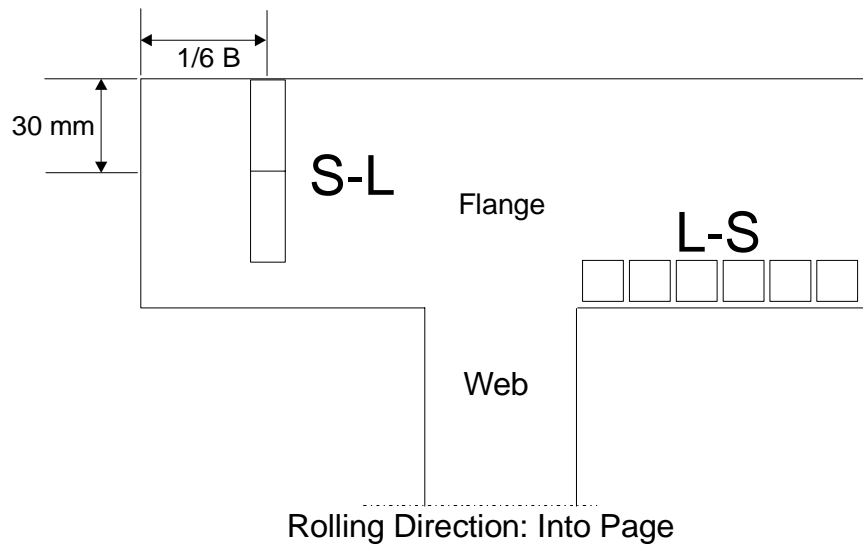
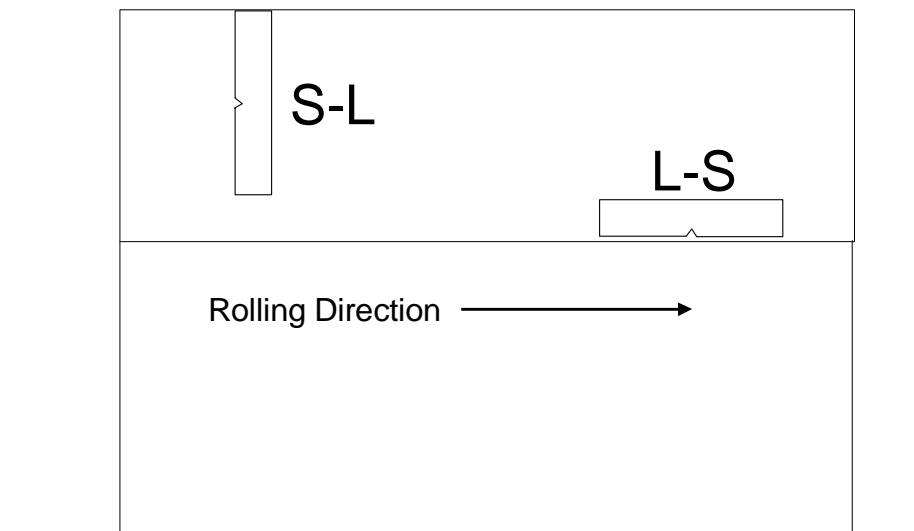


Figure 4-6 Schematic Illustration of Potential Crack Paths in a Bottom Flange Weldment



(A)



(B)

Figure 4-7 Specimen Location and Orientation for CGHAZ Simulation as Part of the SAC Study. Samples Extracted from Column Material were Oriented and Notched so that Crack Propagation Occurred in the S-L Direction. Samples extracted from Beam Material were Oriented so that Crack Propagation Occurred in the L-S Direction.

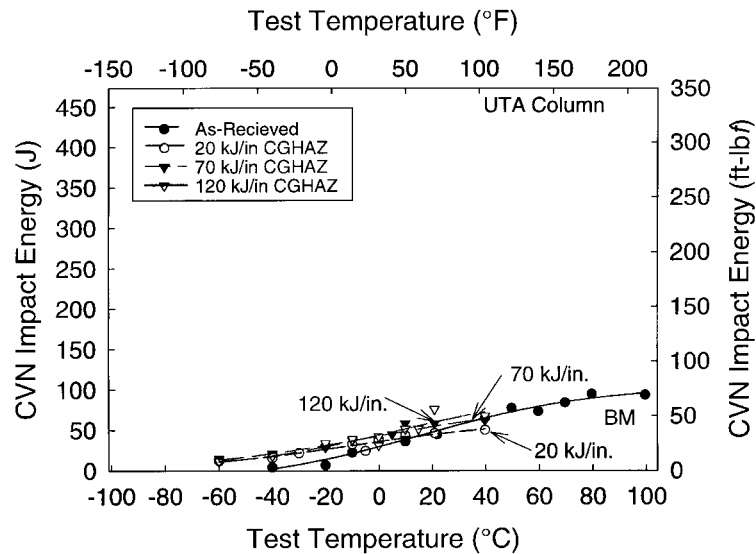


Figure 4-8 Simulated CGHAZ in W14x398 ASTM A572 Gr. 50 Column Material

Figure 4-9 shows the effect of applied simulated thermal cycles on the toughness measured in W36x150 ASTM A572 Gr. 50 beam flange material. Higher as-rolled toughness was measured in this material when compared to the column flange material. As expected, finer microstructures were promoted in the beam flange by higher deformation and faster relative cooling rates. Although the toughness of the simulated HAZ regions was quite high, the potential effects of increasing heat input are evident with an increase in the transformation temperature with the application of thermal cycles corresponding to higher heat input welds.

Although it is not practical to correlate directly the absolute toughness measured in simulated CGHAZ regions with actual welds, the trends in microstructure, hardness, and toughness are expected to be similar. The results from the SAC study suggest that a minor improvement in toughness relative to the hot-rolled toughness may be expected in EAF steel. These results also suggest that toughness is expected to decrease with increasing heat input. Based on these preliminary results, welding with heat inputs ranging from 30 to 70 kJ/in should not result in a substantial degradation of HAZ toughness. It should be pointed out that the steel tested as part of the FEMA/SAC program did not have chemical compositions that fell near the maximum levels allowed in the ASTM specifications. It may be worthwhile to investigate the HAZ properties of steel with a richer composition or steel that is silicon-killed and does not contain microalloying elements such as Al, V, or Nb.

Table 4-1 Chemical Compositions of the Beam and Column Material Subject to CGHAZ Thermal Simulations in the SAC Study

Element	W14x398	W36x150	W14x455
	A572-50	A572-50	A572-50
C	0.077	0.075	0.200
Mn	1.44	1.12	1.33
P	0.015	0.013	0.050
S	0.020	0.017	0.003
Si	0.25	0.22	0.26
Ni	0.13	0.13	0.06
Cr	0.12	0.09	0.03
Mo	0.03	0.03	0.01
Cu	0.34	0.32	0.14
V	0.05	0.03	0.05
Al	<0.01	<0.03	0.02
Ti	<0.01	<0.005	<0.005
Nb	<0.005	<0.005	0.03
Pb	0.01	<0.01	<0.01
Sn	0.01	0.01	<0.01
As	<0.01	<0.01	<0.01
B	<0.0005	<0.0005	<0.0005
CEQ	0.39	0.32	0.45

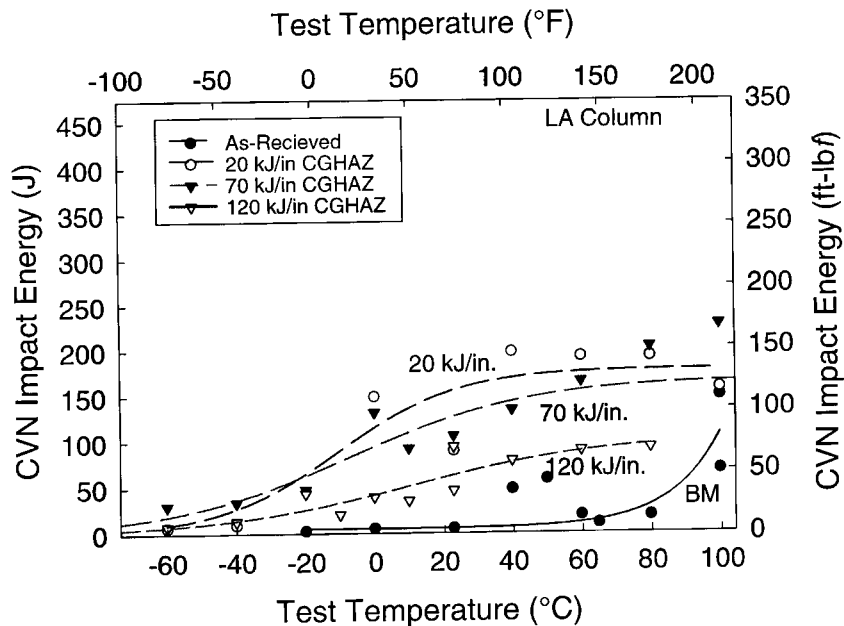


Figure 4-9 The Effect of Thermal Cycles on the CVN Toughness of As-Received W14x455 Column Material Subjected to CGHAZ Thermal Cycles Corresponding to Heat Inputs of 20 kJ/in, 70 kJ/in, and 120 kJ/in. The Column Material was Extracted from a Damaged Building in the Los Angeles Area.

4.4.1.2 HAZ Toughness of QST Jumbo Columns

As part of qualifying steel for API RP 2Z, prEN 10225, and ASTM specifications, the Arbed Group has conducted an extensive testing program on the weldability of QST wide-flange beams. Arbed provided copies of these test reports to EWI for purposes of this review (Trade Arbed, 1989, 1991, 1992, 1993, 1999). This testing was either sub-contracted to an independent facility and witnessed by an agency such as DNV or Lloyds or conducted by Profil Arbed. Testing that was conducted by Arbed was also witnessed. As part of the programs sponsored by Arbed, extensive CVN and CTOD testing of the base metal and weld HAZ regions was undertaken. As will be reviewed below, welds were produced with a variety of welding processes and a range of heat inputs. While this type of testing program is quite costly, it is quite rigorous due to the critical service requirements expected of material produced for offshore applications. QST steel produced to yield Gr. 50, 60, 65, and 70 was evaluated. In addition to evaluation of the various grades of steel, an extensive investigation related to the influence of tramp elements on steel properties was also conducted by Arbed. The work sponsored by Arbed is summarized below. If more information is required, interested parties are encouraged to contact Arbed directly.

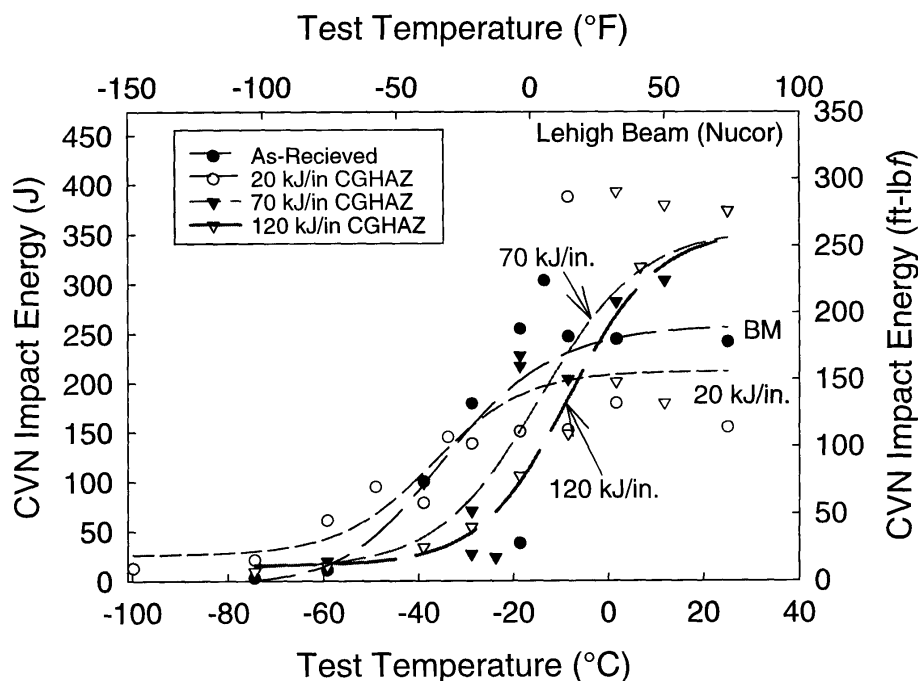


Figure 4-10 The Effect of Simulated CGHAZ Thermal Cycles on the Toughness of W36x150 ASTM A572 Gr. 50 Beam Flange Material

The following base material/consumable combinations were evaluated by Arbed:

- HISTAR 355 TZ OS W14x16 x 311 welded with basic SAW.
- HISTAR 460 TZK OS W14x16x311 (Grade 65) welded with FCAW-G (E80T1-K2), and basic SAW.
- HISTAR 460 W14x730 welded with SMAW (E8018-C3), FCAW (E81T1-Ni1), and SAW (F7A6-EH11K).
- NR 400 (Lincoln Electric FCAW-S) with Grade 50 W14 x 16x730, Grade 60 HEM 550, and Grade 65 W14x16x342 shapes, NR-450H for Grade 70 HEM 300.

Testing of the HISTAR TZ OS W14x16x311 shapes was conducted according to API RP 2Z by Arbed and witnessed by Lloyd's Register of Shipping. As part of this evaluation, the following tests were conducted: Three valid CTOD tests at -10°C in the CGHAZ (including the unaltered CGHAZ, ICCGHAZ, and SCCGHAZ), two valid CTOD tests at -10°C in the unaltered SCHAZ, and CVN transition curves for the CGHAZ and unaltered SCHAZ regions (at the root and 1/4 thickness locations). Evaluation of weld metal toughness, hardness traverses, and sub-surface and mid-thickness base metal CVN toughness was also evaluated. Test specimens were extracted from SA welds deposited using heat inputs of 1.5 kJ/mm, 3.0 kJ/mm, and 50 kJ/mm.

The toughness of the base material at the near surface and mid-thickness locations (in the longitudinal and transverse directions) was quite high, with toughness exceeding 100J at temperatures of -50°C or lower. As expected, slightly lower toughness was measured in the samples extracted from the mid-thickness locations. Consistent with the high quality SAW consumables used in this study, high toughness was measured in the weld root and $\frac{1}{4}$ thickness locations. Toughness of the SAW welds depended on heat input. In the 3.0 and 5.0 kJ/mm welds, 100 J were absorbed at temperatures of -60 and -65°C respectively. In the 1.5 kJ/mm weld metal, 100 J were absorbed at a temperature of -45°C . CVN toughness equivalent to or higher than the weld metal toughness was measured in the CGHAZ and SCHAZ regions. Increasing heat input had little effect on the CTOD toughness measured at -10°C . CTOD values ranging from 1.3 mm to 2.5 mm were measured in both HAZ regions evaluated. These values easily exceeded the 0.25 mm minimum value specified by API. Examination of the hardness data measured at near surface, mid-thickness, and root locations revealed that near matching of the base metal was provided by the weld metal and that no substantial decrease in the SCHAZ hardness occurred.

A similar testing program was carried out by Arbed and Sintef to evaluate HISTAR 460 TZK OS W14x16x311 (Grade 65) shapes. Base metal toughness of the exterior, mid-thickness, and interior regions of the flange were measured. Similar to the Grade 50 material, the lowest toughness was measured at the core region when transverse CVN samples were extracted (100J at -20°C). In all other samples, more than 100 J were absorbed at lower temperatures (below -70°C). A CTOD transition curve was developed for the base material. CTOD values of 2.78 mm were measured at -10°C and toughness decreased in a linear fashion with a CTOD value of 0.57 mm measured at -90°C . CVN samples were notched in the weld, at the fusion line (FL), FL + 2 mm, FL + 5 mm, and in the unaffected base metal. For CVN samples located at the cap and root locations, the base metal and HAZ toughness substantially exceeded the weld metal and fusion line toughness in welds produced at all three heat inputs. For samples extracted from the mid-thickness location, the highest toughness was measured in the FL + 2 mm, FL + 5 mm samples. All WM and HAZ CTOD testing was carried out at -10°C . The CTOD toughness of the FCAW-G weld metal deposited at 0.8 kJ/mm was substantially lower (~ 0.10 mm) than the basic SAW weld metal deposited at higher heat inputs (~ 1.5 mm). As a result, the CGHAZ CTOD toughness barely met the minimum specified toughness of 0.25 mm. The 3.5 and 5.0 kJ/mm CGHAZ toughness ranged from 0.6 mm to 1.10 mm. Higher toughness (~ 1.5 mm to 1.7 mm) was measured in the ICHAZ regions produced during deposition of welds using all three heat inputs. Although the toughness measured in the HAZ at -10°C was substantially lower than the base metal, the values reported by Arbed for Gr. 65 material are still quite high given the range of heat inputs used to produce the experimental welds.

4.4.1.3 Effect of Scrap Quality on the Toughness of A913 Steel

With the use of scrap material as a source of iron, pick-up of tramp elements such as copper, tin, chromium, and nickel can occur. As with many new products or processes, concern has been expressed regarding the effect of tramp elements on the HAZ properties of EAF steel. Although copper is intentionally added as a precipitation strengthening agent in some high-strength low-alloy (HSLA) steels (ASTM A710 for example) and to weathering steels to improve corrosion

resistance, concerns regarding copper levels in EAF steel still exist. It is well known that copper, when added in sufficient quantities (typically more than 1 percent) to steel can promote liquation cracking in the HAZ or solidification hot cracking in the weld metal (particularly at higher weld metal carbon concentrations).

In order to address concerns of the effect of copper and impurity content on the weldability of A913 QST type steels, Arbed has conducted a study with intentional variations in scrap quality. The Arbed study addressed the as-received and as-welded strength and toughness levels of 76 industrial heats of material with a range of strengths. Tramp elements expressed by copper contents ranging from 0.15 to 0.85 wt. pct. were considered. CVN testing at standard locations was undertaken using heats of material with various copper concentrations. For copper contents ranging from 0.40 to 0.60 wt. pct., impact toughness was similar to that of steel with lower copper concentrations (<0.20 wt. pct.). Although some degradation of toughness was measured in steels with high (0.85 wt. pct.) copper, these steels still met minimum toughness requirements of 27 J at 0°C. Similar results were observed when CVN testing of the HAZ region of welds deposited using a range of heat inputs. In all cases, the HAZ CVN values were similar to or slightly below parent properties. For the welding procedures employed by Arbed, relatively little copper dilution from the base metal to the weld metal occurred. The results presented by Arbed are consistent with the results of Hannerz (1987) and Kluken, et al. (1994).

4.5 Summary and Conclusions

Based on the review and discussion above, it is clear that the factors which influence the properties of heat affected zones in steel are numerous and complex. Standardized techniques developed to evaluate multipass heat affected zone toughness were reviewed. It is clear that measurement of multipass heat affected zone toughness using standard CVN test techniques is of limited use due to the heterogeneous nature of the HAZ region. Additionally, the use of CTOD specimens to measure HAZ toughness can be difficult since crack location is critical. If CTOD crack placement does not sample appropriate microstructures, considerable scatter will occur. Thermal simulation can provide an economical alternative for comparing the toughness measured in a single simulated region in one material with another.

The metallurgical factors influencing HAZ evolution and toughness in structural steels have been discussed. It is clear that microalloying additions (either intentional or unintentional) can have a beneficial effect on HAZ toughness. Toughness data collected on HAZ toughness in A572 Gr. 50 steel as part of the FEMA/SAC program of investigations, along with HAZ toughness data on A913 steel, were reviewed. Based on review of the available literature and the information gathered as part of the FEMA/SAC program, it is expected that HAZ toughness of hot rolled and QST steel shapes should be expected to be higher than that of the as-received base metal.

Most of the steel tested in the FEMA/SAC Program was supplied to A572 Gr. 50 or A913 Gr. 50 specifications. These steels contained either Al, Nb, or V microalloying elements that were either intentionally added or introduced through scrap. Review of ASTM A992 suggests that microalloying elements are not required provided that low levels of nitrogen are maintained.

The consequences of deposition of high heat input welds on micro-alloy-free hot-rolled structural steel should be the subject of further study.

5. EFFECT OF HYDROGEN ON WELD METAL PROPERTIES AND INTEGRITY

5.1 Summary

Following the 1994 Northridge earthquake there were concerns that some of the damage to welds in steel moment frames was related to either weld metal hydrogen embrittlement or to the effects of hydrogen assisted cracking. As mentioned elsewhere in this report, the use of weld metal with improved notch toughness is now specified. In many cases, the alloy content of the consumables capable of meeting these specifications has increased so that minimum toughness requirements could be met. In some weld metals deposited using the newer E7XT-X consumables, weld metal tensile and yield strengths have been observed to approach 100 ksi (690 MPa) when using moderate to low heat inputs. This chapter provides a basic review regarding the effects of diffusible hydrogen on the mechanical properties of steel, consideration of preheat to avoid hydrogen-assisted cracking, hydrogen control in FCAW consumables, and low-temperature diffusion of hydrogen from a weld after welding. Recommendations regarding limitations of diffusible hydrogen, appropriate preheat/interpass requirements, consideration of low-temperature PWHT, and hydrogen control in FCAW consumables are made based on consideration of testing conducted as part of the FEMA/SAC program in conjunction with review of relevant literature.

5.2 Effects of Hydrogen in Steel

The effects of hydrogen on the mechanical properties and soundness of steel have been reported in more than 1,000 articles over the past 70 years. Review of early literature shows that the effects of hydrogen on mechanical properties and cracking propensity had first been documented by Swinden and Reeve (1938) and a general theory related to the mechanisms causing hydrogen-assisted cracking had been proposed by Hopkins (1944). While many of the problems associated with hydrogen are not new and have been well documented in the past, some of the mechanisms related to hydrogen degradation are still not well understood, and research in this area still continues today. This section focuses on the effects of hydrogen related to welding of structural steel. Specifically, the following topics are covered:

- Introduction of hydrogen into the weld pool
- Effect of hydrogen on mechanical properties
- Hydrogen-assisted cracking in the heat-affected zone
- Hydrogen-assisted cracking in the weld metal
- Low-temperature PWHT

5.2.1 Introduction of Hydrogen into the Weld Pool

During welding, hydrogen in the arc atmosphere is dissolved into the liquid weld metal (the solubility of hydrogen in liquid iron is quite high (38 ml H₂/100g weld metal at 1 atm and 1600°C) (Graville, 1975) (Coe, 1973), and considerable quantities can be retained at low temperature. The solubility of hydrogen in steel depends on temperature, pressure, and steel composition. The solubility of hydrogen in steel at room temperature is quite low, and a sudden increase in solubility occurs when ferrite (α) transforms to austenite (γ) upon heating. The solubility drops again at higher temperatures when austenite (γ) transforms to delta-ferrite (δ).

Hydrogen may be present in iron and steels in elemental form within the lattice (interstitial) or in molecular form (i.e., gas) at inclusions or internal discontinuities. Many interstitial alloying elements can have a profound effect on the mechanical behavior of alloys. The elements normally considered to be interstitial are carbon, nitrogen, hydrogen, oxygen, and boron. Unlike other interstitial elements, hydrogen will diffuse through and out of steel even at room temperature. Since the late 1940's, many studies have been conducted to determine the diffusion coefficients of hydrogen in steel (Sykes, et al., 1947). Recent reviews (Bollinghaus, et al., 1994, 1995) on the topic of scatterbands for hydrogen diffusion coefficients in microalloyed and low-alloy steels contain data from over 220 studies. Figure 5-1 shows the scatterband for the hydrogen diffusion coefficient in steel up to 600°C. Table 5-1 (Bailey, et al., 1993), (Dallam, et al., 1999), and (Andersson, 1980) gives some typical values for structural steel, basic SMAW weld metal, and FCAW-S weld metal. A single value for overall diffusivity of hydrogen in steel will depend on the type of material under consideration. Based on the information presented in Table 5-1, it is clear that the diffusivity of hydrogen in steel weld metal is much lower than in most mild steel base metals and that the diffusivity of hydrogen in a particular steel will depend on microstructure, alloy content, and inclusion volume fraction. Further consideration of the diffusivity values presented in Table 5-1 will be discussed later in the low-temperature PWHT section.

5.2.2 Sources of Hydrogen

The primary sources of hydrogen found in a welding consumable are (Bailey, et al., 1993):

1. Coating moisture associated with SMAW flux coatings, SAW fluxes, or core ingredients in flux-cored and metal-cored wires.
2. Any other hydrogen bearing compounds in the coating or flux (i.e., cellulose in the case of XX10 type SMAW electrodes).
3. Drawing lubricants, oil, and grease either on the surface of the electrode or trapped in the seam of FCAW and metal core consumables.
4. Hydrated oxide (i.e., rust on the surface of welding wires).
5. Moisture in shielding gas for gas-shielded processes.

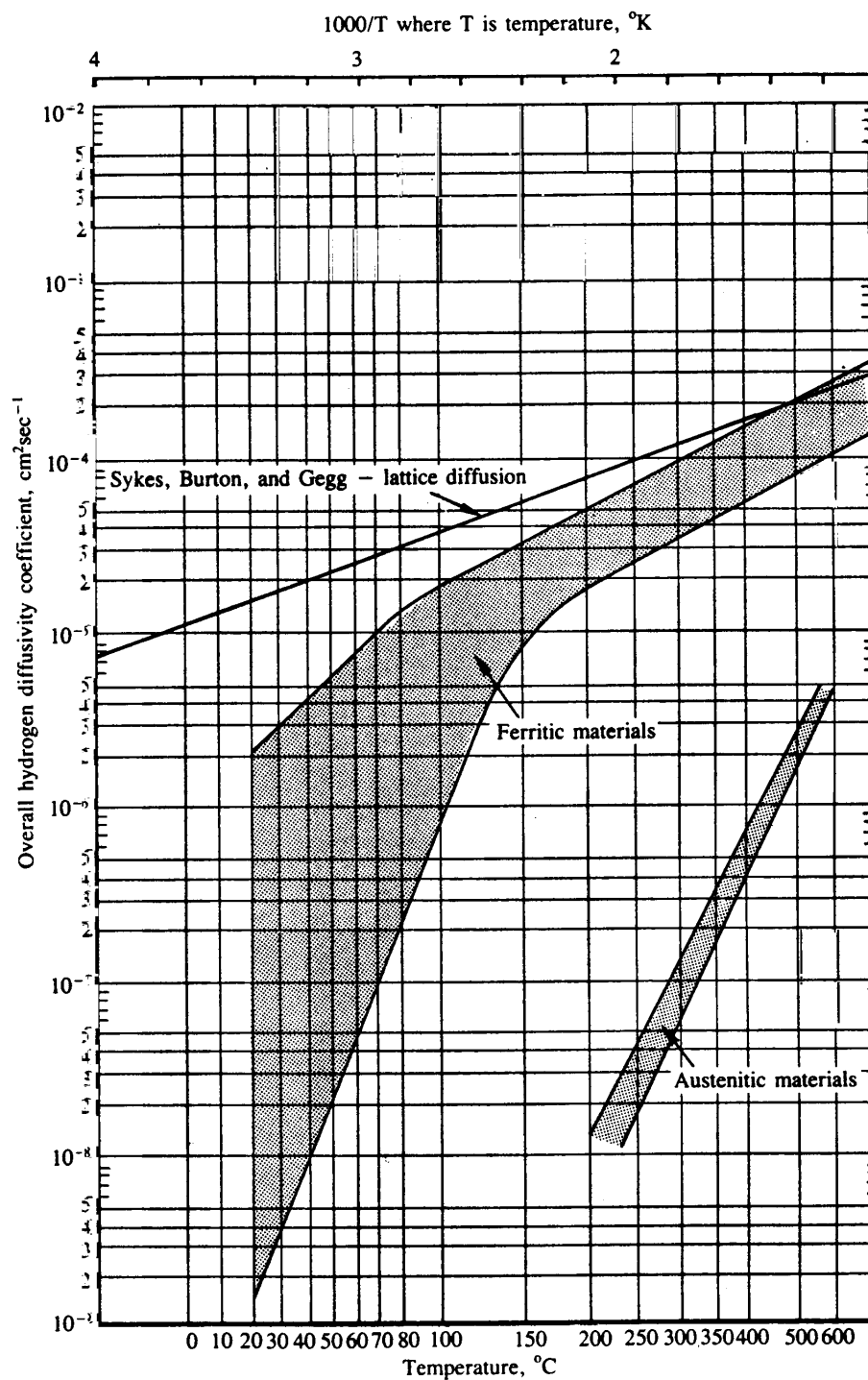


Figure 5-1 Hydrogen Remaining in a Weld Deposit as a Function of Time (Coe, 1973)

Table 5-1 Variation of Overall Diffusivity Coefficient D, with Temperature and Material Type

Location	Reference	Temperature (°C)	D (cm ² /s)
0.06C-1.5Mn Steel, 0.012S	Coe and Chiano (1975)	20	2.0 x 10 ⁻⁶
0.06C-1.5Mn Steel, 0.012S	Coe and Chiano (1975)	40	3.3 x 10 ⁻⁶
0.06C-1.5Mn Steel, 0.012S	Coe and Chiano (1975)	60	8.5 x 10 ⁻⁶
0.06C-1.5Mn Steel, 0.012S	Coe and Chiano (1975)	350	6.4 x 10 ⁻⁵
Basic SMAW	Dallam, et al., (1999)	25	15.5 x 10 ⁻⁷
FCAW-S	Dallam, et al., (1999)	25	8.8 x 10 ⁻⁷
Basic SMAW*	Andersson (1980)	25	7.2 x 10 ⁻⁵
Rutile SMAW*	Andersson (1980)	25	9.3 x 10 ⁻⁶

*Calculated

The primary sources of hydrogen from the material to be welded are as follows:

1. Oil, grease, paint, rust, and moisture on the surface and adjacent to the weld preparation which can subsequently dissociate during welding and enter the arc atmosphere.
2. Degreasing fluids or their residue that may also dissociate and enter the arc atmosphere.
3. Hydrogen from the parent steel. Hydrogen from parent steel can be an important factor when welding heavy castings, welding of parts in service environments where high partial pressures of hydrogen and high temperatures exist, or as a result of corrosion (i.e., sour service).

Another source of hydrogen that is not often considered is humidity in the atmosphere. The absolute atmospheric humidity (i.e., the water vapor partial pressure) of the air rather than the relative humidity can have a pronounced effect on weld metal diffusible hydrogen. The effect of climatic conditions on the diffusible hydrogen measured in SMAW deposits has been reported (Dickehut and Hotz, 1991). The results demonstrate that a given batch of very-low-hydrogen electrodes (less than 5 mlH₂/100g weld metal) may conform to minimum diffusible hydrogen limits in one location but have higher hydrogen in another location with higher absolute humidity. The effect of climatic conditions can be more pronounced when very low hydrogen levels are to be maintained. The availability of FCAW-S consumables that can consistently deposit weld metal with diffusible hydrogen concentrations of less than 5 ml H₂/100g weld metal is not known at the present time.

While the introduction of air into the arc is limited when using the SMAW, FCAW-G, and GMAW processes, the weld pool is in direct contact with air during FCAW-S welding. Prior to

the work conducted as part of the FEMA/SAC program, very little published information regarding the levels of diffusible hydrogen expected in FCAW-S weld deposits was available. Yeo (1988) reported that small-diameter FCAW-S electrodes deposited welds with diffusible hydrogen levels ranging from 3 to 7 ml H₂/100g weld metal. Thus, the effect of absolute humidity may be a more pronounced effect on diffusible hydrogen when using FCAW-S consumables relative to other welding consumables. Chakravarti and Bala (1989) reported that 3.3 and 5.9 ml H₂/100g deposited weld metal was measured in welds produced using two 3/32 in. dia. E70T-4 electrodes.

Table 5-2 (Johnson, 2000a) shows the diffusible hydrogen concentration measured in welds deposited using 3/32-in. dia. E70T-6, 3/32-in. dia. E70TG-K2, and 5/64 in. dia. E71T-8 FCAW-S consumables as part of the FEMA/SAC project. Weld metal diffusible hydrogen concentrations of 8.8, 12.1, and 9.8 ml H₂/100 g were measured in welds deposited using as-received E70T-6, E70TG-K2, and E71T-8 FCAW-S consumables. Depending on atmospheric considerations, an AWS H16 classification (electrode classified to deposit weld metal with less than 16 ml H₂/100g weld metal) may not be met on a consistent basis for the larger diameter electrodes evaluated in the FEMA/SAC study. It should be noted that the electrodes tested as part of this program did not have an AWS hydrogen designation. Additional discussion of weld metal diffusible hydrogen will follow in the section on hydrogen management in FCAW consumables.

Table 5-2 Effect of Atmospheric Exposure on Diffusible Hydrogen of FCAW-S Weld Metal (Johnson, 2000)

	As-Received (ml H ₂ /100g)	Exposed 80-80 (ml H ₂ /100g)	Laboratory Exposure (1 Month) (ml H ₂ /100g)
E71T-8	8.8	11.5	12.5
E70TG-K2	9.8	12.5	25.3
E70T-6	12.1	19.2	19.1

For SMAW coatings and SAW fluxes, there is a correlation between flux coating moisture content and diffusible hydrogen. As part of the manufacture of SMAW electrodes, electrodes are baked to remove moisture associated with the binder and other coating ingredients prior to packaging. In the early 1970's, before moisture resistant SMAW coatings were developed, most SMAW electrodes deposited weld metal with 10-15 ml H₂/100 g weld metal. During the mid-to-late 1970's, moisture resistant coatings became available and many fabrication specifications began to require the maximum weld metal diffusible hydrogen to be controlled to either 10 ml H₂/100g or 5 ml H₂/100 g. Although considerable effort has gone into baking and hermetically sealing SMAW electrodes, moisture reabsorption will eventually occur if the electrodes are exposed to humid conditions (Evans, et al., 1976) (Chew, 1976) (Kotecki, 1992). Effects of atmospheric exposure and operating conditions on the diffusible hydrogen measured in FCAW

welds will be discussed in more detail in the following section on hydrogen management in FCAW electrodes.

5.2.3 Effects of Hydrogen on the Mechanical Properties of Steel

Hydrogen absorbed into the weld metal during welding will evolve from the weld metal by evolution through the surface(s) of the weld and diffusion through the base metal. It is important to know how much hydrogen remains in the weld deposit after different intervals of time. In addition, it is beneficial to know the proportions of residual and diffusible hydrogen that exist after welding. Hydrogen will exist in three forms in a steel weld metal; diffusible hydrogen, residual hydrogen, and elemental hydrogen. The total hydrogen content of a weld metal is the sum of the diffusible, residual, and elemental hydrogen concentrations. Diffusible hydrogen is hydrogen in a weld metal that, at a given temperature, will diffuse through and out of the steel. Residual hydrogen is hydrogen that is “trapped” at particle-matrix interfaces, dislocations, etc. Elemental hydrogen [$H_2(g)$] is hydrogen that exists in a discontinuity as a gas. Shortly after welding, different proportions of diffusible hydrogen, residual hydrogen, and elemental hydrogen may exist at a given temperature. As previously mentioned, hydrogen will diffuse easily at room temperature and will leave the weld.

Considerable progress has been made in identifying factors affecting hydrogen diffusion in steel, and it is well recognized that there is a relationship between the presence of hydrogen in weld metal and fisheyes, flakes, blistering, cold (or hydrogen-assisted) cracking, stress corrosion cracking (SCC), and reduced ductility in weldments. In the case of welds produced for structural applications such as buildings, stress corrosion cracking and blistering are not typically encountered.

For most structural steel applications, residual or elemental hydrogen will have very little if any impact on the mechanical performance of a welded connection. The presence of diffusible hydrogen in steel under ambient conditions, on the other hand, has been shown to influence ductility and toughness (in limited CTOD tests), and contribute to hydrogen assisted cracking. After a given period of time, the concentration of diffusible hydrogen will be reduced below a threshold value that will not affect the mechanical properties of a weld.

The effects of hydrogen on the physical and mechanical properties of iron and steel have been the subjects of considerable study. In addition to the individual studies conducted on this topic, there have been numerous reviews and conferences that have focused exclusively on the effects that hydrogen has on iron and steel. The purpose of this section is to review the effects of hydrogen on the mechanical behavior of structural steel weld metals. Readers interested in more detailed discussion regarding the effects of hydrogen should consider work by Hirth (1980), Beachem (1972), Troiano (1960), and Graville (1967).

The term hydrogen embrittlement is used to characterize the most common effects of hydrogen at temperatures near room temperature in steels. Effects of hydrogen can include loss of ductility and true stress at fracture, loss of load-carrying capacity, cracking, and delayed cracking in the weld metal fusion zone and parent metal heat-affected zone (HAZ).

5.2.3.1 Effect of Hydrogen on Ductility

Diffusible hydrogen in steel can decrease the ductility and true stress at fracture. This effect is typically measured during tension tests as a decrease in the reduction in area and elongation. Reduced notch tensile strength is typically measured when hydrogen is present in notched tensile specimens and, as expected, bend specimens also experience a reduction in bend ductility. The measured tensile properties are influenced by the concentration of hydrogen in the steel at the time of testing, test temperature, strain rate imposed during testing, stress concentrations in the test specimen, and the strength level of the steel being tested. Figure 5-2 shows the effect of temperature on the ultimate tensile strength measured in hydrogen charged notched tensile specimens (Graville, et al., 1967). There is a reduction of strength at temperatures between -100°C and 200°C with a maximum reduction in strength occurring at about 40°C .

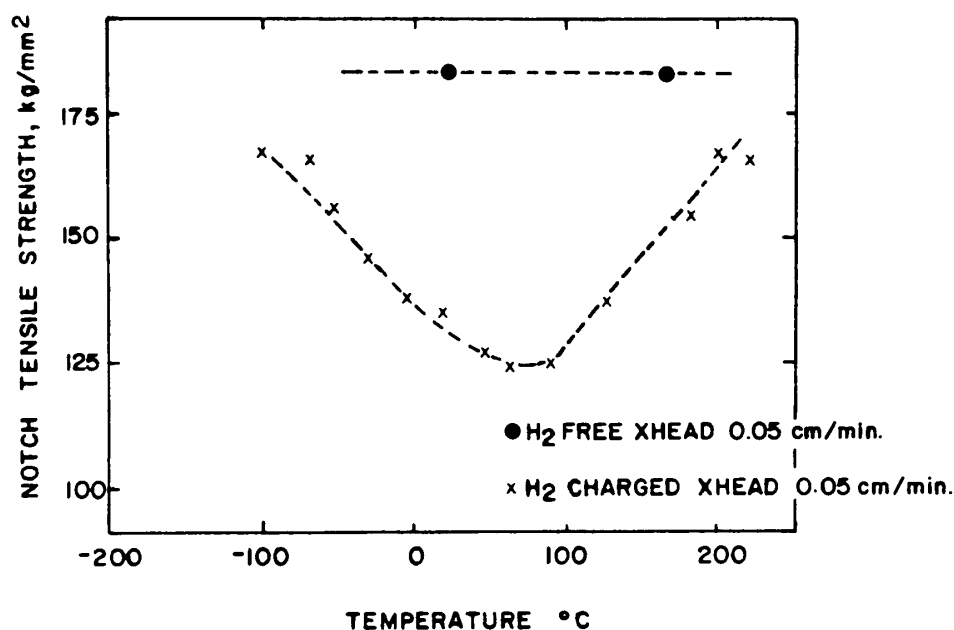


Figure 5-2 Effect of Test Temperature and Strain Rate on the Notched Tensile Strength of Hydrogen Charged Low Alloy Steel (Graville, 1967)

Using conventional tensile test specimens or notched tensile specimens, several investigators have shown a reversible decrease in ductility with increasing test temperature that is independent of strain rate, and a recovery with decreasing temperatures which is strongly dependent on strain rate. In most cases, increasing the crosshead speed during testing reduced the effects of hydrogen on ductility. Brown and Baldwin (1954) investigated the effect of strain rate on the differences between the true fracture strains of charged and uncharged samples at a given temperature using different strain rates. At higher strain rates, the differences in true fracture strain between charged and uncharged specimens decreased. The tensile test data of Brown and Baldwin show that the difference in elongation measured using charged and uncharged samples

(in steel) was >85% for a strain rate of $8 \times 10^{-4} \text{ s}^{-1}$, about 15 percent for a strain rate of 80 s^{-1} , and zero for $3 \times 10^2 \text{ s}^{-1}$.

The magnitude of the ductility reduction when hydrogen is present in steel is primarily a function of the strength level of the steel or weld metal being tested. In higher strength steels (i.e., Ultimate Tensile Strength > 100ksi), comparatively small amounts of hydrogen can lead to large changes in properties, but in steels with lower strength levels, the influence of hydrogen on ductility decreases. The aging of tensile specimens for classification purposes has been a subject of controversy for over 40 years now. Aging is often required to minimize variations in test results. In many cases, aging of tensile specimens results in a 2-5 percent improvement in elongation relative to “as-welded” specimens tested immediately after welding. An example of this effect has been shown by Marianello and Timerman (1990). They compared “as-welded” and artificially aged tensile specimens (100°C for 48 h). In this comparison, weld metal from E6010 electrodes (which typically produce more than 50 ml H₂/100 g of weld metal) and E7018 electrodes (which typically produce less than 5 ml H₂/100 g of weld metal) were tested. Elongation in the E6010 weld specimens averaged 24.4% in the “as-welded” condition and 28.7% in the artificially aged condition. Likewise, weld metal from E7018 electrodes averaged 27.3% in the “as-welded” condition and 28.5% in the artificially aged condition.

Due to constraint experienced in full-scale welds, there is often little direct correlation between a minimum ductility measured in a small-scale tensile specimen and performance of full-scale connections. Current AWS recommendations regarding aging of tensile specimens should still be followed until there is a basis for restricting aging of tensile specimens.

5.2.3.2 Fisheyes in Weld Metal Fracture Surfaces

Fisheyes are found on the fracture surface in ferritic steel weld metal when it is tested in tension at sufficiently slow strain rates near room temperature and contains enough hydrogen to cause some degree of embrittlement. Fisheyes are only seen in tensile tests, bend tests, and similar fracture surfaces produced at slow strain rates; they have not been reported in CVN, or K_{1c}/CTOD test specimens. Examination of a fish-eye at higher magnification shows that the center, or pupil, consists of a small pore, inclusion, or other small defect. The major part of the fish-eye, the ‘iris’, has fractured by brittle fracture (quasi-cleavage) in a pattern radiating from the pupil. The pore or inclusion, usually at the upper end of the size distribution expected in weld metal, is the only pre-existing feature of the fish-eye. Fisheyes on weld metal fracture surfaces are not a weld metal defect. Rather, the presence of fisheyes only indicates that the weld metal has been stressed beyond its yield point while still containing enough hydrogen to cause some degree of local embrittlement. The level of hydrogen required for the formation of fisheyes in a particular type of weld metal has not been documented and can vary for weld metals produced by different processes. Fisheyes are rarely seen in transverse tensile and bend tests because most welds are deposited to overmatch the base metal.

Although fisheyes may be occasionally observed on a weld metal fracture surface, the presence of fisheyes alone is not an indicator of whether or not a particular weld metal is capable of delivering the anticipated level of service. Although several fisheyes were noted on the fracture surface of the T-stub and wide plate specimens tested by Battelle, the peak loads

measured in the test specimens were similar to that expected of the base metal. Testing had little effect on the overall strength level or apparent ductility of these test specimens. It is interesting to note that although some test specimens had been fabricated up to a month earlier, that fisheyes were still observed in specimens joined with undermatching FCAW-S consumables. Similar effects were reported in a study by Yeo and Clark (1986) who noted that when compared to weld metals from other processes, fisheyes were more prevalent in FCAW-S weld metals. Yeo argued that weld metal capable of depositing weld metal with high CTOD values and acceptable levels of strength and ductility, should not be precluded from use due to the occurrence of fisheyes on the tensile and bend specimen fracture surfaces.

5.2.3.3 Hydrogen Assisted Cracking

Hydrogen assisted cracking (HAC) can occur in either the base metal heat affected zone or in the weld metal. It has been well recognized that hydrogen assisted cracking will occur in the HAZ or weld metal if the following four conditions are present simultaneously:

1. Critical concentration of diffusible hydrogen at a crack tip;
2. Stress intensity of sufficient magnitude;
3. A microstructure which is susceptible to hydrogen; and
4. Temperature below 200°C.

Hydrogen assisted cracking is also called “cold-cracking” or delayed cracking because cracking tends to occur after welding in a time period ranging from a few minutes to several days. Hydrogen cracks typically occur in the HAZ near the fusion line or in the weld metal. The cracks often initiate at locations of high stress intensity such as the weld toe or the weld root, and can propagate in a direction that is either longitudinal or transverse to the direction of welding. In single pass welds or the root pass of multipass welds, the root gap provides a stress concentration with respect to stresses transverse to the weld, and this leads to longitudinal cracks in the weld metal. The risk of hydrogen assisted cracking increases with increasing alloy content of the weld or base metal, thickness of parts being welded (thicker parts increase the amount of restraint imposed on the weld), and higher hydrogen levels.

When a steel is welded, the HAZ of the parent steel plate is hardened and becomes susceptible to hydrogen assisted cracking if a sufficient quantity of hydrogen is present. This hydrogen continues to escape at ambient temperatures, so that the local concentration of diffusible hydrogen in a weldment is continually decreasing after welding. Past experience in the welding industry suggests that if a mild steel weld does not crack within 24 hours of welding due to hydrogen, it will not crack at all because the driving force diminishes. The trend to lower carbon content steels and newer steel processing techniques has greatly reduced the risk of hydrogen assisted cracking (HAC) in the HAZ regions, and the problem has shifted to the fusion zone.

Traditionally, over 90% of the problems with hydrogen assisted cracking have been observed in ten percent of the steel materials used in fabrication. Over the years, the structural fabrication industry has adopted practices and procedures so that the occurrence of HAC is now relatively rare. Although there has been a considerable amount of study related to the prediction of appropriate preheat temperatures, approaches developed by Graville (AWS D1.1 and D1.5), Yurioka (AWS D1.5 Fracture Control Plan), (Yurioka and Suzuki, 1990), and Bailey et al., (British Standard 5135) are commonly employed. In general, the approaches recommended by Yurioka are more conservative than those of Graville and Bailey. The individual documents should be consulted for further information.

5.3 Hydrogen Management in Weld Metals Deposited Using Flux-Cored Arc Welding Consumables

5.3.1 Background

Flux cored arc welding (FCAW) electrodes have been in use for many years and their use for welding of critical components in the shop and field has increased. Compared to the many other arc welding processes such as solid wire gas metal arc welding (GMAW), process shielded metal arc welding (SMAW), or gas tungsten arc welding (GTAW), the FCAW process offers higher productivity. Following the Northridge earthquake, some concern was expressed regarding appropriate levels of diffusible hydrogen for construction of steel frame buildings. In industries where the majority of welding has been conducted using the SMAW process, there has been some reluctance to embrace the use of FCAW consumables. One concern that has been expressed is whether or not FCAW consumables are capable of depositing weldments with low hydrogen concentrations over a wide range of operating conditions.

While hydrogen assisted cracking in the base metal HAZ has been extensively studied, factors influencing weld metal cracking have received comparatively less attention. As a result of increased interest, there have been two recent conferences addressing the issue of hydrogen assisted cracking (Johnson and Harwig, 1998). Most investigations of weld metal cracking have focused on weld metals deposited using the SMAW and SAW processes. Few studies have reported hydrogen assisted cracking in FCAW-S weld deposits.

Improvements in steel making and processing techniques have led to the development of C-Mn steels with lower carbon equivalence and hence lower susceptibility of HAZ cracking. The reduced carbon equivalents of ASTM A992 and A913 shapes are good examples of how similar or higher strength steel is produced while maintaining nominally lower carbon concentrations and carbon equivalents.

Accordingly, the availability of more weldable steels and continual pressures for fabricators to reduce costs have resulted in the application of lower preheat temperatures in a range of section thickness while avoiding HAZ cracking. This has effectively caused a shift in the location where hydrogen cracking occurs, from the HAZ of the base metal to the weld metal. In some industrial sectors that utilize modern steels with improved weldability, the selection of preheat is based on avoidance of weld metal cracking rather than HAZ cracking. Unlike selection of welding parameters/preheats for reduced risk of HAZ hydrogen assisted cracking,

the usefulness of empirical predictions of preheat levels and welding procedures to avoid weld metal hydrogen assisted cracking is limited.

Extensive research over the past 40-50 years has led to the development of criteria for selection of welding parameters for a given consumable based on parent metal composition such that hydrogen assisted cracking is avoided (AWS, 1996a, b, 1998c) (BSI, 1984). Examples of these approaches include AWS D1.1 Appendix IX, BS 5135. In the case of the AWS D1.1 Code, the maximum permitted hydrogen concentrations are ambiguous, and there are no provisions to deal with storage conditions, moisture absorption, and welding parameters used to evaluate diffusible hydrogen when using FCAW consumables.

The purpose of this section is to discuss several aspects of hydrogen management in weld metals deposited using FCAW consumables, briefly review tests used to characterize weld metal hydrogen-assisted cracking in SMAW, SAW, and FCAW weld metals, and discuss the challenges of predicting weld metal cracking in multipass welds.

5.3.2 Diffusible Hydrogen in FCAW Weldments

Hydrogen category designators have been used in consumable specifications as an option to enable manufacturers to certify that an electrode is generally capable of achieving a given level of diffusible hydrogen under the classification conditions. In the U.S., designations of H4, H8, and H16 are used to indicate that the consumable is capable of depositing weld metal with less than 4, 8, and 16 ml H₂/100 g weld metal respectively (AWS 1998d). Industrial users of FCAW electrodes have expressed concern regarding the susceptibility of FCAW consumables to moisture absorption and the effect of welding parameters on diffusible hydrogen measured in FCAW weld metals.

Guidelines have been developed to evaluate and control moisture in SMAW electrodes and SAW fluxes (AWS D1.1, 1998) (ANSI/AASHTO/AWS Bridge Welding Code D1.5, 1996). These guidelines typically specify packaging, handling, and storage conditions that help reduce moisture absorption/adsorption that can occur during storage of the electrodes, and after the electrode packaging has been opened. While procedures are well outlined for SMAW electrodes and SAW fluxes, only the AWS D1.5 specification considers handling and storage procedures for FCAW electrodes.

The AWS D1.5 (ANSI/AASHTO/AWS Bridge Welding Code D1.5, 1996) guidelines require that, if welding is to be suspended for more than eight hours, then electrodes must be stored in airtight coverings or placed in a drying oven maintained at a temperature of 120-290°C. Electrodes not consumed after 24 hours of accumulated exposure outside of sealed or heated storage, must be re-dried by baking at 260-290°C or as specified by the manufacturer. The time limits for exposure can be extended following engineer approval. The effectiveness of such storage techniques have not been widely evaluated; experience at EWI suggests that simply storing FCAW consumables in a closed plastic bag or sealed metal cans is not sufficient to prevent moisture absorption during storage. Additionally, some electrodes are packaged on plastic or wood spools and heated storage or re-drying is possible after the original package is opened.

While the guidelines given in the AWS D1.5 specification provide a good starting point that will allow fabricators to control moisture absorption in FCAW electrodes, several limitations of the AWS D1.5 guidelines are apparent. At the present time, the D1.5 guidelines suggest that all FCAW electrodes will experience similar increases in diffusible hydrogen following similar exposure conditions and times. Depending on electrode type (i.e., E70T-1 vs. E70T-5) and manufacturing method (seam type, drawing method, or baking schedule), an increase in diffusible hydrogen after exposure may or may not occur. Thus, the approach recommended in AWS D1.5 may be overly conservative and limit the use of FCAW electrodes unless the engineer is willing to conduct tests to verify that extended exposure times do not result in an increase in diffusible hydrogen. Before the engineer can make an informed decision regarding whether or not a particular electrode will deposit a weld with a higher diffusible hydrogen concentration following atmospheric exposure, a standard approach for an FCAW electrode exposure evaluation technique is required.

As part of the Cooperative Research Program at EWI and the SAC Joint Venture, the effects of welding parameters and atmospheric exposure on the diffusible hydrogen concentration in FCAW-G and FCAW-S weld metals has been evaluated (Johnson, 2000a) and (Harwig, et al., 1999). In these studies, electrode manufacturers were consulted to develop a test that could be used to evaluate the effects of FCAW electrode atmospheric exposure on weld metal diffusible hydrogen. The test procedure used at EWI consists of a single layer of FCAW consumable wrapped on a painted wire spool and exposed to conditions of 80°F (27°C) and 80% relative humidity in a forced air humidity cabinet for one week. Weld metal diffusible hydrogen is evaluated in the as-received condition following exposure. Although this method appears to be a good starting point for evaluating the effects of atmospheric exposure, additional testing may still be required to evaluate the reproducibility amongst several labs. The usefulness of using weight gain or infrared coating analysis techniques to evaluate the effects of atmospheric exposure in FCAW consumables is questionable since it would be difficult to consistently extract flux from the core wire and would not allow effective evaluation of the potential contribution of drawing lubricants.

The results of atmospheric exposure testing conducted as part of the EWI program indicate that it is inappropriate to assume that the response of all FCAW electrodes to atmospheric exposure is the same. Figure 5-3 shows the diffusible hydrogen concentration measured in as-received and exposed (80-80 condition) E71T-1 electrodes from several manufacturers, an E70T-5 electrode, and an ER70S-6 control electrode. It is clear that substantial increases in the weld metal diffusible hydrogen concentration were measured in some rutile-type E71T-1 electrodes as a result of exposure. This increase in diffusible hydrogen can occur in electrodes produced to the same specification (but using different production techniques) by a single manufacturer or among different manufacturers.

Evaluation of a basic E70T-5 electrode in the EWI study seems to suggest that basic FCAW-G electrodes may be less sensitive to atmospheric exposure than rutile FCAW-G electrodes. It is not clear from the EWI study whether or not the E70T-5 electrode absorbed/adsorbed comparable amounts of moisture when compared to the E71T-1 electrodes. It is possible that similar amounts of moisture were absorbed/adsorbed, and hydrogen was reduced by other

mechanisms. These results also do not imply that all E70T-5 electrodes should be impervious to moisture absorption. While electrodes containing high proportions of fluorspar typically deposit weld metals with low concentrations of diffusible hydrogen, the mechanism associated with these lower hydrogen concentrations has not been clearly identified (i.e., whether fluoride reacts with hydrogen in the arc column to form HF, reduces the partial pressure of hydrogen in the arc column, or both).

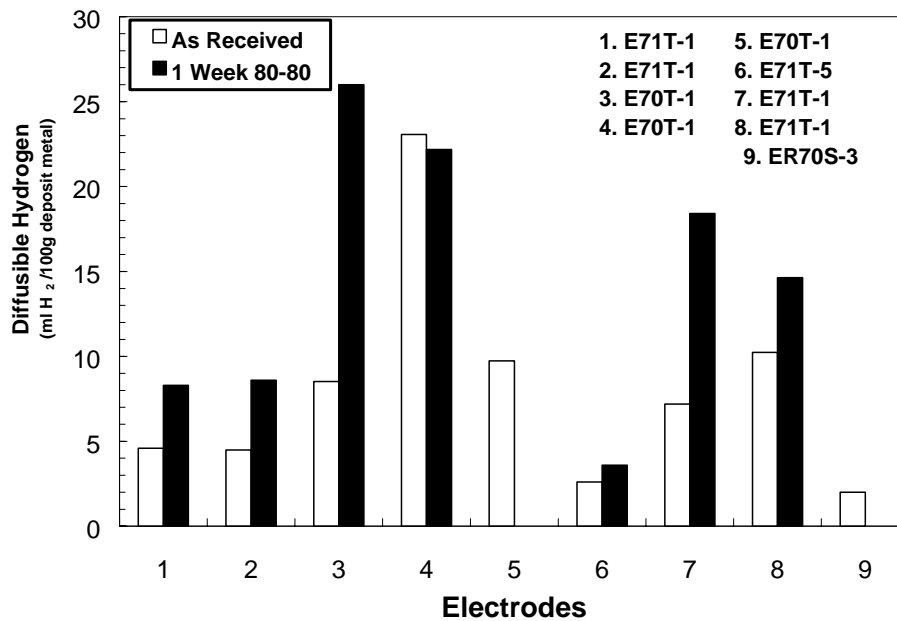


Figure 5-3 Atmospheric Exposure Test Results for Mild-Steel FCAW-G Electrodes Provided by Several Manufacturers (Harwig, 1999)

Figure 5-4 shows the effect of atmospheric exposure on the diffusible hydrogen measured in welds deposited by E71T-8, E70T-6, and E70TG-K2 FCAW-S electrodes. Weld metal diffusible hydrogen determination was conducted using consumables supplied to EWI in the as-received condition (out of the box), after one week of exposure at 80%RH-80°F, and after approximately one month exposure under laboratory conditions. Only a slight increase in diffusible hydrogen was measured in welds deposited using E71T-8 consumables after exposure. The diffusible hydrogen measured in welds deposited using E70TG-K2 electrodes increased from 9.8 ml H₂/100g weld metal to over 12 ml H₂/100g weld metal after exposure for one week at 80%RH/80°F. Saturation of this electrode (>25 ml H₂/100g weld metal) occurred after exposure in ambient laboratory conditions for approximately one month. Evaluation of the E70T-6 electrodes showed that a substantial increase (from 12 to over 19 ml H₂/100g weld metal) in weld metal diffusible hydrogen occurred after exposure in the humidity cabinet and after long term laboratory exposure. It is clear that all of these electrodes should not be expected to meet an H8 classification but should generally be capable of meeting an H16 classification in the as-manufactured condition. At the present time, these consumables are not manufactured to meet an AWS hydrogen designation.

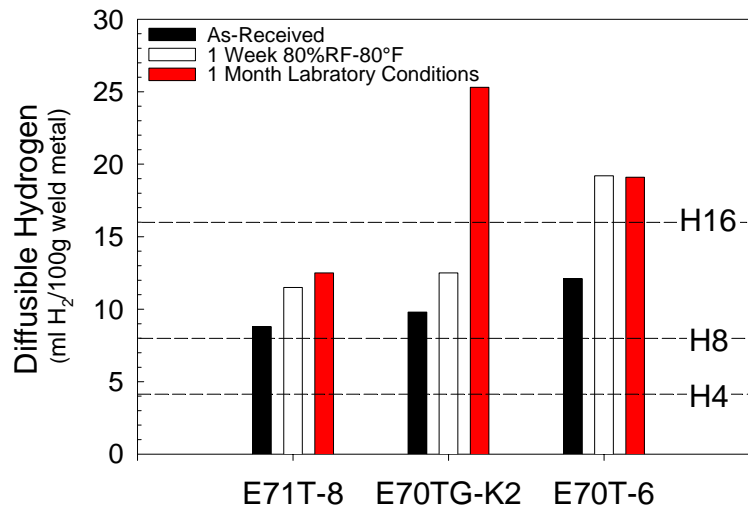


Figure 5-4 Effect of Atmospheric Exposure on FCAW-S Weld Metal Diffusible Hydrogen Concentrations. Electrodes Were Tested in the As-Received Condition, After 1 Week of Exposure in a Forced-Air Humidity Cabinet at 80%RH-80°F, and After 1 Month of Exposure Under Ambient Laboratory Conditions (Johnson, 2000).

In selecting FCAW electrodes, it is important to understand how weld metal diffusible hydrogen is measured. The diffusible hydrogen is measured under very specific conditions, conditions that may not be replicated in production welding. The manufacturer will report “as manufactured” diffusible hydrogen levels, but during electrode storage and when the product is exposed to the atmosphere, the electrode can pick up moisture, leading to higher hydrogen values. Different welding conditions can lead to different hydrogen levels for otherwise identical electrodes. Thus, the value reported by the electrode manufacturer cannot be used as an indication of the level of diffusible hydrogen that will be seen under all production conditions.

Under present AWS electrode specifications, manufacturers producing electrodes with an “H” designator only report that their products are capable of meeting a given diffusible hydrogen level (H4, H8, H16). The operating window in which consumables will maintain a given level of diffusible hydrogen is not typically given. Similarly, UK and European electrodes have designations corresponding to diffusible hydrogen concentrations of 5, 10, and 15 ml/100g deposited weld metal. European standard EN 758 (PrEN, 1996) requires manufacturers to define the conditions under which their flux-cored electrodes provide the claimed weld metal diffusible hydrogen class (and minimum mechanical property requirements). This includes the operating envelope of welding parameters for which the claimed diffusible hydrogen classification can be guaranteed, and the storage recommendations for retaining this classification.

Currently in the U.S., welding parameters used for diffusible hydrogen tests are typically the same as those used to measure mechanical properties. The effects of welding parameters on

rutile FCAW-G, basic FCAW-G, and metal core weld metal diffusible hydrogen concentrations have been reported by several authors (White, et al., 1992) and (Harwig et al., 1999). As shown in Figure 5-5, increased diffusible hydrogen concentrations were measured in some rutile FCAW-G weld metals with increasing current and decreasing contact tip-to-work distance. Figure 5-5 shows the effect of welding current and electrode extension in constant area welds deposited using an E71T-1 rutile flux cored electrode. The weld metal diffusible hydrogen concentration increased from 2.3 ml H₂/100 g deposited weld metal when a welding current of 140 A was used, to over 11.6 ml H₂/100 g deposited weld metal when a welding current of 345 A was used. Tests were conducted using an as-received electrode. Considerably higher levels of diffusible hydrogen may be expected after electrode exposure. The fused metal hydrogen concentration increased from 2.0 ml to 7.1 ml over the same current range.

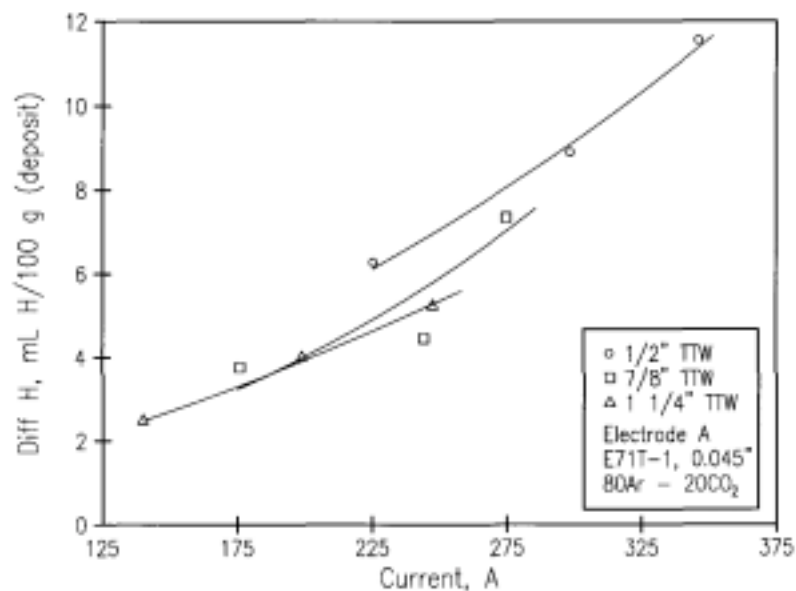


Figure 5-5 Effect of Electrode Extension and Welding Current on Diffusible Hydrogen in E71T-1 Rutile FCAW-G Weld Metal (Harwig, 1999)

Another study (Marianetti, 1998) using a different E71T-1 electrode reported that diffusible hydrogen increased from 4.3 ml H₂/100g deposited weld metal when a welding current of 170 A was used to 13.2 ml H₂/100 g deposited weld metal when a welding current of 290 A was used. Following exposure of this electrode exposure to laboratory conditions (50% RH, 20°C) for two weeks, diffusible hydrogen concentrations of 8 ml H₂/100 g and 20 ml H₂/100g were measured in welds produced using low and high currents. Similar increases in weld metal diffusible hydrogen as a function of welding parameters were not measured when using basic E70T-5 electrodes (Harwig, 1999) (Marianetti, 1998).

Based on the results shown in Figure 5-5, it is clear that welding parameters used to measure weld metal diffusible hydrogen during conformance testing and diffusible hydrogen measured in welds produced using welding parameters closer to those experienced in actual fabrication may

be entirely different. Testing according to European Specification EN 758 (PrEN 758, 1996) may be helpful in providing an added level of assurance that a particular consumable will be able to consistently deposit weld metal with a given hydrogen concentration (provided that electrodes are stored properly). However, the natural consequence of this specification may be a limited operating range or that manufacturers may choose not to supply electrodes under that specification. Additionally, the maximum concentration of diffusible hydrogen is likely to be measured using the highest recommended wire feed speed and the shortest electrode extension.

5.3.3 Hydrogen Assisted Cracking in FCAW Weldments

There have been a number of published investigations (Marianetti, 1998), (North, 1982), (Graville, 1974), (Hart, 1986), (Hannerz, 1993), (Graville, 1975), (Graville, 1976), (Hart, 1982), (Hannerz, 1996), (Chakravarti, 1989), (Sawhill, 1974), (Okuda, 1987), (Fujii, 1974), and several review articles (Yurioka, 1990), (Fujii, 1974), and (Vuik, 1992) related to hydrogen assisted cracking in weld metals. Most of these studies have used small-scale laboratory tests to compare weld metal cracking tendency. Susceptibility to weld metal cracking has been evaluated using tests such as the Tekken test, with a sloping Y-preparation and a straight Y-preparation, WIC test, controlled thermal severity test (CTS), and the gapped bead on plate test (GBOP).

In practice, Y-groove tests are representative of welding under highly restrained conditions with an adverse root geometry such as incomplete root penetration found in the root pass of a butt weld. Similarly, WIC tests have been successfully used to select appropriate arc energies and preheat levels for root passes in pipeline girth welds. Recent investigations at The Welding Institute (TWI) (ANSI/AASHTO/AWS Bridge Welding Code D1.5, 1996) using the CTS test technique suggest that HAZ cracking can be adequately predicted in FCAW weldments using the TWI nomograms. However, Kinsey (1996) found that root profile in some welds could increase the risk of cracking and, consistent with previous studies at TWI, weld metal cracking was typically eliminated before HAZ cracking in the CTS test.

Y-Groove, WIC, and CTS tests give a good indication of welding parameters that can be used to avoid HAZ hydrogen cracking and cracking that can occur in the root pass of a butt weld. It is well known that weld metal cracking can be strongly influenced by dilution from the base metal. If weld metal cracking in a number of consumables is to be evaluated over a period of time, tests must be conducted using the same heat of base material to ensure consistent results. While this approach is useful in determining preheat levels appropriate for the root pass in a multipass weld, the results of this testing approach are then applicable only to the particular base metal and weld metal combination evaluated.

The gapped bead-on-plate (G-BOP) test was developed strictly as a weld metal cracking test (Hart, 1986), (Graville, 1975), and (Graville, 1976). Early work was conducted by depositing welds directly onto 50-mm thick plate. The test was later modified to include a butter layer such that dilution from the base plate was negligible and consumables could be directly compared to each other by determining a critical preheat as a comparative index. The G-BOP test has been used to study hydrogen cracking in weld metals deposited by a variety of welding processes and evaluate the effect of microstructure and composition. Two approaches have been used to

describe cracking in the G-BOP test: cracking that occurs with a room temperature preheat, and the preheat temperature at which 10% cracking occurs.

Following the discussion on moisture and hydrogen presented above, Figures 5-6 and 5-7 show hydrogen cracking as a function of preheat G-BOP tests conducted using buttered test blocks with E71T-1 and E70T-5M weld metal. Figure 5-6 shows that cracking in E71T-1 weld metal deposited with two different heat inputs (heat input was varied by increasing current) had a similar cracking response. In this case, the beneficial effect of higher heat input was offset by the higher concentrations of hydrogen introduced at higher wire feed speeds. Hardness decreased from approximately 225 VHN in weld metals deposited with the low heat input and 20°C preheat to approximately 195 VHN when higher heat inputs were used. Alternately, Figure 5-7 shows that little or no cracking was measured in E70T-5 weld metals deposited using similar heat inputs despite comparable hardness (198-220 VHN). The lower level of cracking in the E70T-5 weld metal is presumably due to the lower hydrogen concentration. Accordingly, moisture was added to the shielding gas to produce diffusible hydrogen concentrations in the E70T-5 weld metals that were comparable to those measured in the E71T-1 weld metals. When comparing cracking in the E71T-1 and E70T-5 weld metals with similar diffusible hydrogen concentrations at a given preheat temperature, cracking was generally less in the E70T-5 weld metal. Additional study is required to determine the cause of this apparent difference.

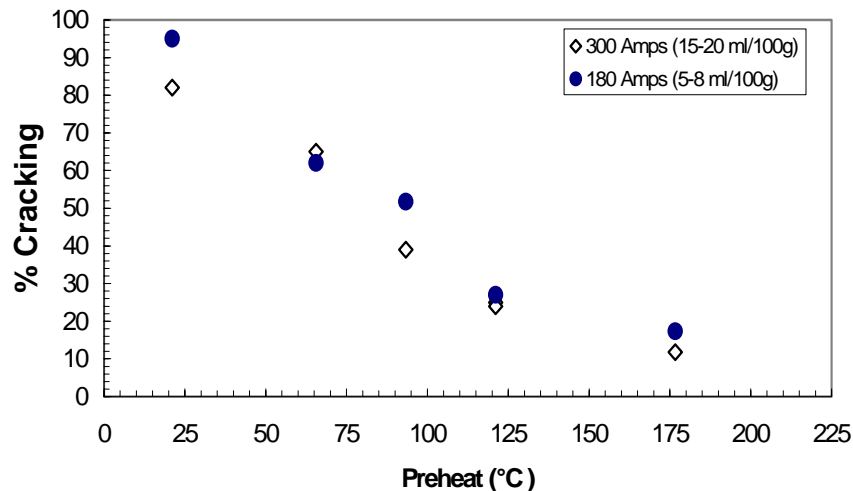


Figure 5-6 Effect of Preheat on E71T-1M Weld Metal Cracking Using Low and High Welding Currents (The Nominal Heat Inputs were 0.95 and 1.85 kJ/mm Respectively)

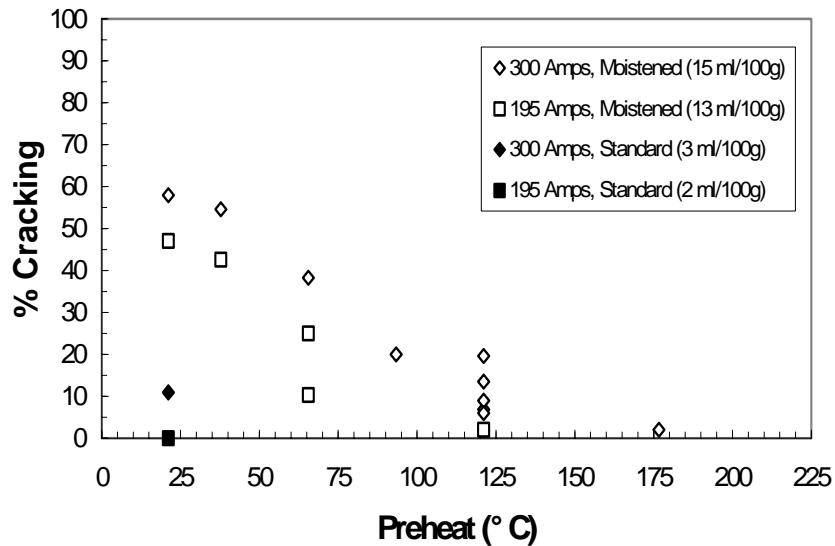


Figure 5-7 Effect of Preheat and Hydrogen on E70T-5M Weld Metal Cracking. Welds were Produced with Heat Inputs of 0.95 and 1.85 kJ/mm. The Filled Symbols Represent Welds Produced using Dry 80/20 Ar/CO₂ and the Open Symbols Represent Welds Produced with Moistened Gas.

The effect of preheat and heat input on hydrogen assisted cracking in FCAW-S weld deposits was evaluated as part of an investigation, task 5.2.3 using the Y-Groove test technique. A 1-in. thick ASTM A572 Gr. 60 plate was used for the evaluation. Although the plate met ASTM A572 Gr. 60 mechanical property requirements, the chemical composition of the plate did not exceed ASTM A572 Gr. 50 maximum elemental restrictions. Consumables were tested in the as-received condition, and the diffusible hydrogen concentrations correspond to the as-received values shown in Table 5-2. Figure 5-8 shows that, even under high restraint conditions, cracking should be prevented in single pass welds when following prescribed AWS D1.1 preheat requirements. Additionally, Figure 5-8 suggests that preheat should be applied even when higher heat inputs are used when high restraint conditions are expected (i.e., 70°F preheat was not adequate). As is typical for this test technique, the majority of cracking occurred in the weld metal rather than the base metal.

The effect of hydrogen accumulation (especially when high hydrogen concentrations are present) during deposition of a multipass weld can be significant. Review of preheat requirements corresponding to an H16 condition suggests that heat affected zone HAC may be effectively avoided with the minimum AWS preheats provided that moderate heat inputs are utilized. Given the service requirements of moment-resisting connections and AWS D1.1 inspection techniques, consumables with an H16 classification may be acceptable, but uncontrolled diffusible hydrogen concentrations would be highly undesirable.

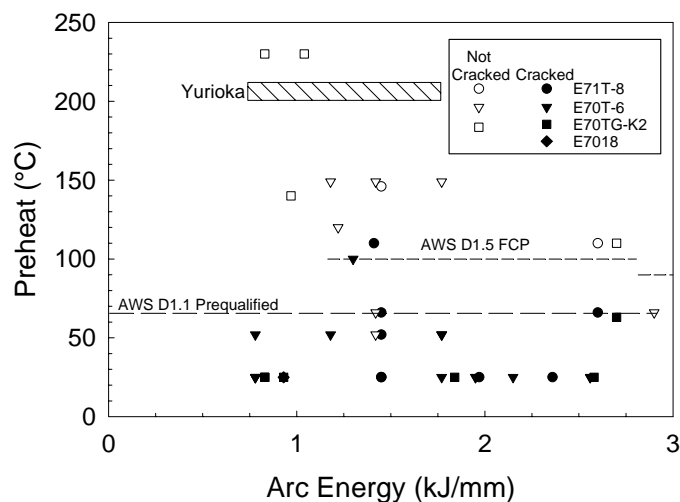


Figure 5-8 Effect of Preheat and Arc-Energy on Hydrogen-Assisted Cracking in Y-Groove Test Specimens. FCAW-S Electrodes were Used to Deposit Welds in 1-in. Thick A572Gr. 60 plate. The Nominal Diffusible Hydrogen Concentration in the FCAW-S Weld Metals Ranged from 8-12 ml H₂/100 g Deposited Weld Metal.

Weld metal hydrogen cracking in multipass submerged arc, GMAW, FCAW-G, and FCAW-S welds has occasionally been observed. If higher than expected hydrogen concentrations occur during multipass welding (either due to moisture absorption or an increase in hydrogen with increasing current), cracking in multipass welds similar to that as shown in Figure 5-9 can occur. Figure 5-9 shows transverse and longitudinal cracking observed in multipass E70TG-K2 welds deposited using manufacturer recommended parameters and low heat inputs. The cracking observed in this weld was attributed to the low heat input employed (~20 kJ/in) and high hydrogen (~25 ml H₂/100 g weld metal) conditions as the result of exposure. While cracking was not observed in other SAC tests deposited using these consumables, this example illustrates the need for manufacturers to specify operating ranges (in this case, minimum heat inputs) for their consumables and recommended appropriate storage conditions.

According to many manufacturers of FCAW-S consumables and fabricators that use FCAW-S consumables, the incidence of hydrogen-assisted cracking is reportedly very low. Additional testing to confirm this observation may allow relaxation of preheat requirements and/or storage requirements for FCAW-S weld deposits. The use of full-scale restraint tests may be appropriate. It has been possible to produce weld metal cracking under laboratory conditions using a large restrained test plate into which a multipass weld metal is deposited. While no standard test plate geometry has been developed to study cracking in multipass welds, several investigators have been successful in producing cracking in laboratory multipass welds (Pargeter, 1989), (Okuda, et al., 1987), and (Fujii, 1974). These test plates are sufficiently long such that a high residual tensile stress is developed in the welding direction and sufficiently thick so that the effects of hydrogen accumulation in the multipass weld can be determined. In many cases, detection of cracking in these test plates is difficult, and costly sectioning is required to

verify whether or not cracking has occurred when enhanced ultrasonic inspection techniques fail to detect cracking.

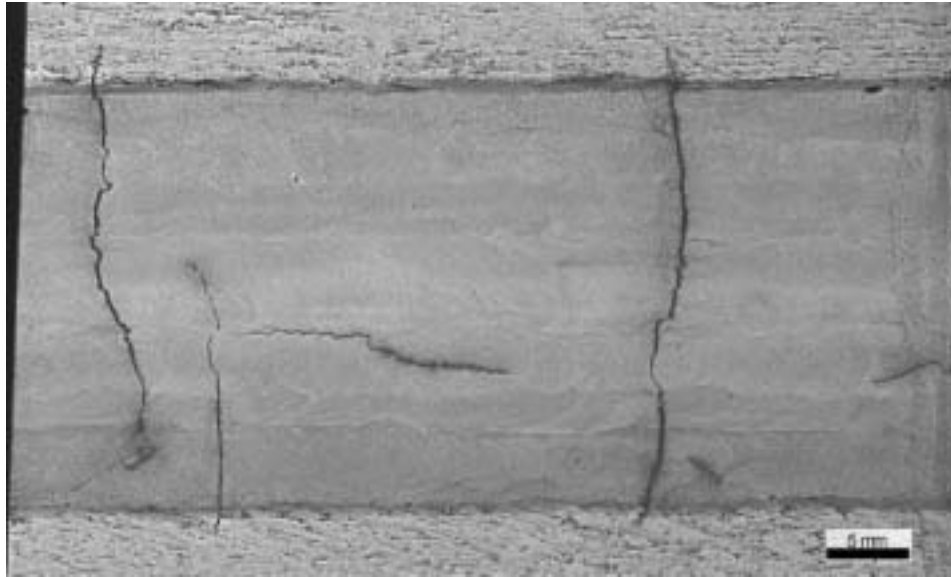


Figure 5-9 Longitudinal and Transverse Cracks Occurring in a Multipass Weldment

It is intuitive that deposition of weld metals with a very low heat input will result in a high strength weld deposit with higher risk of hydrogen assisted cracking. The risk of weld metal hydrogen assisted cracking can also increase with the use of high heat inputs. A key parameter controlling cracking in multipass welds is hydrogen accumulation during welding. On this basis, cracking in high heat input welds has been observed because larger bead sizes are deposited and it takes less time to fill the joint. Hydrogen accumulation in a multipass weld is controlled by residual hydrogen concentration of the underlying beads, bead size, and delay time between layers. Deposition of welds with an intermediate heat input with a moderate interpass temperature will allow for deposition of a softer weld while allowing hydrogen to escape the weld in-between passes.

Multipass welds deposited using some rutile (titanium dioxide) FCAW-G and some FCAW-S consumables may be particularly susceptible to hydrogen cracking for several reasons. First, in some consumables, hydrogen will increase with increasing heat input, which will result in a higher hydrogen concentration in the multipass weld when compared to welds deposited using other consumables in which hydrogen does not vary with heat input. Second, compared to many other consumables within a given strength range, higher levels of alloy addition are typically used to ensure that minimum toughness requirements are met. This may result in a weld deposit with higher than expected strength and thus reduced cracking resistance. Third, a recent study by Hart and Evans (1997) suggested that residual hydrogen concentrations in 6013-type deposits were considerably higher than that of the basic weld. Although a similar analysis has not been performed using rutile FCAW-G weld metals, it is possible that hydrogen may be effectively

trapped at inclusions (due to the higher oxygen concentration in these weld metals) and thus a higher residual hydrogen may exist. Upon deposition of subsequent passes, dilution of hydrogen from the underlying beads may effectively increase the weld metal diffusible hydrogen and increase the risk of cracking.

5.3.4 Low Temperature PWHT

As discussed above, hydrogen will generally enter the weld pool during welding. The presence of hydrogen in sufficient quantity can cause embrittlement and cracking in steel. Diffusible hydrogen in quantities exceeding 5 ml H₂/100g have been shown to cause embrittlement of notched tensile samples while embrittlement in steel forgings has occurred with hydrogen concentrations ranging from 2-5 ml H₂/100g. The problem of hydrogen embrittlement is reversible since hydrogen will diffuse out of the steel given enough time at a given temperature. The process of hydrogen removal can take place during and after welding. A considerable amount of work has been conducted to describe methods that will allow an engineer to determine the amount of hydrogen remaining after welding and how to determine an appropriate thermal treatment to ensure that hydrogen is reduced to a safe level (Coe, 1973), (Bailey, et al., 1993), and (Coe and Chiano, 1975). Much of the following discussion and analysis is presented by Bailey, et al. (1993) and the reader should refer to this reference for additional information.

It is desirable to identify the initial hydrogen concentrations in a multipass weld, and the critical hydrogen levels above which the risk of cracking and reduction of mechanical properties takes place. It has thus far been impossible to determine a general answer to these questions that applies directly to a wide range of materials and situations. The diffusible hydrogen values shown in Table 5-2 refer to the diffusible hydrogen measured in a single bead deposited under standardized AWS test conditions. When following AWS test procedures, the weld is quenched rapidly following welding and stored at low temperature prior to measurement of diffusible hydrogen. Thus, the values of diffusible hydrogen shown in Table 5-2 do not necessarily represent the final diffusible hydrogen concentration that would be expected in a single pass weld that was allowed to cool normally or the diffusible hydrogen in a multipass weld. During deposition of a multipass weld, the weld would not be quenched, and the weld would lose a considerable amount of hydrogen before the next bead is deposited.

The quantity of hydrogen that evolves in-between weld passes is a function of the bead size, low temperature cooling rate (a strong function of heat input, interpass temperature, and plate thickness), weld metal composition, and the time elapsed between weld passes. The evolution of diffusible hydrogen from single pass welds has been effectively modeled using empirical and numerical techniques. The situation with multipass welds is much more complex since hydrogen diffusion and accumulation (from previous passes) is taking place simultaneously. Thus the levels reported in Table 5-2 are not representative of the diffusible hydrogen concentrations that would be expected to remain in a multipass weld after welding.

Limited experimentation has demonstrated that the hydrogen remaining shortly after deposition of a multipass weld is often 20 to 50% of the original values. In the case of pipeline welds deposited with 6010 electrodes (AWS diffusible hydrogen > 40 ml H₂/100g weld metal),

diffusible hydrogen levels of less than 5 ml H₂/100g weld metal were measured in the multipass weld shortly after welding (Gordon, et al., 1999) and (Lancaster, 1992). As discussed by Bailey, et al. (1993) and Coe (1973), a good rule of thumb is to assume that approximately 50% of diffusible hydrogen measured in a single pass AWS test will remain in the multipass weld following welding. This assumption is conservative and will depend on a number of factors.

Complex numerical techniques have been developed to describe hydrogen diffusion out of steel. Despite the precise results given by these techniques, a good approximation of the hydrogen remaining in a given weldment can often be obtained by simplification of the geometry and making some assumptions regarding material homogeneity and diffusion coefficients. Figure 5-10 shows loss of hydrogen from different specimen geometries as a function of time. In Figure 5-10, D represents the appropriate overall diffusivity coefficient for hydrogen in steel [cm²/s], t is the time [s], and L is the critical half-thickness of the plate, rod, or cylinder under consideration. Figure 5-1 shows the range of values for D , the apparent diffusivity of hydrogen in steel as a function of temperature. As shown from Figure 5-1, the diffusivity hydrogen in steel strongly depends on temperature and impurity content.

Some simple assumptions, along with Figures 5-1 and 5-10, can be used to estimate the diffusible hydrogen remaining in a weld after a given time. Figure 5-11 shows a schematic of a beam-to-column weld and the assumption of a cylindrical weld volume with a radius (L) and an infinite length. Assuming maximum and minimum values of D by consulting Table 5-1 or Figure 5-10 at a given temperature and equivalent diffusion on all directions, and geometry (an infinite cylinder in the case of beam-to-column welds) allows estimation of remaining hydrogen after a given time. Table 5-3 shows the time required to reduce the original concentration to 10% at room temperature assuming a range of flange thickness and diffusion coefficients. Consideration of the hydrogen diffusion coefficients given by Dallam, et al. (1999) for FCAW-S consumables suggests that diffusible hydrogen can be reduced to 10% in approximately five days, when a flange thickness of 3/4 in. was assumed, to over 34 days when a 2 in. flange was assumed. As previously mentioned, the diffusion coefficient, D , of hydrogen in steel can vary considerably with impurity concentration. Although the values given by Dallam in Table 5-1 are likely to be representative of some FCAW-S welds, this value is likely to be reduced further in weld metal with higher carbon and aluminum concentrations. Considering the lower bound diffusion coefficients reported in the literature, it may be possible for significant levels of diffusible hydrogen to remain in a moment connection for more than a year. Additionally, the distribution of hydrogen will be non-uniform with lower levels of diffusible hydrogen measured in the near-surface regions.

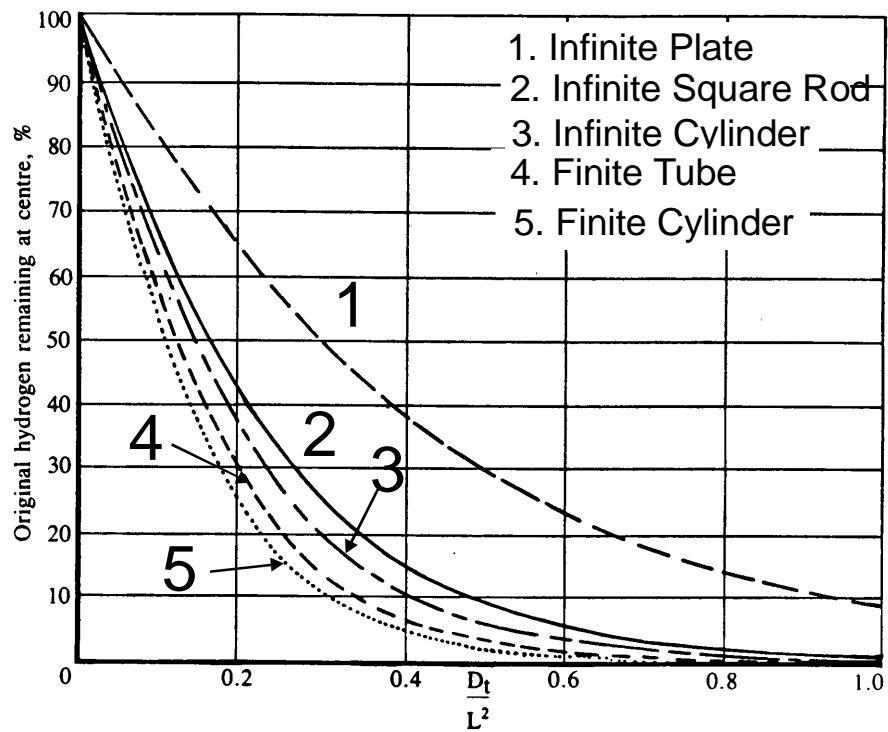


Figure 5-10 Proportion of Diffusible Hydrogen Remaining in Different Geometry Shapes after Exposure in Air for Time at Constant Temperature (Bailey, 1993)

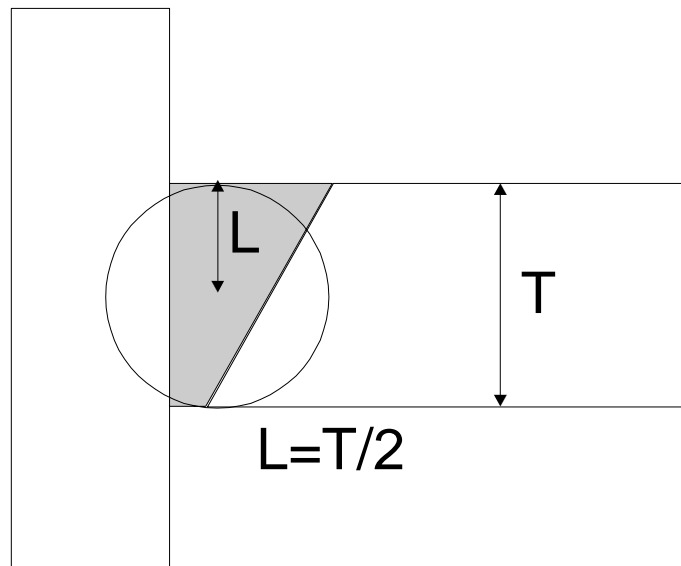


Figure 5-11 Simplified Geometry and Assumption of Infinite Cylinder to Estimate Hydrogen Remaining after a Given Period of Time

Table 5-3 Expected Time for Diffusion of 90% of Hydrogen from FCAW-S Weld Metal from Flanges of Different Thickness

Beam Flange Thickness (in.)	Half Thickness (cm)	Days Until 10% Remains	
		Dmax	Dmin
0.75	0.9525	2.1	4.8
1	1.27	3.7	8.5
1.5	1.905	8.4	19.1
2	2.54	14.9	33.9

Diffusion rates: Dmax 2.00E-06 cm²/s

Dmin 8.80E-07 cm²/s

No weld metal failures were observed in specimens fabricated using the E70TG-K2, E71T-8, or E70T-6 consumables. Many of the full-scale connection tests were tested within weeks after fabrication. Although there was some evidence of fisheyes on some of the fracture surfaces, no direct evidence of a reduction of weld metal performance as a result of the presence of diffusible hydrogen exists. On this basis, the use of low temperature PWHT to increase the rate of diffusible hydrogen removal may not be entirely justified provided that appropriate consumables and welding procedures are employed. The following factors should also be considered when deciding whether or not to employ a low temperature PWHT:

- Cost and logistics: Simply applying insulating blankets over the welds would provide little benefit, and the cost of using electrical heating blankets can be high.
- Elapsed time after welding and before service: In many cases, more than six months will elapse after welding prior to service.
- Demand on weld: Many of the post-Northridge connection designs reduce the demand on the weld considerably and thus yield-level stresses may not be expected in all cases.

Consumables and welding procedures employed:

- Maintenance of an adequate interpass temperature will allow for some hydrogen diffusion to take place in between weld passes.
- Specification of a maximum interpass temperature will ensure that welds are not rapidly deposited and allows for interpass hydrogen diffusion.
- Weld metal carbon and aluminum concentrations should be equivalent to, or lower than, those measured in E70T-6 and E70TG-K2 weld metals since both carbon and aluminum can considerably reduce the diffusivity of hydrogen in steel.
- Initial diffusible hydrogen concentrations expected in the weld metal.

5.4 Summary and Conclusions

1. Weld metal diffusible hydrogen can increase substantially after atmospheric exposure of certain FCAW-G and FCAW-S welding consumables. This increase in diffusible hydrogen can be attributed to the use of hygroscopic core ingredients and/or hygroscopic drawing lubricants. Electrodes should be evaluated on a “consumable-by-consumable” basis to determine the risk of atmospheric exposure.
2. In some consumables, weld metal diffusible hydrogen can increase with increasing wire feed speed and shorter electrode extension. As with atmospheric exposure, this effect should be evaluated on a “consumable-by-consumable” basis.
3. Evaluation of weld metal diffusible hydrogen in FCAW consumables should be conducted using welding parameters that include wire feed speeds near the upper end of the range recommended by the manufacturer at the shortest recommended electrode extension.
4. Although some FCAW-S consumables can be manufactured to meet an AWS H8 designation, it may be difficult to maintain this level of diffusible hydrogen on a consistent basis due to the contribution of hydrogen to the weld pool from the atmosphere during welding.
5. With the use of lower carbon equivalent steel base materials, the location of hydrogen assisted cracking has shifted from the HAZ to the weld metal. Although appropriate models and approaches have been developed to reduce the risk of base metal hydrogen assisted cracking, similar approaches have not been developed for hydrogen assisted cracking in the weld metal.
6. The risk of hydrogen-assisted cracking was evaluated using the E71T-8, E70T-6, and E70TG-K2 consumables using 1 in. thick ASTM A572Gr. 60 plate material. Based on these tests, it appears that the minimum preheat values for prequalified welding procedure specifications as contained in AWS D1.1 are adequate to prevent hydrogen assisted cracking in single pass weld metal deposited with moderate heat inputs. These tests were evaluated using as-received consumables depositing welds with 8 to 12 ml H₂/100g weld metal.
7. Based on the results of the full-scale tests welded with the E70T-6, E70TG-K2, and E71T-8 consumables, and employing a post-Northridge design, low-temperature PWHT was not required to increase removal of diffusible hydrogen from the beam-to-column weldments.

5.5 Recommendations

5.5.1 Recommendations: Present Problems

Based on discussions at recent FEMA/SAC sponsored workshops, it is apparent there are two views regarding hydrogen management in FCAW consumables. These two opposing views are discussed below:

View 1: Some level of hydrogen control should be maintained and only “low hydrogen” consumables should be used.

In many industrial sectors where fabrication of fracture critical components exist (off-shore, pressure vessel, and naval applications), the use of consumables depositing weld metal with diffusible hydrogen concentrations of less than 5 ml H₂/100 g weld metal is often specified. Some fabricators allow the use of consumables classified to AWS hydrogen designation H8 along with moderate preheat. These restrictions are typically imposed to limit the risk of hydrogen assisted cracking. Depending on the duration of time between fabrication and service, low hydrogen electrodes may be desirable when welding thicker sections so that effects of diffusible hydrogen on weld ductility are reduced. In some cases, high temperature PWHT is specified to ensure reduction of diffusible hydrogen and reduction of residual stress in a weld deposit. Note: high temperature PWHT is not recommended for structural steel due to variability in toughness following heat treatment.

When appropriate, many fabricators that use FCAW electrodes to fabricate critical components in other industrial sectors utilize storage ovens for their consumables and apply the same exposure requirements for SMAW electrodes to FCAW electrodes.

Recent work by Devletian (2000) evaluated HAC in structural grades of steel deposited with FCAW-G electrodes depositing weld metal with 4 ml H₂/100g weld metal and ~8 ml H₂/100g weld metal. Although only a single heat input was evaluated in this study, Devletian observed cracking in the welds containing higher levels of diffusible hydrogen despite preheat levels that were expected to be “safe” according to criteria specified in AWS D1.1.

View 2: Maximum hydrogen limits are not required in the fabrication of steel moment connections.

In the initial stages of the FEMA/SAC program, some of the moment connection failures were attributed to hydrogen-assisted cracking. At the present time, no published studies exist that indicate that hydrogen or hydrogen-assisted cracking contributed to weld fractures during the Northridge earthquake. Additionally, the E70TG-K2, E70T-6, and E71T-8 consumables have been extensively tested during the FEMA/SAC program. Presumably these electrodes deposited weld metal with diffusible hydrogen concentrations equivalent to or higher than those listed in Table 5-2. While fisheyes have been observed in some of the fracture surfaces, there has been no indication that hydrogen assisted cracking occurred or that the presence of hydrogen reduced the plastic capacity of the moment connections during testing. Many of the fabricators participating in project workshops indicated that there have not been any problems with using either the FCAW-S electrodes mentioned above or using FCAW-G electrodes in the shop. The argument that the connection re-design should reduce the demand on the weld should hydrogen assisted cracking go un-noticed and that delayed inspection procedures should improve chances of detecting cracking was also presented.

At the present time, the definition of “low-hydrogen” in the AWS D1.1 code as applied to the use of prequalified electrodes is not defined, and there are no provisions requiring hydrogen

control in current guidelines. As such, there are no mandatory requirements requiring control of weld metal diffusible hydrogen in the codes that govern steel frame construction.

Many fabricators at the FEMA/SAC workshops also suggested that control of electrode exposure would be prohibitively expensive and that tracking the exposure of a given spool or wire would be impractical. Concern was also expressed regarding the level of knowledge regarding exposure of FCAW consumables, including:

- Is the test method consistent from lab to lab?
- Can only the top layer of exposed electrodes be removed?
- Are the exposure conditions consistent with exposure conditions in a large drum of wire?
- Are there data regarding the combined effect of time and relative humidity on absorbed moisture in FCAW consumables?

Based on the lack of test data, the argument was presented that no exposure restrictions should be imposed, and no restrictions on diffusible hydrogen are required.

5.5.2 Recommendations: Proposed Specifications

It is clear that both viewpoints expressed above are valid. While hydrogen control is utilized in many industries during fabrication of critical components, all testing under the FEMA/SAC program was conducted shortly after welding and, in most cases, performance of the test connections was not limited by weld performance. With the exception of the EWI study, weld metal diffusible hydrogen was not measured in all of the consumables used to fabricate the test connections. Electrode formulation and welding procedure can have a pronounced effect on the mechanical properties, ductility, and hydrogen assisted cracking resistance. The results of the SAC testing applies only to the specific electrodes tested in the SAC program when welds are deposited under similar conditions. Since electrode composition and hydrogen can vary considerably in different electrodes produced to a given specification by a single manufacturer or by several manufacturers, the engineer must rely on test data to make an educated decision regarding selecting appropriate consumables and welding procedures.

While additional study related to the determination of maximum permitted diffusible hydrogen for fabrication of structural steel is clearly warranted, there are numerous studies that have been conducted in the past that illustrate the need for control of diffusible hydrogen when conditions of high restraint and high consequence exist. It is clear that conditions of high restraint and high consequence exist when welds are deposited as part of the moment resisting system. The risk is further increased by the lack of reliable UT inspection to detect transverse weld metal cracks.

When compared to consumables used in the pre-Northridge era, electrode formulations have changed considerably. In order to meet minimum mechanical properties over a range of heat inputs, the alloy content, and risk of hydrogen assisted cracking, in the weld metal has increased. Many of the E7XT-X consumables are more than capable of depositing weld metal with tensile

and yield strengths of over 90 ksi even when moderate heat inputs are used. Given the critical nature of fabrication of steel frame moment connections, along with the possibility of higher weld metal strength levels, high restraint, and high levels of weld metal diffusible hydrogen, approaches to control diffusible hydrogen are warranted. While the maximum permissible levels and approaches should be the subject of future research, the following recommendations are made based on the present testing and consideration of previous work related to hydrogen assisted cracking in steel.

Recommendation 1: FCAW-S consumables to be used in the construction of steel moment frames designed for seismic resistance should be purchased to meet an AWS H16 classification. FCAW-G electrodes should be purchased to meet an AWS H8 classification.

Commentary: Uncontrolled diffusible hydrogen concentrations are not technically justified for fabrication of critical components under conditions of high weld metal strength and high restraint, and when inspection techniques may not be reliable. Preferably, electrodes that are capable of meeting an H8 classification should be specified. At the present time, limiting diffusible hydrogen to a level of H8 would limit the number of consumables that could be used in the fabrication of moment frames without adequate justification of this recommendation. Given the ambiguity of the AWS D1.1 code, specification of some level of hydrogen control is just a step in the right direction, and further thought should be given to whether or not lower levels of diffusible hydrogen are technically justified. The FCAW-S consumables evaluated in the FEMA/SAC program should be capable of meeting an AWS H16 classification. Many FCAW-G consumables on the market today should be capable of meeting an H8 classification. The higher alloy content in some FCAW-G consumables may warrant more stringent control of diffusible hydrogen.

Recommendation 2: Weld metal diffusible hydrogen should be reported for each lot of electrode purchased. Electrodes should be evaluated using a welding current and wire feed speed that corresponds to 80% of the maximum range specified by the manufacturer, at the shortest electrode extension recommended by the manufacturer.

Commentary: Reporting of weld metal diffusible hydrogen levels must also accompany the mechanical test results. At the present time, no information is available to an engineer wishing to make a decision regarding the selection of appropriate consumables or welding procedures to control hydrogen. Test methods specified in the current versions of A5.20 and A5.29 may give a non-conservative measure of the weld metal diffusible hydrogen. Operating ranges specified by most manufacturers only imply that a stable arc can be maintained over a given range. Additional guidance from the manufacturer is required so that appropriate decisions can be made regarding the selection of welding procedures and consumables.

Recommendation 3: Electrode manufacturers should recommend appropriate storage and handling conditions such that as-manufactured hydrogen levels can be maintained after packaging is opened.

Commentary: Electrode manufacturers can only guarantee that a particular level of diffusible hydrogen will be measured in as-manufactured electrodes. No guarantee can be made that the same level of diffusible hydrogen will be measured after shipping and storage, or in the case of package damage. Where hydrogen control is justified, fabricators will typically have a procedure established to verify hydrogen levels reported by the manufacturer and to verify that extensive absorption of moisture did not occur during storage, due, for example, to damage to packaging. At the present time, most fabricators erecting steel to the AWS D1.1 code do not have appropriate staff, equipment, or other measures to successfully implement any type of hydrogen control program. As such, it may be unrealistic to expect this type of effort to occur without further justification. Without some evaluation of weld metal diffusible hydrogen, an engineer wishing to select welding procedures and welding consumables must rely on input information from the manufacturer. Given the present circumstances, this recommendation is the best compromise that can be expected, based on the test data on hand.

Imposition of strict exposure limits on all consumables is not technically justified. Some FCAW consumables may deposit welds with high levels of diffusible hydrogen, while other consumables manufactured to the same AWS classification may not. Although it is clear that moisture absorption can lead to dramatically higher hydrogen concentrations in weld metal deposited using some consumables, such restrictions would be virtually meaningless unless the fabricators are committed to controlling diffusible hydrogen. The electrode manufacturer should provide information regarding appropriate operating windows and storage conditions that could be followed should a fabricator decide that control of diffusible hydrogen is warranted. Preferably, testing should be conducted to provide some guidance on whether a given electrode is susceptible to moisture absorption and whether or not special storage requirements are in fact needed.

5.5.3 Recommendations: Future Research

Based on the data reviewed in this chapter, it is clear that the following technical topics should be the subject of additional research:

- Clarification of the minimum diffusible hydrogen concentrations permitted in the AWS D1.1 is required. At the present time, the term “low hydrogen” can be interpreted in many ways.
- A standardized method of atmospheric exposure testing is required for FCAW consumables. Determination of exposure limits for FCAW consumables will prevent overly conservative restrictions on exposure that would otherwise limit their use.

- At the present time, storage and handling conditions to ensure low hydrogen FCAW consumables are not reported by many manufacturers. Many users of FCAW electrodes would like improved assurance that the electrodes they use will consistently meet hydrogen classification levels claimed by the suppliers over a range of welding conditions. This may be achieved by specifying that diffusible hydrogen measurements are made at 80% of the manufacturers maximum recommended operating range using the lowest electrode extension.

6. EFFECT OF WIND SPEED

6.1 Introduction and Background

The selection of appropriate welding consumables for a given application is dependent on the ambient conditions encountered at the point of welding. This chapter deals with the tolerance of different welding consumables and processes to wind during welding. The wind speeds that can be tolerated for shielded metal arc welding (SMAW), gas-shielded welding processes, and FCAW-S welding processes are different. The primary effect of a strong cross wind is to displace (or blow away) the shielding gas used to protect the weld metal during metal transfer and solidification. Loss of shielding gas can result in absorption of nitrogen into the weld metal. For many processes, the absorption of nitrogen, even in small amounts, has been shown to cause a substantial decrease in toughness. Higher levels of nitrogen absorption can also cause porosity.

SMAW electrodes have been used for field welding operations since their development, and are widely accepted. Cellulosic and rutile electrodes generate a CO/CO₂ shielding gas with a high proportion of hydrogen during welding, while limestone (CaCO₃) is used in basic electrodes to effectively generate a CO/CO₂ shielding gas during welding. Despite the use of SMAW electrodes for field use, there are surprisingly few studies related to the effect of wind speed on either weld metal nitrogen pick-up, porosity, or mechanical properties. Although the “flux cup” that forms at the end of SMAW electrodes during welding is capable of mechanically shielding the weld from wind, variations in arc length can result in an increase in atmospheric contamination. Low nitrogen values and sound weld metal can typically be maintained through the use of a short arc length.

Several studies have shown that the use of gas-shielded arc welding processes are sensitive to wind disturbances (Boniszewski, 1992), (Yeo, 1986, 1988, 1989), (Prior, et al., 1986), (Millington, 1970), (Henrie and Long, 1982), (Schinkler, 1992), and (Autio, et al., 1981). Even a slow wind speed of 0.73 m/s (1.6 mph) can cause a disturbance in shielding gas and contamination of the weld deposit. When GMAW or FCAW-G is employed in an enclosed shop or welding booth, care must be exercised in orienting fume extraction equipment so that no disturbance of air flow occurs. Likewise, when gas-shielded processes are used for field welding operations, a wind screen is erected to eliminate drafts. As reviewed by Bonieszewski, several investigators (Shlepakov, et al., 1989) determined that increasing wind speed had little effect on the mechanical properties of most FCAW-S electrodes while the CVN impact energy, elongation, and weld integrity of GMAW deposits was substantially degraded when wind speed increased.

Figure 6-1 shows the effect of increasing wind speed (up to 5.5 m/s or ~12 mph) on weld metal nitrogen concentration of three FCAW-S weld metals. No increase in weld metal nitrogen was measured in weld metals deposited using two of the three experimental electrodes. A slight increase in nitrogen (410 to 500 ppm N) was measured in the third electrode. Unfortunately, the effect of wind speed on the mechanical properties was not reported as part of the study by Houldcroft (1977).

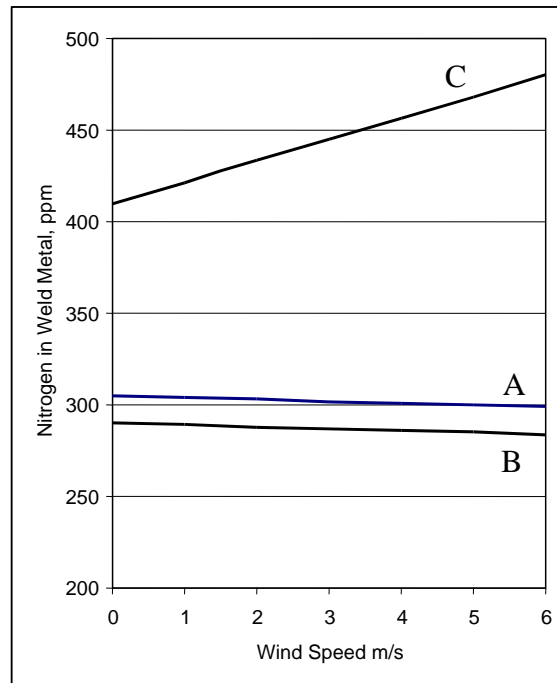


Figure 6-1 Effect of Wind Speed on Nitrogen Concentration in Three FCAW-S Weld Deposits

Similarly, Sheplekov reports that increasing wind speed up to 13 m/s did not cause an increase in weld metal nitrogen in two different FCAW-S electrodes. Combining data from two references, Boneszowski showed that the elongation and impact energy decreased with increasing impact energy when using a CO₂ shielded GMAW electrode (Figures 6-2 and 6-3).

The electrodes used to deposit welds in the previously mentioned studies were smaller diameter electrodes used for the construction of offshore platforms. The formulation, deposition rates, and welding procedures employed when using these smaller diameter consumables are not representative of those used in construction of moment frames in the U.S. When compared to the small diameter electrodes used in the fabrication of offshore platforms (welds with very high toughness), electrodes used in the fabrication of moment frames in the U.S. typically do not have core ingredients designed to provide additional shielding gas and have much higher deposition rates. Review of the applicable literature revealed very little data related to the effects of wind speed on the properties of weld metals deposited using large diameter FCAW-S electrodes. Therefore, under the FEMA/SAC program, an investigation was performed to evaluate the effect of increasing wind speed on the soundness and mechanical properties of FCAW-S weld metals. This study is described in the following section.

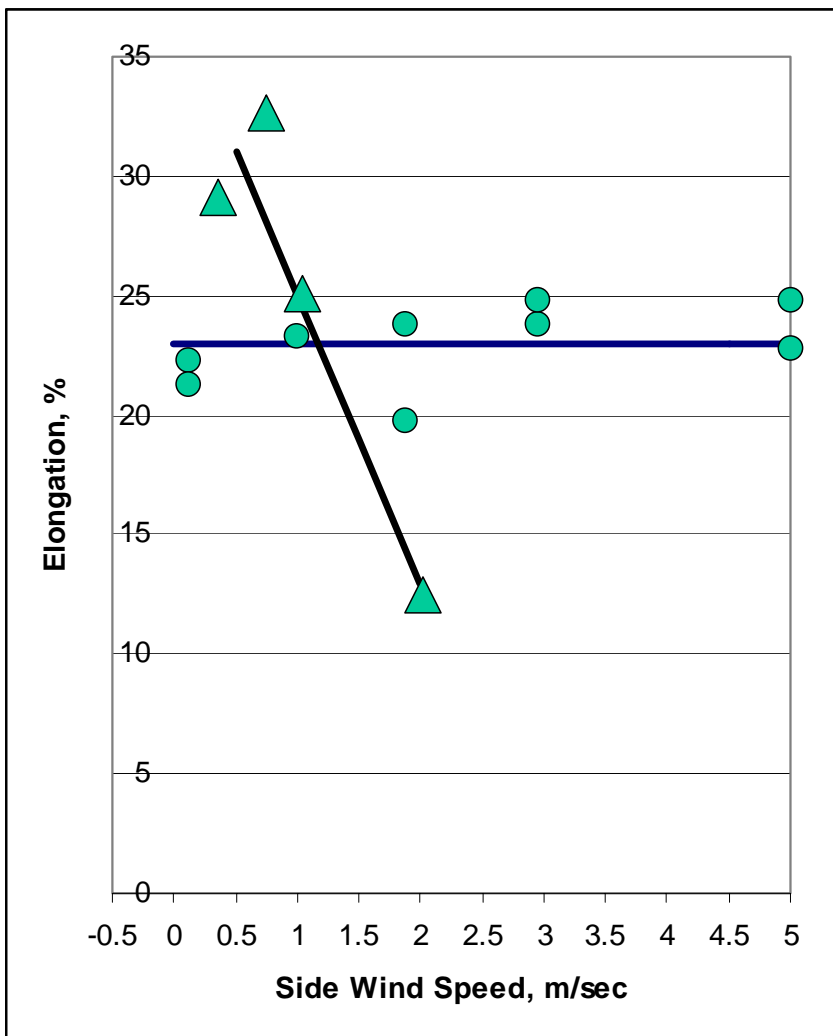


Figure 6-2 Effect of Wind Speed on Tensile Ductility of All Weld Metal Tensile Specimens Produced Using the FCAW-G and FCAW-S Processes

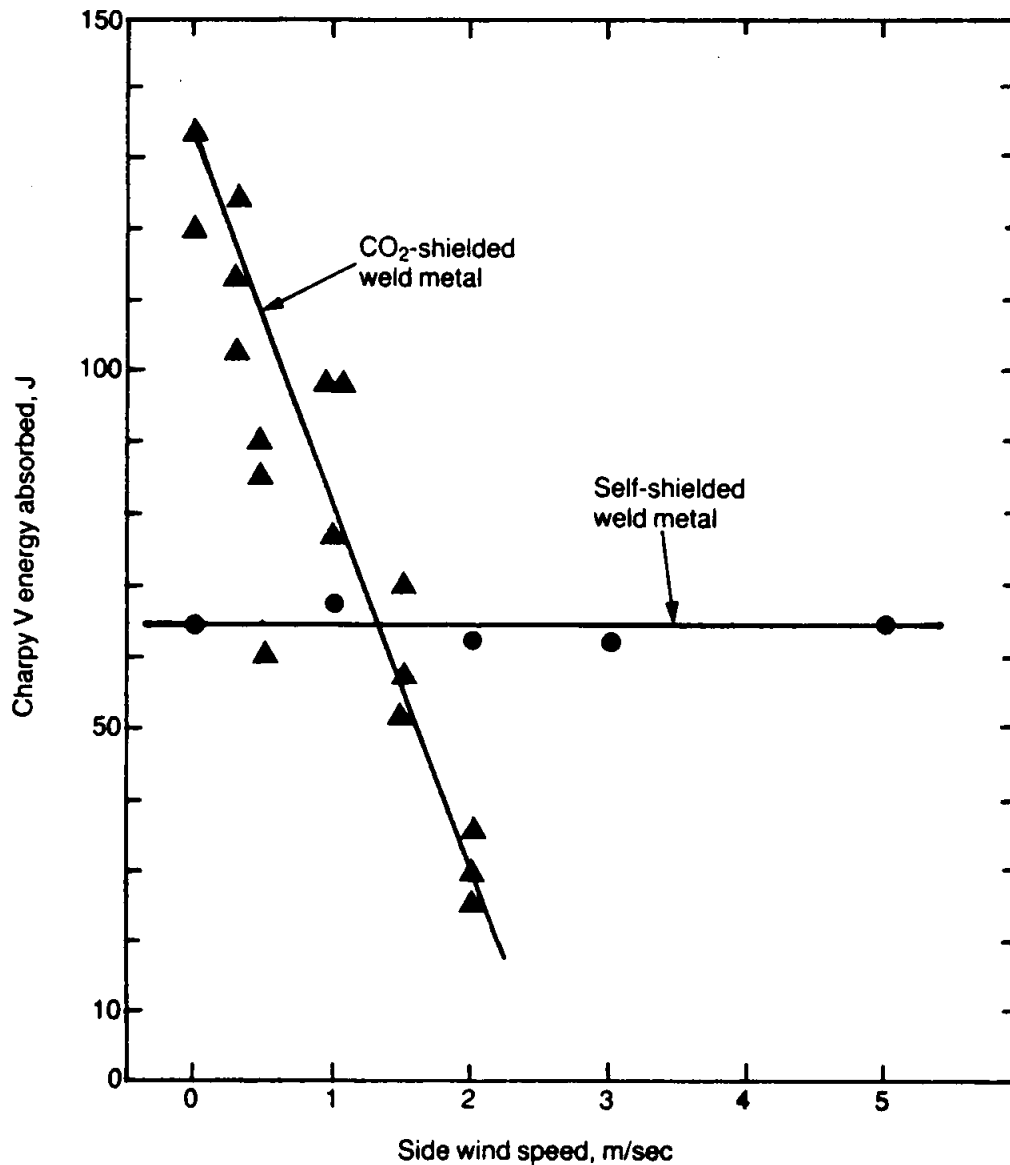


Figure 6-3 Effect of Wind Speed on CVN Impact Energy Measured in Welds Deposited Using the FCAW-G and FCAW-S Processes

6.2 Experimental Approach

6.2.1 Weld Metal Soundness Study

As part of investigation Task 5.2.3 (Johnson, 2000a) welds were deposited to evaluate the effect of wind speed on the soundness of GMAW, FCAW-G, and FCAW-S weld metals. Bead-on-plate welds were deposited using the consumables and welding parameters listed in Table 6-1. Welds were deposited on 10- × 10- × 1/2-in. thick A36 steel plate. The surface of the plate was prepared using a Blanchard grinder and degreased prior to welding. A preheat of 70°F was used for all experimental welds. The welding parameters used were within the range specified

by the manufacturer. Wind speed was varied by changing fan speed or by positioning a standard box fan at different distances from the weld joint during welding as shown schematically in Figure 6-4. The fan was positioned so that air flow occurred in a direction that was perpendicular to the direction of welding, allowing a constant wind speed to be maintained at all locations along the weld length. The length of the bead-on-plate welds ranged from 8 to 10 in. Wind speed was measured at locations corresponding to the weld centerline using a hand-held anemometer. For each consumable evaluated in this study, mechanized welds were deposited at wind speeds of 0.5, 1, 2, 3, 4, 5, 8, 10, 15, and 18 mph. Welds were visually inspected and radiographed to determine the nature and extent of porosity.

Table 6-1 Welding Parameters Used to Produce the Bead-on-Plate Welds Deposited Used to Evaluate the Effect of Wind Speed on Weld Soundness

Weld	Electrode Name	Current (A)	Voltage (V)	Travel speed (ipm)	ESO (in.)	Gas	Flow Rate
A	5/64 E61T8-K6 (NR203NiC)	250	22	6	0.75	N/A	
B	5/64 E71T-8 (NR232)	320	23	12	0.5	N/A	
C,G	3/32 E70TG-K2 (NR311Ni)	330	27	12	1	N/A	
E	0.045 E71T-1	200	27	12	0.75	80/20	30 CFH
D,J	0.045 E70T-5	195	30	12	0.75	80/20	30 CFH
F	0.045 ER70S-6	200	22	12	3/8	80/20	30 CFH
H	3/32 E70T-6 (NR305)	425	24	12	1.5	N/A	

6.2.2 Weld Metal Mechanical Property Study

In addition to the bead-on-plate welds deposited to determine the effect of wind speed on weld soundness, multipass groove welds were deposited manually under windy conditions in order to determine the effect of wind speed on weld metal mechanical properties. As will be discussed later, the FCAW-S welds produced sound weld metal under conditions where the wind speed exceeded 18 mph. Based on the weld soundness study and practical safety considerations, multipass groove welds were deposited with a wind speed of 10 mph. Mechanical property specimens were extracted from the multipass groove welds.

Three FCAW-S (3/32 E70TG-k2, 3/32 E70T-6, and 5/64 E71T-8) electrodes and one SMAW (3/32 E7018) electrode were used to fill a single-V joint (60 deg. included angle, 1/2-in. root opening) in 1-in. thick ASTM 572 Gr. 50 plate. The test plate dimensions are shown in Figure 6-5. The welding parameters used to deposit the multipass welds are listed in Table 6-2. In order to make a comparison to welds deposited in still air (welds deposited in the mechanical property portion of this investigation), welding parameters corresponding to the medium cooling rate welding parameters (as discussed in the section on weld metal robustness in this study) were used. A preheat and interpass temperature of 300°F was maintained through the use of electric

heating blankets. Standard full-size CVN specimens and all weld metal 0.505-in. diameter tensile specimens were machined from the groove welds. The CVN specimens were extracted along the weld centerline at the mid-thickness location as shown in Figure 6-5. Mechanical testing was conducted following FEMA/SAC protocols.

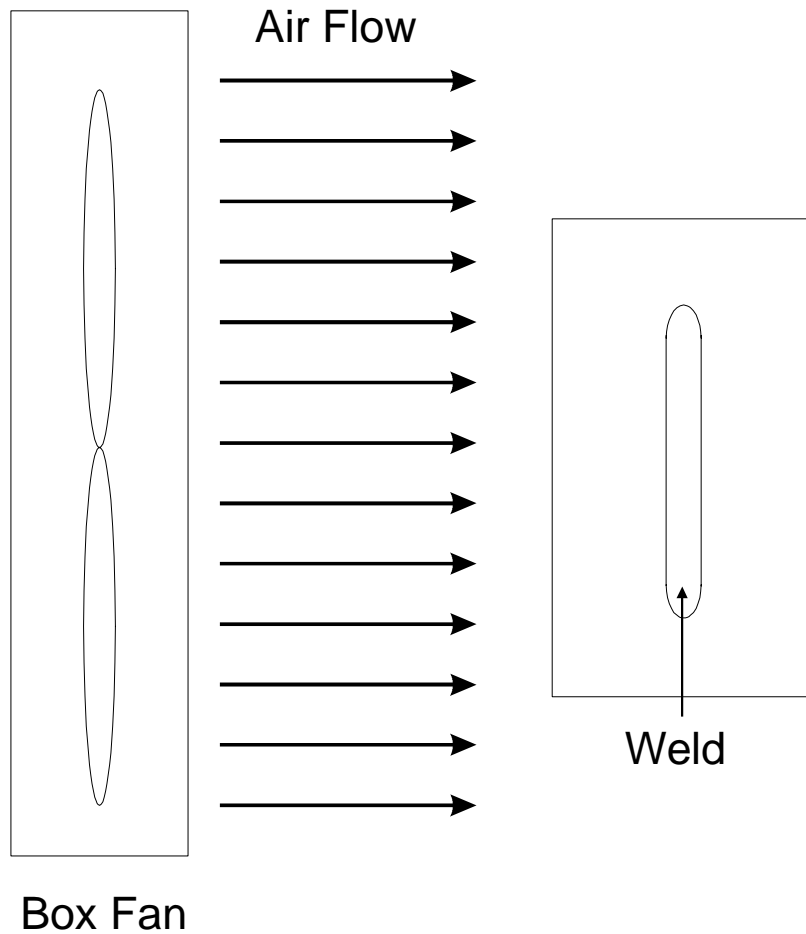


Figure 6-4 Schematic of Equipment Used to Vary Wind Speed. Wind Velocity was Varied by Adjusting Fan Speed and by Varying Distance to the Weld. Wind Velocity was Measured at the Weld Centerline Using a Hand-Held Anemometer.

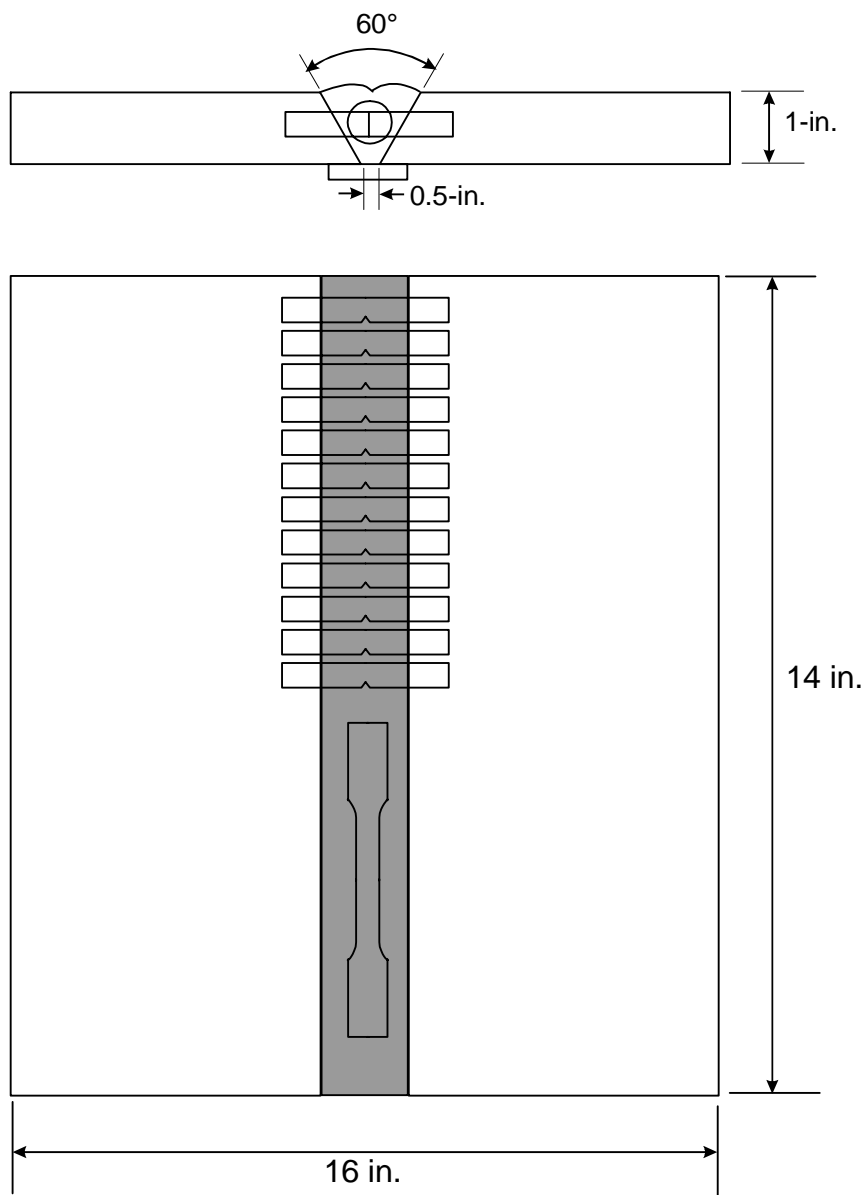


Figure 6-5 Groove Weld Joint Geometry, Test Plate Dimensions, and Sample Locations for the Mechanical Properties of Welds Deposited with a Wind Speed of 10 mph

Table 6-2 Welding Parameters Used to Deposit Multipass Weld Metal Used for Mechanical Property Measurement

Electrode	Current (A)	Voltage (V)	Travel Speed (ipm)	Electrode Extension (in)	Interpass (°F)	No. of Passes	Heat Input (kJ/in)
3/32 E70T-6	425	24	12	1.5	300	16	51.0
3/32 E70TG-K2	330	26	12	1	300	19	42.9
5/64 E71T-8	310	19	12	0.75	300	35	29.5
3/32 E7018	240	26	7	N/A	300	26	53.5

6.3 Results and Discussion

Increasing the wind speed above 2 mph caused porosity in welds deposited using the gas shielded arc welding processes. Initially, fine porosity was visually observed on the face of the weld bead. Additional increases in wind speed resulted in a corresponding increase in porosity observed both visually and in the radiographs. Although the arch characteristics changed, and spatter increased substantially when using the gas shielded processes, when wind speeds exceeded 8 to 10 mph, porosity was not evident when visually inspected. Radiographs of weld metals indicated that porosity occurred in the bead-on-plate welds deposited under high wind velocities. Figure 6-6 shows a macrophotograph of the face of E71T-1 weld metal deposited using a range of side wind velocities and corresponding radiographs. In Figure 6-6, extensive porosity is observed when the wind speed was 5 mph. Careful examination shows that although porosity is present in the weld at higher wind speeds, porosity was not visible on the face of the welds when wind speed exceeded 8 to 10 mph.

Inspection of the welds, deposited using the various FCAW-S weld metals evaluated in the wind speed trials, revealed that no porosity was observed in welds deposited using as-received consumables. Figure 6-7 shows that, even at wind velocity of 18 mph, sound weld metal was deposited using an E70T-6 consumable. A second experiment was conducted using an FCAW-S electrode that had been exposed to the atmosphere. This electrode produced deposited welds that were porous even under normal welding conditions. Exposure of the E70TG-K2 consumable under laboratory conditions for one month resulted in contamination of the electrode and caused an increase in the weld metal diffusible hydrogen concentration to 25 ml H₂/100 g weld metal. Similar to welds deposited using the gas shielded welding processes, porosity was not visible on the face of these weld metals when wind speed exceeded 12 mph while radiographs indicated the presence of porosity in the contaminated FCAW-S weld metals.

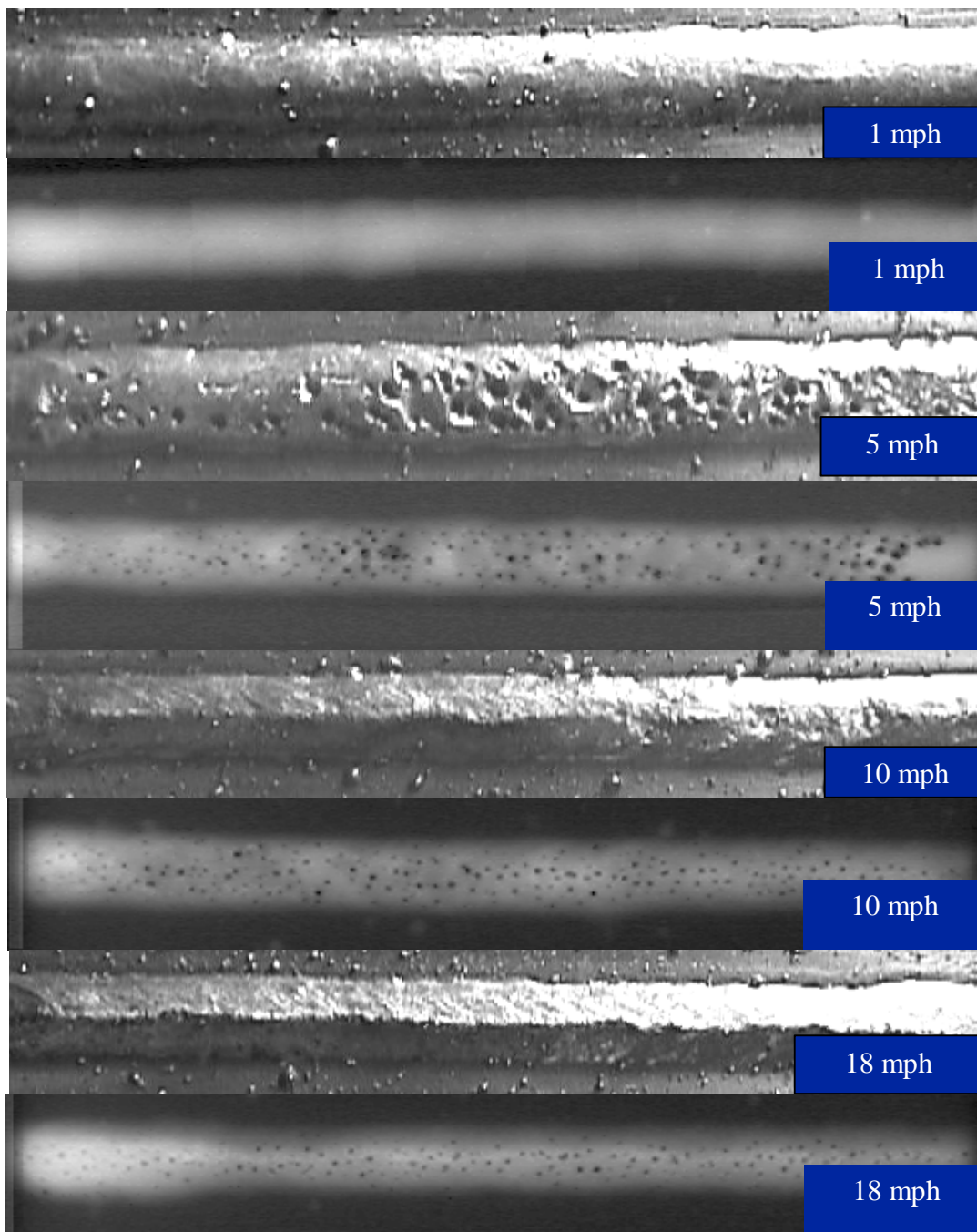


Figure 6-6 Macrophotograph (top pictures) and Radiographs (bottom pictures) of the E71T-1 Bead-on-Plate Welds Deposited Under a Range of Wind Conditions

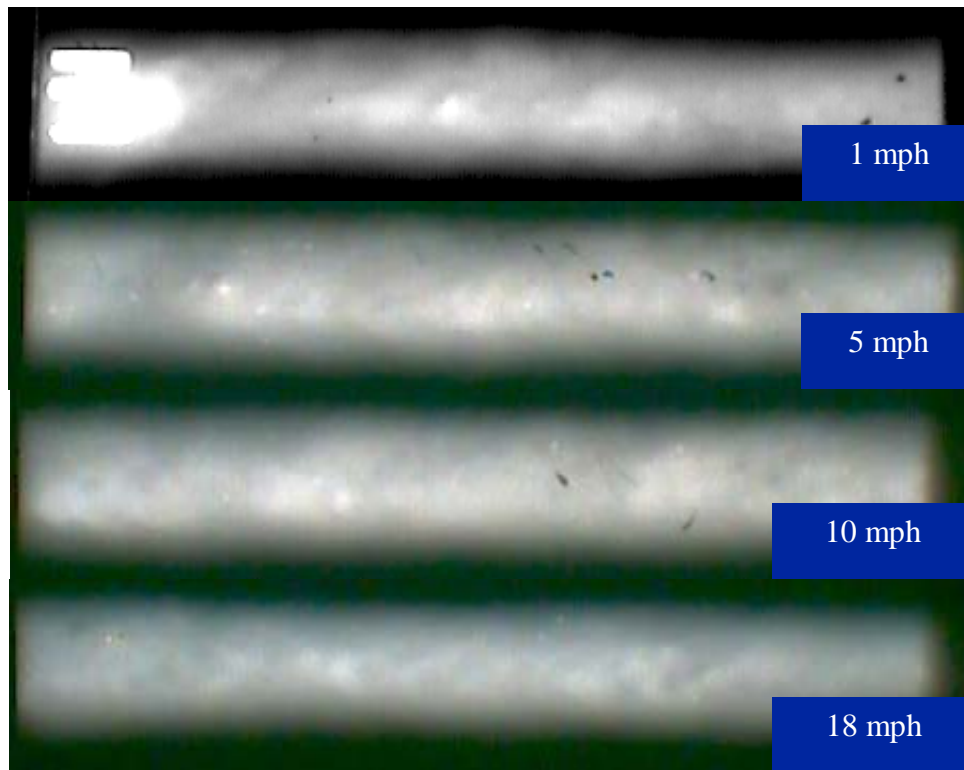


Figure 6-7 Radiographs of Bead-on-Plate Welds Deposited Under Different Wind Conditions Using an E70T-6 FCAW-S Consumable

It is clear from the above discussion that it is possible to have porosity in a weld metal which is detectable through the use of radiography or ultrasonic inspection but not visible on the face of the weld. For the welds produced in this study, the effectiveness of visual inspection was limited when the wind speed exceeded 10 to 12 mph (~5 m/s). One possible explanation of this observation is likely related to how the high wind velocity alters heat flow from the weld during welding. When welding in conditions of high wind velocity, it is possible that the wind causes a thin layer at the weld surface to solidify prior to the remainder of the weld. This surface layer (or skin) does not permit the evolution of gas through the surface of the weld as occurs under normal welding conditions or conditions of lower wind speed.

From an inspection standpoint, the inability to visually inspect for porosity may represent a problem, especially when no other techniques are employed to evaluate weld metal soundness. Welder safety considerations excluded, the results of this study indicate that weld soundness of gas shielded processes is compromised even at low wind speeds (1 to 2 mph - comparable to a slow walk) and that the FCAW-S consumables evaluated in this study are capable of depositing sound weld metal even at very high wind velocities. For the range of welding parameters employed in this study, it appears that wind velocities in excess of 10 mph may reduce an inspector's ability to evaluate weld soundness when using visual inspection alone.

Welding in the presence of a strong side wind can have a pronounced effect on weld properties. Several investigations have reported that the mechanical properties of small diameter FCAW-S consumables were maintained even when welding under high wind speed conditions. Review of relevant literature suggests that similar studies of welds deposited under windy conditions using large diameter FCAW-S consumables was limited. As part of investigation Task 5.2.3, the toughness of welds deposited using several FCAW-S and SMAW electrodes has been measured.

Figures 6-8 through 6-11 show a comparison of the CVN impact energy measured in welds deposited using E70T-6, E70TG-K2, and E7018 weld metals under conditions of still air and with a 10 mph (4.5 m/s) side wind. Surprisingly, improved toughness was measured in the E70T-6 welds deposited with a side wind (Figure 6-8). Inspection of the weld cross section revealed that the CVN notch sampled very little (~20 percent) primary weld metal in the welds deposited with a side wind and a large amount of primary weld metal (~60 percent) in welds deposited with no side wind. Although the welds were produced with similar arc energies and interpass temperatures, it is often difficult to precisely control CVN notch position. This drop in toughness when the CVN notch samples a large proportion of primary weld metal (with an as-deposited microstructure) is the most likely explanation for the difference in weld toughness measured in the E70T-6 deposits discussed above.

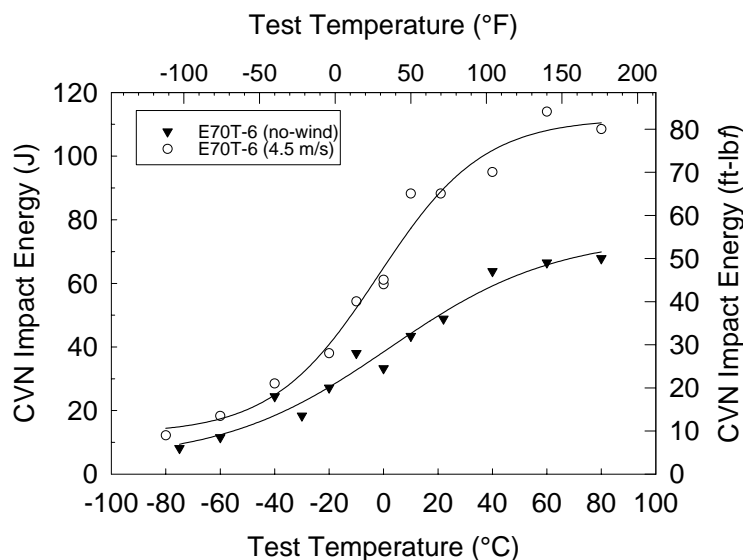


Figure 6-8 CVN Impact Energy Measured in E70T-6 Multipass Welds Deposited in Still Air and Under Wind Speeds of 10 mph (4.5 m/s)

Figure 6-9 shows that welding with a side wind had very little effect on the toughness of welds deposited using an E70TG-K2 consumable. This finding is consistent with earlier literature reporting the effects (or lack thereof) of wind velocity on FCAW-S toughness. Figure 6-10 shows that welding with a side wind had very little effect on the toughness of welds deposited using an E71T-8 consumable. The data presented in Figures 6-8 through 6-10 confirm

the findings of previous studies which report that very little degradation in toughness is expected in welds deposited using FCAW-S electrodes under conditions of high wind velocity.

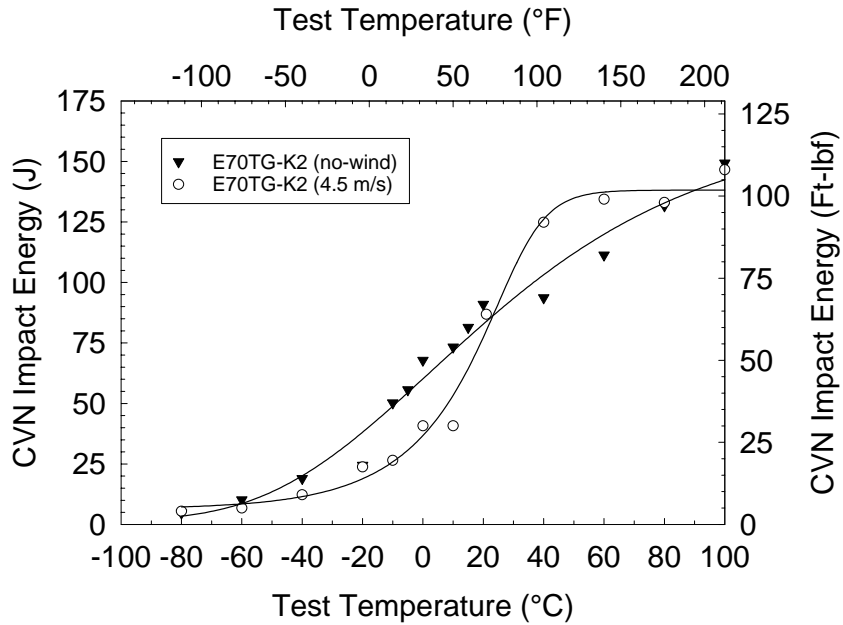


Figure 6-9 CVN Impact Energy Measured in E70TG-K2 Multipass Welds Deposited in Still Air and Under Wind Speeds of 10 mph (4.5 m/s)

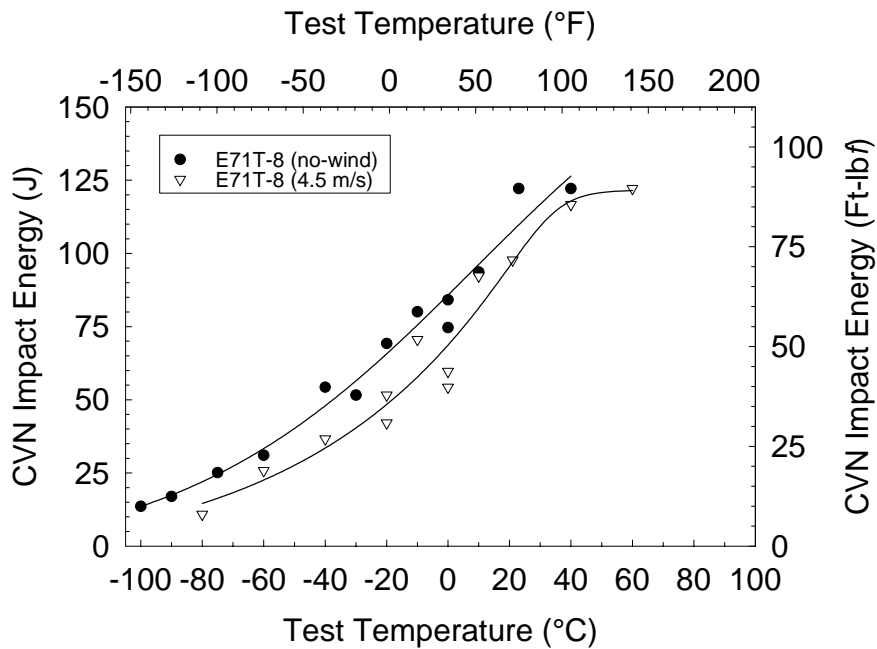


Figure 6-10 CVN Impact Energy Measured in E71T-8 Multipass Welds Deposited in Still Air and Under Wind Speeds of 10 mph (4.5 m/s)

Figure 6-11 shows that welding with a 10 mph side wind had a pronounced effect on the toughness of weld metal deposited using an E7018 electrode. Despite a substantial reduction in upper shelf toughness and a substantial increase in transition temperature, welds deposited using the E7018 weld metal in a side-wind would still meet the recommended toughness requirements for critical welded joints in moment resisting frames intended for seismic applications. Although chemical analysis of welds deposited under conditions of a side wind was not conducted, this drop in toughness in the E7018 deposits is consistent with the drop in toughness expected in SMAW deposits containing increased concentrations of nitrogen. Very little porosity was observed in the SMAW welds deposited with a side wind of 10 mph (4.5 m/s). The lack of porosity in welds deposited under these wind conditions is consistent with the observations of Henrie and Long (1982) who reported that sound SMAW welds could be produced with side winds of up to 50 mph if arc voltage (arc length) was carefully controlled.

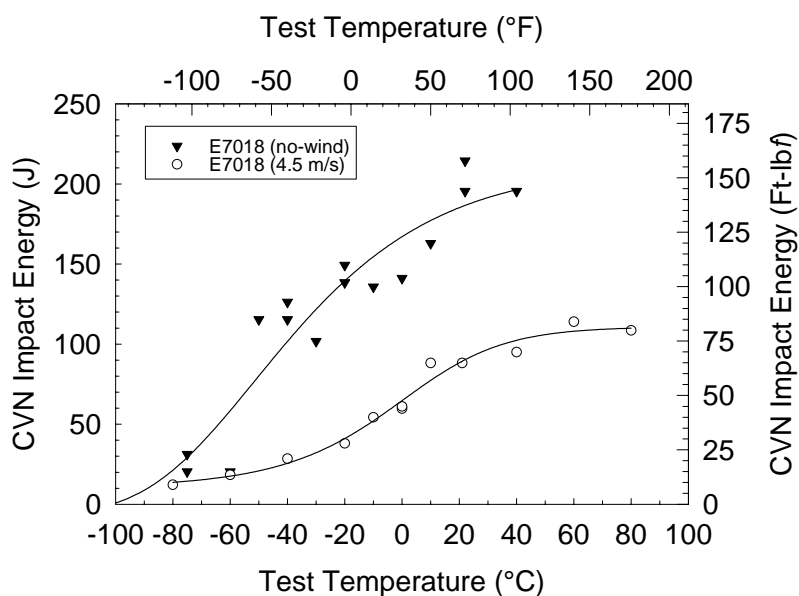


Figure 6-11 CVN Impact Energy Measured in E7018 Multipass Welds Deposited in Still Air and Under Wind Speeds of 10 mph (4.5 m/s)

Although the toughness of FCAW-G/GMAW weld metals deposited under windy conditions was not measured in this study, a similar reduction in weld metal toughness would be expected to occur due to the effects of nitrogen on weld metal toughness. Of particular concern would be welds deposited using microalloyed rutile (MAR) FCAW-G consumables that rely on a balance of titanium and boron. In these weld metals, titanium forms titanium-rich inclusions that serve as nucleation sites for acicular ferrite and combines with excess nitrogen. If enough titanium is added (typically >400 ppm) the boron will not react with nitrogen and, according to many theories, will segregate to austenite grain boundaries. The presence of boron is believed to “poison” the grain boundaries and reduce the volume fraction of grain boundary nucleated microstructures, which reduce toughness. An increased nitrogen content would be expected to disrupt this balance and reduce the effectiveness of the boron.

The results of the tensile tests are shown in Table 6-3. A slight decrease in strength and elongation was measured in welds produced while exposed to a side wind. Given the slight decrease in tensile properties, it is questionable whether or not the change in tensile properties is due directly to welding under windy conditions or associated with the inherent scatter expected when comparing welds produced manually. This decrease in tensile and elongation measured in welds produced with the 4.5 m/s side wind in this study are much smaller than the decrease in elongation measured by Autio, et al. (1981) using the CO₂ welding process. In their experiments, elongation dropped from over 40% in still air to less than 5% with a side wind of only 2.0 m/s. Autio's results demonstrated an obvious decline in weld metal properties beginning with a side wind speed of 0.3-0.5 m/s (0.7-1.2 mph).

Table 6-3 Summary of All Weld Metal Tensile Tests from Weld Metal Deposited with a Side Wind of 10 mph (4.5 m/s) and Under Laboratory Conditions (0 mph)

Specimen No.	Welding Conditions	Ultimate Strength		Yield Strength		% Elong.	% R.A.
		MPa	ksi	MPa	ksi		
E70TG-K2	4.5 m/s	561	81.3	463	67.2	24.2	70.0
E71T-8	4.5 m/s	561	81.3	456	66.1	23.5	63.8
E70T-6	4.5 m/s	595	86.3	528	76.6	24.4	69.4
E7018	4.5 m/s	561	81.3	463	67.2	26.2	70.0
E70TG-K2	0 m/s	592	85.9	509	73.8	29.3	71.9
E71T-8	0 m/s	598	86.7	455	66.0	28.9	63.8
E70T-6	0 m/s	638	92.6	550	79.8	25.6	54.8
E7018	0 m/s	561	81.3	492	71.4	28.9	72.8

If gas shielded arc welding processes are to be conducted in windy conditions, several approaches can be taken to reduce the effects of shielding gas loss (Okupnik, et al., 1993), (Kvirikadze, et al., 1968), (Bezbakh, 1971), (Verhagen, et al., 1972), and (Singh, et al., 1976). Most recommendations center on increasing shielding gas flow rate and nozzle design. One consequence of increasing shielding gas flow rate, however, is that at higher flow rates, the economic advantages of using gas shielded arc welding processes diminishes rapidly. Other suggestions include the use of an air stream in the opposite direction to that of the side wind (provided that the wind direction is constant). Although the SMAW process is capable of depositing sound welds under high wind velocities, the use of a short arc length is critical.

The results of this investigation demonstrate that it is possible to deposit sound welds that are capable of depositing weld metal meeting minimum expected mechanical properties with strong side winds. The results of this study are consistent with other studies reviewed in the literature. Although it is possible to deposit welds under conditions of high wind speed, the safety of an operator must be of primary concern, especially while fitting and welding in high winds. Job site safety is of primary importance and cannot be overlooked.

Current guidelines in the AWS D1.1 code state that gas metal arc welding (GMAW), gas tungsten arc welding (GTAW), electro gas welding (EGW), and gas shielded flux cored arc welding (FCAW-G) shall not be done in a draft or side wind unless the weld is protected by a shelter. Such shelter shall be of material and shape appropriate to reduce wind velocity in the vicinity of the weld to a maximum of three (3) miles per hour (2.3 m/s). This measurement should be based on the average windspeed over an hour's time at the point of welding. Welding in the shop can also reduce the shielding gas effectiveness. This loss in shielding gas is often the result of inappropriate application of fume extraction equipment. In light of this study and other studies reviewed, it may be beneficial to reduce the maximum wind speed permitted by AWS D1.1.

6.4 Conclusions

1. Surface breaking porosity was observed in bead-on-plate welds deposited using the FCAW-G and GMAW processes when side wind velocity exceeded 1-2 miles per hour. Further increases in wind speed to over 8-10 mph resulted in welds that contained significant proportions of internal porosity without visual indication of surface breaking porosity.
2. Welds deposited using several FCAW-S welding consumables did not contain porosity when welds were deposited using side winds exceeding 18 mph. This observation is consistent with other studies reported in the literature.
3. Welding with a side wind of 10 mph did not result in decrease in CVN impact energy in of welds deposited using E70T-6, E70TG-K2, and E71T-8 electrodes.
4. A significant reduction in upper shelf toughness and transition toughness was measured in SMAW welds deposited under conditions of a 10 mph cross wind.
5. A slight decrease in tensile properties was measured in welds deposited with a 10 mph side wind. Given the minor decrease in tensile properties, it was unclear whether this decrease was caused by variations in welding procedure or wind velocity.

6.5 Recommendations

1. Based on the results of this study and a review of literature, it can be concluded that the FCAW-S process is capable of depositing sound welds without degradation of mechanical properties in high winds. The SMAW should also be considered in situations where wind may be of concern. In conditions of high wind, operator safety should be of primary concern.
2. Wind speeds as low as 1-2 mph caused porosity in welds deposited using gas shielded arc welding processes. Review of relevant literature suggests that mechanical properties may also be substantially reduced when welding with a 1-2 mph side wind. Some consideration should be given to reducing the 5 mph maximum wind speed permitted in AWS D1.1.

7. INSPECTION AND ACCEPTANCE CRITERIA

7.1 Introduction

As part of any manufacturing or construction process, inspection and acceptance criteria are typically established by code or contract. Over the years, a range of inspection and acceptance criteria have been developed for different industrial sectors. While there are more sophisticated inspection and acceptance criteria utilized in different industrial sectors, AWS D1.1 has done an exceptional job of providing guidelines for such inspection efforts – in many cases, better than some other industry standards. Much of what was learned in the studies related to inspection following the Northridge earthquake was that AWS D1.1 had addressed many of the critical issues related to monitoring and verifying weld quality, but the execution of production welding and related welding inspection could have been improved.

It is widely recognized that the NDT procedures specified in the AWS D1.1 Structural Welding Code are not adequate for the evaluation of planar type discontinuities. The amplitude-based evaluation technique does not provide for adequate evaluation for planar type discontinuities. As part of the FEMA/SAC program of investigations, samples with flaws representative of those typically observed in beam-to-column welds were fabricated by Southwest Research Institute (SwRI). These samples were utilized in round robin tests to evaluate the reliability of standard AWS D1.1 ultrasonic (UT) techniques and alternative flaw sizing procedures developed by Southwest Research Institute (SwRI). The results of the round robin testing are briefly reviewed in this section along with results of the SwRI testing. The advantages and limitations of inspection criteria developed for other industrial sectors are contrasted with those specified by AWS D1.1. Additionally, alternative non-destructive inspection techniques are reviewed.

When welds are inspected, judgements can be made as to whether the welds should be kept or removed, repaired, or replaced. To keep such judgements from being arbitrary and variable, written acceptance criteria are placed within welding codes such as AWS D1.1. These acceptance criteria take the available information from inspection and other easily accessed sources and put out a recommended course of action, basically, to accept or reject. Welds with flaws that impact the service performance and safety should be rejected. Welds without such flaws should, in most cases, be accepted, leaving a margin of conservatism that allows for the occasional rejection of imperfections that are not severe. Factors affecting acceptance criteria and alternative acceptance criteria are discussed below.

7.2 Overview of Inspection Methods

7.2.1 Visual Inspection

Visual inspection, as a form of nondestructive testing, is the visual observation and measurement of base metal, thermally cut surfaces, weld surfaces, and completed components. It is the first nondestructive testing method applied, and if the inspected item fails to meet visual criteria, more extensive nondestructive testing should not be conducted until the visual criteria is satisfied. Visual inspection requires good vision, and is normally conducted without the use of

magnifiers and other enhancements. Such instruments tend to distort the perception of the inspector. When surface defects such as cracks are suspected, the use of magnifying devices to further investigate the area is permitted. The existence of suitable lighting is necessary for adequate visual inspection.

Visual inspection includes the measurement of the work, which may include the smoothness of thermally cut edges, and the measurement of root openings, groove angles, weld size, convexity and other profile values, porosity, undercut, and other discontinuities. To perform such work, specific tools such as weld gauges are required.

Advantages and Limitations of Visual Inspection

- Visual inspection is effective for all surface-breaking discontinuities, including piping porosity, arc strikes, excessive convexity, overlap, toe cracks, undersized welds, undercut, seams, and laminations at exposed edges. Not all listed discontinuities are structurally significant, but they may indicate improper WPS application or poor welding technique.
- Visual inspection cannot reveal subsurface discontinuities such as cracks, incomplete fusion, slag inclusions, incomplete penetration, buried laminations, or lamellar tearing. See Table 7-1 and Table 7-2.
- Visual inspection cannot provide information regarding the mechanical properties of the weld or surrounding heat-affected zone (HAZ).
- The cost of visual inspection is usually less, per unit length of weld, than other methods of NDT. Inspection costs can increase dramatically if inspection includes recording of all measurements, rather than simple verification measurements and recording of unsatisfactory workmanship.

7.2.2 Penetrant Testing (PT)

Penetrant testing, also called dye penetrant or liquid penetrant testing, is the use of a specifically designed liquid penetrating dye to detect discontinuities at the surface of a weld or base metal. The penetrant is applied to the surface, allowed to remain on the surface for a specified time to penetrate cracks, pores, or other surface-breaking discontinuities, and then is carefully removed. A developer is then applied to the surface, which draws the penetrant out of the discontinuities. This leaves a visible contrasting indication in the developer, which may be removed for closer visual examination of the area providing indications. One method of penetrant testing uses a visible dye, usually red, which contrasts with the developer, usually white. The second method uses a fluorescent dye, visible under ultraviolet light. Fluorescent methods are usually more sensitive, but require a darkened area for testing.

Table 7-1 Applicability of NDE Techniques for Finding Discontinuities

Discontinuity Type	NDE Method				
	VI	PT	MT	UT	RT
Micro-cracks	X	A	A	S	X
Shrinkage Cavity	X	X	X	S	A
Undercut	A	S	S	S	A
Excessive Reinforcement	A	X	X	X	A
Excessive Convexity	A	X	X	S	A
Excessive Penetration	A	X	X	S	A
Misalignment	A	X	X	X	A
Excessive Melt Through	A	X	X	S	A
Underfilled Groove	A	X	X	A	A
Irregular Bead	A	X	X	S	A
Root Concavity	A	X	X	A	A
Poor Restart	A	A	A	A	A
Miscellaneous Surface Defects	A	A	A	A	A
Crater Cracks	A	A	A	S	A
Group Discontinuous Cracks	A	A	A	A	A
Branching Cracks	A	A	A	A	A
Surface Pore	A	A	A	S	A
Incomplete Penetration	A	X	X	A	A
Incomplete Fusion (Overlap)	S	A	A	A	X
Longitudinal Cracks	A	A	A	A	A
Transverse Cracks	A	A	A	S	A
Radiating Cracks	A	A	A	A	A
Uniform Porosity	A	A	A	A	A
Aligned Porosity	A	A	A	A	A
Elongated Porosity	A	A	A	A	A
“Worm Hole” Porosity	X	X	X	A	A
Incomplete Fusion (Interpass)	X	X	X	A	X
Incomplete Fusion at Root	S	A	A	A	A
Slag Inclusion	X	X	X	A	A
Oxide Inclusion	X	X	X	A	A
Metallic (e.g., Tungsten) Inclusion	X	X	X	A	A

Note: A = Acceptable method

S = Satisfactory, provided special procedures (e.g., VI enhanced with magnification) are used

X = Not recommended

1. VI and PT are surface tests only. These methods will not detect defects that lie beneath the surface. For purposes of developing this table, MT is not considered reliable for detecting subsurface discontinuities.
2. See Table 7-2 for applicable weld joint geometries.
3. The table is a guide only. Not every defect will be detected every time with each acceptable or satisfactory process. Recommendations are based on structural welds.
4. This table does not take into account operator training and qualifications. It is based on an average NDE Level II, as defined by ASNT SNT-TC-1A.

Table 7-2 Applicability of NDE Techniques for Weld Joint Geometry

Weld Joint Configuration (access to one side only)	NDE Method				
	VI	PT	MT	UT	RT
Butt Joint	A	A	A	A	A
Lap Joint	A	A	A	S	S
T-Joint	A	A	A	S	X
Corner Joint	A	A	S	X	X
Edge Joint	A	A	S	X	X

Note: A = Acceptable method

S = Satisfactory, provided special procedures (e.g., VI enhanced with magnification) are used

X = Not recommended

1. These are based on typical situations. Using special procedures, other NDE methods can be used for specific weld joint geometries.

Advantages and Limitations of Penetrant Testing

- Penetrant testing is relatively economical compared to ultrasonic testing, and especially economical when compared to radiographic testing.
- Testing materials are small, portable, and inexpensive, with no specialized equipment required unless an ultraviolet light is used.
- A relatively short period of training is necessary for technicians who will be performing PT.
- PT can be performed relatively quickly, depending upon the penetrant used and the required dwell time.
- A disadvantage with some penetrants and developers is the safe handling and disposal of used liquids and cleaning rags.
- Cleaning after inspection to remove residual penetrant and developer prior to weld repairs or the application of coating systems can sometimes be difficult and time-consuming. Unless penetrant materials are properly removed from the area to be repaired, subsequent defects may be introduced.
- Rough surface conditions, and irregular profile conditions such as undercut and overlap, can sometimes provide false indications of weld toe cracks when cleaning is not thoroughly performed. Weld spatter can also make surface removal of the penetrant more difficult.
- PT cannot be performed when the surface remains hot, unless special high-temperature PT materials are used, so waiting time is sometimes necessary with PT that would not be required with magnetic particle testing.

- Existing coatings should be removed prior to PT because the coating may bridge narrow cracks, preventing the entry of the penetrant.
- PT is especially effective with small surface-breaking cracks, such as toe cracks, and also surface-breaking piping porosity, crater cracks, laminations along exposed edges and joint preparations, and other surface flaws.
- PT is ineffective for any discontinuity below the surface, such as buried cracks, slag inclusions, lack of fusion, or incomplete penetration. See Tables 7-1 and 7-2.

7.2.3 Magnetic Particle Testing (MT)

Magnetic particle testing uses the relationship between electricity and magnetism to induce magnetic fields in the steel. Magnetic particles, commonly in the form of iron powder colored for better visibility, are dusted onto the magnetized surface. Cracks and other discontinuities on or near the surface disturb the lines of magnetic force, essentially acting as poles of a magnet, attracting the magnetic particles. After the area has been magnetized, the particles are applied, then removed with gentle dusting or application of air. Particles attracted to discontinuities remain on the surface at the flaw, attracted to the magnetic poles. The MT technician then evaluates the location and nature of the indicating particles. Tight lines are indicative of surface cracks or other flaws. Subsurface cracks and slag inclusions would show a broader indication. A permanent record of detected discontinuities can be made with the use of transparent adhesive tape or photography.

The magnetic fields can be induced using either prods, which directly magnetize the steel through direct contact with the steel and the induction of current flow in the steel, or with a yoke, which does not transfer electrical current but provides magnetic flux between the two elements of the yoke.

MT equipment may be operated either DC (rectified AC) or AC. DC provides higher magnetization levels, which allows for inspection for discontinuities somewhat below the surface. Inspection with AC is generally limited to surface-breaking and very near-surface discontinuities, and is considered more effective for surface discontinuities because the particles are more mobile.

Advantages and Limitations of Magnetic Particle Testing

- MT is relatively fast and economical.
- The equipment is relatively inexpensive, compared with ultrasonic or radiographic equipment.
- A source of electric power is necessary.
- Inspection costs are generally equal to or slightly more than PT, but considerably less than UT or RT.

- More training is necessary for MT, compared to PT, but substantially less than that required for UT or RT.
- MT can be performed effectively while the joint is still warm from welding or postheating.
- After inspection, removal of magnetic particles is quick and thorough, not delaying repairs or affecting coating application.
- Existing coatings may reduce the effectiveness of MT.
- Prods can cause arcing, requiring base metal repair for arc strikes, if improperly used.
- The depth of inspectability depends upon the equipment, selection of current, and the type of particles used. Although opinions vary as to the maximum depth that can be effectively inspected using MT, 8 mm (5/16 in.) is generally considered the deepest flaw that can be detected under ideal conditions.
- MT is effective for detecting surface-breaking discontinuities such as cracks and laminations. It is also effective for cracks, laminations, incomplete fusion, slag inclusions, and incomplete penetration if slightly below the surface. Rounded discontinuities such as porosity do not disturb the magnetic flux lines sufficiently to be effectively detected. See Tables 7-1 and 7-2.

7.2.4 Ultrasonic Testing (UT)

Ultrasonic testing requires specialized equipment to produce and receive precise ultrasonic waves induced into the steel using piezoelectric materials. The unit sends electric pulses into the piezoelectric crystal, which converts electrical energy into vibration energy. The vibration is transmitted into the steel from the transducer using a liquid couplant. The vibration is introduced into the steel at a known angle, depending upon the design of the transducer, with a known frequency and waveform. The speed of travel of the vibration in steel is also known. The vibration pulse travels through the steel until it strikes a discontinuity, or the opposite face of the steel, either of which reflects energy back to the transducer unit or another receiving transducer. Using a system of calibration and measurements, the location, relative size and nature of the discontinuity, if any, can be determined by close evaluation of the reflected signals. Small reflections are generally ignored, unless located in specific regions such as along edges. Locations of flaws can be determined using the display screen scale and simple geometry.

AWS *D1.1* Section 6, Part F provides the UT inspection procedures, including calibration, scanning methods, scanning faces, and transducer angles, and weld acceptance criteria, including reflected signal strength, flaw lengths, and locations for weld discontinuities. Report forms, generally hand written, are prepared by the UT technician, recording weld defects and other material flaws that exceed the acceptance criteria specified.

More expensive and sophisticated UT equipment can be operated in digital mode, recording and printing display screen images with input data. Very sophisticated automated UT equipment

can record the transducer location and the corresponding reflections, then use computer software systems to produce representative two-dimensional images, from various directions, of the inspected area and discontinuities. Such equipment is rarely used in normal construction inspection applications, but is available and sometimes used for very complex and critical inspections.

Even with conventional equipment, more complex inspection methods can be used to locate, evaluate, and size weld discontinuities. These techniques include tip diffraction and time-of-flight techniques, and can be incorporated into project inspection through the use of AWS *D1.1* Annex K provisions. Annex K requires the use of written UT procedures specific to the application, with experienced and qualified UT technicians tested in the use of the procedures, and also provides for alternate acceptance criteria in lieu of the tables found in Section 6, Part F of AWS *D1.1*. Such provisions are necessary when using miniature transducers, alternate frequencies, or scanning angles other than those prescribed.

The key to any successful ultrasonic examination is to have personnel, who are trained, qualified, and certified, to implement the procedures. The Southwest Research Institute (SwRI) procedure, developed under the FEMA/SAC program of investigations, is an example of an ultrasonic test procedure that is capable of detecting discontinuities not readily found by the AWS *D1.1* Code. However, the procedure requires an extensive amount of operator training, qualification, and performance demonstration prior to use in the production environment.

The development of any new ultrasonic testing procedure will require a significant investment in the time and training of the UT operators. This is especially true in procedures that vary significantly from the standard “code” testing procedures. Most codes used in the USA do not require defect sizing and classification as found in the Southwest Research Institute Procedure and API Recommended Practice 2X. Hence, when defect sizing and classification is critical, using trained and qualified personnel will be mandatory for successful execution of the ultrasonic inspection.

Advantages and Limitations of Ultrasonic Testing

- Ultrasonic testing is a highly sensitive method of NDT, and is capable of detecting flaws in welds and base metal in a wide variety of joint applications and thicknesses.
- AWS *D1.1* provisions are applicable for thickness ranges from 8 mm (5/16 in.) to 200 mm (8 in.). Both thinner and thicker materials may be examined and evaluated using UT, but Annex K must be used for technique and acceptance.
- Although capable of locating flaws and measuring flaw length, it is less capable of directly sizing flaws or determining flaw height without the use of advanced techniques.
- A primary disadvantage of ultrasonic testing is that it is highly dependent upon the skill of the UT technician. The cost of the equipment is considerably more than for MT, but less

than RT. The cost of more sophisticated UT units, capable of computer-generated imaging, approaches, and can exceed the cost of RT equipment.

- UT indications are difficult to interpret in certain geometric applications. It is ineffective for fillet welds unless very large, and then only for the root area for fillet welds above approximately 18 mm (3/4 in.). When backing bars remain in place, it is difficult to distinguish between the backing bar interface and cracks, slag lines, or lack of penetration or fusion at the root. With partial joint penetration groove welds, it is difficult to distinguish between the unfused root face and discontinuities near the root. In welded beam-to-column moment connections, the interference of the web with inspection of the bottom flange makes direct evaluation of the area beneath the weld access hole difficult. Second-leg inspections, not as accurate or as reliable as first-leg inspections, are necessary to evaluate the entire depth of many welds unless the weld face is ground flush. Discontinuities located just below the weld or material surface are also difficult to detect.
- UT is best suited for planar flaws such as cracks and lack of fusion, flaws which are generally most detrimental to joint performance when oriented transverse to the direction of loading. These defects tend to be irregular with rough surfaces, and therefore reflect signals even when not exactly perpendicular to the direction of the pulse. Laminations and lamellar tears are also easily detected. Smooth surfaces, such as unfused root faces, would redirect a signal and provide a weak response unless oriented perpendicular to the pulse. Rounded and cylindrical discontinuities such as porosity disperse the signal, also providing a weak response, but such rounded discontinuities are rarely detrimental to joint performance. Slag inclusions are irregular and provide easily identifiable responses. See Tables 7-1 and 7-2.
- The cost of ultrasonic testing is considerably more than PT or MT, and considerably less than RT. However, UT is the best method for detection of the most serious weld defects in a wide variety of thicknesses and joints. The time, and therefore cost, of UT inspection can vary greatly, depending upon the quality of the weld to be inspected. A good quality weld will provide few responses, requiring little evaluation time. A difficult configuration, or a poor quality weld, will require numerous time-consuming evaluations and recording of test data.

7.2.5 Radiographic Testing (RT)

Radiographic Testing (RT) uses a radioactive source and, typically, a film imaging process similar to X-ray film. The film provides a permanent record of the inspection. When a weld is exposed to penetrating radiation, some radiation is absorbed, some scattered, and some transmitted through the weld onto the film. Image Quality Indicators (IQIs) are used to verify the quality and sensitivity of the image. Most conventional RT techniques involve exposures that record a permanent image on film, although other image recording methods are also used. Real-time radiography uses a fluoroscope to receive radiation, then presents an on-screen image for evaluation. The two types of radiation sources commonly used in weld inspection are x-ray machines and radioactive isotopes:

1. X-rays are produced by portable units capable of radiographing relatively thin objects. A large 2000 kV X-ray unit is capable of penetrating approximately 200 mm (8 in.) of steel, a 400 kV unit to 75 mm (3 in.), and a 200 kV unit to 25 mm (1 in.) of steel.
2. Radioisotopes are used to emit gamma radiation. The three most common RT isotopes are cobalt 60, cesium 137, and iridium 192. Cobalt 60 can effectively penetrate up to approximately 230 mm (9 in.) of steel, cesium 137 to 100 mm (4 in.), and iridium 192 to 75 mm (3 in.) of steel.

Advantages and Limitations of Radiographic Testing

- RT can detect subsurface porosity, slag, voids, cracks, irregularities, and lack of fusion. See Tables 7-1 and 7-2.
- Accessibility to both sides of the weld is required.
- RT is limited to butt joint applications by AWS *DI.1*. Because of the constantly changing thickness for the exposure, RT is not effective when testing fillet welds or groove welds in tee or corner joints.
- To be detected, an imperfection must be oriented roughly parallel to the radiation beam. As a consequence, RT may miss laminations and cracks parallel to the film surface. Because they are usually volumetric in cross-section, discontinuities such as porosity or slag are readily detected.
- The limitations on RT sensitivity are such that defects smaller than about 1% of the metal thickness may not be detected.
- The radiographic images provide a permanent record for future review, and aid in characterizing and locating discontinuities for repair.
- RT is generally unaffected by grain structure, which is particularly helpful with ESW and EGW welds.
- RT is a potential radiation hazard to personnel, and strict safety regulations must be monitored and enforced.
- The cost of radiographic equipment, facilities, safety programs, and related licensing is higher than any other NDT process.
- There is usually a significant waiting time between the testing process and the availability of results.

7.2.6 Acoustic Emission Testing

There has been some research of Acoustic Emission (AE) testing of bridges. However, most of this work is in the stages of testing evaluation, and no viable commercial alternatives have been developed for buildings. It is recommended to explore and promote AE applications for inspection of seismically loaded welded connections in the future.

7.2.7 New NDE Techniques

There are several new technologies being developed for nondestructive examination of structural welds. These include:

- Semi-automated and fully automated UT
- Phased Array UT

7.2.7.1 Semi-Automated and Fully Automated UT

Semi-automated and fully automated ultrasonic testing provide several advantages when compared to manual ultrasonic testing. In a semi-automated system, the crawler or search unit is moved by hand, and UT data is collected automatically. In a fully automated system, the scanning is mechanized. Both methods offer the advantage of having a permanent image for viewing. This image can allow for a third party evaluation of critical discontinuities. These methods take some of the “human factor” out of the process by allowing for more consistent, reliable inspections. These methods are faster than manual UT, once specific procedures have been developed.

The disadvantages of these systems are higher capital costs and operator training and qualification. Typical semi-automated systems can cost three to four times what a manual UT system costs. A fully automated UT system can cost seven to ten times as much as a manual UT system. These estimates are based on the features and options of each individual system. Operators will need special training and qualifications prior to using any type of automated inspection system.

7.2.7.2 Phased Array UT

The next technology step after a fully automated UT system is a phased array ultrasonic test system. This system allows for beam steering, focusing, and control of the beam focal spot size, using a transducer made up of multiple piezoelectric crystals controlled electronically. This allows for better visualization of indications and better detectability of the critically sized defects. Additionally, a permanent record of images can be saved for third-party evaluation. As only one transducer can produce multiple types of transverse waves, the system allows for greater flexibility in complex weld geometries.

The phased array UT system has several disadvantages. A phased array system can cost ten to fifteen times that of a manual UT system, depending on options and features. Ultrasonic operators will require specialized training due to the specialized controls and features inherent in

the phased array system. Another disadvantage of the phased array system is how the system can be incorporated into current construction codes.

7.2.8 Types of Inspectors

AWS D1.1 is one of the few standards that clearly stipulates a delineation between a “fabrication/erection” inspector, who is the duly designated representative who acts for, or on behalf of, the contractor, and the “verification” inspector, who acts for, or on behalf of, the owner or engineer. The specific responsibilities of each type of inspector are stipulated in Sections 6.1.2.1 and 6.1.2.2 of AWS D1.1 for the fabrication/erection inspector and verification inspector, respectively. In quality circles, this would be recognized as the delineation between the activities and responsibilities of an individual working in quality control (fabrication/erection inspector) and quality assurance (verification inspector). While the Code makes the distinction, when the term inspector is used, it is intended to apply equally to both types of inspectors.

7.2.9 Inspector Qualification Requirements

In Section 6.1.4, AWS D1.1 specifies the qualification requirements for a visual welding inspector. Here, three different options exist:

1. AWS Certified Welding Inspector (CWI), currently or previously qualified per the requirements of AWS QC1, *Standard and Guide for Qualification and Certification of Welding Inspectors*, or
2. Canadian Welding Bureau (CWB) equivalent, currently or previously qualified per the requirements of Canadian Standard Association (CSA) Standard W178.2, *Certification of Welding Inspectors*, or
3. An engineer or technician who, by training or experience, or both, in metals fabrication, inspection, and testing, is competent to perform inspection of the work.

While the qualifications and performance of individuals meeting either of the first two options is fairly well understood and quantified, the third category certainly provides some room for interpretation.

7.3 Discussion of Ultrasonic Inspection Approaches

AWS D1.1 has done an exceptional job of providing guidelines for the inspection effort – in many cases, better than some other industry standards. Much of what was learned in the studies related to inspection following the Northridge earthquake was that the AWS D1.1 code had addressed many of the critical issues related to monitoring and verifying weld quality, but the execution of the production welding and related welding inspection could have been improved.

It is widely recognized that the AWS D1.1 Structural Welding Code is not adequate for the evaluation of planar type discontinuities. The amplitude based evaluation technique does not provide for adequate evaluation for planar type discontinuities. As part of the FEMA/SAC

investigations, samples with flaws representative of those typically observed in welded beam-to-column joints were fabricated by Southwest Research Institute (SwRI). These samples were utilized in round robin tests to evaluate the reliability of standard AWS D1.1 ultrasonic (UT) and alternative flaw sizing procedures by Southwest Research Institute (SwRI). The results of the round robin testing are briefly reviewed in this section along with results of the SwRI testing. The advantages and limitations of inspection criteria developed for other industrial sectors are contrasted with AWS D1.1. Additionally, alternative non-destructive inspection techniques are reviewed.

7.3.1 Summary of SAC UT Round-Robin Testing

As part of the FEMA/SAC program, specimens for round robin ultrasonic testing were fabricated by Southwest Research Institute (SwRI) and subjected to inspection by fifteen technicians at different locations around the country (Shaw, 2000). The specimens and defects utilized for this study were representative of full and partial penetration welds utilized in the construction of steel frame buildings. Although “average” technicians were requested, the participating technicians were generally higher qualified than the average technician, including several with Level III status, and were often selected by the testing agencies based upon their experience and skill level.

Technicians were instructed to evaluate the samples using *AWS D1.1 Structural Welding Code - Steel*, Section 6 methodology, using acceptance criteria for cyclically loaded structures. Following this testing, the technicians were encouraged to use any enhanced testing techniques at their disposal to further evaluate the specimens. Technicians were encouraged to use *AWS D1.1*, Annex D standard forms, but could use whatever form was standard for their firm, and were encouraged to draw sketches to accompany their test reports.

Although all participants were invited to use whatever special techniques they had at their disposal for further evaluation of the samples, none used techniques beyond the AWS D1.1 prescribed methodology.

Shaw (2000) reached the following conclusions regarding the SAC round robin UT investigation:

1. The scatter in UT results is broad, particularly in the “indication rating” or “db value” used for acceptance criteria under the AWS D1.1 code (see Table 7-1). Scatter as much as 15 db, and sometimes higher, for an indication rating was common for a given discontinuity. For a given discontinuity, the average of indication rating standard deviations is approximately 4 db, with a standard deviation over 7 db for some discontinuities.
2. On average, approximately 25% of the known discontinuities were missed.
3. On average, 16% of the reported rejectable indications were for locations where no known discontinuities were implanted (false calls). There was little consistency to these indications to cause one to suspect that an unknown discontinuity existed in the specimens. Of the false

calls, 12 were for backing indications and 7 were from the root of a partial penetration groove weld. If these forms of false calls are discounted, the rate of false calls drops to 7%.

4. Joints that have backing bars remaining in place have a higher incidence of false indications (false calls) than joints without backing bars in place. Most false calls were based upon rejections from the backing bar itself. If root indications are considered, the rate of false calls is 20%. If these rejections are ignored, the rate of false calls drops to 8%. By comparison, in similar joints with the backing removed, only one false call out of 34 indications was made. Joints with web interference, such as at the bottom flange of a beam-to-column connection, had 17 misses out of a possible 52 indications, or 33%. There were also 9 false calls out of a total of 43 reported indications, or 21%. Seven of the nine false calls were on the specimen without backing, which contradicts the conclusions drawn from data mentioned in the previous paragraph. Joints representative of cover-plated connections had a total of four misses out of a possible 24 indications, or 17%. This is not outside the boundary of normal performance expectations, so it cannot be stated with certainty that such joints cannot be inspected with confidence equal to that of other joints, although that confidence may be limited.
5. The size of embedded discontinuities varied in both height and length. There was no correlation noted between the size of discontinuity and the rate of misses. A commonly accepted value is that discontinuities of 1/8" in height are the smallest that can be detected using AWS D1.1 techniques. None of the implanted discontinuities were of a size to validate this assumption.
6. When detected, discontinuity length measurement was fairly consistent, within 1/4" for the start or end of a given discontinuity 67% of the time. Accuracy in total discontinuity length within 1/4" was achieved 65% of the time, and within 1/2" approximately 85% of the time. Current AWS D1.1 acceptance criteria use length as a basis, with acceptance cut-offs at 3/4" and 2" lengths.
7. Technicians were generally able to indicate the relative position of the discontinuity in relation to the throat dimension (height) of the weld. Standard UT reporting procedure is to indicate the depth of maximum indication, rather than locate the top and bottom of the discontinuity. Similarly, technicians were generally able to locate the discontinuity along the "x-axis" (measured distance away from the column face) within 1/8" when located at the fusion line between beam and column. Only one of thirteen technicians accurately identified the depth of a lamellar tear located in column material, the others noting the discontinuity at the column fusion line. When the discontinuity is located away from the column fusion line, in the weld or the fusion line between weld and beam material, the position of the discontinuity was within 1/4" 50% of the time, and within 1/2" 70% of the time. Problems in locating the "x-axis" dimension were not specific to any one type of joint.

For backing bars, some technicians rejected joints based upon backing bar indications, attributing them to root discontinuities, while others ignored those indications. The methods used by the technicians in this evaluation were rarely stated in their reports.

7.3.2 Demonstrated Limitations of the Current D1.1 Acceptance Criteria

During examination of fractures from welds in moment-resisting frames in the Los Angeles area after the Northridge earthquake, root flaws were observed (typically, lack of root fusion and slag inclusions) that were believed to be in the original welding rather than caused by the earthquake. These flaws were common to many failed welds with a T-joint geometry using backing bars. They particularly occurred at the root on the column flange side and often had their greatest depth centered in the beam flange width, adjacent to the beam web.

In addition to the round robin UT trials, the sizes of these flaws from original fabrications examined at Lehigh University (Kaufman, et al., 1997) ranged in depth up to 0.4 in. and in length up to the full flange width. The mean depth from the study at Lehigh was 0.15 in. These flaws were found in welded joints that had been inspected to D1.1 during the construction process. These depths and lengths for original fabrication imperfections significantly exceed those that the ultrasonic acceptance criteria in AWS D1.1 had been expected to reject.

Investigators (Paret and Freeman, 1997) and (Paret, 1999) have suggested that the large difference between the flaw sizes expected to be rejected by D1.1 and the fabrication flaw sizes that actually remain in complete joint penetration welds can be caused by the geometry of the welds being inspected. Large imperfections may be judged as acceptable for three general types of reasons:

1. The area including the flaw was hidden from ultrasonic inspection.
2. The area including the flaw could only be inspected by ultrasonics from long range.
3. The area including the flaw had other structures that returned ultrasonic echoes but were known to be acceptable, so that the flaw response was confused with the acceptable response.

One area where flaws may be hidden in beam-to-column connections is the area below the beam web in the weld of the bottom beam flange to the column. That section of the weld cannot be reliably inspected with a single transducer from the top surface of the lower beam flange since the web interferes with placement of the transducer. The beam web shape and the weld access hole surface prevent a single transducer on the lower face from transmitting ultrasound to this region also.

The hidden region under the beam web can be inspected using a dual probe technique. The two probes are adjacent to the beam web and angled so that one sends ultrasound into this region and the other receives the echoes from this region. This approach is not currently described in AWS D1.1. Also it can be expected to provide different amplitude responses from single transducer techniques used on other parts of the same weld, since the path length of the ultrasound beam will change and the beam will be approaching the plane of the imperfection from a different angle.

Paret has discussed the difficulty of reaching the area of the weld adjacent to the column face when scanning from the top surface of the beam. The minimum inspection during construction

uses a single transducer from the top surface of the beam (Face A) and inspects using leg one (no reflections from the beam surface) of the sound path. If the weld cap is wide compared to the beam flange thickness, a region at the cap side adjacent to the column will not be in the ultrasound path. Weld spatter or a wider weld cap may push the transducer further away and expand the region not in the ultrasound path on leg one.

If the transducer is moved further from the weld, longer ultrasound paths can reach these areas. However, the correction for a longer sound path in D1.1 tends to underestimate the effect of a longer sound path on reducing the echo amplitude. So imperfections that may be rejected from scanning at close range may be accepted with a longer ultrasound path.

The area adjacent to the backing bar in complete joint penetration T-joints with backing can cause difficulties in interpreting the ultrasonic response. The surfaces of the backing bar add locations where the ultrasound may be returned to the detector. A weld without imperfections will have a more complicated ultrasonic response with a backing bar than without one. The inspector must be able to judge the backing bar geometry as acceptable when it has no imperfections. This complicated response can prevent the interpretation of some types of imperfection. In particular, the weld root area adjacent to the column flange surface poses interpretation difficulties. Lack of fusion or slag in this region can appear to be an extension of the surface of the backing bar adjacent to the column flange. No change in amplitude may be present to allow differentiation between the acceptable backing bar surface and the additional imperfection that is to be judged by its amplitude and length as acceptable or requiring rejection.

Discussions in the literature and research have recognized the complexity of interpretation in this region. Innovations in scanning methods have been the most active area of investigation, since changes in angles and beam directions should cause different responses from welding imperfections and the cut surface of the backing bar. However, the response may be dependent upon the particular type of welding imperfection and the surface condition of the backing bar. Modifications specific to this geometry have not been included in AWS D1.1.

The limitations described above could be minimized by a system where the results of the ultrasonic inspection were reported based upon the size of the imperfection rather than the amplitude of the response and the length. Methods exist to get ultrasound in to inspect hidden areas. However, these methods currently do not provide comparable results to those for areas where access is not a problem, since the amplitudes of the response will differ. If imperfection sizes were reported by each method, these sizes could be directly compared.

For cases where interpretation is a problem, recording based upon flaw size would allow additional information about the geometry to be brought to bear to determine whether an ultrasonic echo was generated at an imperfection or on part of the connection geometry. For instance, responses from the backing bar must come from at least a minimum distance from the transducer. Smaller distances could be unambiguously interpreted as coming from other indications.

FEMA-267B removes the recommendation contained in FEMA-267 that ultrasonic inspection be provided after an earthquake to check for damage. The basis for this removal is the difficulty of inspection of the areas adjacent to the backing bar notch and under the web in the bottom beam flange combined with the determination that many flaws that were detected by ultrasonics had remained since original construction. (Both FEMA-267 and FEMA-267B have been superseded by FEMA-350 to 353.)

The primary argument against extensive use of ultrasonic inspection is basically that it does not effectively distinguish between welds that are more likely to fail in service and welds which are less likely to fail. This inability to distinguish between conditions that are important and those that are not important, need not be entirely the fault of the technique applied to the inspection. It can instead be a fault of the criteria applied to the inspection.

The acceptance criteria applied by AWS D1.1 use the amplitude of the ultrasonic response from an imperfection as the parameter used to judge acceptance. Such criteria are of limited use when other sources of ultrasonic response, as at the backing bar, are present, or there are changes in procedures required to access a certain area, as under the bottom beam flange.

7.3.3 Contrast of AWS D1.1 Annex K and API Recommended Practice 2X

AWS D1.1 attempts to provide some guidance on alternative techniques for ultrasonic testing in its nonmandatory Annex K. The purpose of this annex is to describe alternative techniques for the ultrasonic examination of welds. The annex requires qualified procedures, special calibrations, and operator qualifications. However, as this is a nonmandatory annex, none of the requirements detailed are applicable unless required by the Engineer in writing.

Annex K is similar to API RP 2X in that it provides special calibration and scanning techniques, classification of indications, and defect sizing and acceptance criteria. Annex K recommends final evaluation and acceptance/rejection by the Engineer.

Annex K relies on a detailed written and approved procedure for the examination of welds. The requirements of this procedure are detailed in Section K3. Section 6, in the main body of the AWS D1.1 Code, provides detailed procedures for calibrating, scanning, performing, and evaluating indications when using ultrasonic testing. In contrast, Annex K allows the UT operator to develop detailed written procedures for UT testing that require approval by the Engineer.

The detailed procedure is required to contain the following: (Subsections of Section 6 refer to AWS D1.1.)

- Type of weld joint configurations to be examined
- Acceptance criteria for each type of weld joint examined (if different than section 6, Part C)
- Type of UT equipment

- Type of transducer including frequency, size, shape, angle, and type of wedge (if different than section 6.22.6 or 6.22.7)
- Scanning surface preparation and couplant requirements
- Type of calibration test block and reference reflectors
- Method of calibration and calibration interval
- Method for examining for laminations prior to weld examination if different than section 6.26.5
- Weld root index marking and other preliminary marking methods
- Scanning pattern and sensitivity requirements
- Methods for determining discontinuity location, height, length, and amplitude level
- Transfer correction methods
- Method of verifying accuracy of the completed examination (can include re-examination by UT by others, other NDE methods, macroetch specimen, gouging, or other visual techniques as approved by the Engineer.
- Documentation requirements for examinations and any verifications performed
- Documentation retention requirements

In addition, Annex K requires the written procedure to be proven on mock-up test samples that represent production welds. The mock-up samples are sectioned, properly examined, and documented to prove satisfactory performance of the procedure. The procedure and all qualifying data must be approved by an individual who has been certified as Level III in UT by testing in accordance with ASNT SNT-TC-1A and who is further qualified by experience in the specific types of welds joints to be examined.

One significant difference between API RP 2X and AWS D1.1 Annex K is the emphasis on operator qualification and certification. Section K4 of Annex K requires that the “operator demonstrate ability to use the written procedure, including all special techniques required, and, when sizing of discontinuity height and length are required, must establish ability and accuracy for determining these dimensions.” API RP 2X requires a minimum of 400 hours of UT experience with particular weld geometries before applying to take a qualification test. The qualification examination includes written, practical, and physical (visual acuity) testing.

The API document acknowledges that average ultrasonic operators need significantly more training and qualification in order to adequately apply special defect sizing and classifying techniques used in the recommended practice.

7.3.4 Southwest Research Institute Alternative Manual UT Procedures

Under the FEMA/SAC investigations, Southwest Research Institute (SwRI) developed two sets of manual UT procedures that are alternatives to the AWS D1.1 inspection methodology. As discussed in subsection 7.5.1, the shear-wave probes recommended in AWS D1.1 have significant difficulties in seeing planar flaws adjacent to the column flange surface. The ultrasonic technician faces signal interpretation difficulties due to the presence of wide weld caps and backing bars. Appendix B of the SwRI final report provides some guidance on improving the flaw detection reliability of the AWS Code procedures. The key feature of the SwRI-supplemental procedures is the use of a dual-element, pitch-catch type transducer consisting of a straight-beam longitudinal-wave transducer and a 60-degree shear-wave transducer mounted on a common wedge, as shown on page B-8 of the SwRI report (Grueber and Light, 1999).

During testing conducted in the course of the FEMA/SAC investigations, twelve mockup specimens representative of the worst-case weld geometries and containing a total of approximately 20 planar flaws were fabricated. Both the written AWS Code and the SwRI-supplemental (Appendix B of the Subtask 5.2.4 final report) procedures were evaluated for flaw detection reliabilities against the project mockup specimens under blind-test conditions. A summary of results obtained is discussed in the following sections.

The SwRI procedure requires a greater degree of operator skill, training, qualification, and knowledge prior to inspection of production welds. The procedure requires the use of unique transducer configurations and testing procedures to accurately identify and quantify weld discontinuities. The procedures developed by SwRI cannot be reliably employed without sufficient operator training and experience. Typically, the average UT operator would not be familiar with these types of procedures and transducer configurations.

AWS Code Flaw Detection Procedure

Application of the AWS D1.1-based UT procedures on the test samples resulted in four missed flaws and more than ten false calls, resulting in a detection reliability index of only 60 percent.

SwRI-Supplemented Code Flaw Detection Procedure

The least missed calls and least false calls were obtained by using the SwRI-supplemental procedure with 70-degree and 45-degree shear-wave probes operated in the pulse-echo mode and a 60-degree shear-wave (S) probe in conjunction with the 0-degree longitudinal-wave (L) probe operated in the pitch-catch mode. The latter S&L transducer detected all four of the planar flaws near the column flange face that were missed by the standard AWS Code procedure. With only one false call, the SwRI-supplemented Code procedure's detection reliability index was calculated to be 90 percent.

SwRI Advanced Flaw Location and Sizing Procedures

Only the Appendix A (Grueber and Light, 1999) procedures were used to locate and size the detected flaws. These procedures have many similarities to those contained in Annex K of the 1996 edition of the AWS D1.1 Code. Ninety-five percent of the time, the XYZ flaw location and the YZ size (length and depth, respectively) estimates obtained by using SwRI advanced flaw location and sizing procedures were within 0.2 inch (5 mm) of their intended values.

In summary, the alternative procedure qualification test results demonstrated that not only reliable flaw detection but also accurate flaw location and sizing are possible.

Ultrasonic Operator Training Requirements

The implementation of the SwRI alternative procedures (SwRI-supplemental Code and the SwRI advanced flaw location and sizing procedures) in the field would require significant additional training and subsequent proficiency testing of UT operators.

7.3.5 Ultrasonic Inspection Summary

Ultrasonic testing can be the most reliable tool in the detection of flaws and defects in moment-resisting connections. However, when using this nondestructive testing method, it is important to understand that the reliability of the manual UT method is extremely operator dependent. When specifying new techniques and procedures in the construction contract, the engineer must consider the abilities of the operator. The average UT operator in the United States is not familiar with defect sizing and classification procedures. When specifying that these methods be used, the engineer must take into account that it may take several attempts to find a qualified UT operator to perform these types of examinations.

Without specific guidelines, there is no way to ensure that an adequate inspection has been performed. The engineer should include in the specifications detailed requirements for the UT operator to prove their capabilities on “mock-up” samples of actual production welds to be inspected. It is recommended to establish an ASNT performance demonstration program for qualifying UT operators to perform flaw detection and sizing of critical seismically loaded welded connections. For example, ASNT CP-189 provides a more vigorous program than ASNT SNT-TC-1A.

7.4 Acceptance Criteria

The purpose of weld inspection is to permit judgements on whether the welds should be accepted, or removed, repaired, or replaced. To keep such judgements from being arbitrary and variable, written acceptance criteria are placed within welding codes such as AWS D1.1. These acceptance criteria are used to take the available information from inspection and other easily accessed sources to suggest a recommended course of action, basically, accept or reject. Welds with flaws that have significant negative impact on the ability of a weldment to resist anticipated loading should be rejected. Welds without such flaws should, in most cases, be accepted. In making these acceptance judgements, a margin of conservatism should be provided that allows

for the occasional rejection of imperfections that are not excessively severe, while avoiding the routine acceptance of imperfections that could be detrimental to structure performance.

7.4.1 Alternative Acceptance Criteria

The limitations described above relative to construction inspection using ultrasonic testing methods, as specified in the main sections of the D1.1 code, strongly suggest that alternative, improved inspection techniques and acceptance criteria could be defined. Such alternative procedures and acceptance criteria can potentially be derived by several means resulting in quite different features. Mohr (1999) surveyed existing structural codes from the United Kingdom, Japan, and New Zealand, for ultrasonic testing procedures and acceptance criteria, finding wide deviation from the D1.1 acceptance criteria, and little agreement.

The sections below describe three alternative approaches to improving existing weldment inspection and acceptance criteria that may be considered for application to structures intended to resist seismic loading. The first consists of modifying the existing UT procedures and altering the acceptable ultrasonic amplitude at which accept/reject decisions are made, in order to improve the overall reliability of the inspection. For instance, one way to do this would be by changing from the static loading criteria contained in D1.1 to that provided for cyclically loaded structures. The second approach includes the use of alternative scanning procedures and acceptance criteria, such as the use of flaw sizing techniques developed by SwRI. The third involves the use of inspection procedures other than ultrasonics.

7.4.2 More Stringent Ultrasonic Amplitude-Based Criteria

In addition to the acceptance criteria for statically loaded structures, AWS D1.1 currently includes acceptance criteria for cyclically loaded structures. These more stringent criteria are intended for use in structural joints in which fatigue is a possible failure initiator. These criteria specify more stringent limits on the ultrasonic amplitude used to indicate rejectable conditions. It has been suggested by some that the use of these alternative criteria would substantially improve the reliability of structural joint inspections using UT. However, more stringent limits on amplitude would not directly address the three problems with detection and recognition of large imperfections previously described.

The use of more severe amplitude limits, such as those for cyclically loaded structures, has the potential to mitigate the difficulty with long-range inspections and inspections of hidden regions of weldments. Return signals from defects that are detected in long range scans return a lower amplitude signal, so use of lower amplitude limits as rejectable indications would result in a greater number of these defects being detected and rejected. Similarly, defects present in “hidden” areas of weldments, such as the root of beam flange to column welds beneath the beam web, may return a weak signal that would be identified as rejectable with more stringent amplitude limits. However, the use of the more stringent amplitude criteria would also result in far more false calls or identification of defects that are not really of detrimental size. It is highly undesirable to use criteria that result in excessive false calls, as this weakens the credibility of the inspector and results in unwillingness to accept inspection results.

More important, the use of a single set of amplitude criteria does not provide the inspector to base acceptance/rejection decisions on the true significance of a defect to the serviceability of a weld. Mohr has compared the fracture resistance of connections with embedded flaws to ones with surface flaws and shown that weldments can tolerate much larger embedded flaws than surface flaws. Chi, et al. (1997) and Burdekin and Suman (1999) made similar checks on the acceptability of larger embedded flaws. Criteria which are based only on amplitude do not take this important parameter, defect location, into account.

7.4.3 Ultrasonic Size-Based Criteria

Rather than the use of amplitude-based criteria for acceptance or rejection, it is possible to use alternative parameters. For example, decisions to accept or reject defects can be based on flaw sizing techniques, with acceptance based on the apparent size of a defect. Second, the position of the defect within the weld, and in particular, the position of the notch tip within the weld, can be used. Such criteria would result in a more refined screen of the returns obtained during UT scanning such that only defects that are important would be rejected. Mohr (1999) proposed a set of acceptance criteria based on the size of the imperfection rather than the amplitude of returning ultrasound. A size-based criteria could be integrated with current AWS D1.1 Annex K inspection procedures.

However, there are a number of factors that limit the potential application of size-based acceptance criteria for structural welding. Flaw size cannot be determined during the quick scans that are routinely performed during an initial detection. Accurate flaw sizing requires the use both of alternative transducers and also more scanning time. There are currently few structural ultrasonic inspectors in North America that have commonly used sizing techniques. Therefore, adoption of size-based acceptance criteria would require substantial training of inspectors. This training must include instruction on how to perform flaw sizing and also identification of acceptable as opposed to rejectable conditions. Finally, current ultrasonic technology is somewhat limited in its ability to accurately size and locate flaws, though the newer, automated techniques with computer assisted signal processing are quite promising in their ability to do this. In summary, although flaw sizing based criteria have the potential to provide significantly improved inspection and accept/reject decisions, routine implementation would require a substantial increment in inspection costs. The section below describes a set of size based acceptance criteria, developed by Mohr (1999) as part of the FEMA/SAC investigations, for welds having the toughness and strength recommended for application in critical joints of moment-resisting frames intended for seismic applications, and anticipated to be loaded to the plastic range at intermediate strain rates typical of those seen under seismic response.

7.4.3.1 Alternative Acceptance-Rejection Criteria

Under this criteria, if a flaw is detected, but has a height dimension that is below the size that can be measured, the flaw height is assumed to be 1/8 in. (3mm). If the separation from the surface cannot be measured, the flaw is categorized as a surface flaw. Surface flaws with measured height greater than 1/8 in. (3mm) or length greater than 3/4 in. (19mm) are rejectable. Embedded flaws are rejectable if their height exceeds 1/4 in. (6mm), or if their area, as

calculated by multiplying the maximum discontinuity height by the maximum discontinuity length, exceeds the thickness of the thinner parent metal multiplied by the thickness of the thicker parent metal.

Embedded flaws either individually or as a group within a length of weld 12 in. (300mm) or less are rejectable if they exceed a total area (the sum of the areas of individual discontinuities) of 10% of the thickness of the thinner parent metal multiplied by the weld length. The weld length used for this calculation should not exceed 12 in. (300 mm). For the application of this criteria to longer welds, the weld is broken into 12-in. maximum length segments, and the criteria individually applied to each segment.

Aligned discontinuities of lengths L_1 and L_2 separated by less than $(L_1+L_2)/2$ are evaluated as continuous. Parallel discontinuities of heights H_1 and H_2 separated by less than $(H_1+H_2)/2$ are also evaluated as continuous.

The position of notch tips that extend into the weld metal must be determined. Notches are rejected if they extend greater than 1/8 in. (3mm) into the thickness of the weld.

7.4.3.2 Commentary on Alternative Criteria

Any size-based acceptance criteria must be based on an understanding of the flaw sizes and orientations that can cause failure and an understanding of the size and orientation of flaws capable of detection by available equipment. The criteria presented above, and developed by Mohr (1999), are similar to criteria recommended by Burdekin and Suman (1999). They recommended a three-level approach to acceptance criteria. The three categories for NDT and defect sizes are given as follows:

1. Backing strip removed; controlled welding procedures and qualified welders; and NDT carried out using ultrasonics to ensure maximum defect height not greater than the larger of 0.15 x beam flange thickness and 1/8 in. (3mm).
2. Backing strip left in place; either controlled welding procedures and qualified welders or NDT carried out using ultrasonics to ensure maximum anticipated defect height is not greater than the larger of 0.3 x beam flange thickness and 6 mm.
3. Backing strip left in place; no control on welding procedures/operators; no NDT carried out.

The acceptance criteria provided by Mohr (1999) cover similar situations to those of the first two categories described by Burdekin and Suman. The Burdekin and Suman criteria also use 1/8 in. (3mm) as the minimum defect height at which rejection can be determined. The differences relate to Mohr providing only one accept/reject level for seismic service rather than two, not allowing an increase in defect height as a function of member thickness, and having less stringent requirements for embedded imperfections. Mohr also has a specific requirement for notch tip positions more stringent than that provided in category 2, where backing strips are allowed. The Mohr criteria are based on fracture mechanics analyses of typical welded beam-column joints subjected to plastic seismic loading.

Mohr's fracture mechanics analyses show that one aspect of the backing bar notch was that it concentrated stresses not only from the beam but also from the column flange. Beam to column connections where the backing bar has been removed are much less likely to locate any welding imperfections where stresses can be concentrated from both members. Mohr's analysis also suggests that fracture risk can increase for the same size flaw as flange thickness increases. Thus, the approach of allowing flaw depths that increase with flange thickness may increase the sensitivity to flaws of thick connections.

The acceptance-rejection criteria presented in Section 7.4.3 have been designed for steel structures with demand plastic deformation at or adjacent to welds during service, loaded at intermediate strain rates, like those typically encountered in seismic response. They are based on base metals with strengths as large as those encountered in modern Grade 50 structural steels, including ASTM A572, Gr. 50, ASTM A913, Gr. 50, and ASTM A992; and CVN toughness of both base and weld metals of at least 20 ft-lb. at -20°F.

UT acceptance criteria require a full inspection to be effective. Regions of welds adjacent to access holes may have to be inspected with multiple probe techniques. It may not be possible to inspect some regions of welds. In such cases the engineer should be notified of the lack of inspection, so that determination can be made as to the potential impacts of joint failure.

The default flaw size of 1/8 in.(3mm) in the above acceptance criteria has been selected because this is the smallest size measurement that can reliably be made using current standard UT methods. Different size criteria are proposed for surface as opposed to embedded flaws because surface flaws represent a much more severe condition. Separate height and area criteria are provided because brittle fracture initiation is particularly sensitive to flaw height. Height is not used as the only criteria because initiation of ductile fracture is sensitive to flaw area. It has been noted that, in several full-scale tests of welded beam-column connections, ductile failure has been observed initiating from surface imperfections smaller than those allowed by the criteria. Ductile failure mechanisms are not specifically addressed in the derivation of the acceptance criteria. However, making the size-based acceptance criteria more stringent for surface imperfections in high-strain locations is not an available option as discussed above. Amplitude-based acceptance criteria for these surface flaws may be more appropriate in regions where high plastic strains could be expected.

The criteria requires the location of notch tips because these features were found after the 1994 Northridge earthquake to have been initiation sites for many fractures. Notch tips are frequently found at welds between three or more members, or where two members are joined using a permanent backing bar.

7.4.4 Acceptance Criteria Using Other Inspection Techniques

In addition to ultrasonics, inspection methods can also use liquid penetrant or dry magnetic particle testing. These methods can detect surface cracks on all exposed weld surfaces. Some methods of magnetic particle testing can also detect imperfections slightly below the surface. Sensitivity cannot be arbitrarily increased, since areas such as weld toes and corners can trap penetrant or magnetic particles and appear as an indication of an imperfection at high sensitivity.

Dry magnetic particle testing may be preferred because it is less likely to be sensitive to acceptable surface contours.

Liquid penetrant and magnetic particle techniques both allow imperfection sizes to be determined visually. These methods do not generally allow a depth or width measurement for a crack-like flaw. Therefore, any acceptance criteria for planar defects detected by these techniques must relate to the length across the surface. The criterion for planar defects in AWS codes and standards has generally been to reject all cracks observed by these methods. This is equivalent to accepting only flaws below the size that can be determined visually to be cracks. Although this length may differ under different observation conditions, it should generally be less than 2 mm.

Surface inspection techniques cannot provide information on areas away from exposed surfaces. Areas located under backing bars, behind sealing fillet welds, or behind cover plates can only be assessed by these techniques for flaws that extend to an exposed surface. The significant potential for flaws at these locations suggests that these surface inspection methods should not be relied on as the sole inspection technique for these geometries. A combination of surface inspection with visual inspection during welding may be appropriate for welds made with hidden surfaces such as those behind backing bars or cover plates. Visual inspection before and during welding should become the primary method of limiting the size of embedded internal imperfections in such locations.

REFERENCES, FEMA REPORTS, SAC REPORTS, AND ACRONYMS

References.

- Abson, D.J., and Pargeter, R.J., 1986, "Factors Influencing the As-Deposited Strength, Microstructure and Toughness of Manual Metal Arc Welds Suitable For C-Mn Steel Fabrications," *International Metals Reviews*, 31(4), pp. 141-194.
- Aihara, S., and Okamoto, K., 1990, "Influence of Local Brittle Zone on HAZ Toughness of TMCP Steels," *Proc. Int. Conf. Metallurgy, Welding, and Qualification of Microalloyed (HSLA) Steel Weldments*, AWS, pp. 402-426.
- AISC, November 1, 1978, "The Specification for the Design, Fabrication & Erection of Structural Steel for Buildings," *Manual of Steel Construction, Eighth Edition*, Supplement No. 2 dated January 1, 1989, American Institute of Steel Construction.
- AISI, 1979, *The Variations of Charpy V-Notch Impact Test Properties In Steel Plates, Report SU/24*, American Iron and Steel Institute.
- ASTM, 1994a, *Standard Specification for Carbon Structural Steel, A 36/A 36 M*, American Society for Testing and Materials.
- ASTM, 1994b, *Standard Specification for High-Strength Low-Alloy Columbium-Vanadium Structural Steel, A 572/A 572 M*, American Society for Testing and Materials.
- ASTM, 1994c, *Standard Specification for High-Strength Low-Alloy Structural Steel with 50 ksi [345 MPa] minimum Yield Point to 4 in. [100 mm] Thick, A 588/A 588 M*, American Society for Testing and Materials.
- ASTM, 1995, *High-Strength Low-Alloy Steel Shapes of Structural Quality, Produced by Quenching and Self-Tempering Process (QST)*, A 913/A 913 M, American Society for Testing and Materials.
- AWS, *Welding Handbook, 7th Edition*, Volume 2, pp. 530-550, American Welding Society.
- AWS, 1991, *AWS A5.1-91: Specification of Carbon Steel Electrodes for Shielded Metal Arc Welding*, American Welding Society.
- AWS, 1995, *AWS A5.20-95: Specification of Carbon Steel Electrodes for Flux Cored Arc Welding*, American Welding Society.
- AWS, 1996a, *ANSI/AASHTO/AWS Bridge Welding Code D1.5*, American Welding Society.
- AWS, 1996b, *ANSI/AWS 5.20, Specification for Carbon Steel Electrodes for Flux Cored Arc Welding*, American Welding Society.
- AWS, 1998a, *AWS B4.0-98: Standard Methods for Mechanical Testing of Welds*, American Welding Society.
- AWS, 1998b, *AWS 5.29-98: Specification of Low Alloy Steel Electrodes for Flux Cored Arc Welding*, American Welding Society.
- AWS, 1998c, *AWS D1.1-98: Structural Steel Welding Code-Steel*, American Welding Society.
- AWS, 1998d, *ANSI/AWS 5.29, Specification for Low Alloy Steel Electrodes for Flux Cored Arc Welding*, American Welding Society.
- AWS D1.1, 2000, *Structural Welding Code – Steel*, American Welding Society.

- Andersson, B.A.B., 1980, "Diffusion and Trapping of Hydrogen in a Bead-on-Plate Weld," *Journal of Engineering Materials and Technology*, 102, 64.
- Applied Technology Council, 1992, *Guidelines for Cyclic Seismic Testing of Components of Steel Structures*, ATC-24, Redwood City, CA.
- Autio, J., Kettunen, P., and Strom, K., 1981, "Detrimental Effects of Air Currents and their Elimination in MIG-Welding," *Weld Pool Chemistry and Metallurgy, Proceedings, International Conference, London*, 15-17, Welding Institute, ISBN 0-853001-38-3, Vol. 1, Session IV, Paper 32, pp. 187-196, Abington Publishing, Cambridge CB1 6AL, UK.
- Bailey, N., Coe, F.R., Gooch, T.G., Hart, P.H.M., Jenkins, N., and Pargeter, R.J., 1993, *Welding Steels Without Hydrogen Cracking, 2 ed.*, Abington Publishing and ASM International.
- Banks, E., 1974, "Toughness Properties of HAZ Structures in Structural Steel," *Weld. J.*, Vol. 53, No. 7, pp. 299s-306s.
- Barsom, J., 1999, *Failure Analysis of Welded Beam to Column Connections*, SAC/BD-99/23.
- Barsom, J., 2000, "Development of Fracture Toughness Requirements for Weld Metals in Seismic Applications," *Proc. 4th. US/Japan Workshop on Steel Fracture Issues*, San Francisco, CA, February 28-29, 2000.
- Barsom, J.M., and Reisdorf, B.G., 1988, "Characteristics of Heavyweight Wide-Flange Structural Shapes," *WRC Bulletin 332*, Welding Research Council, pp. 1-19.
- Barsom, J., and Rolfe, S.T., 1987, *Fracture and Fatigue Control in Structures, 2nd ed.*, Prentice-Hall, Inc.
- Barsom, J.M., and Rolf, S.T., 1999, *Fracture and Fatigue Control in Structures-Applications of Fracture Mechanics, 3rd edition*, ASTM MNL41, American Society for Testing and Materials West Conshohocken, PA.
- Barsom, J.M., and Frank, K., 2000, *State of the Art Report on Base Metals and Fracture*, FEMA-355A.
- Beachem, C.D., A 1972, "New Model for Hydrogen Assisted Cracking (Hydrogen "Embrittlement)," *Metallurgical Transactions*, 3, pp. 437-451.
- Bezbakh, D.K., 1971, "Effects of Wind on the Jet of Shielding Gas during Welding," *Avtomaticheskaya Svarka*, Vol. 24 (5) pp. 57-59.
- Bollinghaus, T., Hoffmeister, H., and Dangeleit, A., 1994, *A Scatterband for Hydrogen Coefficients in Microalloyed and Low Carbon Structural Steels*, IIW DOC 1767-94, AWS American Delegation, Miami, FL.
- Bollinghaus, T., Hoffmeister, H., and Middel, C., 1995, *Scatterbands for Hydrogen Diffusion Coefficients in Low and High Alloyed Steels with an Austenite Decomposition Microstructure and High Alloyed Steels with an Austenitic Microstructure*, IIW DOC IX-812-1995, AWS American Delegation, Miami, FL.
- Boniszewski, T., 1992, *Self-Shielded Arc Welding*, Abington Publishing.
- BSI, 1979, *Methods for Crack Opening Displacement (COD) Testing*, BS5762, British Standards Institution.
- BSI, 1984, *BS 5135: Specification for Arc Welding of Carbon and Carbon Manganese Steels*, British Standards Institution.

- Burdekin, F.M., and Suman, A., 1998, *Further Thoughts on the Relationship Between Toughness, Workmanship and Design for Earthquake Resistance Structures*, IIW DOC X-1431-98, XV-998-98, and XVG-43-98.
- Cane, M.W.F., and Dolby, R.E., 1973, *Metallurgical Factors Controlling the HAZ Fracture Toughness of Submerged-Arc Welded C-Mn Steels*, TWI Research Report M/72/73, TWI.
- Cattan, J., 1996, "Statistical Analysis of Charpy V-Notch Toughness for Steel Wide Flange Structural Shapes," *Modern Steel Construction*, Vol. 36, No. 5, pp. 38-44.
- Chew, B., 1976, "Moisture Loss and Regain by Some Basic Flux Covered Electrodes," *Welding Journal*, 55(5), pp. 127-s to 134-s.
- Coe, F.R., 1973, *Welding Steels Without Hydrogen Cracking*, The Welding Institute.
- Coe, F.R., and Chiano, Z., 1975, "Hydrogen Distribution and Removal for a Single Bead Weld During Welding," *Welding International*, 5(1), pp. 33-90.
- Dallam, C.D., Quintana, M.A., and VanderMee, V., 1999, *Capabilities and Limitations of FCAW-S, Proc. of First International Conference on Weld Metal Hydrogen Cracking in Pipeline Girth Welds*, Wollongong, Australia.
- Dawson, G.W., and Judson, P., 1982, *Procedural Guidelines for the Achievement of Tough Welded Joints in Structural Steels for Offshore Applications, Second International Conference on Offshore Welded Structures*, 16-18, London, England.
- Deierlein, G., 1999. *SAC Sub-Task 5.3.3 Fracture Behavior and Acceptance Criteria for Welded Connections*, SAC Joint Venture.
- Denys, R., and McHenry, H. I., 1988, "Local Brittle Zones in Steel Weldments: An Assessment of Test Methods," *Proc. 7th Int. Conf. Offshore Mechanics and Arctic Engineering*, Vol. III, pp. 379-385, American Society of Mechanical Engineers.
- DePatto, L.R., and Pense, A.W., 1983, "The Effect of Thermal and Mechanical Treatments on the Properties of A572 Grade 50 Steel," *WRC Progress Reports*, Vol. 38, No. 11, Welding Research Council.
- Dickehut and Hotz, 1991, "Effect of Climatic Conditions on Diffusible Hydrogen Content in Weld Metal," *Welding Journal*, 70(1), 1s-6s.
- Dong, P., Kilinski, T., Zhang, J., and Brust, F.W., 1999, *Effects of Strength/Toughness Mismatch on Structural and Fracture Behavior in Weldments*, SAC Steel Project Report SAC/BD-99/04.
- Dorling, D.V., Rodrigues, P.E.L.B, and Rogerson, J.H, 1976, "Part 2-Through-Thickness Toughness Variation," *Welding and Metal Fabrication*, 44(7), pp. 479-481.
- Dorling, D.V, and Rogerson, J.H., 1977, "The Effect of Heat input on the Weld Metal Properties of Self-Shielded Arc Welds in BS-4360 Material," *Welding and Metal Fabrication*, 45(3), pp. 157-161.
- Dorling, D.V., Rodrigues, P.E.L.B, and Rogerson, J.H., 1976, "A Comparison of the Toughness of Self-Shielded Arc Welding and Submerged-Arc Weld Metal in C-Mn-Nb Steel," Part 1-Effect of Consumables and Procedure Variables on Weld Metal Toughness," *Welding and Metal Fabrication*, 44(6), 419-423.
- Dubois, D., Devaux, J., and Leblond, J.B., 1984, "Numerical Simulation of a Welding Operation: Calculation of Residual Stresses and Hydrogen Diffusion," *Proc. Conf. Pressure Vessel Technology*, 1210-1239, San Francisco.

- Easterling, K., 1992, *Introduction to the Physical Metallurgy of Welding*, Butterworth-Heinemann.
- El-Tawil, S., Mikesell, T., Vidarsson, E., and Kunnath, S., 1998, *Strength and Ductility of FR Welded-Bolted Connections*, SAC Joint Venture Report SAC/BD-98/01.
- Engelhardt, M.D., and Venti, M., 1999, *Summary of Moment Connection Tests on Dog-Bone Weak-Panel Zone Tests*, SAC Joint Venture Report SAC/BD-00/18.
- Engelhardt, M., Fry, G., Johns, S., Venti, M., and Holliday, S., *Behavior and Design of Radius-Cut, Reduced Beam Section Connections*, SAC Joint Venture Report SAC/BD-00/17
- Evans, G.M., and Baach, H., 1976, *Hydrogen Content of Welds Deposited by Different Welding Processes*, IIW DOC IIW-1976-MTC. Also in *Metals Technology Conference, Sydney*, Paper 4-2.
- Evans, G.M., and Bailey, N., 1997, *Metallurgy of Basic Weld Metal*, Abington Publishing.
- Fairchild, D.P., 1990, "Fracture Toughness Testing of Weld Heat-Affected Zones in Structural Steel," *Fatigue and Fracture of Weldments*, ASTM STP 1058, pp. 117-141, American Society of Testing and Materials.
- Fairchild, D.P., Bangaru, N.V., Koo, J.Y., Harrison, P.L., and Ozekcin, A., 1991, "A Study Concerning Intercritical HAZ Microstructure and Toughness in HSLA Steels," *Welding Journal*, 70 (12), pp. 321s-329s.
- Fujii, T., 1975, *On the Prevention of Hydrogen-Induced Weld Cracking in Steel Weldments*, IIW DOC IX-876-74.
- Fujimoto, M., and Izumi, M., 1980, *The Effect of Incomplete Root Penetration on the Low Cycle Fatigue Behavior of T-Butt Welds*, IIW DOC XIII-942-80, International Institute of Welding.
- Fujimoto, M., and Izumi, M., 1981, "Deformation Capacity of Defective Welded Joints – Low Cycle Plastic Fatigue Test of Butt Welded T-Joints Parts 1 and 2," *Transactions of the Architectural Institute of Japan*, 303, pages 21-30.
- Fukada, Y., and Komizo, Y., 1992, "Study on Critical CTOD Property in HAZ of C-Mn Microalloyed Steel," *Trans. Jap. Weld. Soc.*, Vol. 23, No. 2, pp. 3-10.
- Gordon, J.R., Hammond, J., and Swank, G., 1999, "Welding Challenges for Strain-Based Design," presented at the International Conference on Advances in Welding Technology, Pipeline Welding and Technology Conference, Galveston, TX.
- Graville, B.A., 1975, *The Principles of Cold Cracking Control in Welds*, Dominion Bridge Company, Ltd.
- Graville, B.A., Baker, R.G., and Watkinson, F., 1967, "Effect of Temperature and Strain Rate on Hydrogen Embrittlement Of Steel," *British Welding Journal*, 337-342.
- Graville, B.A., and McParlan, M., 1974, "Weld Metal Cold Cracking," *Metal Const.*, 6(2), 62-63.
- Graville, B.A., and McParlan, M., 1975, IIW DOC IX-922-75, International Institute of Welding.
- Graville, B.A., and McParlan, M., 1976, "Hydrogen Cracking in Weld Metals," *Welding Journal*, 55 (4), 95s-102s.
- Graville, B., 1986, "A Survey Review of Weld Metal Hydrogen Cracking," *Welding in the World*, Vol. 24, No. 9/10.

- Graville, B.A., 1995, "Interpretive Report on Weldability Tests for Hydrogen Cracking of Higher Strength Steels and Their Potential for Standardization," *WRC Bul. 400*, Welding Research Council.
- Grong, O., and Matlock, D.K., 1986, "Microstructure Development in Mild and Low-Alloy Steel Weld Metals," *International Metals Reviews*, 31(1), pp. 27-48.
- Grong, O., Kluken, A.O., and Bjorbakk, B., 1988. "Effect of Nitrogen on Weld Metal Toughness in Self-Shielded Flux Cored Arc Welding," *Joining and Materials*, pp. 164-169.
- Graville, B.A., Malik, L., Pussegoda, L.N., and Glover, A.G., 1996, "Effect of Repair Geometry and Temperature on Delayed Cracking in Pipeline Girth Welds," *Conf. Proc. ICAWT '96, Intl. Conf. on Adv. In Weld. Technol.*, Columbus, OH, pp. 461-474.
- Hannerz, N.E., 1987, *Review on the Influence of Copper Content on Weld Metal Properties*, IIW DOC IX-1487-87, International Institute of Welding.
- Hannerz, N.E., and Xu, L.C., 1993, "High Strength Cored Wire Weld Metal Hydrogen Content and Weld Metal Cracking," *OMAE*, III-A, 69-74, American Society of Mechanical Engineers.
- Hannerz, N.E., and Limu, 1996, "Influence of Vanadium and Niobium on Weld Solid State Cracking," *Int. J. for the Joining of Materials*, 8(4), 134-144.
- Harrison, P.L., and Hart, P.H.M., 1990, "Influences of Steel Composition and Welding Procedure on the HAZ Toughness of Thick Section Structural Steels," *Proc. Int. Conf. Metallurgy, Welding, and Qualification of Microalloyed (HSLA) Steel Weldments*, AWS, pp. 626-658, American Welding Society.
- Harrison, P.L., and Hart, P.H.M., 1995, "HAZ Microstructure and its Role in the Fracture of Microalloyed Steel Weld", *The Institute of Materials 2nd Griffith Conference*, pp. 57-68.
- Hart, P.H.M., 1982, "Hydrogen Cracking in Ferritic Steel Weld Metals," *Third Int. Conf. Hydrogen and Materials*, Paris, France.
- Hart, P.H.M., 1986, "Resistance to Hydrogen Cracking in Steel Weld Metals," *Welding Journal*, 65(1), 14s-22s.
- Hart, P.H.M., and Evans, G.M., 1997, "Hydrogen Content of Single and Multipass Steel Welds," *Welding Journal*, 76(2).
- Harwig, D.D., Longenecker, D.P., and Cruz, J.H., 1999, "Effects of Welding Parameters and Electrode Atmospheric Exposure on the Diffusible Hydrogen Content of Gas Shielded Flux Cored Arc Welds," *Welding Journal*, 78(9), pp. 314-s to 321-s.
- Haze, T., and Aihara, S., 1988, "Influence of Toughness and Size of Local Brittle Zone on HAZ Toughness of HSLA Steels," *Proc. 7th Int. Conf. Offshore Mechanics and Arctic Engineering*, Vol. III, pp. 515-523, American Society of Mechanical Engineers.
- Hehemann, R.F., 1984, *Hydrogen Embrittlement and Stress Corrosion Cracking*, ASM International.
- Heisterkamp, F., Hulka, K., and Batte, A.D., 1990, "HAZ [HAZ] Properties of Thick Section Microalloyed Steels – A Perspective," *WRC Bulletin 373*, pp. 17-24, Welding Research Council.
- Henrie, K.W., and Long, R.E., 1982, "Effects of Wind on Radiographic Quality of Weld Metal Deposited with Low-Hydrogen SMA [Manual Metal Arc Welding] Electrodes," *Welding Journal*, Vol. 61(4), pp. 45-50.

- Herman, W.A., Erazo, M.A., DePatto, L.R., Sekizawa, M., and Pense, A.W., 1987, "Strain Aging Behavior of Microalloyed Steels," *WRC Bulletin 322*, pp. 1-13, Welding Research Council.
- Hirth, J.P., 1980, "Effects of Hydrogen on the Properties of Iron and Steel," *Metallurgical Transactions A*, 11A, pp. 861-890.
- Hopkins, G.L., 1944, "A Suggested Cause and a General Theory to the Cracking of Alloy Steels on Welding," *Trans. Inst. Welding*, 7, pp. 76-78.
- Houldcroft, P.T., 1977, *Welding Process Technology*, Cambridge University Press, Cambridge.
- Interrante, C.G., and Pressouyre, G.M., 1982, *Current Solutions to Hydrogen Problems in Steels*, Washington.
- Johnson, M.Q., 2000a, *Evaluation of the Effect of Welding Procedure on the Mechanical Properties of FCAW-S and SMAW Weld Metal Used in the Construction of Seismic Moment Frames*, SAC Joint Venture Report SAC/BD-00/12.
- Johnson, M.Q., 2000b, *Preliminary Evaluation of Heat Affected Zone Toughness in Structural Shapes Used in the Construction of Seismic Moment Frames*, SAC Joint Venture Report SAC/BD-00/13.
- Johnson, M.Q., Mohr, W.C., and Barsom, J., 2000c, *Evaluation of Mechanical Properties in Full-Scale Connections and Recommended Minimum Weld Toughness for Moment Resisting Frames*, SAC Joint Venture Report SAC/BD-00/14.
- Johnson, M.Q., Harwig, D.D., and Gordon, J.R., 1998, "Hydrogen Management In Weld Metals Deposited Using Flux-Cored Arc Welding Consumables," *International Workshop on Hydrogen Management*, Ottawa, Canada.
- Kaplan, H.I., and Hill, DC., 1976, "Thermodynamics Of Air-Operated Flux-Cored Electrodes and an Analysis Of Toughness," *Welding Journal*, 55(1), pp. 15-19.
- Kaufman, E.J., Fisher, J.W., et al., 1997, *Failure Analysis of Welded Steel Moment Frames Damaged in the Northridge Earthquake*, National Institute of Standards and Technology Report NISTIR 5944.
- Kaufman, E.J., and Fisher, J.W., 1995, "A Study of the Effects of Material and Welding Factors on Moment Frame Weld Joint Performance Using a Small-Scale Tension Specimen," SAC Joint Venture 95-08, Paper 2.
- Keeler, T., 1981, "Innershield Welding Part-1 Development of Applications," *Metal Construction*, 13(11), pp. 667-673.
- Keeler, T., 1981, "Innershield Welding Part 2-"Properties," *Metal Construction*, 13(12), pp. 750-753.
- Keeler, T., and Garland, J.G., 1983, *Welding and Metal Fab.*, 51(4), 193-199.
- Killing, R., 1980, "Welding With Self-Shielded Wires-The Mechanisms of Shielding and Droplet Transfer," *Metal Construction*, 12(9), pp. 433-436.
- Kim, B.C., Lee, S., Kim, N.J., and Lee, D.Y., 1991, "Microstructure and Local Brittle Zone Phenomena in High-Strength Low-Alloy Steel Welds," *Metallurgical Transactions A*, Vol. 22A, pp. 139-149.
- Kinsey, A.J., 1996, *Heat Affected Zone Hydrogen Cracking of C-Mn Steels When Welding with Tubular Cored Wires*, TWI Member Report 578/1996, The Welding Institute.

- Klimpel, A., and Makosz, P., 1993, "Effect of Repair Welding on the Mechanical Properties of Welded Butt Joints," *JOM-6 Proc. Intl. Conf. On Joining of Materials*, Helsingor, Denmark, 5-7 Apr., pp. 575-580.
- Kluken, A.O, Siewert, T.A., and Smith, R., 1994, "Effect of Copper, Nickel and Boron on Mechanical Properties of Low-Alloy Steel Weld Metals Deposited at High Heat Input," *Welding Journal*, 73(8), pp. 193s-199s.
- Koçak, M., Chen, L., Terlinde, G., Gnriss, G., and Schwalbe, K.H., 1990, "CTOD Testing of HAZ and Analysis of Pop-In Behavior," *Trans. ASME – J. Offshore Mechanics and Arctic Engineering*, Vol. 112, No. 8, American Society of Mechanical Engineers, pp. 214-222.
- Konkol, P.J., 1988, "Effects of Long-Time Postweld Heat Treatment on the Properties of Constructional-Steel Weldments," *WRC Bulletin 330*, pp. 11-26, Welding Research Council.
- Kotecki, D.J., and Moll, R.A., 1970. "A Toughness Study of Steel and Weld Metal From Self-Shielded Flux Cored Arc Electrodes-Part 1," *Welding Journal*, 49(4), 157s-165s.
- Kotecki, D.J., and Moll, R.A.; 1972. "A Toughness Study of Steel and Weld Metal From Self-Shielded Flux Cored Arc Electrodes-Part 2," *Welding Journal*, 51(3), 138s-155s.
- Kotecki, D.J., 1992, "Hydrogen Reconsidered," *Welding Journal*, 71(8), pp. 35-43.
- Kuwamura, H., and Yamamoto, K., 1997, "Ductile Crack as Trigger of Brittle Fracture in Steel," *ASCE Journal of Structural Engineering*, pp. 729-735.
- Kvirikadze, D.G., Novozhilov, N.M., and Savin, V.K., 1968, "Effects of Wind on Gas Shielding in CO₂ Welding," *Avt. Svarka*, Vol. 21(7), pp. 21-24.
- Kwansniewski, L., Stojadinovic, B., and Goel, S.C., 1999, *Local and Lateral-Torsion Buckling of Wide Flange Beams*, SAC Joint Venture SAC/BD-99/20.
- Lancaster, 1992, *Handbook of Structural Welding*, Abington Publishing.
- Lau, T.W., Bowker, J.T., and Lazor, R.B., 1985, "First Report of HAZ Study", *Proc. of Welding for Challenging Environments*, pp.167-180, Ontario.
- Maraniello, E., and Timerman, R., 1990, *Influence of the Type of Aging on the All Weld Metal Tension Test Results*, IIW DOC II-A-803-90, International Institute of Welding.
- Marianetti, C., 1998, *The Development of the G-BOP Test and the Assessment of Weld Metal Hydrogen Cracking*, M.S. Thesis, The Ohio State University. See also EWI Project Report 01231, Edison Welding Institute.
- Masubuchi, K., Monroe, R.E., and Martin, DC., 1966, Interpretive Report on Weld-Metal Toughness, WRC Bulletin 111, Welding Research Council.
- Matos, C.G., and Dodds, R.H., 1999, "Modeling the Effects of Residual Stresses on Defects in Welds of Steel Frame Connections," *Engineering Structures*.
- Millington, D., 1970, "Gas Shielding Efficiency in MIG Welding," *Welding Institute Bulletin*, pp. 347-352.
- Mitchell, P.S., Hart, P.H.M., and Morrison, W.B., 1995, "The Effect of Microalloying on HAZ Toughness," *Microalloying '95 Conf. Proc.*, pp. 149-162.
- Mohr, W.C., 1999, *Weld Acceptance Criteria for Seismically-Loaded Welded Connections*, SAC Joint Venture SAC/BD-99/24
- Nakanishi, M., Komizo, Y.I., and Fukada, Y., 1986, "Study on the Critical CTOD Properties in the HAZ of C-Mn Micro Alloyed Steel," *The Sumitomo Search*, No. 33, pp. 22-34.

- North, T.H., Rothwell, A.B., Glover, A.G., and Pick, R.J., 1982, "Weldability of High Strength Line Pipe Steels," *Welding Journal*, 61(8), 243-257s.
- Okuda, N., Ogata, Y., Nishikawa, Y., Aoki, T., Goto, A., and Abe, T., 1987, "Hydrogen Induced Cracking Susceptibility in High Strength Weld Metal," *Welding Journal*, 66(5), 141-s to 146-s.
- Okupnik, E.I., Zhiznyakov, S.N., Doroshenko, F.E., Novozhilov, N.M., and Steklov, O.I., 1993, "Arc Welding in a Shielding Gas in Wind (Review)," *Welding International*, Vol. 7(7), pp. 550-553.
- Ostertag, C.P., 1997, "Microstructural Characteristics of Failed Steel Moment-Resisting Beam-Column Connections," *Earthquake Engineering Research Center News*, Vol. 18, No. 3.
- Ostertag, C.P., 1998, "Effect of Local Microstructure Parameters on Performance of Welded Steel Moment Connections," *Third U.S.-Japan Workshop on Steel Fracture Issues*, Tokyo, Japan.
- Paret, T.F., and Freeman, W., 1997, "Is Steel Frame Damage Being Diagnosed Correctly," *Proceedings of Structures Congress XV*, Volume 1, pp.261-266, ASCE.
- Paret, T.F., 1999, *Nine Studies Aimed at Explaining the W1 Issue and the Related Issue of UT Inspection Reliability*, Report to SAC on Subtask 3.1.3.
- Pargeter, R.J., 1989, *The Effects of Arc Energy, Plate Thickness, and Preheat on C-Mn Weld Metal Hydrogen Cracking When Welding C-Mn Steels*, Report 7930.02/89/627.2, The Welding Institute.
- Paterson, S., Vaillancourt, H., and Kuntz, T., 1998, "Variability and Statistical Bounds of the Strength and Fracture Toughness of Common Structural Steel Shapes and Weld Metals Used in Welded Steel Moment Frame Connections in Building Construction," *Proc. Int. Conf. on Welded Structures in Seismic Areas*, pp. 123-144, American Welding Society.
- Pisarski, H.G., Jones, R.L., and Harrison, P.L., 1987, "Influence of Welding Procedure Variables on the Fracture Toughness of Welds Made with Self-Shielded Flux Cored Wire," *6th Int. Symp. on Offshore Mechanics and Arctic Engineering (OMAE)*, Houston, TX.
- Pisarski, H.G. and Pargeter, R.J., 1984, "Fracture Toughness of HAZs in Steels for Offshore Platforms," *Metal Construction*, Vol. 16, No. 7, pp. 412-417.
- PrEN 758, 1996, *European Standard-Welding Consumables: Tubular Cored Electrodes for Metal Arc Welding with and without a Gas Shield on Non-Alloy and Fine Grain Steels-Classification*
- Prior, H., Clark, J., Stoddart, D.W., Brown, M.A.S., and Yeo, R.B.G., 1986, "Welding with Self-Shielded Flux Cored Wire," *Metal Construction*, Scottish Branch Sponsored Meeting, Vol. 18(8), pp. 491-494.
- Quintana, M.A., and Johnson, M.Q., 1998, "Effects of Intermixed Weld Metal on Mechanical Properties-Part 3," *Proc. of International Conference on Welded Constructions in Seismic Areas*, Maui, Hawaii.
- Quintana, M.A., and Johnson, M.Q., 1999a, "Effects of Intermixed Weld Metal on Mechanical Properties-Part 1," *Welding Journal*, 78(3), pp.87s-99s.
- Quintana, M.A. and Johnson, M.Q., 1999b, "Effects of Intermixed Weld Metal on Mechanical Properties-Part 2," *Welding Journal*.
- Ricles, J.M., Mao, C., Kaufmann, E.J., and Fisher, J.W., 2000, *Dynamic Tension Tests of Simulated Beam Flange Connections*, SAC Joint Venture SAC/BD-00/07.

- Rogers, K.J., and Lockhead, J.C., 1987, "Self-Shielded Flux Cored Arc Welding-A Route to Good Fracture Toughness," *Welding Journal*, 66(7), pp. 49-59.
- Rorvik, G., Onsoien, M., Kluken, A.O., and Akselsen, O.M., 1992, "High Heat Input of Offshore Structures Procedures and Weld Properties," *Welding Journal*, 71(9), pp. 331s-339s.
- SAC Joint Venture, 1995, *Interim Guidelines, Inspection, Evaluation, Repair, Modification and Design, Welded Moment Resisting Steel Structures*, Report No. FEMA 267. Federal Emergency Management Agency, Washington, DC.
- SAC Joint Venture, 1999, *Interim Guidelines Advisory No. 2, Supplement to FEMA-267 Interim Guidelines*, SAC Joint Venture SAC-99-01.
- Sagan, S., and Campbell, H.C., 1960, "Factors which affect Low-Alloy Weld Metal Notch-Toughness," *WRC Bulletin 59*, pp. 1-15, Welding Research Council.
- Sawhill, J.M., Dix, A.W., and Savage, W.F., 1974, "Modified Implant Test for Studying Delayed Cracking," *Welding Journal*, pp. 554s-560s.
- Schinkler, T., 1992, "Evaluating E71T-11 Flux Cored Electrodes for Structural Carbon Steel Applications," *Welding Journal*, Vol. 71(5), pp. 73-75.
- Scholz, W., Diekman A., and Scherer, J., 1998, "Low Cycle, High Strain Rate, Inelastic Performance of Welded, Moment-Resisting Connections," *Proceedings on Welded Construction in Seismic Areas*, Maui, Hawaii.
- Shaw, R.E., 2000, *Round Robin Testing of Ultrasonic Testing Technicians*, SAC Joint Venture SAC/BD-00/06.
- Shiga, C., Gotoh, A., Kojima, T., Hori, Y., Fukada, Y., Ikeuri, K., and Matsuda, F., 1996, *Welding in the World*, Vol. 37, No. 4, 163-176.
- Shlepakov, V.N., Suprun, S.A., Kotelchuk, A.S., 1989, "Estimating the Characteristics of Flux-Cored Wire Welding under the Wind Flow Effect," In: *Welding Under Extreme Conditions. Proceedings, International Conference*, Helsinki, Finland, ISBN 0-08-037863-3. Paper 4.1, pp.171-179, Pergamon Press for the International Institute of Welding, Oxford OX3 0BW, UK.
- Singh, D.V., Khanna, O.P., and Gupta, R.L., 1976, "Effects of Welding Parameters and Wind Velocity on Metal Transfer," *Welding Research Abroad*, Vol. 22(5), pp. 48-59.
- Smith, S.D., and Blunt, F.J., 1993, *An Application of a Simple Numerical Model for Hydrogen Diffusion in Multipass Submerged Arc Welds in C-Mn Steels*, TWI Member Report 473/1993, The Welding Institute.
- Sparkes, D. J., 1986, *Effect of Postweld Heat Treatment on HAZ Microstructure and Toughness of Microalloyed C-Mn Submerged Arc Welds*" TWI Research Report 323/1986, The Welding Institute.
- Squirrell, S. J., Pisarski, H.G., and Dawes, M.G., 1986, *Recommended Procedures for the Crack Tip Opening Displacement (CTOD) Testing of Weldments*, TWI Research Report 311/1986, The Welding Institute.
- Suzuki, S., Bessyo, K, Toyoda, M., and Minami, F., 1996, "HAZ Microstructure and its Role in the Fracture of Microalloyed Steel Weld A Property Distribution Map to Explain HAZ CTOD Toughness: Study of Microcrack Initiation Properties of a Steel HAZ having Microscopic Strength Inhomogeneities (2nd Report)," *Welding International*, Vol. 10, No.1, pp. 36-43.

- Svensson, L.E., 1994, *Control of Microstructures and Properties and Steel Arc Welds*, CRC Press.
- Swinden, T., and Reeve, L., 1938, "Metallurgical Aspects of the Welding of Low Alloy Structural Steels," *Trans. Inst. Welding*, 1, pp. 7-24.
- Sykes, Burton, and Gregg, 1947, *Journal of the Iron and Steel Institute*, Vol. 157, pp. 155-180.
- Takahashi, E., Iwai, K., and Horitsuji, T., 1979, "Prevention of the Transverse Cracks in Heavy Section Butt Weldments of 2 ¼ Cr-1Mo Steel Through Low Temperature Post Weld Heat treatment (Reports 2 and 3)," *Trans. Japan Welding Society*, 10 (2) pp. 22-23.
- Threadgill, P.L., Leggatt, R.H., 1984, *Effects of Postweld Heat Treatment on Mechanical Properties and Residual Stress Levels of Submerged-Arc Welds in a C-Mn-Nb-Al Steel*, TWI Research Report 253, The Welding Institute.
- Timmins, P.F., 1997, *Solutions to Hydrogen Attack in Steels*, ASM International.
- TradeArbed, 1991, *Histar 355 TZ OS: Weldability Evaluation in Accordance with API RPI 2Z*, Available from Arbed.
- TradeArbed, 1992, *Histar 469: Weldability of Histar 460 Complying to ASTM A 913 Gr. 65, Study Conducted by AWI/Lehigh*, American Welding Institute Report 91-002.
- Trade Arbed, 1993, *Histar 460 TZK OS: Weldability Evaluation in Accordance with prEN 10225, Joint Study by Profil-Arbed and Sintef*. Available from Arbed.
- TradeArbed, 1999a, Personal Communication, *Report on Recycling of Scrap for High Quality Products, Part 4.1a*, Draft Final Report ECSC Agreement 7210-CB/501. Provided by Arbed.
- TradeArbed, 1989b, *Welding of Sections Using a Self-Shielded Flux Cored Process*, ECSC Agreement 501 7210-KA/501 (FS. 1/89). Provided by Arbed.
- Trautnor, J., 1998, Unpublished Research, presented at the Third US-Japan Workshop on Steel Fracture Issues.
- Troiano, A.R., 1960, "The Role of Hydrogen and Other Interstitials on the Mechanical Behavior of Metals," *Transactions of ASM*, 52, pp. 54-80.
- Verhagen, J.G., Liefkens, R., and Tichelaar, G.W., 1972, "Gas Shielding for CO₂ Welding," *Metal Construction and British Welding Journal*, Vol. 4(2), pp. 47-50.
- Vuik, J, 1992, *An Update of the State of the Art of Weld Metal Hydrogen Cracking*, IIW DOC IX-1686-92, International Institute of Welding.
- Weber, R.A., 1981, "Weldability Characteristics of Construction Steels A36, A514, and A516," *U.S. Army Construction Engineering Research Laboratory*, Report No. CERL-TR-M-302, 100 pp.
- Webster, S.E., and Bateson, P.H., 1990, "The Relative Influence of Centreline Segregation and Grain Coarsened Microstructures on the HAZ Toughness of Grade 50DD Steels," *Welded Structures '90 (Proc. Int. Conf.)*, Paper 13, pp. 237-248.
- White, D., Pollard, B., and Gee, R, 1992, *The Effect of Welding Parameters on Diffusible Hydrogen Levels in Steel Welds Produced with Cored Wires*, International Conference in Welding Science and Technology, Gatlinburg, TN
- Widgery, D.J., 1994, *Tubular Wire Welding*, Abington Publishing.
- Xu, P., Somers, B.R., and Pense, A.W., "Vanadium and Columbium Additions in Pressure Vessel Steels," *WRC Bulletin 395*, pp. 1-14, 57-59, Welding Research Council.

- Yeo, R.B.G., 1988, "Specifications for the Welding of Offshore Oil Structures," *Australian Welding Journal*, pp. 15-26.
- Yeo, R.G.B., and Clark, J., 1986, "Fisheyes in Weld Procedure Tension Tests," *Metal Construction*, pp. 377-378.
- Yeo, R.B.G., 1989, "Effect of Nitrogen on Weld Metal Toughness," *Joining and Materials*, Vol. 2(1), pp. 9-10.
- Yurioka, N., 1989, *Review of Numerical Analyses on the Hydrogen Diffusion in Welding of Steel*, IIW DOC IX-1553-89, International Institute of Welding.
- Yurioka, N., and Suzuki, H., 1990, "Hydrogen Assisted Cracking in C-Mn and Low Alloy Weldments," *International Materials Reviews*, 35(4), pp. 217-249.
- Zhang, J., and Dong, P., 1998, "Residual Stress in Welded Moment Frames and Implications on Structural Performance," *Proceedings on Welded Construction in Seismic Areas*, Maui, Hawaii.

FEMA Reports.

FEMA reports are listed by report number.

- FEMA-178, 1992, *NEHRP Handbook for the Seismic Evaluation of Existing Buildings*, developed by the Building Seismic Safety Council for the Federal Emergency Management Agency, Washington, DC.
- FEMA-267, 1995, *Interim Guidelines, Inspection, Evaluation, Repair, Upgrade and Design of Welded Moment Resisting Steel Structures*, prepared by the SAC Joint Venture for the Federal Emergency Management Agency, Washington, DC. Superseded by FEMA 350 to 353.
- FEMA-267A, 1996, *Interim Guidelines Advisory No. 1*, prepared by the SAC Joint Venture for the Federal Emergency Management Agency, Washington, DC. Superseded by FEMA 350 to 353.
- FEMA-267B, 1999, *Interim Guidelines Advisory No. 2*, prepared by the SAC Joint Venture for the Federal Emergency Management Agency, Washington, DC. Superseded by FEMA 350 to 353.
- FEMA-273, 1997, *NEHRP Guidelines for the Seismic Rehabilitation of Buildings*, prepared by the Applied Technology Council for the Building Seismic Safety Council, published by the Federal Emergency Management Agency, Washington, DC.
- FEMA-274, 1997, *NEHRP Commentary on the Guidelines for the Seismic Rehabilitation of Buildings*, prepared by the Applied Technology Council for the Building Seismic Safety Council, published by the Federal Emergency Management Agency, Washington, DC.
- FEMA-302, 1997, *NEHRP Recommended Provisions for Seismic Regulations for New Buildings and Other Structures, Part 1 – Provisions*, prepared by the Building Seismic Safety Council for the Federal Emergency Management Agency, Washington, DC.
- FEMA-303, 1997, *NEHRP Recommended Provisions for Seismic Regulations for New Buildings and Other Structures, Part 2 – Commentary*, prepared by the Building Seismic Safety Council for the Federal Emergency Management Agency, Washington, DC.
- FEMA-310, 1998, *Handbook for the Seismic Evaluation of Buildings – A Prestandard*, prepared by the American Society of Civil Engineers for the Federal Emergency Management Agency, Washington, DC.

- FEMA-350, 2000, *Recommended Seismic Design Criteria for New Steel Moment-Frame Buildings*, prepared by the SAC Joint Venture for the Federal Emergency Management Agency, Washington, DC.
- FEMA-351, 2000, *Recommended Seismic Evaluation and Upgrade Criteria for Existing Welded Steel Moment-Frame Buildings*, prepared by the SAC Joint Venture for the Federal Emergency Management Agency, Washington, DC.
- FEMA-352, 2000, *Recommended Postearthquake Evaluation and Repair Criteria for Welded Steel Moment-Frame Buildings*, prepared by the SAC Joint Venture for the Federal Emergency Management Agency, Washington, DC.
- FEMA-353, 2000, *Recommended Specifications and Quality Assurance Guidelines for Steel Moment-Frame Construction for Seismic Applications*, prepared by the SAC Joint Venture for the Federal Emergency Management Agency, Washington, DC.
- FEMA-354, 2000, *A Policy Guide to Steel Moment-Frame Construction*, prepared by the SAC Joint Venture for the Federal Emergency Management Agency, Washington, DC.
- FEMA-355A, 2000, *State of the Art Report on Base Metals and Fracture*, prepared by the SAC Joint Venture for the Federal Emergency Management Agency, Washington, DC.
- FEMA-355B, 2000, *State of the Art Report on Welding and Inspection*, prepared by the SAC Joint Venture for the Federal Emergency Management Agency, Washington, DC.
- FEMA-355C, 2000, *State of the Art Report on Systems Performance of Steel Moment Frames Subject to Earthquake Ground Shaking*, prepared by the SAC Joint Venture for the Federal Emergency Management Agency, Washington, DC.
- FEMA-355D, 2000, *State of the Art Report on Connection Performance*, prepared by the SAC Joint Venture for the Federal Emergency Management Agency, Washington, DC.
- FEMA-355E, 2000, *State of the Art Report on Past Performance of Steel Moment-Frame Buildings in Earthquakes*, prepared by the SAC Joint Venture for the Federal Emergency Management Agency, Washington, DC.
- FEMA-355F, 2000, *State of the Art Report on Performance Prediction and Evaluation of Steel Moment-Frame Buildings*, prepared by the SAC Joint Venture for the Federal Emergency Management Agency, Washington, DC.

SAC Joint Venture Reports.

- SAC Joint Venture reports are listed by report number, except for SAC 2000a through 2000k; those entries that do not include a FEMA report number are published by the SAC Joint Venture.
- SAC 94-01, 1994, *Proceedings of the Invitational Workshop on Steel Seismic Issues, Los Angeles*, September 1994, prepared by the SAC Joint Venture for the Federal Emergency Management Agency, Washington, DC.
- SAC 94-01, 1994b, *Proceedings of the International Workshop on Steel Moment Frames, Sacramento*, December, 1994, prepared by the SAC Joint Venture for the Federal Emergency Management Agency, Washington, DC.
- SAC 95-01, 1995, *Steel Moment Frame Connection Advisory No. 3*, prepared by the SAC Joint Venture for the Federal Emergency Management Agency, Washington, DC.

- SAC 95-02, 1995, *Interim Guidelines: Evaluation, Repair, Modification and Design of Welded Steel Moment Frame Structures*, prepared by the SAC Joint Venture for the Federal Emergency Management Agency, Report No. FEMA-267, Washington, DC.
- SAC 95-03, 1995, *Characterization of Ground Motions During the Northridge Earthquake of January 17, 1994*, prepared by the SAC Joint Venture for the Federal Emergency Management Agency, Washington, DC.
- SAC 95-04, 1995, *Analytical and Field Investigations of Buildings Affected by the Northridge Earthquake of January 17, 1994*, prepared by the SAC Joint Venture for the Federal Emergency Management Agency, Washington, DC.
- SAC 95-05, 1995, *Parametric Analytic Investigations of Ground Motion and Structural Response, Northridge Earthquake of January 17, 1994*, prepared by the SAC Joint Venture for the Federal Emergency Management Agency, Washington, DC.
- SAC 95-06, 1995, *Technical Report: Surveys and Assessment of Damage to Buildings Affected by the Northridge Earthquake of January 17, 1994*, prepared by the SAC Joint Venture for the Federal Emergency Management Agency, Washington, DC.
- SAC 95-07, 1995, *Technical Report: Case Studies of Steel Moment-Frame Building Performance in the Northridge Earthquake of January 17, 1994*, prepared by the SAC Joint Venture for the Federal Emergency Management Agency, Washington, DC.
- SAC 95-08, 1995, *Experimental Investigations of Materials, Weldments and Nondestructive Examination Techniques*, prepared by the SAC Joint Venture for the Federal Emergency Management Agency, Washington, DC.
- SAC 95-09, 1995, *Background Reports: Metallurgy, Fracture Mechanics, Welding, Moment Connections and Frame Systems Behavior*, prepared by the SAC Joint Venture for the Federal Emergency Management Agency, Report No. FEMA-288, Washington, DC.
- SAC 96-01, 1996, *Experimental Investigations of Beam-Column Subassemblages, Part 1 and 2*, prepared by the SAC Joint Venture for the Federal Emergency Management Agency, Washington, DC.
- SAC 96-02, 1996, *Connection Test Summaries*, prepared by the SAC Joint Venture for the Federal Emergency Management Agency, Report No. FEMA-289, Washington, DC.
- SAC 96-03, 1997, *Interim Guidelines Advisory No. 1 Supplement to FEMA-267 Interim Guidelines*, prepared by the SAC Joint Venture for the Federal Emergency Management Agency, Report No. FEMA-267A, Washington, DC.
- SAC 98-PG, *Update on the Seismic Safety of Steel Buildings – A Guide for Policy Makers*, prepared by the SAC Joint Venture for the Federal Emergency Management Agency, Washington, DC.
- SAC 99-01, 1999, *Interim Guidelines Advisory No. 2 Supplement to FEMA-267 Interim Guidelines*, prepared by the SAC Joint Venture, for the Federal Emergency Management Agency, Report No. FEMA-267B, Washington, DC.
- SAC, 2000a, *Recommended Seismic Design Criteria for New Steel Moment-Frame Buildings*, prepared by the SAC Joint Venture for the Federal Emergency Management Agency, Report No. FEMA-350, Washington, DC.
- SAC, 2000b, *Recommended Seismic Evaluation and Upgrade Criteria for Existing Welded Steel Moment-Frame Buildings*, prepared by the SAC Joint Venture for the Federal Emergency Management Agency, Report No. FEMA-351, Washington, DC.
-

- SAC, 2000c, *Recommended Postearthquake Evaluation and Repair Criteria for Welded Steel Moment-Frame Buildings*, prepared by the SAC Joint Venture for the Federal Emergency Management Agency, Report No. FEMA-352, Washington, DC.
- SAC, 2000d, *Recommended Specifications and Quality Assurance Guidelines for Steel Moment-Frame Construction for Seismic Applications*, prepared by the SAC Joint Venture for the Federal Emergency Management Agency, Report No. FEMA-353, Washington, DC.
- SAC, 2000e, *A Policy Guide to Steel Moment-Frame Construction*, prepared by the SAC Joint Venture for the Federal Emergency Management Agency, Report No. FEMA-354, Washington, DC.
- SAC, 2000f, *State of the Art Report on Base Metals and Fracture*, prepared by the SAC Joint Venture for the Federal Emergency Management Agency, Report No. FEMA-355A, Washington, DC.
- SAC, 2000g, *State of the Art Report on Welding and Inspection*, prepared by the SAC Joint Venture for the Federal Emergency Management Agency, Report No. FEMA-355B, Washington, DC.
- SAC, 2000h, *State of the Art Report on Systems Performance*, prepared by the SAC Joint Venture for the Federal Emergency Management Agency, Report No. FEMA-355C, Washington, DC.
- SAC, 2000i, *State of the Art Report on Connection Performance*, prepared by the SAC Joint Venture for the Federal Emergency Management Agency, Report No. FEMA-355D, Washington, DC.
- SAC, 2000j, *State of the Art Report on Past Performance of Steel Moment-Frame Buildings in Earthquakes*, prepared by the SAC Joint Venture for the Federal Emergency Management Agency, Report No. FEMA-355E, Washington, DC.
- SAC, 2000k, *State of the Art Report on Performance Prediction and Evaluation*, prepared by the SAC Joint Venture for the Federal Emergency Management Agency, Report No. FEMA-355F, Washington, DC.
- SAC/BD-96/01, *Selected Results from the SAC Phase I Beam-Column Connection Pre-Test Analyses*, submissions from B. Maison, K. Kasai, and R. Dexter; and A. Ingrassia and G. Deierlein.
- SAC/BD-96/02, *Summary Report on SAC Phase I - Task 7 Experimental Studies*, by C. Roeder (a revised version of this document is published in Report No. SAC 96-01; the original is no longer available).
- SAC/BD-96/03, *Selected Documents from the U.S.-Japan Workshop on Steel Fracture Issues*.
- SAC/BD-96/04, *Survey of Computer Programs for the Nonlinear Analysis of Steel Moment Frame Structures*.
- SAC/BD-97/01, *Through-Thickness Properties of Structural Steels*, by J. Barsom and S. Korvink.
- SAC/BD-97/02, *Protocol for Fabrication, Inspection, Testing, and Documentation of Beam-Column Connection Tests and Other Experimental Specimens*, by P. Clark, K. Frank, H. Krawinkler, and R. Shaw.
- SAC/BD-97/03, *Proposed Statistical and Reliability Framework for Comparing and Evaluating Predictive Models for Evaluation and Design*, by Y.-K. Wen.

- SAC/BD-97/04, *Development of Ground Motion Time Histories for Phase 2 of the FEMA/SAC Steel Project*, by P. Somerville, N. Smith, S. Punyamurthula, and J. Sun.
- SAC/BD-97/05, *Finite Element Fracture Mechanics Investigation of Welded Beam-Column Connections*, by W.-M. Chi, G. Deierlein, and A. Ingrassia.
- SAC/BD-98/01, *Strength and Ductility of FR Welded-Bolted Connections*, by S. El-Tawil, T. Mikesell, E. Vidarsson, and S. K. Kunnath.
- SAC/BD-98/02, *Effects of Strain Hardening and Strain Aging on the K-Region of Structural Shapes*, by J. Barsom and S. Korvink
- SAC/BD-98/03, *Implementation Issues for Improved Seismic Design Criteria: Report on the Social, Economic, Policy and Political Issues Workshop* by L. T. Tobin.
- SAC/BD-99/01, *Parametric Study on the Effect of Ground Motion Intensity and Dynamic Characteristics on Seismic Demands in Steel Moment Resisting Frames* by G. A. MacRae.
- SAC/BD-99/01A, *Appendix to: Parametric Study on the Effect of Ground Motion Intensity and Dynamic Characteristics on Seismic Demands in Steel Moment Resisting Frames* by G. A. MacRae.
- SAC/BD-99/02, *Through-Thickness Strength and Ductility of Column Flange in Moment Connections*, by R. Dexter and M. Melendrez.
- SAC/BD-99/03, *The Effects of Connection Fractures on Steel Moment Resisting Frame Seismic Demands and Safety*, by C. A. Cornell and N. Luco.
- SAC/BD-99/04, *Effects of Strength/Toughness Mismatch on Structural and Fracture Behaviors in Weldments*, by P. Dong, T. Kilinski, J. Zhang, and F.W. Brust.
- SAC/BD-99/05, *Assessment of the Reliability of Available NDE Methods for Welded Joint and the Development of Improved UT Procedures*, by G. Gruber and G. Light.
- SAC/BD-99/06, *Prediction of Seismic Demands for SMRFs with Ductile Connections and Elements*, by A. Gupta and H. Krawinkler.
- SAC/BD-99/07, *Characterization of the Material Properties of Rolled Sections*, by T. K. Jaquess and K. Frank.
- SAC/BD-99/08, *Study of the Material Properties of the Web-Flange Intersection of Rolled Shapes*, by K. R. Miller and K. Frank.
- SAC/BD-99/09, *Investigation of Damage to WSMF Earthquakes other than Northridge*, by M. Phipps.
- SAC/BD-99/10, *Clarifying the Extent of Northridge Induced Weld Fracturing and Examining the Related Issue of UT Reliability*, by T. Paret.
- SAC/BD-99/11, *The Impact of Earthquakes on Welded Steel Moment Frame Buildings: Experience in Past Earthquakes*, by P. Weinburg and J. Goltz.
- SAC/BD-99/12, *Assessment of the Benefits of Implementing the New Seismic Design Criteria and Inspection Procedures*, by H. A. Seligson and R. Eguchi.
- SAC/BD-99/13, *Earthquake Loss Estimation for WSMF Buildings*, by C. A. Kircher.
- SAC/BD-99/14, *Simplified Loss Estimation for Pre-Northridge WSMF Buildings*, by B. F. Maison and D. Bonowitz.
- SAC/BD-99/15, *Integrative Analytical Investigations on the Fracture Behavior of Welded Moment Resisting Connections*, by G. G. Deierlein and W.-M. Chi.

- SAC/BD-99/16, *Seismic Performance of 3- and 9- Story Partially Restrained Moment Frame Buildings*, by B. F. Maison and K. Kasai.
- SAC/BD-99/17, *Effects of Partially-Restrained Connection Stiffness and Strength on Frame Seismic Performance*, by K. Kasai, B. F. Maison, and A. Mayangarum.
- SAC/BD-99/18, *Effects of Hysteretic Deterioration Characteristics on Seismic Response of Moment Resisting Steel Structures*, by F. Naeim, K. Skliros, A. M. Reinhorn, and M. V. Sivaselvan.
- SAC/BD-99/19, *Cyclic Instability of Steel Moment Connections with Reduced Beam Section*, by C.-M. Uang and C.-C. Fan.
- SAC/BD-99/20, *Local and Lateral-Torsion Buckling of Wide Flange Beams*, by L. Kwasniewski, B. Stojadinovic, and S. C. Goel.
- SAC/BD-99/21, *Elastic Models for Predicting Building Performance*, by X. Duan and J. C. Anderson.
- SAC/BD-99/22, *Reliability-Based Seismic Performance Evaluation of Steel Frame Buildings Using Nonlinear Static Analysis Methods*, by G. C. Hart and M. J. Skokan.
- SAC/BD-99/23, *Failure Analysis of Welded Beam to Column Connections*, by J. M. Barsom and J. V. Pellegrino.
- SAC/BD-99/24, *Weld Acceptance Criteria for Seismically-Loaded Welded Connections*, by W. Mohr.
- SAC/BD-00/01, *Parametric Tests on Unreinforced Connections, Volume I – Final Report*, by K.-H. Lee, B. Stojadinovic, S. C. Goel, A. G. Margarian, J. Choi, A. Wongkaew, B. P. Reyher, and D.-Y. Lee.
- SAC/BD-00/01A, *Parametric Tests on Unreinforced Connections, Volume II – Appendices*, by K.-H. Lee, B. Stojadinovic, S. C. Goel, A. G. Margarian, J. Choi, A. Wongkaew, B. P. Reyher, and D.-Y. Lee.
- SAC/BD-00/02, *Parametric Tests on the Free Flange Connections*, by J. Choi, B. Stojadinovic, and S. C. Goel.
- SAC/BD-00/03, *Cyclic Tests on Simple Connections Including Effects of the Slab*, by J. Liu and A. Astaneh-Asl.
- SAC/BD-00/04, *Tests on Bolted Connections, Part I: Technical Report*, by J. Swanson, R. Leon, and J. Smallridge.
- SAC/BD-00/04A, *Tests on Bolted Connections, Part II: Appendices*, by J. Swanson, R. Leon, and J. Smallridge.
- SAC/BD-00/05, *Bolted Flange Plate Connections*, by S. P. Schneider and I. Teeraparbwong.
- SAC/BD-00/06, *Round Robin Testing of Ultrasonic Testing Technicians*, by R. E. Shaw, Jr.
- SAC/BD-00/07, *Dynamic Tension Tests of Simulated Welded Beam Flange Connections*, by J. M. Ricles, C. Mao, E. J. Kaufmann, L.-W. Lu, and J. W. Fisher.
- SAC/BD-00/08, *Design of Steel Moment Frame Model Buildings in Los Angeles, Seattle and Boston*, by P. Clark.
- SAC/BD-00/09, *Benchmarking of Analysis Programs for SMRF System Performance Studies*, by A. Gupta and H. Krawinkler.

- SAC/BD-00/10, *Loading Histories for Seismic Performance Testing of SMRF Components and Assemblies*, by H. Krawinkler, A. Gupta, R. Medina, and N. Luco.
- SAC/BD-00/11, *Development of Improved Post-Earthquake Inspection Procedures for Steel Moment Frame Buildings*, by P. Clark.
- SAC/BD-00/12, *Evaluation of the Effect of Welding Procedure on the Mechanical Properties of FCAW-S and SMAW Weld Metal Used in the Construction of Seismic Moment Frames*, by M. Q. Johnson.
- SAC/BD-00/13, *Preliminary Evaluation of Heat Affected Zone Toughness in Structural Shapes Used in the Construction of Seismic Moment Frames*, by M. Q. Johnson and J. E. Ramirez.
- SAC/BD-00/14, *Evaluation of Mechanical Properties in Full-Scale Connections and Recommended Minimum Weld Toughness for Moment Resisting Frames*, by M. Q. Johnson, W. Mohr, and J. Barsom.
- SAC/BD-00/15, *Simplified Design Models for Predicting the Seismic Performance of Steel Moment Frame Connections*, by C. Roeder, R. G. Coons, and M. Hoit.
- SAC/BD-00/16, *SAC Phase 2 Test Plan*, by C. Roeder.
- SAC/BD-00/17, *Behavior and Design of Radius-Cut, Reduced Beam Section Connections*, by M. Engelhardt, G. Fry, S. Jones, M. Venti, and S. Holliday.
- SAC/BD-00/18, *Test of a Free Flange Connection with a Composite Floor Slab*, by M. Venti and M. Engelhardt.
- SAC/BD-00/19, *Cyclic Testing of a Free Flange Moment Connection*, by C. Gilton, B. Chi, and C. M. Uang.
- SAC/BD-00/20, *Improvement of Welded Connections Using Fracture Tough Overlays*, by James Anderson, J. Duan, P. Maranian, and Y. Xiao.
- SAC/BD-00/21, *Cyclic Testing of Bolted Moment End-Plate Connections*, by T. Murray, E. Sumner, and T. Mays.
- SAC/BD-00/22, *Cyclic Response of RBS Moment Connections: Loading Sequence and Lateral Bracing Effects*, by Q. S. Yu, C. Gilton, and C. M. Uang.
- SAC/BD-00/23, *Cyclic Response of RBS Moment Connections: Weak Axis Configuration and Deep Column Effects*, by C. Gilton, B. Chi, and C. M. Uang.
- SAC/BD-00/24, *Development and Evaluation of Improved Details for Ductile Welded Unreinforced Flange Connections*, by J. M. Ricles, C. Mao, L.-W. Lu, and J. Fisher.
- SAC/BD-00/25, *Performance Prediction and Evaluation of Steel Special Moment Frames for Seismic Loads*, by K. Lee and D. A. Foutch.
- SAC/BD-00/26, *Performance Prediction and Evaluation of Low Ductility Steel Moment Frames for Seismic Loads*, by S. Yun and D. A. Foutch.
- SAC/BD-00/27, *Steel Moment Resisting Connections Reinforced with Cover and Flange Plates*, by T. Kim, A. S. Whittaker, V. V. Bertero, A. S. J. Gilani, and S. M. Takhirov.
- SAC/BD-00/28, *Failure of a Column K-Area Fracture*, by J. M. Barsom and J. V. Pellegrino.
- SAC/BD-00/29, *Inspection Technology Workshop*, by R. E. Shaw, Jr.
- SAC/BD-00/30, *Preliminary Assessment of the Impact of the Northridge Earthquake on Construction Costs of Steel Moment Frame Buildings*, by Davis Langdon Adamson.

Acronyms.

2-D, two-dimensional	C, carbon
3-D, three-dimensional	CA, California
A, acceleration response, amps	CAC-A, air carbon arc cutting
A2LA, American Association for Laboratory Accreditation	CAWI, Certified Associate Welding Inspector
ACAG, air carbon arc gouging	CGHAZ, coarse-grained HAZ
ACIL, American Council of Independent Laboratories	CJP, complete joint penetration (weld)
AE, acoustic emission (testing)	CMU, concrete masonry unit, concrete block
AISC, American Institute for Steel Construction	COD, crack opening displacement
AISI, American Iron and Steel Institute	“COV,” modified coefficient of variation, or dispersion
AL, aluminum	CP, Collapse Prevention (performance level)
ANSI, American National Standards Institute	Connection Performance (team)
API, American Petroleum Institute	Cr, chromium
ARCO, Atlantic-Richfield Company	CSM, Capacity Spectrum Method
As, arsenic	CTOD, crack tip opening dimension or displacement
ASD, allowable stress design	CTS, controlled thermal severity (test)
ASME, American Society of Mechanical Engineers	Cu, copper
ASNT, American Society for Nondestructive Testing	CUREe, California Universities for Research in Earthquake Engineering
ASTM, American Society for Testing and Materials	CVN, Charpy V-notch
ATC, Applied Technology Council	CWI, Certified Welding Inspector
AWS, American Welding Society	D, displacement response, dead load
B, boron	DMRSF, ductile, moment-resisting, space frame
BB, Bolted Bracket (connection)	DNV, Det Norske Veritas
BD, background document	DRAIN-2DX, analysis program
BF, bias factor	DRAIN-3DX, analysis program
BFO, bottom flange only (fracture)	DRI, direct reduced iron
BFP, Bolted Flange Plates (connection)	DST, Double Split Tee (connection)
BM, base metal	DTI, Direct Tension Indicator
BO, Boston, Massachusetts	EAF, electric-arc furnace
BOCA, Building Officials and Code Administrators	EBT, eccentric bottom tapping
BOF, basic oxygen furnace	EE, electrode extension
BSEP, Bolted Stiffened End Plate (connection)	EERC, Earthquake Engineering Research Center, UC Berkeley
BSSC, Building Seismic Safety Council	EGW, electrogas welding
BUEP, Bolted Unstiffened End Plate (connection)	ELF, equivalent lateral force
	EMS, electromagnetic stirring
	ENR, Engineering News Record
	ESW, electrosag welding
	EWI, Edison Welding Institute

FATT, fracture appearance transition temperature	LMF, ladle metallurgy furnace
fb, fusion boundary	LRFD, load and resistance-factor design
FCAW-G, flux-cored arc welding – gas-shielded	LS, Life Safety (performance level)
FCAW-S or FCAW-SS, flux-cored arc welding – self-shielded	LSP, Linear Static Procedure
FEMA, Federal Emergency Management Agency	LTH, linear time history (analysis)
FF, Free Flange (connection)	LU, Lehigh University
FGHAZ, fine-grained HAZ	M, moment
FL, fusion line	MAP, modal analysis procedure
FR, fully restrained (connection)	MAR, microalloyed rutile (consumables)
GBOP, gapped bead on plate (test)	MCE, Maximum Considered Earthquake
gl, gage length	MDOF, multidegree of freedom
GMAW, gas metal arc welding	MMI, Modified Mercalli Intensity
GTAW, gas tungsten arc welding	Mn, manganese
HAC, hydrogen-assisted cracking	Mo, molybdenum
HAZ, heat-affected zone	MRF, steel moment frame
HBI, hot briquetted iron	MRS, modal response spectrum
HSLA, high strength, low alloy	MRSF, steel moment frame
IBC, <i>International Building Code</i>	MT, magnetic particle testing
ICBO, International Conference of Building Officials	N, nitrogen
ICC, International Code Council	Nb, niobium
ICCGHAZ, intercritically reheated CGHAZ	NBC, <i>National Building Code</i>
ICHAZ, intercritical HAZ	NDE, nondestructive examination
ID, identification	NDP, Nonlinear Dynamic Procedure
IDA, Incremental Dynamic Analysis	NDT, nondestructive testing
IMF, Intermediate Moment Frame	NEHRP, National Earthquake Hazards Reduction Program
IO, Immediate Occupancy (performance level)	NES, National Evaluation Services
IOA, Incremental Dynamic Analysis	NF, near-fault, near-field
ISO, International Standardization Organization	Ni, nickel
IWURF, Improved Welded Unreinforced Flange (connection)	NLP, nonlinear procedure
L, longitudinal, live load	NLTH, nonlinear time history (analysis)
LA, Los Angeles, California	NS, north-south (direction)
LACOTAP, Los Angeles County Technical Advisory Panel	NSP, Nonlinear Static Procedure
LAX, Los Angeles International Airport	NTH, nonlinear time history (analysis)
LB, lower bound (building)	NVLAP, National Volunteer Laboratory Accreditation Program
LBZ, local brittlezone	O, oxygen
LDP, Linear Dynamic Procedure	OHF, open hearth furnace
LEC, Lincoln Electric Company	OMF, Ordinary Moment Frame
	OTM, overturning moment
	P, axial load
	P, axial load, phosphorus
	Pb, lead
	PGA, peak ground acceleration
	PGV, peak ground velocity
	PIDR, pseudo interstory drift ratio

PJP, partial joint penetration (weld)	SMRSF, special moment-resisting space frame (in 1988 UBC)
PPE, Performance, Prediction, and Evaluation (team)	SN, strike-normal, fault-normal
PQR, Performance Qualification Record	Sn, tin
PR, partially restrained (connection)	SP, Side Plate (connection)
PR-CC, partially restrained, composite connection	SP, strike-parallel, fault-parallel
PT, liquid dye penetrant testing	SP, Systems Performance (team)
PWHT, postweld heat treatment	SPC, Seismic Performance Category
PZ, panel zone	SRSS, square root of the sum of the squares
QA, quality assurance	SSPC, Steel Shape Producers Council
QC, quality control	SSRC, Structural Stability Research Council
QCP, Quality Control Plan, Quality Certification Program	SUG, Seismic Use Group
QST, Quenching and Self-Tempering (process)	SW, Slotted Web (connection)
RB, Rockwell B scale (of hardness)	SwRI, Southwest Research Institute
RBS, Reduced Beam Section (connection)	T, transverse
RCSC, Research Council for Structural Connections	TBF, top and bottom flange (fracture)
RT, radiographic testing	Ti, titanium
S, sulphur, shearwave (probe)	TIGW, tungsten inert gas welding
SAC, the SAC Joint Venture; a partnership of SEAOC, ATC, and CUREe	TMCP, Thermo-Mechanical Processing
SAV, sum of absolute values	TN, Tennessee
SAW, submerged arc welding	TT, through-thickness
SBC, <i>Standard Building Code</i>	TWI, The Welding Institute
SBCCI, Southern Building Code Congress International	UB, upper bound (building)
SCCGHAZ, subcritically reheated CGHAZ	UBC, <i>Uniform Building Code</i>
SCHAZ, subcritical HAZ	UCLA, University of California, Los Angeles
SCWB, strong column, weak beam	UM, University of Michigan
SCWI, Senior Certified Welding Inspector	URM, unreinforced masonry
SDC, Seismic Design Category	US, United States of America
SDOF, single degree of freedom	USC, University of Southern California
SE, Seattle, Washington	USGS, US Geological Survey
SEAOC, Structural Engineers Association of California	UT, ultrasonic testing
SFRS, seismic-force-resisting system	UTA, University of Texas at Austin
Si, silicon	UTAM, Texas A & M University
SMAW, shielded metal arc welding	V, vanadium
SMF, Special Moment Frame	VI, visual inspection
SMRF, special moment-resisting frame (in 1991 UBC)	w/o, without
SMRF, Steel Moment Frame	WBH, Welded Bottom Haunch (connection)
	WCPF, Welded Cover Plate Flange (connection)
	WCSB, weak column, strong beam
	WF, wide flange
	WFP, Welded Flange Plate (connection)
	WFS, wire feed speed
	WPQR, Welding Performance Qualification Record

WPS, Welding Procedure Specification
WSMF, welded steel moment frame
WT, Welded Top Haunch (connection)
WTBH, Welded Top and Bottom Haunch
(connection)
WUF-B, Welded Unreinforced Flanges –
Bolted Web (connection)
WUF-W, Welded Unreinforced Flanges –
Welded Web (connection)

SAC PHASE II PROJECT PARTICIPANTS**FEMA Project Officer**

Michael Mahoney
Federal Emergency Management Agency
500 C St. SW, Room 404
Washington, DC 20472

FEMA Technical Advisor

Robert D. Hanson
Federal Emergency Management Agency
DFO Room 353
P.O. Box 6020
Pasadena, CA 91102-6020

Joint Venture Management Committee (JVMC)

William T. Holmes, Chair
Rutherford and Chekene
427 Thirteenth Street
Oakland, CA 94612

Christopher Rojahn
Applied Technology Council
555 Twin Dolphin Dr., Suite 550
Redwood City, CA 94065

Edwin T. Huston
Smith & Huston, Inc.
8618 Roosevelt Way NE
Seattle, WA 98115

Arthur E. Ross
Cole/Yee/Shubert & Associates
2500 Venture Oaks Way, Suite 100
Sacramento, CA 95833

Robert Reitherman
California Universities for Research in
Earthquake Engineering
1301 South 46th St.
Richmond, CA 94804

Robin Shepherd
Earthquake Damage Analysis Corporation
40585 Lakeview Drive, Suite 1B
P.O. Box 1967
Big Bear Lake, CA 92315

Project Management Committee (PMC)

Stephen A. Mahin, Project Manager
Pacific Earthquake Engr. Research Center
University of California
Berkeley, CA 94720

William T. Holmes, JVMC
Rutherford and Chekene
427 Thirteenth Street
Oakland, CA 94612

Ronald O. Hamburger, Project Director for
Project Development
EQE International
1111 Broadway, 10th Floor
Oakland, CA 94607-5500

Christopher Rojahn, JVMC
Applied Technology Council
555 Twin Dolphin Dr., Suite 550
Redwood City, CA 94065

James O. Malley, Project Director for
Topical Investigations
Degenkolb Engineers
225 Bush St., Suite 1000
San Francisco, CA 94104-1737

Robin Shepherd, JVMC
Earthquake Damage Analysis Corporation
40585 Lakeview Drive, Suite 1B
P.O. Box 1967
Big Bear Lake, CA 92315

Peter W. Clark, Technical Assistant to PMC
SAC Steel Project Technical Office
1301 South 46th St.
Richmond, CA 94804

Project Administration

Allen Paul Goldstein, Project Administrator
Allen Paul Goldstein and Associates
1621B 13th Street
Sacramento, CA 95814

Lori Campbell, Assistant to the Project
Administrator
4804 Polo Court
Fair Oaks, CA 95628-5266

Project Oversight Committee (POC)

William J. Hall, Chair
3105 Valley Brook Dr.
Champaign, IL 61821

James R. Harris
J.R. Harris and Co.
1580 Lincoln St., Suite 550
Denver, CO 80203-1509

Shirin Ader
International Conference of Building
Officials
5360 Workman Mill Rd.
Whittier, CA 90601-2298

Richard Holguin
520 Kathryn Ct.
Nipomo, CA 93444

John M. Barsom
Barsom Consulting, Ltd.
1316 Murray Ave, Suite 300
Pittsburgh, PA 15217

Nestor Iwankiw
American Institute of Steel Construction
One East Wacker Dr., Suite 3100
Chicago, IL 60601-2001

Roger Ferch
Herrick Corporation
7021 Koll Center Parkway
P.O Box 9125
Pleasanton, CA 94566-9125

Roy Johnston
Brandow & Johnston Associates
1600 West 3rd St.
Los Angeles, CA 90017

Theodore V. Galambos
University of Minnesota
122 CE Building, 500 Pillsbury Dr. SE
Minneapolis, MN 55455

Leonard Joseph
Thornton-Tomassetti Engineers
641 6th Ave., 7th Floor
New York, NY 10011

John L. Gross
National Institute of Stds. & Technology
Building and Fire Research Lab,
Building 226, Room B158
Gaithersburg, MD 20899

Duane K. Miller
The Lincoln Electric Company
22801 St. Clair Ave.
Cleveland, OH 44117-1194

John Theiss
EQE/Theiss Engineers
1848 Lackland Hills Parkway
St. Louis, MO 63146-3572

John H. Wiggins
J.H. Wiggins Company
1650 South Pacific Coast Hwy, Suite 311
Redondo Beach, CA 90277

Team Leaders for Topical Investigations

Douglas A. Foutch
University of Illinois
MC-250, 205 N. Mathews Ave.
3129 Newmark Civil Engineering Lab
Urbana, IL 61801

Karl H. Frank
University of Texas at Austin
10100 Bornet Rd.
Ferguson Lab, P.R.C. #177
Austin, TX 78758

Matthew Johnson
Edison Welding Institute
1250 Arthur E. Adams Drive
Columbus, OH 43221

Helmut Krawinkler
Department of Civil Engineering
Stanford University
Stanford, CA 94305

Charles W. Roeder
University of Washington
233-B More Hall FX-10
Dept. of Building and Safety
Seattle, WA 98195-2700

L. Thomas Tobin
Tobin and Associates
134 California Ave.
Mill Valley, CA 94941

Lead Guideline Writers

John D. Hooper
Skilling Ward Magnusson Barkshire, Inc.
1301 Fifth Avenue, Suite 3200
Seattle, WA 98101-2699

Lawrence D. Reaveley
University of Utah
Civil Engineering Dept.
3220 Merrill Engineering Building
Salt Lake City, UT 84112

Thomas A. Sabol
Englekirk & Sabol Consulting Engineers
P.O. Box 77-D
Los Angeles, CA 90007

C. Mark Saunders
Rutherford & Chekene
303 Second St., Suite 800 North
San Francisco, CA 94107

Robert E. Shaw
Steel Structures Technology Center, Inc.
42400 W Nine Mile Road
Novi, MI 48375-4132

Raymond H. R. Tide
Wiss, Janney, Elstner Associates, Inc.
330 Pflingsten Road
Northbrook, IL 60062-2095

C. Allin Cornell, Associate Guideline Writer
Stanford University
Terman Engineering Center
Stanford, CA 94305-4020

Technical Advisory Panel (TAP) for Materials and Fracture

John M. Barsom, POC
Barsom Consulting, Ltd.
1316 Murray Ave, Suite 300
Pittsburgh, PA 15217

Serge Bouchard*
TradeARBED
825 Third Avenue, 35th Floor
New York, NY 10022

Michael F. Engestrom*
Nucor-Yamato Steel
P.O. Box 678
Frederick, MD 21705-0678

Karl H. Frank, Team Leader
University of Texas at Austin
10100 Burnet Rd.
Ferguson Lab, P.R.C. #177
Austin, TX 78758

Nestor Iwankiw*
American Institute of Steel Construction
One East Wacker Dr., Suite 3100
Chicago, IL 60601-2001

Dean C. Krouse*
705 Pine Top Drive
Bethlehem, PA 18017

Frederick V. Lawrence
University of Illinois at Urbana-Champaign
205 N. Mathews Ave.
Room 2129 Newmark Lab
Urbana, IL 61801

Robert F. Preece
Preece, Goudie & Associates
100 Bush St., Suite 410
San Francisco, CA 94104

Raymond H. R. Tide, Guideline Writer
Wiss, Janney, Elstner Associates, Inc.
330 Pflingsten Road
Northbrook, IL 60062-2095

TAP for Welding and Inspection

John M. Barsom
Barsom Consulting, Ltd.
1316 Murray Ave, Suite 300
Pittsburgh, PA 15217

John W. Fisher
Lehigh University
117 ATLSS Drive
Bethlehem, PA 18015-4729

J. Ernesto Indacochea
University of Illinois at Chicago
Civil and Materials Engineering (mc 246)
842 West Taylor Street
Chicago, IL 60607

Matthew Johnson, Team Leader
Edison Welding Institute
1250 Arthur E. Adams Drive
Columbus, OH 43221

David Long
PDM Strocal, Inc.
2324 Navy Drive
Stockton, CA 95206

Duane K. Miller, POC
The Lincoln Electric Company
22801 St. Clair Ave.
Cleveland, OH 44117-1194

Robert Pyle*
AISC Marketing
10101 South State Street
Sandy, Utah 84070

Douglas Rees-Evans*
Steel Dynamics, Inc.
Structural Mill Division
2601 County Road 700 East
Columbia City, IN 46725

Richard I. Seals
P.O. Box 11327
Berkeley, CA 94712-2327

Robert E. Shaw, Guideline Writer
Steel Structures Technology Center, Inc.
42400 W Nine Mile Road
Novi, MI 48375-4132

TAP for Connection Performance

Charlie Carter*
American Institute of Steel Construction
One East Wacker Drive, Suite 3100
Chicago, IL 60601-2001

Robert H. Dodds
University of Illinois at Urbana-Champaign
205 N. Mathews Ave.
2129 Newmark Lab
Urbana, IL 61801

Roger Ferch, POC
Herrick Corporation
7021 Koll Center Parkway
P.O. Box 9125
Pleasanton, CA 94566-9125

John D. Hooper, Guideline Writer
Skilling Ward Magnusson Barkshire, Inc.
1301 Fifth Avenue, Suite 3200
Seattle, WA 98101-2699

Egor Popov
University of California at Berkeley
Department of Civil and Environmental
Engineering, Davis Hall
Berkeley, CA 94720

Steve Powell*
SME Steel Contractors
5955 W. Wells Park Rd.
West Jordan, UT 84088

Charles W. Roeder, Team Leader
University of Washington
233-B More Hall FX-10
Dept. of Building and Safety
Seattle, WA 98195-2700

Stanley T. Rolfe
University of Kansas
Civil Engineering Department
2006 Learned Hall
Lawrence, KS 66045-2225

Rick Wilkinson*
Gayle Manufacturing Company
1455 East Kentucky
Woodland, CA 95695

TAP for System Performance

Jacques Cattan*
American Institute of Steel Construction
One East Wacker Drive, Suite 3100
Chicago, IL 60601-2001

Gary C. Hart
Hart Consultant Group
The Water Garden, Ste. 670E
2425 Olympic Blvd.
Santa Monica, CA 90404-4030

Y. Henry Huang*
Los Angeles County Dept. of Public Works
900 S. Fremont Avenue, 8th Floor
Alhambra, CA 91803

Helmut Krawinkler, Team Leader
Department of Civil Engineering
Stanford University
Stanford, CA 94305

Dennis Randall*
SME Steel Contractors
5955 West Wells Park Road
West Jordan, UT 84088

Andrei M. Reinhorn
State University of New York at Buffalo
Civil Engineering Department
231 Ketter Hall
Buffalo, NY 14260

Arthur E. Ross, JVMC
Cole/Yee/Shubert & Associates
2500 Venture Oaks Way, Suite 100
Sacramento, CA 95833

C. Mark Saunders, Guideline Writer
Rutherford & Chekene
303 Second St., Suite 800 North
San Francisco, CA 94107

W. Lee Shoemaker*
Metal Building Manufacturers Association
1300 Summer Avenue
Cleveland, OH 44115

John Theiss, POC
EQE/Theiss Engineers
1848 Lackland Hills Parkway
St. Louis, MO 63146-3572

TAP for Performance Prediction and Evaluation

Vitelmo V. Bertero
University of California at Berkeley
Pacific Earthquake Engr. Research Center
1301 S. 46th St.
Richmond, CA 94804

Bruce R. Ellingwood
Johns Hopkins University
Department of Civil Engineering
3400 N. Charles St.
Baltimore, MD 21218

Douglas A. Foutch, Team Leader
University of Illinois
MC-250, 205 N. Mathews Ave.
3129 Newmark Civil Engineering Lab
Urbana, IL 61801

Theodore V. Galambos, POC
University of Minnesota
122 CE Building, 500 Pillsbury Dr. SE
Minneapolis, MN 55455

Lawrence G. Griffis
Walter P. Moore & Associates
3131 Eastside, Second Floor
Houston, TX 77098

Edwin T. Huston, JVMC
Smith & Huston, Inc.
8618 Roosevelt Way NE
Seattle, WA 98115

Thomas A. Sabol, Guideline Writer
Englekirk & Sabol Consulting Engineers
P.O. Box 77-D
Los Angeles, CA 90007

Harry Martin*
American Iron and Steel Institute
11899 Edgewood Road, Suite G
Auburn, CA 95603

Tom Schlafly*
American Institute of Steel Construction
One East Wacker Drive, Suite 3100
Chicago, IL 60601-2001

Technical Advisors

Norm Abrahamson
Pacific Gas & Electric
P.O. Box 770000, MC N4C
San Francisco, CA 94177

Robert Kennedy
RPK Structural Mechanics Consultants
18971 Villa Terr
Yorba Linda, CA 92886

C.B. Crouse
URS – Dames and Moore
2025 First Avenue, Suite 500
Seattle, WA 98121

Social Economic and Policy Panel

Martha Cox-Nitikman
Building and Owners and Managers
Association, Los Angeles
700 South Flower, Suite 2325
Los Angeles, CA 90017

Alan Merson
Morley Builders
2901 28th Street, Suite 100
Santa Monica, CA 90405

Karl Deppe
27502 Fawnskin Dr.
Rancho Palos Verdes, CA 90275

Joanne Nigg
University of Delaware
Disaster Research Center
Newark, DE 19716

Eugene Lecomte
Institute for Business and Home Safety
6 Sheffield Drive
Billerica, MA 01821

William Petak
University of Southern California
Lewis Hall, Room 201
650 Childs Way
Los Angeles, CA 90089

James Madison
Attorney at Law, Mediator and Arbitrator
750 Menlo Avenue, Suite 250
Menlo Park, CA 94025

Francine Rabinovitz
Hamilton, Rabinovitz and Alschuler
1990 South Bundy Drive, Suite 777
Los Angeles, CA 90025

Dennis Randall
SME Steel Contractors
5955 West Wells Park Road
West Jordan, UT 84088

Stephen Toth
TIAA-CREF
730 Third Avenue
New York, NY 10017-3206

David Ratterman
Stites and Harbison
400 West Market St., Suite 1800
Louisville, KY 40202-3352

John H. Wiggins, POC
J.H. Wiggins Company
1650 South Pacific Coast Hwy, Suite 311
Redondo Beach, CA 90277

L. Thomas Tobin, Panel Coordinator
134 California Ave.
Mill Valley, CA 94941

Performance of Steel Buildings in Past Earthquakes Subcontractors

David Bonowitz
887 Bush, No. 610
San Francisco, CA 94108

Peter Maranian
Brandow & Johnston Associates
1660 West Third Street
Los Angeles, CA 90017

Peter Clark
SAC Steel Project Technical Office
1301 South 46th St.
Richmond, CA 94804

Terrence Paret
Wiss Janney Elstner Associates, Inc.
2200 Powell St. Suite 925
Emeryville, CA 94602

Michael Durkin
Michael Durkin & Associates
22955 Leanora Dr.
Woodland Hills, CA 91367

Maryann Phipps
Degenkolb Engineers
225 Bush Street, Suite 1000
San Francisco, CA 94104

James Goltz
California Institute of Technology
Office of Earthquake Programs
Mail Code 252-21
Pasadena, CA 91125

Allan Porush
Dames & Moore
911 Wilshire Blvd., Suite 700
Los Angeles, CA 90017

Bruce Maison
7309 Lynn Ave
Elcerrito, CA 94530

Access Current Knowledge Subcontractors

David Bonowitz
887 Bush , No. 610
San Francisco, CA 94108

Stephen Liu
Colorado School of Mines
Mathematics and Computer Science
Department
Golden, CO 80401

Materials and Fracture Subcontractors

Robert Dexter
University of Minnesota
122 Civil Engineering Building
500 Pillsbury Drive SE
Minneapolis, MN 55455-0116

Karl H. Frank
University of Texas at Austin
10100 Burnet Rd.
Ferguson Lab, P.R.C. #177
Austin, TX 78758

Welding and Inspection Subcontractors

Pingsha Dong / Tom Kilinski
Center for Welded Structures Research
Battelle Memorial Institute
501 King Avenue
Columbus, OH 43201-2693

Glenn M. Light / George Gruber
Southwest Research Institute
6220 Culebra Road, P. O. Drawer 28510
San Antonio, TX 78228-0510

Matthew Johnson
Edison Welding Institute
1250 Arthur E. Adams Drive
Columbus, OH 43221

William C. Mohr
Edison Welding Institute
1250 Arthur E. Adams Drive
Columbus, OH 43221

Connection Performance Subcontractors

Gregory Deierlein
Stanford University
Terman Engineering Center
Department of Civil and Environmental Engr.
Stanford, CA 94305-4020

Sherif El-Tawil / Sashi Kunnath
University of Central Florida
Civil and Environmental Engr. Department
Orlando, FL. 32816-2450

Charles W. Roeder
University of Washington
233-B More Hall FX-10
Seattle, WA 98195-2700

Anthony Ingraffea
Cornell University
School of Civil Engineering
363 Hollister Hall
Ithaca, NY 14853

System Performance Subcontractors

Paul Somerville
Woodward-Clyde Federal Services
566 El Dorado St., Suite 100
Pasadena, CA 91101-2560

Andrei M. Reinhorn
State University of New York at Buffalo
Civil Engineering Department
231 Ketter Hall
Buffalo, NY 14260

Farzad Naeim
John A. Martin & Associates
1212 S. Flower Ave.
Los Angeles, CA 90015

C. Allin Cornell
Stanford University
Terman Engineering Center
Stanford, CA 94305-4020

Helmut Krawinkler
Dept. of Civil Engineering
Stanford University
Stanford, CA 94305

Kazuhiko Kasai
Tokyo Institute of Technology
Structural Engineering Research Center
Nagatsuta, Midori-Ku
Yokohama 226-8503, JAPAN

Gregory MacRae
University of Washington
Civil Engineering Department
Seattle, WA 98195-2700

Bruce F. Maison
7309 Lynn Avenue
El Cerrito, CA 94530

Performance Prediction and Evaluation Subcontractors

James Anderson
University of Southern California
Civil Engineering Department
Los Angeles, CA 90089-2531

Gary C. Hart
Department of Civil and Environmental
Engineering
University of California
Los Angeles, CA 90095

Douglas A. Foutch
University of Illinois
MC-250, 205 N. Mathews Ave.
3129 Newmark Civil Engineering Lab
Urbana, IL 61801

Y.K. Wen
University of Illinois
3129 Newmark Civil Engineering Lab
205 N. Mathews Ave.
Urbana, IL 61801

Testing Subcontractors

Subhash Goel / Bozidar Stojadinovic
University of Michigan
Civil Engineering Department
Ann Arbor, MI 48109

Thomas Murray
Virginia Tech, Dept. of Civil Engineering
200 Patton Hall
Blacksburg, VA 24061

Roberto Leon
Georgia Institute of Technology
School of Civil & Environmental Engr.
790 Atlantic Ave.
Atlanta, GA 30332-0355

James M. Ricles / Le-Wu Lu
Lehigh University
c/o ATLSS Center
117 ATLSS Drive, H Building
Bethlehem, PA 18015-4729

Vitelmo V. Bertero / Andrew Whittaker
UC Berkeley
Pacific Earthquake Engr. Research Center
1301 S. 46th St.
Richmond, CA 94804

John M. Barsom
Barsom Consulting, Ltd.
1316 Murray Ave, Suite 300
Pittsburgh, PA 15217

Hassan Astaneh
University of California at Berkeley
Dept. of Civil and Environmental Engr.
781 Davis Hall
Berkeley, CA 94720

Michael Engelhardt
University of Texas at Austin
Ferguson Laboratory
10100 Burnet Road, Building 177
Austin, TX 78712-1076

Gary T. Fry
Texas A&M University
Department of Civil Engineering
Constructed Facilities Division, CE/TTI
Building, Room 710D
College Station, TX 77843-3136

Chia-Ming Uang
University of California at San Diego
Dept. of AMES, Division of Structural Engr.
409 University Center
La Jolla, California 92093-0085

Stephen Schneider
University of Illinois at Urbana-Champaign
3106 Newmark Civil Engr. Lab, MC-250
205 N. Mathews Avenue
Urbana, IL 61801

Matthew Johnson
Edison Welding Institute
1250 Arthur E. Adams Drive
Columbus, OH 43221

James Anderson
University of Southern California
Civil Engineering Department
Los Angeles, CA 90089-2531

Bozidar Stojadinovic
Dept. of Civil & Environmental Engr.
University of California
Berkeley, CA 94720

Inspection Procedure Consultants

Thomas Albert
Digiray Corporation
2235 Omega Road, No. 3
San Ramon, CA 94583

Randal Fong
Automated Inspection Systems, Inc.
4861 Sunrise Drive, Suite 101
Martinez, CA 94553

Andre Lamarre
R.D Tech, Inc.
1200 St. Jean Baptiste, Suite 120
Quebec City, Quebec, Canada G2ZE 5E8

Glenn Light
Southwest Research Institute
6220 Culebra Road
San Antonio, TX 78228

Andrey Mishin
AS & E High Energy Systems
330 Keller Street, Building 101
Santa Clara, CA 95054

Robert Shaw
Steel Structures Technology Center, Inc.
42400 W. Nine Mile Road
Novi, MI 48375-4132

Carlos Ventura
Dept of Civil Engineering
University of British Columbia
2324 Main Hall
Vancouver, BC, Canada V6T 1Z4

Guideline Trial Applications Subcontractors

John Hopper
Skilling Ward Magnusson Barkshire, Inc.
1301 Fifth Avenue, Suite 320
Seattle WA 98101-2699

Lawrence Novak
Skidmore, Owings, and Merrill
224 S. Michigan Ave, Suite 1000
Chicago, IL 60604

Leonard Joseph
Thornton-Tomassetti Engineers
641 6th Avenue, 7th Floor
New York, NY 10011

Maryann Phipps
Degenkolb Engineers
225 Bush Street, Suite 1000
San Francisco, CA 94104

Economic and Social Impact Study Subcontractors

Ronald Eguchi
EQE Engineering and Design
300 Commerce Dr., Ste. 200
Irvine, CA 92602

Charles Kircher
Charles Kircher & Associates
1121 San Antonio Road, Suite D-202
Palo Alto, CA 94303

Martin Gordon / Peter Morris
Adamson Associates
170 Columbus Avenue
San Francisco, CA 94133

Lizandro Mercado
Brandow & Johnston Associates
1600 West 3rd St.
Los Angeles, CA 90017

Richard Henige
Lemessurier Consultants Inc.
675 Massachusetts Ave.
Cambridge, MA 02139-3309

Greg Schindler
KPF Consulting Engineers
1201 3rd Ave.
Seattle, WA 98101-3000

Report Production and Administrative Services

A. Gerald Brady, Technical Editor
Patricia A. Mork, Administrative Asst.
Peter N. Mork, Computer Specialist
Bernadette A. Mosby, Operations Admin.
Michelle S. Schwartzbach, Pub. Specialist
Applied Technology Council
555 Twin Dolphin Drive, Suite 550
Redwood City, CA 94065

Carol Cameron, Publications Coordinator
Ericka Holmon, Admin. Assistant
California Universities for Research in
Earthquake Engineering
1301 S. 46th Street
Richmond, CA 94804

*indicates industrial or organizational contact representative